Study on Stereochemistry and Regioselective Methylation in 1,4-β-Glucomannan

Von der Fakultät für Lebenswissenschaften

der Technischen Universität Carolo-Wilhelmina zu Braunschweig

zur Erlangung des Grades einer

Doktorin der Naturwissenschaften

(Dr. rer. nat.)

genehmigte

D i s s e r t a t i o n

von Qimeng Zhang

aus Beijing, China

1. Referentin: Professorin Dr. Petra Mischnick

2. Referent: apl. Professor Dr. Hans-Joachim Jördening

eingereicht am: 12.09.2018

mündliche Prüfung (Disputation) am: 17.12.2018

Druckjahr 2019

Vorveröffentlichungen der Dissertation

Teilergebnisse aus dieser Arbeit wurden mit Genehmigung der Fakultät für Lebenswissenschaften, vertreten durch die Mentorin der Arbeit, in folgenden Beiträgen vorab veröffentlicht:

Publikationen

Q. Zhang, P. Mischnick. Influence of Stereochemistry on Relative Reactivities of Glucosyl and Mannosyl Residues in Konjac Glucomannan (KGM). Macromolecular Chemistry and Physics 218 (17): 1700119 doi.org/10.1002/macp.201700119 (2017).

Q. Zhang, P. Mischnick. Borate-Mediated Stereo- and Topo-Selective Methylation of 1,4-β-Glucomannan. Macromolecular Chemistry and Physics 219 (6): 1700502 doi.org/10.1002/macp.201700502 (2018).

J. Raßloff, Q. Zhang, P. Mischnick. Potential of dibutyltin oxide for the manno/gluco- and regioselective methylation of Konjac glucomannan. Cellulose 25 (9): 4929-4940, doi.org/10.1007/s10570-018-1911-3 (2019).

Tagungsbeiträge

Q. Zhang and P. Mischnick: Reductive-cleavage and alditol acetate analysis for the analysis of the substitution pattern in *O*-methylated 1,4-β-glucomannans. (Poster). Seventh International Symposium on the Separation and Characterization of Natural and Synthetic Macromolecules-SCM 7, Amsterdam, Netherlands (2015).

Q. Zhang and P. Mischnick: Reductive-cleavage and alditol acetate analysis for the analysis of the substitution pattern in *O*-methylated 1,4-β-glucomannans. (Poster). Sixth Braunschweiger Jungchemikertagung, Braunschweig, Germany (2015).

Q. Zhang and P. Mischnick: Monomer and oligomer analysis for the investigation of the substitution pattern in *O*-methylated 1,4-β-glucomannans. (Poster). 4th EPNOE International Polysaccharide Conference-EPNOE 4, Warsaw, Poland (2015).

Q. Zhang and P. Mischnick: Borate effects in the modification of 1,4-β-glucomannans. (Poster). Seventh Braunschweiger Jungchemikertagung, Braunschweig, Germany (2016).

Q. Zhang and P. Mischnick: Borate-mediated Stereoselective Alkylation of 1,4-β-glucomannans. (Poster). Eighth International Symposium on the Separation and Characterization of Natural and Synthetic Macromolecules-SCM 8, Amsterdam, Netherlands (2017).

Acknowledgement

Working as a PhD student at TU Braunschweig has been a challenging and memorable experience for me. In all these years, many people were involved and influenced my academic career. Without this support, I would not have finished my PhD study here.

First of all, I would like to thank my supervisor Prof. Dr. Petra Mischnick for the interesting topic and for her inspiration and supervision during my doctoral working time. She was available for discussion at any time and to support me to participate in international conferences. My experience in her working group was very fruitful.

I would like to thank Prof. Dr. Hans-Joachim Jördening to be my second supervisor and Prof. Dr. Ulrich Engelhardt to be the chairman of the examination.

The China Scholarship Council (CSC) is acknowledged for the 4 years financial support of my PhD studies.

Special thanks to my lovely colleagues and friends in the institute of food chemistry, Silke Lehmann, Fanziska Sydow, Matthias Bol, Julia Cuers, Sheetal Gangula, Payam Hashemi, Patrick Sudwischer, Christian Bork, Marko Rother, Nico Lämmerhardt and Anna-Lena Korf for generously sharing your knowledge with me and providing the warm and helpful working atmosphere. Janick Raßloff is gratefully acknowledged for his work as a Diploma-student. Not the least, I have really good memory for doing sport with my friends Maggie and Julia.

Most importantly, completing my PhD studies aboard would not have been possible without the love, concern and support of my family and friends. I really appreciate my parents for supporting my decision and giving me so much love. My husband, Rinie, I feel blessed to have met you in Germany and to be part of your life. My little angel, Jinmao, you are the most precious gift I have ever gotten in my life. Especially at the end phase of my PhD work, these difficult but happy months, many thanks for the supporting of my family and my supervisor Prof. Mischnick.

List of abbreviations and symbols

ABA	Aminobenzoic Acid
AAM	Alditol Acetate Method
Ac	Acetylation
ACN	Acetonitrile
Ac-KGM	*O*-Acetyl-KGM
AGU	Anhydro Glucose Unit
AMU	Anhydro Mannose Unit
ATR-IR	Attenuated Total Reflection-Infrared Spectroscopy
B	Borate Complexation
c_i	Molar Fraction of *i*-fold Substituted Monomer Units
DIPEA	Diisopropylethylamine
CM-KGM	Carboxymethyl Konjac Glucomannan
DMSO	Dimethylsulphoxide
DP	Degree of Polymerization
DM-KGM	*O*-Methyl-d_3/*O*-Methyl-KGMs
DMF	Dimethylformamide
DS	Degree of Substitution
DTG	Differential Thermal Gravimetry
DSC	Differential Scanning Calorimetry
ECR	Effective Carbon Response
EI	Electron Impact
EIC	Extracted Ion Chromatograms
EM-KGM	*O*-Ethyl-*O*-Methyl-KGM
ESI	Electrospray Ionization
Et	Ethyl
Exo>	Exothermic
FID	Flame Ionization Detector
G/Glc	D-Glucosyl, D-Glucose
GGM	Galactoglucomannan
GLC	Gas Liquid Chromatography
G_mM_n	Mixed Oligomer of Glucosyl and Mannosyl Units
H_1	Heterogeneity Parameter

H_c	Diversity Parameter
HCl	Hydrogen Chloride
HOAc	Acetic Acid
HPLC	High Performance Liquid Chromatography
HPMC	Hydroxypropylmethylcellulose
KGM	Konjac Glucomannan
M/Man	D-Mannosyl, D-Mannose
MC	Methylcellulose
Me	Methyl
MeOH-Ac	Methanolysis and subsequent acetylation
MeOH-TMS	Methanolysis and subsequent trimethylsilylation
M-Glc	Methyl α-D-glucoside
M-KGM	Methylated KGM
MM	Methylated Mannan
M-Man	Methyl α-D-mannoside
MS	Mass Spectrometry
NMR	Nuclear Magnetic Resonance
RCM-Ac	Reductive cleavage and subsequently acetylation
RCM-Bz	Reductive cleavage and subsequently benzoylation
SGM	Spruce Glucomannan
s_i	Molar Fraction of Monomer Substituted at Position *i*
sono-KGM	Sonificated KGM
stan-KGM	Stannylated KGM
TMS	Trimethylsilylation
TFA	Trifluoroacetic Acid
TGA	Thermogravimetric Analysis
UV	Ultraviolet
x_i	Partial DS in Position *i*

Contents

1 Introduction

1.1 Konjac glucomannan structure

The plant genus *Amorphophallus konjac* (Konjac)[1] is one of the family Araceae (aroidae) family and it has been used as food and food additive in China and Japan for more than 1000 years.[2] Konjac glucomannan (KGM) is isolated from the konjac tuber and it is a water-soluble non-ionic polysaccharide.[3] Employing konjac root, the industrial processes to produce KGM consist of a sequence of steps including washing, slicing it into chips, and pulverizing dried chips. The common konjac flour (food grade) is finally obtained after removal of impurities such as starch, protein, cellulose, and low molecular weight sugars (e.g. D-glucose and D-fructose) from the crude flour via wind shifting or by ethanol precipitation.[4] Tsuji reported that the tuber of *Amorphophallus konjac* root contains a very large proportion of mannan.[5] Smith and Srivastava found that this polysaccharide is composed of D-glucosyl (G) and D-mannosyl (M) residues connected by β-1,4-glycosidic linkages.[6] The ratio of mannosyl and glucosyl units was determined to be 1.6 by Kato and Matsuda.[7] The molecular weight is reported to be in the range of 1×10^4 to 1.9×10^6.[8] Branching at either position 3 or 6 of both sugar constituents has been reported by several authors,[6,9–11] however, other studies did not find any hint on branching whatsoever. This absence of branching was found by methylation analysis,[12] the same technique as used in the present study. KGM is acetylated to an extent of 5-10%,[9] but the acetyl groups are split off under strong alkaline conditions.[13] A possible structural element of KGM is shown in Figure 1.1.

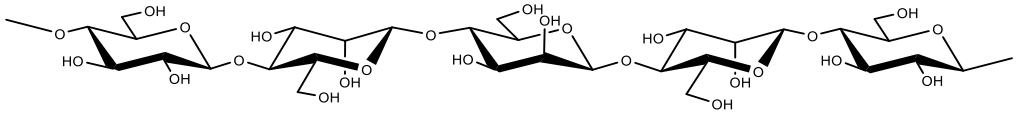

Figure 1.1 Structure of KGM, built of β-1,4-linked glucosyl and mannosyl units.

Reports about the possible arrangement of G and M in the KGM main chains are contradictory. By applying cellulase and sulfuric acid, Kato et al. identified some oligomers obtained by carbon column chromatography. Among the di- to pentasaccharides (e.g. M-M, M-G, G-G, M-M-G, M-G-M, M-M-M-M-G), structures with up to four β-1,4-linked mannoses were found.[14] Shimahara et al. degraded KGM with crude β-mannanase and isolated and characterized the generated oligomers.[15] They suggested the presence of repeating domains dominated by short manno-oligosaccharides up to mannopentaose. Cescutti performed enzymatic hydrolysis of KGM by cellulase and two β-mannanases and concluded that the distribution of mannose and glucose in the products of enzymic digestion does not indicate blockiness.[16] In contrast, on basis of ^{13}C NMR measurements, Katsuraya et al.

reported that the structure of KGM is not random, but typically G–M–G–M_2–G–M_3–G_2–M–G_2–M_2–G_2–M_3–G_2–M_4–G_2–M_5.[10] By means of capillary electrophoresis with laser-induced fluorescence detection (CE-LIFD), Albrecht et al. analyzed KGM which had been partially degraded with different enzymes, and concluded that the KGM polysaccharide backbone was built of short mannose and glucose sequences.[11] All these studies suffer from the fact that they deduce the polysaccharide structure from single structural features which do not represent the whole.

1.2 Konjac glucomannan, its derivatives and application potential

KGM has good water binding and gelation capacity as well as film forming property. Therefore, due to these functional properties, KGM and its derivatives have a wide spectrum of applications, e.g. as emulsifier in food production, for drug-delivery in pharmaceuticals, as body weight reducer in health-care agents, for pulp and paper industry, and generally in the textile manufacturing and the petroleum industry.[17–21]

Nowadays, the product market for ready-to-eat food and minimally processed food are growing each year. Therefore, it is important to minimize the change in taste, texture, and drip loss of frozen food after thawing. KGM acts as hydrocolloid, if added into food matrices before freezing, and the texture and rheological properties of food and beverages can be improved since KGM can retain the moisture by the interactions with starch.[22,23] Moreover, KGM has attracted much interest for using it for the formulation of functional food in last decades.[3] It is reported that KGM has the ability to lower blood cholesterol level by binding bile acids in the gut and carry them out of the body in the feces, requiring the body to convert more cholesterol into bile acids.[24] Furthermore, KGM can help with weight loss by filling the stomach and making a person feel saturated.[25] It is possible to add KGM as fat analogue in mayonnaise[26] or replace beef fat by KGM in merguez sausage.[27]

Native KGM has limited uses and has been chemically/physically modified to various derivatives to expand the range of application, and the interested reader is referred to the recent review paper by Zhu.[25] Such derivatives are of interest to researchers to improve the solubility of KGM in various solvents. The chemical modifications of KGM include esterification, etherification, acetylation and cationization.

The first partial methylation of KGM has been performed by Haworth et al.[28] while permethylation became possible by the method of Hakomori, an important step in the characterization of the linking positions of polysaccharides.[29] To obtain a water-soluble methylated KGM, An et al. performed the methylation directly in aqueous NaOH/CH_3I to

yield water-soluble *O*-methyl-glucomannan derivatives with a degree of substitution (DS) in the range of 0.09-0.18.[30] They suggested that the resulting *O*-methylated KGM has promising film-forming properties for production of packaging, encapsulating of liquid or as a stabilizer in preparation of metal nanoparticle.[30]

Carboxymethyl KGM (CM-KGM) is one of the most common KGM ethers. CM-KGM with a DS of 0.53 was prepared in 80 % ethanol/chloroacetic acid at pH 12 at 55 °C for 3 hours. It showed both, a higher rate of hydration and hydrosol transmittance, and it could be further utilized for improving the appearance of the product as well as the shelf life of the product.[31] CM-KGM has been used as a paper strengthening agent, where the dry and wet tensile indices are proportional to the DS of CM-KGM.[20]

KGM sulfates with DS of 1.3-1.4 and molecular weight of 0.4×10^4-1.0×10^4 have been obtained KGM after partial hydrolysis by diluted sulfuric acid and subsequent sulfation with piperidine-*N*-sulfonic acid in dimethyl sulfoxide (DMSO) or with SO_3-pyridine complex in pyridine at 60 °C.[32] The anti-HIV capacity of the sulfate was astonishing and comparable to that of an anti-HIV drug (e.g. 2' 3'-dideoxycytidine).

Enomoto-Rogers et al. prepared KGM acetates (Ac-KGM) with different DS up to 3.0 for thermoplastic film production. They reported that Ac-KGM with increasing DS increased the thermal stability of the products, i.e. increasing DS increased the decomposition temperatures of Ac-KGM and decreased the glass transition temperature (e.g. from 219 °C at DS 1.3 to 178 °C at DS 3.0).[33] With respect to application, a transparent films was produced from KGM acetate by casting the solution, and increasing DS of Ac-KGM reduced the elongation at break and the tensile strength of the films.

From economic and environmental perspectives, there is a demand for the application of waste water processes by using efficient natural polysaccharide derivatives. Cationic KGM was prepared by reacting with (2-methacryloyloxyethyl)trimethyl-ammonium chloride and 3-chloro-2-hydroxypropyl trimethylammonium chloride in NaOH/urea aqueous solution as a flocculant for waste water treatment. In a model system, the cationic KGM with a DS of 0.2 decreased the turbidity of a kaolin suspension (0.1%) by up to 90% at pH 7.[32]

1.3 Analysis of the structure of KGM

The study of the structure of starch and cellulose derivatives are quite complicated since the different hierarchical levels need to be considered, i.e. from supramolecular structures to molecular sub-structures, as well as the substituent distribution within one glycosyl unit.[34]

The following sections focusses on the analysis of substituent distribution in the glycosyl units and the substitution pattern on the oligomer level.

1.3.1 Determination of substitution pattern in the glycosyl units (monomer analysis)

To evaluate the relationships between structure and physiochemical, or where applicable, biological functions and transfer this knowledge to manufacture, a detailed analysis of the substitution pattern of the product is necessary. The analysis of the monomer composition, i.e. the molar proportions of the eight (e.g. methylcellulose) or more (eight for M units and eight for G units in methyl KGM) different glucosyl monomers, is the basis for studying the substitution pattern at all structural levels.[34] Due to the high polarity, hydrophilicity and low volatility, polysaccharides have to be converted into volatile and stable derivatives. First of all, depolymerization of polysaccharides is essential and their monomeric constituents of appropriate derivatives are submitted to subsequent separation and quantification by chromatographic or electrophoretic techniques. In general, aqueous acid hydrolysis by hydrogen chloride (HCl) or trifluoroacetic acid (TFA), methanolysis by methanolic HCl and reductive depolymerization by lewis acids and triethylsilane are commonly applied in the depolymerization step. Afterwards, several classical derivatization methods consist in the substitution of the polar groups (i.e. 2-, 3-, 6-OH groups in methylcellulose) of carbohydrates in order to increase their volatility. The most common derivatives used for carbohydrate composition determination are methyl ethers, acetates, trifluoroacetates and trimethylsilyl ethers.[35] In this thesis, three monomer derivatization method were applied, such as alditol acetated methods (AAM),[36] reductive cleavage and subsequently acetylation[37] or benzoylation (RCM-Ac/Bz),[38] and methanolysis and subsequently acetylation or trimethyl-silylation(MeOH-Ac/TMS).[39] A comparison between these three methods is performed with respect to advantage and disadvantage for the determination of monosaccharide composition in polysaccharides.

The advantage of AAM is that by this method half of the diastereoisomers can be eliminated by the reduction step (no α- and β-anomers). During sample preparation of AAM, each step has a critical moment that needs to be dealt with carefully, for instance, sample losses by side reactions during hydrolysis (e.g. formation of anhydro sugars and further eliminations, reversion products), selective losses due to volatility during evaporation steps and due to polarity during extraction steps. During evaporation of acid, the TFA concentrates in the residual water and can cause formation of reversion products from the depolymerized polysacchrides.[34,40] Therefore, samples require full alkylation before hydrolysis in case of

sample with low DS. Moreover, AAM is a time-consuming derivatization method, normally three days working time.

The reductive cleavage method is an alternative to AAM for fully alkylated glycans applying Lewis acid in dichlormethane instead of aqueous Bronsted acid and performing in situ reduction with triethylsilane to cyclic anhydroalditols.[34] Advantage of RCM in the analysis of starch and cellulose derivatives are the relative short preparation time at room temperature (one to two days working time). However, a few drawbacks of RCM need to be mentioned. First, permethylation is a prerequisite for reductive depolymerization and not only facultative. Further, the reagents are very sensitive to humidity and the Lewis acids might also catalyze rearrangement and isomerization reactions.[34,41,42]

While derivatization does not essentially require full protection of the OH groups, methanolysis (with dry methanol/HCl) is a faster alternative to acid hydrolysis (one day working time). Compared to AAM (applying aqueous acid), the application of methanolic HCl enables better dissolution and accessibility of the less polar partly or peralkylated polysaccharides, especially when methyl glycans have been perethylated Furthermore, applying methanolysis followed by silylation to get methyl glucosides, and reductive cleavage to produce 1,5-anhydro-4-*O*-benzoyl-2,3,6-tri-*O*-(m)ethyl alditols could protect or eliminate the reactive aldehyde function by glycosidation or by reduction.[36] Although the methyl glycosides obtained are less sensitive to aforementioned side reactions, they cannot be further converted (reduced) to alditols by $NaBD_4$. Therefore, eight substituent patterns of corresponding methyl α- and β-pyranosides would be observed in GLC analysis, respectively.

By coupling GLC with mass spectrometry (MS), alkyl groups (e.g. methyl/ethyl) can be easily located due to characteristic shifts of *m/z* of primary and secondary fragments with respect to the well-known spectra of partially methylated alditol acetates,[43] partially methylated and acetylated or benzoylated 1,5-anhydro-D-mannitols[42] and acetylated or trimethylsilylated methyl glycosides.[44] GLC-FID is the quantitation method to evaluate the relative molar composition of monomers (peak area corrected according to the effective carbon response (ECR) concept[45]) and monomer substituent composition for polysaccharides. Besides GLC-FID, CE coupled with UV detector has been applied for the determination of the constituent composition of glycan derivatives, e.g. MC or CMC.[35,46,47] To obtain UV-detectable analytes, carbohydrates are usually labeled with a chromophore by reductive amination and charge necessary for separation is introduced by reversible complex formation of diols groups with borate (stability: *cis* > *trans*) in an alkaline buffer.[48] Wang et al. reported

a better separation of sugars (labeled with 1-phenyl-3-methyl-5-pyrazolone) with increasing amount of methanol as modifier in the background electrolyte solution.[49] The optimized condition was 4% methanol in 175 mM borate buffer at pH 11.

1.3.2 Determination of substitution pattern over the polysaccharide chains (oligomer analysis)

Control over physicochemical properties of modified cellulose or KGM (such as solubility, thermoreversible gelation, viscosity, and flocculation) will lead to more tailor-made application hereof. For this purpose, not only the investigation of DS and molar mass distribution needs to be performed, but also the analysis of the substituent distribution along and over the polymer chains is required. The local substitution in oligomeric sequences determines the interaction between chains and thus will influence the physicochemical properties.[50]

In general, enzymatical hydrolysis and determine the amount of released monosaccharide is a common measure for the homo- or heterogeneity of substitution in polysaccharide derivates, e.g. by using cellulase for cellulose ether[50] and applying cellulase and mannanase for KGM.[16] Depending on the enzyme's specificity, different mono- and oligosaccharide profiles will be released from the polysaccharide derivatives and allow comparison of samples with the same average data. Opposed to this, partial degradation of peralkylated homoglycans e.g. perdeuteromethylated MC by acid promotes random cleavage nearly independent of the position of the substituent, DS and distribution pattern.[51,52]

Modified cellulose ethers can be cleaved to smaller oligosaccharides and the DS/DP (degree of depolymerization) pattern of these oligomers can be analyzed by electrospray ionization mass spectrometry (ESI-MS or LC-ESI-MS) or matrix assisted laser desorption ionization – time of flight mass spectrometry (MALDI-ToF-MS).[53,54] Perdeuteromethylation of methyl cellulose is performed before acid hydrolysis to reduce chemical and mass differences of the representatives of one DP.[34,55,56] The methyl pattern of oligomeric domains obtained by MS is compared with the methyl distribution calculated from the monomer composition. Some typical case examples are displayed in Figure 1.2.[57]

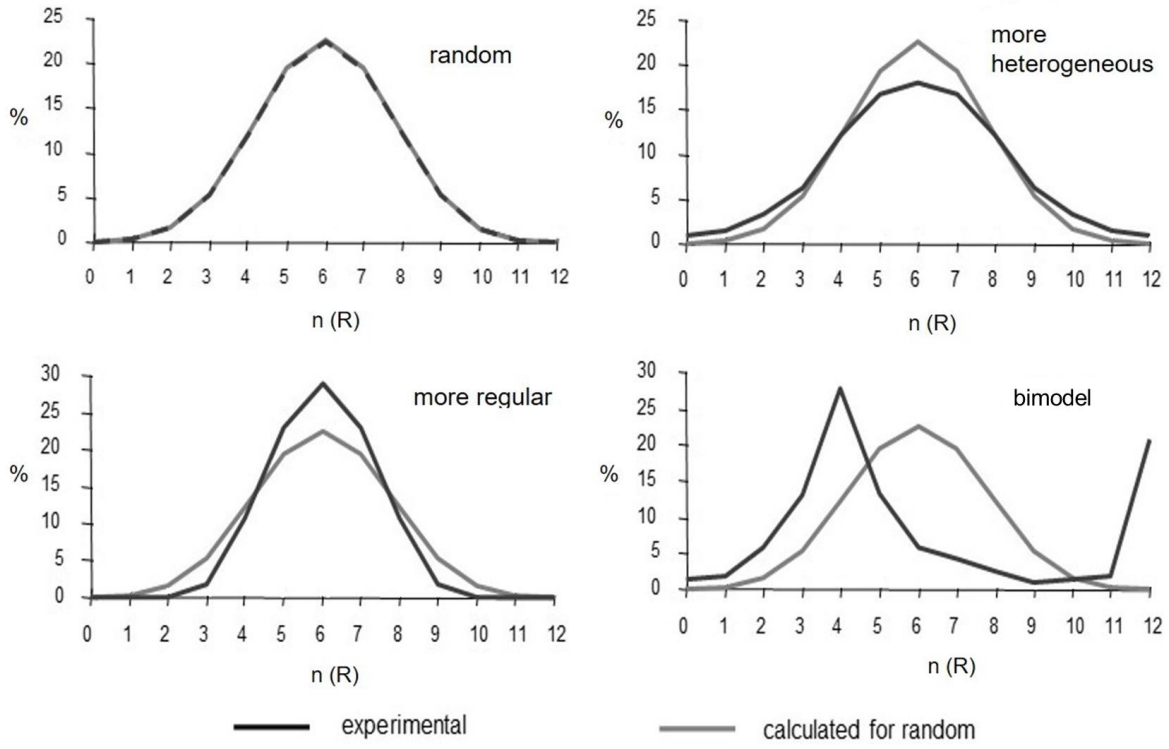

Figure 1.2 Comparison between experimental and calculated substitution pattern in DP4, to study the substitution pattern on cellulose chains, modified from ref.57.

In heteroglycans like KGM, the distribution of the sugar constituents additionally is of interest beside the substitution pattern in these constituents. Figure 1.3 shows possible distributions of mannose and glucose units over KGM polymer chains (a random distribution referred to as homogeneous, a block distribution, and a regular distribution).

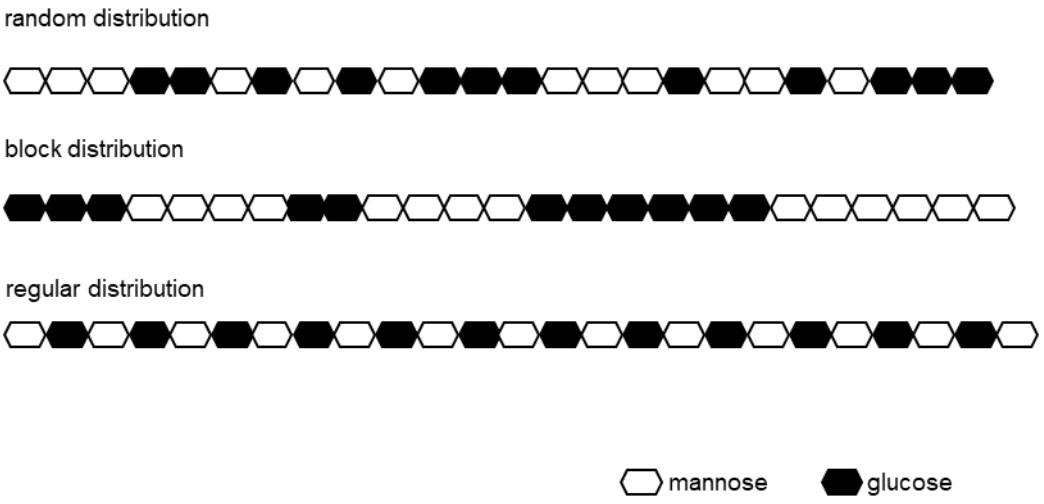

Figure 1.3 Three types of distribution of mannose and glucose unit over KGM chains. The real ratio of M and G in KGM (1.6) is neglected.

2 Objectives of the Thesis

Compared with cellulose, KGM only differs with respect to the orientation of OH group at C-2 (i.e. axial in M and equatorial in G) in about 60% of the glycosyl units, and can thus be considered as a stereoisomer of the well-known and widely applied β-1,4-glucan. While chemical modification of cellulose does not allow to differentiate between the constituents in a chain, the difference in stereochemistry of G and M opens the chance to generate different substitution patterns within one chain. Thus, in this study, the influence on stereochemistry on relative reactivity of M and G in KGM was investigated and methylation of KGM was performed by various methods. This investigation includes the following:

- Investigation of the relative reactivities of the different OH groups of KGM in both mannosyl and glucosyl units
- Studying regio- and M/G-selective methylation of KGM by making use of the stereochemistry-related differences in reactivity of G and M or in stability of their transient protected intermediates, respectively (borate or stannylene acetal intermediates)
- Determination of the substituent distribution in the sugar units for the partially methylated KGM products and deducing information of the G-M-distribution in KGM chains from the methyl pattern.

3 Influence of Stereochemistry on Relative Reactivities of Glucosyl and Mannosyl Residues in KGM

3.1 Introduction

The structure study of natural polysaccharides (e.g. KGM), their further chemical modification and application have attracted much interest in the last decades.[3,20,31,58,59] As mentioned in the introduction (Chapter 1), reports about the possible arrangement of G and M in the KGM main chains are contradictory. Therefore, the arrangement of G and M in KGM backbone is one point of the discussion in this chapter.

Independent on the distribution of M and G, KGM can be considered as a stereoisomer of cellulose, since it only differs with respect to the orientation of hydroxyl group at C-2, i.e. axial in M and equatorial in G (Figure 3.1). Due to this difference in stereochemistry the relative reactivities of the hydroxyl groups at position 2, 3, and 6 of glucose and mannose are expected to be different, as is known for the monosaccharides.[60] Such differences have been previously found for low molecular weight spruce glucomannan (SGM), methylated in DMSO/Li-dimsyl/CH_3I, with the order of reactivities in glucose being $k_2 > k_3 > k_6$ and $k_3 > k_2 > k_6$ in mannose.[61] Xu et al. prepared carboxymethylated galactoglucomannan (GGM) with DS in the range 0.1-1.1 in water/2-propanol/NaOH/chloroacetate.[62] Based on the analysis by means of GLC-MS and NMR spectroscopy, they reported for a CM-GGM with DS of 0.7 that the easiest accessible position for carboxymethylation was the primary 6-OH group, followed by O-2 and O-3, in both glucose and mannose units. GGM has also been functionalized for further grafting or cross-linking. Maleki et al. introduced thiol functions up to a DS of about 0.16 and used these reactive intermediates as a platform for various “click”-reactions.[63]

In general, it is a prominent challenge to achieve regioselective substitution in carbohydrates. The regioselectivity of reactions on carbohydrates will not only influence the substituent patterns within one sugar unit, it furthermore effects the substituent distribution over the polymer chains as well as the physical properties.[64] The stereoisomerism along the β-1,4-glycan chain opens the chance to establish sequences with changing substituent patterns in the molecular range.[65] By using NMR spectroscopy, Coleman et al. investigated the relative reactivity of phosphorylated alginates with respect to four possible substitution positions, i.e. 2-OH and 3-OH positions of D-mannuronic acid and L-guluronic acid, respectively.[66] By preparing a sample with the DS value of 0.26, they reported that the phosphorylation was strongly favored at the 3-OH (equatorial) groups compared to the 2-OH (axial) groups in D-mannuronic acid units, while the regioselectivity in L-guluronic acid

residues was not clearly determined. Based on ^{1}H and ^{13}C NMR analysis, An et al. reported the methylation of KGM in aqueous NaOH/CH_3I to yield water-soluble *O*-methyl-glucomannan derivatives with the DS values of 0.09-0.18.[30] They determined the overall order of reactivity under the conditions applied being O-6 > O-3 > O-2. The positions of the methyl groups in individual glucosyl and mannosyl residues, however, were not differentiated. Analysis of a tosylated KGM with DS 2.06 determined by NMR spectroscopy revealed complete esterification of C-6 hydroxyl groups, whereas, C-2 hydroxyl groups of glucose units were tosylated to a larger extent than mannose units, and C-3 hydroxyl groups showed lowest reactivity.[59]

In summary, there are not many studies comparing the relative reactivities of hydroxyl groups at different positions of KGM in both glucose and mannose residues in kinetically controlled etherification, and the consequence for the substituent pattern over the macromolecules has not been studied at all, while at the same time the distribution of mannosyl and glucosyl units within the long chain is not exactly known.

In this chapter methylation in water with NaOH/CH_3I is applied to investigate the influence of stereochemistry on the relative reactivities of mannosyl units compared to glucosyl units. It is of interest to study the relative reactivities of different OH groups in M and G residues in a aqueous solution at constant pH. The reactivities are influenced by their different acidities and by axial or equatorial orientation of OH in M and G, and dependent on the conditions applied their *cis*- or *trans*-relation as well (see Chapter 4 and Chapter 5). We now report on the synthesis of *O*-methyl Konjac glucomannans (M-KGM), the analysis of the methyl patterns obtained, and the kinetic evaluation of a time course study. In a next step, partially methylated KGM were perdeuteromethylated, partially hydrolyzed, and subsequently analyzed with respect to the distribution of the various *O*-methyl-glucosyl and *O*-methyl-mannosyl units over the polysaccharide chains. Moreover, thermal properties of M-KGMs obtained were analyzed by differential scanning calorimetry and thermogravimetric analysis.

3.2 Results and discussion

3.2.1 Relative reactivities in KGM

In the Williamson etherification, OH groups are deprotonated under alkaline conditions in order to form good nucleophiles which then attack methyl halides (or dimethyl sulfate) to form methyl ethers. In general, the alcoholic OH of the carbohydrates are more acidic than common aliphatic mono-alcohols with the OH at C-2 next to the electron-withdrawing anomeric center being the most acidic (pK_a ca. 13).[67] On the other hand, primary alcohols are

usually more acidic than secondary ones and especially better accessible for the nucleophiles. Therefore, the secondary OH at C-2 is the most favorable position in kinetically controlled reactions, as long as base concentration and pH are comparably low, followed by the primary OH at C-6 and then 3-OH.[68] The pK_a of 2-OH of stereoisomers are slightly different, where OH in the axial configuration (like in mannose) is less acidic then in the equatorial configuration (like in glucose).[67] The *cis*-configuration of the 2,3-diol feature in mannose compared to the *trans*-configuration in glucose can also play a role. E.g. for ribose in adenosine, a "shared acidity" of the vicinal *cis*-diol with a pK_a of about 12.5 is reported.[69]

During the methylation process reported here, the pH of the aqueous solution was hold constant at 13.6 by addition of NaOH-solution over the course of the reaction. CH_3I was applied in access and the reaction mixture was vigorously stirred to bring the KGM and the alkylating agent in good contact. Aliquots were taken after various reaction times (1, 5, 10, 22, 48 hours), and the residual portion was quenched after 54 hours.

To check the progress of methylation of KGM, ATR-IR spectra were recorded. For better comparison, all IR spectra, shown in Figure 3.2, were normalized to the most intense absorption band at 1020 cm^{-1} (C-O). The shift of the characteristic hydroxyl stretching vibration peak for sugars at 3400-3200 cm^{-1} (-OH) to higher wave numbers due to decreasing possibilities of hydrogen bond formation between OH when methylation proceeds was considered as a convenient tool to monitor the degree of methyl substitution in KGM.

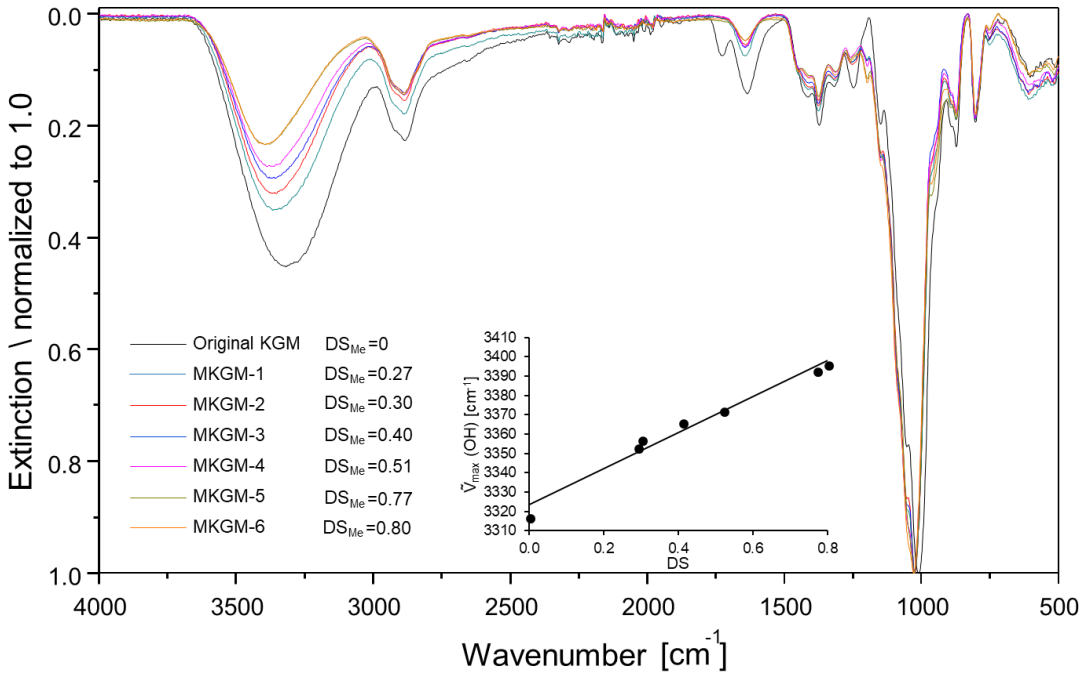

Figure 3.2. ATR-IR spectra of KGM and M-KGM-1 – M-KGM-6 obtained by methylation in aqueous NaOH/CH_3I (pH=13.6) after different reaction times. The lines are in the order of decreasing OH absorption at 3320-3400 cm^{-1} for M-KGMs, i.e. with increasing DS. The DS values were determined by AAM of corresponding EM-KGM. Inset: Correlation between the DS and the $\tilde{\nu}_{max}$ of ν(OH) in M-KGM.

In the insertion in Figure 3.2, the maximum wavenumber of OH absorption is plotted against the corresponding DS values of M-KGMs. For the DS range of up to 0.80 considered here, the increase of $\tilde{\nu}_{max}$ of ν(OH) with DS value is quasi linear, allowing an estimation of the average DS in this range. The absorption band at 1727 cm^{-1} probably indicating tiny amounts of carbonyl ester groups was only observed in the original KGM. Under the strong alkaline conditions of methylation, acetates present in native KGM were saponified.

After depolymerization of M-KGM or EM-KGM, the quantities of the differently methylated sugar units were calculated from the peak areas of the corresponding derivatives in the GLC.

The quantities of the different methylated sugar units were calculated from the peak areas of the corresponding derivates in the GLC. In this study, the detector connected with GLC is flame ionization detector (FID), the number of carbon atoms and their neighbors in glycose derivatives must be considered for the response of the FID. The contribution of a carbon is reduced when bound to a more electronegative atom, such as O or O(C=CO)R. The effective carbon response (ECR) can be calculated from experimental data for certain structural features. Thus, the relative molar composition of the constituents in all GLC quantification evaluation can be determined after correction of the peak areas by the ECR concept.[45,70]

From the analysis of a fully-methylated KGM, 62.7% of *O*-methyl-mannitol acetates and 37.3% of *O*-methyl-glucitol acetates were detected and the ratio of M and G thus 1.68 (M-KGM-7, see Table 9.8 in appendix). This result was in good agreement with the data provided by the KGM supplier (M : G = 1.6 : 1). Other than 2,3,6-methyl patterns were only detected in very tiny amounts (< 0.3 mol%) with no preference for any particular pattern and thus interpreted as arising from incomplete methylation. Therefore, the original KGM was considered as a linear polymer.

To determine the substituent distribution in the M-KGM from the time course study, the polysaccharide transformed to proper monosaccharide derivatives for GLC analysis. Various methods can be applied for the depolymerization step which is catalyzed or promoted by Brönsted or Lewis acids. In the latter case, full protection of all OH is a prerequisite, but also for hydrolysis or methanolysis, protection of free OH by perethylation will improve the accuracy of the results since discriminating side reactions are reduced. As shown in Scheme 3.1, M-KGM samples were analyzed by methanolysis and acetylation (MeOH-Ac) and methanolysis and trimethylsilylation (MeOH-TMS), while EM-KGM samples were analyzed by alditol acetate method (AAM), reductive cleavage and acetylation (RCM-Ac) and reductive cleavage followed by benzoylation (RCM-Bz).

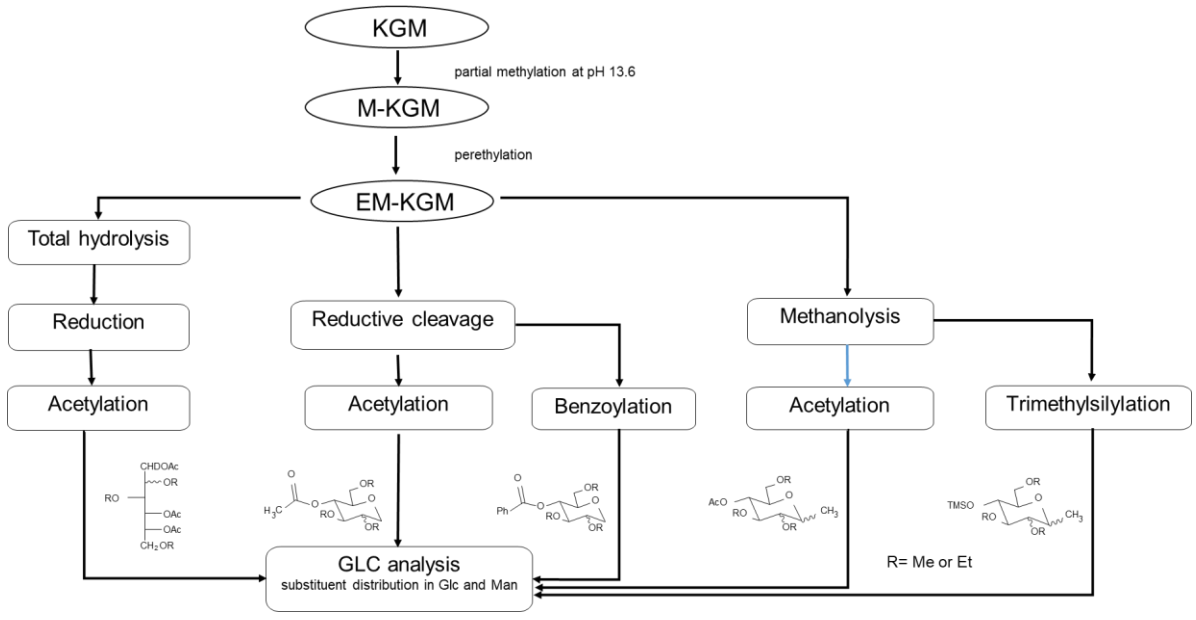

Scheme 3.1. Procedures applied to the analysis of methyl patterns in M-KGM or after perethylation: alditol acetate method, reductive cleavage and methanolysis.

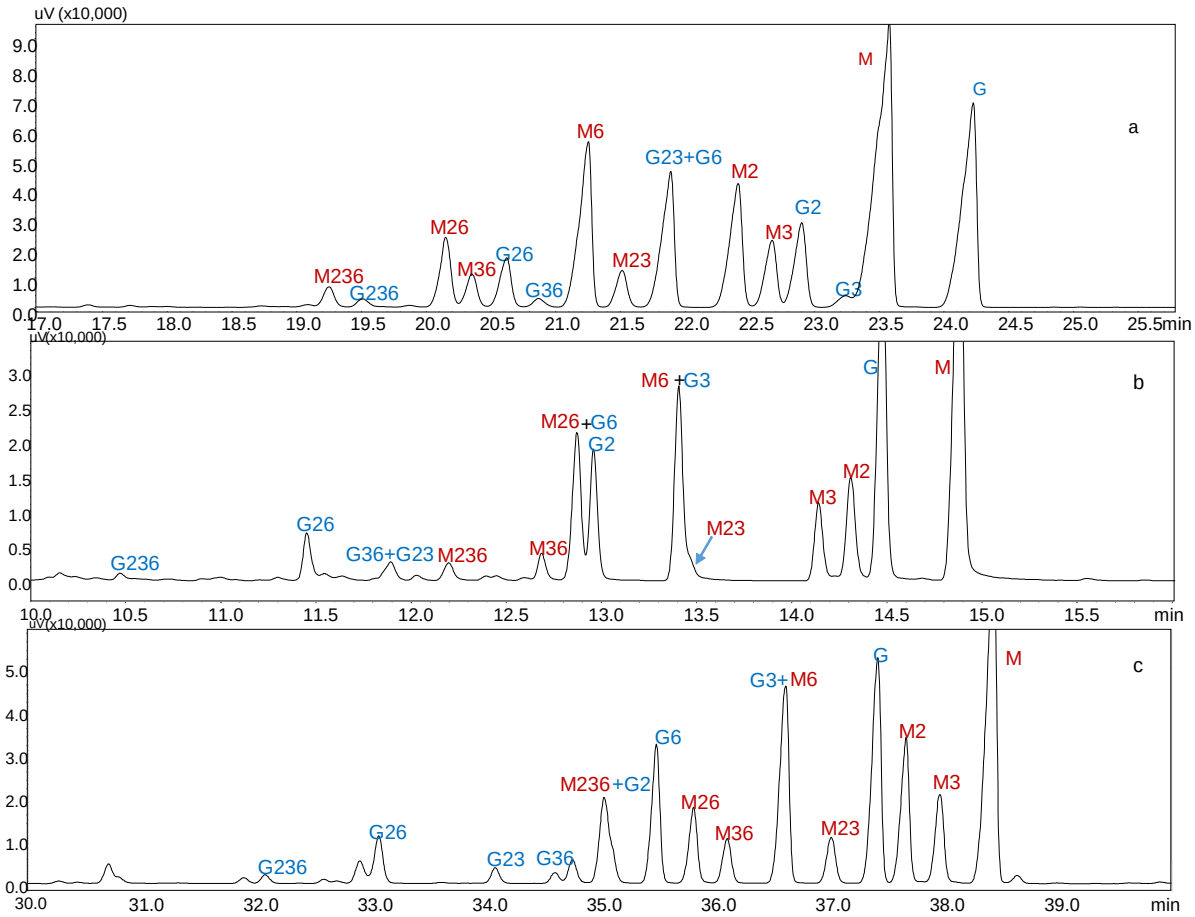

Figure 3.3. Gas chromatograms of EM-KGM-6 (DS 0.80); (a) alditol acetates, (b) reductive cleavage and acetylation, (c) reductive cleavage and benzoylation. Peaks from glucose (G) and mannose (M) are assigned according to the methylated position.

The gas chromatogram of EM-KGM-6 of *O*-ethyl-*O*-methyl alditol acetates is shown in Figure 3.3a. To distinguish the stereoisomers (mannitols and glucitols), standards of alditol acetates from *O*-ethyl-*O*-methyl cellulose and corresponding β-1,4-mannan were prepared and co-injected and submitted to GLC-MS. The corresponding mass spectra is referred to thesis of Kristin Voiges.[71] Positions of ethyl and methyl groups can be easily located due to characteristic shifts of *m/z* of primary and secondary fragments with respect to the well-known spectra of partially methylated alditol acetates.[43] Only 6-*O*-ethyl-2,3-di-*O*-methyl-glucitol and 2,3-di-*O*-ethyl-6-*O*-methyl-glucitol were not separated (indicated by G_{23}+G_6 in Figure 3.3a). However, the ratio of these components could be calculated from the areas of the corresponding peaks of 1,5-anhydro-4-*O*-benzoyl-alditols (prepared by reductive cleavage and subsequent benzoylation, as shown in Figure 3.3c, corresponding mass spectra are listed in appendix).[42] On the other hand, the overlapping peaks presented in Figure 3.3c (indicated by M_{236}+G_2 and G_3+M_6) can be differentiated by the ratio of corresponding peak areas in Figure 3.3a. In addition, as shown in Figure 3.3b, the portions of overlapping peaks of

anhydro-alditol acetates can be deduced from the ratios of the corresponding benzoyl derivatives (as shown in Figure 3.3c), i.e., 2-*O*-ethyl-3,6-di-*O*-methyl-glucosyl and 6-*O*-ethyl-2,3-di-*O*-methyl-glucosyl (indicated by G_{36}+G_{23}), 3-*O*-ethyl-2,6-di-*O*-methyl-mannosyl and 2,3-di-*O*-ethyl-6-*O*-methyl-glucosyl (indicated by M_{26}+G_6), 2,3-di-*O*-ethyl-6-*O*-methyl-mannosyl and 2,6-di-*O*-ethyl-3-*O*-methyl-glucosyl (indicated by M_6+G_3).

By methanolysis of M-KGM, methyl α- and β-pyranosides of mannose and glucose are obtained, respectively. Since eight substitution patterns are possible for each monosaccharide (M and G), 16 substitution patterns (i.e. up to 32 peaks) could be observed in GLC analysis. The chemical similarity of mannosyl and glucosyl units caused some overlapping of peaks, which made the complete evaluation of all components more difficult. In the case of the acetylated methyl glycosides, five unresolved peak pairs were observed which concern ten constituents (as shown in Figure 3.4a), while three overlapping peak pairs (G36+M3, M6+G26, M+G2) are observed in the case of TMS derivatives (as shown in Figure 3.4b). Therefore, the two derivatizations were necessary to calculate the ratio of non-resolved constituents from the information of the other type of derivative for which fortunately those peaks were separated. Since in the case of acetylated derivatives the peaks of the most relevant 2- and 3-*O*-methyl mannosides were fully separated, these data are used and the ratio of non-separated peaks (α-G2 and α-G3, α-G6 and β-M6, α-G23 and α-M23, and β-G23 and α-M26; G = Glucose, M = Mannose, number = position of methylation) were taken from the GLC evaluation of the TMS derivatives.

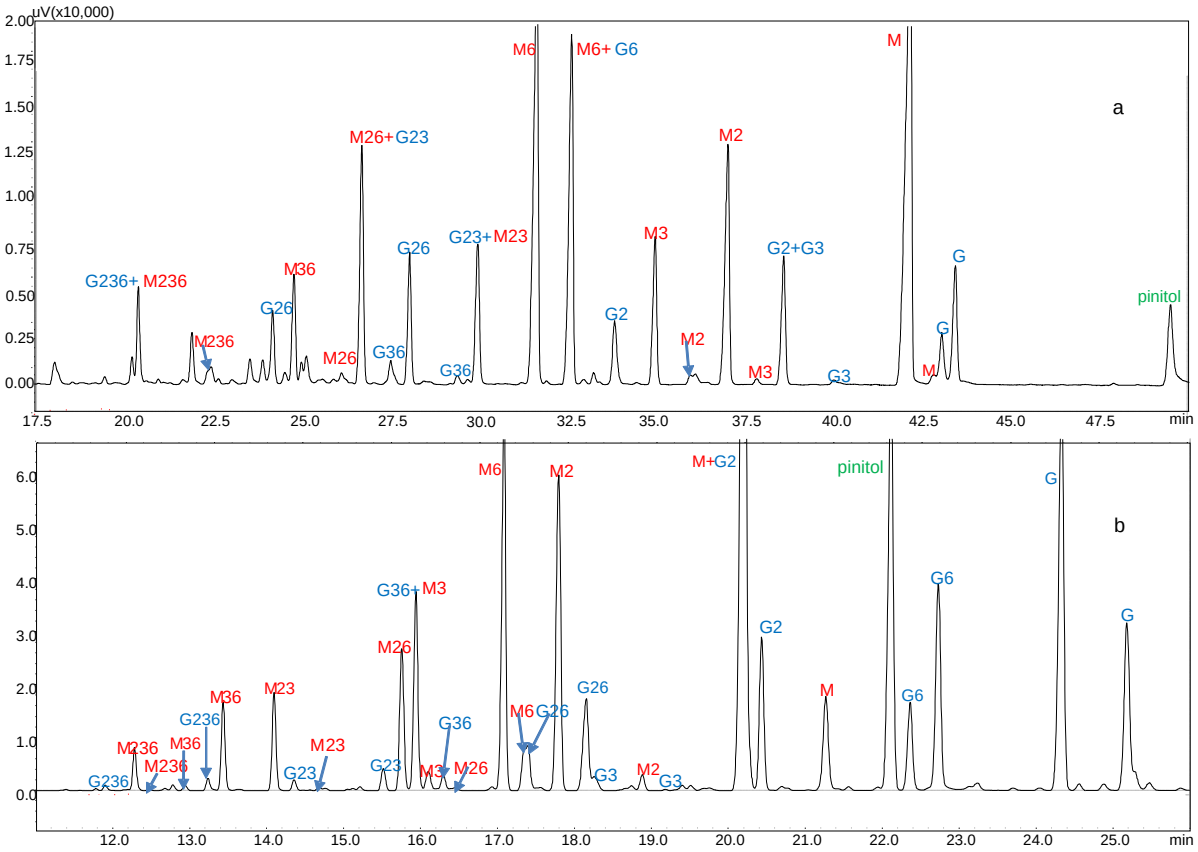

Figure 3.4. Gas chromatograms of M-KGM-6 after methanolysis and acetylation (a), and after methanolysis and trimethylsilylation (b). The DS of M-KGM-6 is 0.80 determined by MeOH/H^+/Ac, the peaks from glucose (G) and mannose (M) are assigned according to the methylated position.

To distinguish the epimers (α- and β-glucosides and mannosides, respectively), corresponding derivatives derived from *O*-methyl cellulose and *O*-methyl mannan were prepared and submitted to GLC-MS. The corresponding mass spectra are listed in appendix. Positions of methylation were deduced from the mass spectra recorded by GLC. It has to be pointed out that the equilibrium ratio of α- and β-glycosides depends on pH and solvent and thus also from the work-up procedure (during evaporation of methanolic HCl and subsequent co-distillation these conditions change). Thus, methanolysis and subsequent acetylation of one portion and trimethylsilylation of the other should be in parallel (i.e. substrate of acetylation and trimethylsilylation came from the same residue of methanolysis).

From the corrected peak areas, the relative molar composition (mol%) of EM-KGM samples with respect to mannose and glucose substituted at position *i* (s_i), molar fraction in % of *i*-fold substituted monomer units (c_i), partial DS-values x_i for individual hydroxyl group in position *i*, and total DS were calculated and listed in Table 3.1 (determined by AAM). The data obtained by the other four methods are listed in Table 9.1 - 9.6 in appendix. Data were compared with the random model of Spurlin.[73] An average heterogeneity parameter H_1 was calculated to

show the deviation of the experimentally determined distribution from the statistical model:[74]

$$H_1=\sqrt{\frac{\sum(si(exp.)-si(calc.))^2}{8}} \qquad (3.1)$$

The H_1 values for the individual EM-KGM and M-KGM samples are also listed in the corresponding Tables, just mentioned. For better comparison, the molar compositions of mannosyl units and glucosyl units of each EM-KGM was normalized to 100 %, independently.

Table 3.1. Relative molar composition (mol%) of EM-KGM regarding the glucose and mannose substituted at position i (s_i), molar fraction of i-fold substituted monomer units (c_i), partial DS-values x_i for individual hydroxyl groups in position i, and total DS. Data are independently normalized for both glucose and mannose (n=3). Sample preparation parameters are described at 7.3.1 and derivatization methods are described at 7.4.1.

Me in position	**M-KGM-1**		**M-KGM-2**		**M-KGM-3**		**M-KGM-4**		**M-KGM-5**		**M-KGM-6**	
	Man	Glc	Man	Glc	Man	Glc	Man	Glc	Man	Glc	Man	Glc
s_0	75.94±0.05	76.28±0.02	72.85±0.05	73.79±0.60	65.32±0.74	68.06±0.05	57.62±0.10	58.60±0.92	41.25±0.18	43.50±0.21	39.59±0.38	41.75±0.31
s_2	7.50±0.14	8.42±0.02	8.34±0.04	9.02±0.09	9.66±0.22	10.60±0.31	11.84±0.06	13.80±0.33	14.36±0.10	15.39±0.06	14.79±0.04	15.80±0.05
s_3	4.21±0.08	0.79±0.17	4.56±0.09	1.18±0.02	5.22±0.22	1.43±0.04	5.73±0.09	1.73±0.38	7.24±0.07	1.94±0.20	7.35±0.07	2.30±0.33
s_6	9.80±0.23	11.62±0.02	10.56±0.07	12.76±0.31	13.05±0.04	15.17±0.33	15.43±0.04	18.09±0.09	19.05±0.08	23.36±0.06	19.54±0.07	23.67±0.10
s_{23}	0.52±0.01	0.52±0.00	1.09±0.01	0.60±0.01	1.49±0.00	0.78±0.02	2.12±0.03	1.63±0.01	4.12±0.04	2.82±0.01	4.27±0.09	2.88±0.01
s_{26}	1.44±0.00	1.75±0.03	1.61±0.02	2.01±0.18	2.72±0.31	3.16±0.13	4.19±0.14	5.19±0.14	7.72±0.06	9.41±0.11	8.07±0.09	9.84±0.12
s_{36}	0.59±0.03	0.61±0.12	0.99±0.04	0.64±0.22	1.73±0.20	0.81±0.10	2.09±0.16	0.96±0.05	3.64±0.03	1.74±0.01	3.78±0.08	1.78±0.06
s_{236}	0.00±0.00	0.00±0.00	0.00±0.00	0.00±0.00	0.81±0.20	0.00±0.00	0.99±0.03	0.00±0.00	2.62±0.20	1.84±0.11	2.60±0.11	1.98±0.13
c_0	75.94±0.05	76.28±0.02	72.85±0.30	73.79±0.60	65.32±0.74	68.06±0.05	57.62±0.10	58.60±0.92	41.25±0.18	43.50±0.21	39.59±0.38	41.75±0.31
c_1	21.51±0.01	20.83±0.17	23.46±0.26	22.96±0.20	27.93±0.04	27.20±0.09	32.99±0.19	33.63±0.73	40.65±0.22	40.69±0.09	41.69±0.07	41.77±0.18
c_2	2.55±0.04	2.89±0.15	3.69±0.04	3.25±0.41	5.94±0.51	4.74±0.12	8.40±0.26	7.78±0.20	15.47±0.12	13.98±0.12	16.12±0.26	14.50±0.18
c_3	0.00±0.00	0.00±0.00	0.00±0.00	0.00±0.00	0.81±0.20	0.00±0.00	0.99±0.03	0.00±0.00	2.62±0.20	1.84±0.11	2.60±0.11	1.98±0.13
H_1	1.15	0.56	0.47	0.43	0.91	0.49	1.02	0.74	1.08	1.36	0.91	1.24
x_2	0.09±0.1%	0.11±0.0%	0.11±0.0%	0.12±0.0%	0.15±0.7%	0.15±0.0%	0.19±0.0%	0.21±0.0%	0.29±0.0%	0.29±0.0%	0.30±0.0%	0.30±0.0%
x_3	0.05±0.0%	0.02±0.1%	0.07±0.0%	0.02±0.0%	0.09±0.2%	0.03±0.0%	0.11±0.2%	0.04±0.0%	0.18±0.0%	0.08±0.0%	0.18±0.2%	0.09±0.0%
x_6	0.12±0.3%	0.14±0.2%	0.13±0.0%	0.15±1.0%	0.18±0.7%	0.19±0.0%	0.23±0.0%	0.24±0.0%	0.33±0.0%	0.36±0.0%	0.34±0.0%	0.37±0.0%
M/G ratio	1.63		1.69		1.61		1.60		1.68		1.68	
DS_M and DS_G	0.27	0.27	0.31	0.29	0.42	0.37	0.53	0.49	0.79	0.74	0.82	0.77
DS_{KGM}	0.27		0.30		0.40		0.51		0.77		0.80	

Before discussing the methyl substitution in M-KGMs, the accuracy of the monomer analysis methods needs to be considered. Due to the free OH groups in M-KGMs which were not methylated in first methylation process, some side reaction might happen during the hydrolysis and subsequent work-up. Therefore, the fully ethylated M-KGMs are more suitable for constituent analysis. Furthermore, from the literature and the information from the KGM supplier, the ratio of M and G is around 1.6, which could be used as a judgement tool (AAM, RCM-Bz and MeOH-TMS obtained M/G ratio around 1.65). However, the MeOH-TMS yields at least double number of products which are not fully separated in GLC. This made the evaluation complicated. Above all, the alditol acetate and reductive cleavage method with subsequent benzoylation were found to give the most reproducible and plausible results. Therefore, we choose the results obtained from AAM for relative rate constants of OH groups in KGM for further discussion, and the results from the other four methods are presented as well in the appendix.

Average DS_{KGM} values of M-KGM were in the range of 0.3 - 0.8. In general, the individual DS of mannose was slightly higher than that of glucose. Similar to commercial MCs which are prepared after activation with aqueous NaOH, the most acidic 2-OH and the primary OH at C-6 are strongly favoured in both glucose and mannose residues. While commercial MCs with DS about 1.9 usually show a slightly larger partial DS in position 2, methylation of 6-OH clearly dominates in KGM in aqueous solution at pH 13.6. In contrast, in the methylation of SGM with Li-dimsyl/CH_3I in DMSO, order of reactivity was $2 > 3 > 6$ for glucose and $3 > 2 > 6$ for mannose.[61] For CM-GGM with the average DS 0.7, prepared in water/isopropanol, Xu et al. reported the CM-distribution on O-2, O-3 and O-6 to be 27, 15, and 58% for glucose and 35, 20 and 45% for mannose.[62] This preference of the primary OH, followed by positions 2 and 3 corresponds with our results.

According to the above mentioned random model of Spurlin[73] the relative reactivity of different hydroxyl groups (at C-2, C-3 and C-6) should remain constant over the course of the reaction, as long as the glycosyl units are equally accessible and primary substitution does not influence subsequent reactions. Therefore, the relative reactivity constants k_i can be obtained from a logarithmic plot when these requirements are fulfilled. A linear relationship with a slope corresponding to the relative reactivity constant k_i is presented in Figure 3.5. Instead of time, the decrease in the unsubstituted glucosyl (or mannosyl) units $-\ln c_0$ was taken as the reaction coordinate. For better comparison of the relative reactivities between glucose and mannose, it is necessary to use the same reaction coordinate. Therefore, the average c_0 of

EM-KGMs (M/G=1.68) was taken instead of the c_0 of individual glucose and mannose. As shown in Figure 3.5, by alditol acetated methods, the relative reactivities for glucose and mannose followed the order G-k_6 > M-k_6 > G-k_2 ≈ M-k_2 > M-k_3 > G-k_3 with the ratio 5.5 : 4.9 : 4.2 : 4.1 : 2.3 : 1.0. Same order was obtained by other four analysis methods as shown in Figures 3.6 and 3.7.

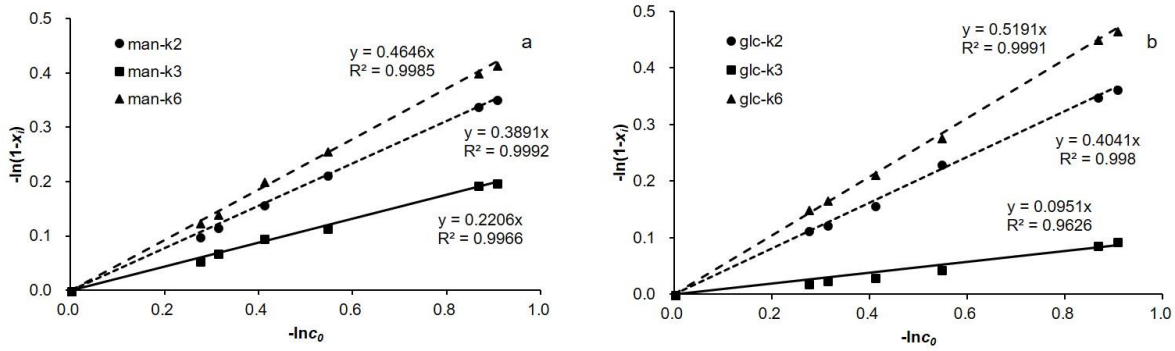

Figure 3.5. Relative rate constants k_2 , k_3 , and k_6 calculated independently for mannose (a) and glucose (b) for the methylation time course study; data from ethylation analysis of M-KGM-1 – M-KGM-6 by alditol acetate method (AAM).

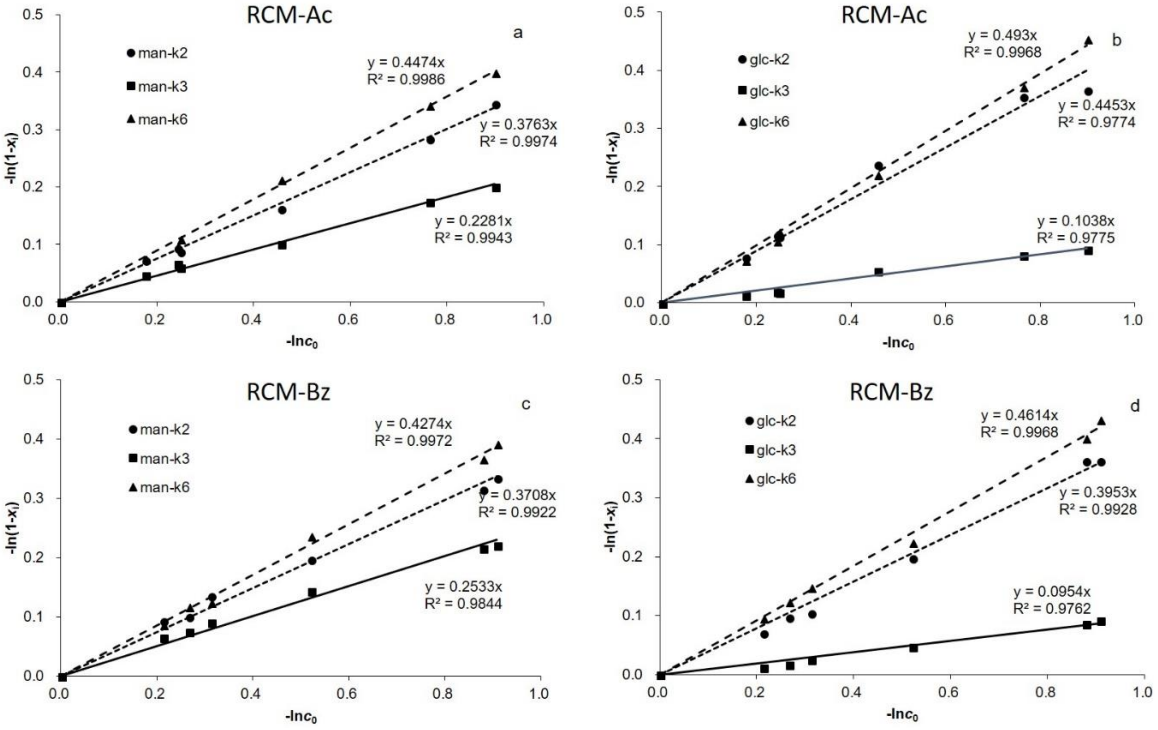

Figure 3.6. Relative rate constants k_2 , k_3 , and k_6 calculated independently for mannose (ac) and glucose (bd) for the methylation time course study; data from methylation analysis of M-KGM-1 – M-KGM-6 by reductive cleavage and subsequent acetylation or benzoylation (RCM-Ac / RCM-Bz).

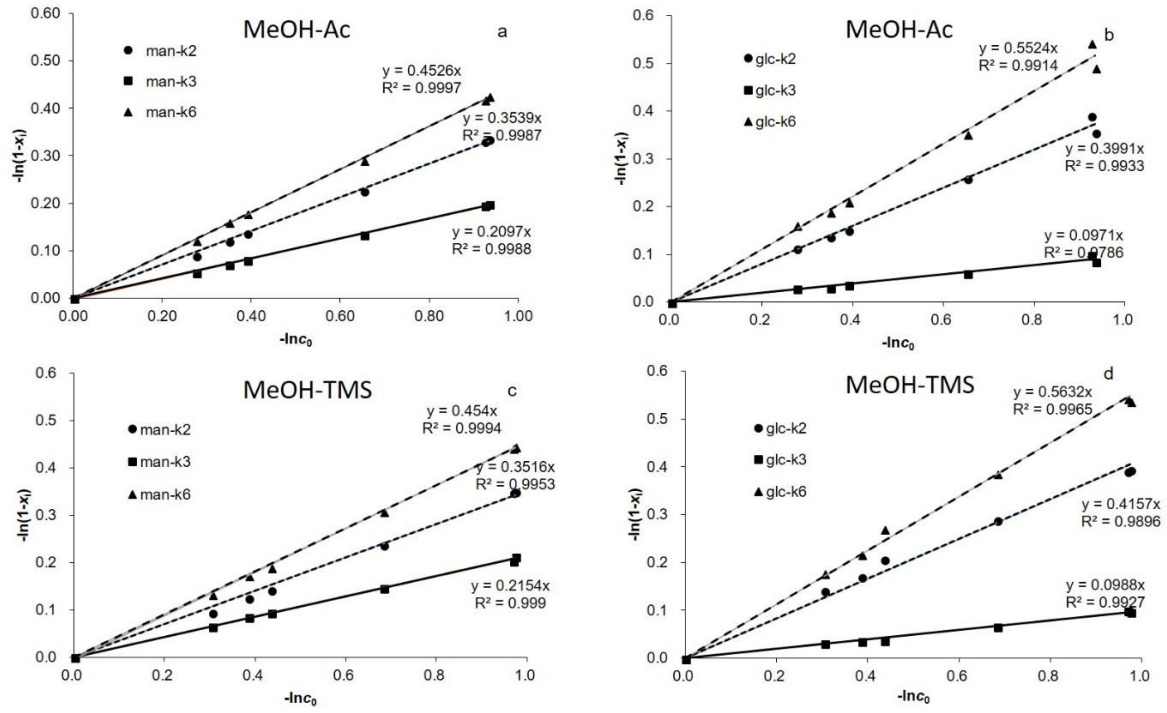

Figure 3.7. Relative rate constants k_2 , k_3 , and k_6 calculated independently for mannose (ac) and glucose (bd) for the methylation time course study; data from methylation analysis of M-KGM-1 – M-KGM-6 by methanolysis and subsequent acetylation or trimethylsilylation (MeOH-Ac / MeOH-TMS).

While relative rate constants for 6-OH and 2-OH only show a slight difference for G and M, the secondary 3-OH were least reactive with a pronounced preference for Mover G (about 2.3:1, data from AAM). This means that 3-OH profits from acidity of 2-OH by the *cis*-relationship of these two secondary OH in M units. The highest reactivity at 6-OH in both glucose and mannose are a result of their acidity[75] coupled with lower steric requirements of a primary OH. De Belder et al. partially methylated β-D-glucopyranoside in the system $NaOH/Me_2SO_4/H_2O$ and reported the relative rates to be $k_2 : k_3 : k_4 : k_6 = 4 : 1 : 0.5 : 4$.[76] With $k_2 : k_3 : k_4 : k_6 = 7.3 : 1 : 3.1 : 12$, Norrman reported larger differences for methyl β-D-glucopyranoside.[77] Based on studies on the selectivity of methylation of methyl α-D-manno-pyranoside, in the Haworth system ($NaOH/Me_2SO_4/H_2O$), Handa et al. determined the ratio of substitution for the positions 2, 3, 4, and 6 to be 2.5 : 1.8 : 1 : 3.2. [60] The results from this study are similar to that cited above.

For mannosyl residues in KGM, the relative reactivity of O-3 remained unaffected with increasing methylation of O-2, while, however, for glucose it increased. Thus, the equatorial 3-OH in glucose residues seemed to profit from the methylation of the equatorial 2-OH what is not known for cellulose. But the correlation coefficient R^2 for rate constant calculation is only 0.96 in this case, while all others are above 0.99 (Figure 3.5b). However, methyl

celluloses in this low DS range are uncommon and thus no data are available for direct comparison. It should be mentioned that such a tendency has been reported in some older work.[76,78] Under the conditions of Haworth methylation, k_3 of glucosides was doubled when 2-OH was substituted.[76] Furthermore, 4-*O*-methyl-β-D-xylopyranoside (which has the same *trans*-2,3-diol configuration as glucose) was found to enhance the reactivity of 3-OH three times after methylation of 2-OH, while methylation of 3-OH did not alter the reactivity of 2-OH.[78] These results are, however, questionable since the data at that time were obtained gravimetrically after preparative isolation of the products from partial methylation.

The reaction system plays an important role for the relative reactivities of different hydroxyl groups in polysaccharides. In the aqueous system, during the overnight dissolving process, KGM was very well swollen, and after addition of NaOH, it was clearly dissolved. Water can well solvate ROH and RO^- as well. Thus, the deprotonated OH groups can act independently as nucleophiles. While at the amount of base applied the differences in acidity were no longer relevant for 2- and 6-OH, the sterically less hindered primary group can attack the nucleophile at the highest rate. In contrast, in DMSO/Li-dimsyl methylation of SGM preferentially happened at the secondary 2,3-diol side.[61] Since the aprotic solvent cannot stabilize anions, the $2\text{-}O^-$ will interact with the vicinal 3-OH and vice versa. For 6-OH no such neighbor effect is possible and thus perhaps therefore, the deprotonation less favored.

In summary, different regioselectivities were detected for glucose and mannose of M-KGMs in the aqueous methylation system. While the primary 6-OH exhibited overall highest reactivity with only slight preference for the glucosyl residues, secondary OH showed pronounced differences. The axial OH at C-2 in mannose mainly affected 3-OH resulting in a 2.3 times larger rate constant in this position compared to glucose. This means, that the degree of methylation at O-3 will vary along the chain in accordance with the distribution of mannosyl and glucosyl residues. In cellulose, this regiospecific degree of methylation is of great importance for the properties. Moreover, methylation at position O-3 impairs chain-stiffening by intramolecular hydrogen bonds between 3-O-H and the neighbored ring oxygen O-5' for both glucose and mannose.[79,80] In G-G and G-M diades, additional O-2'···H-O-6 and 2'-O-H···O-6 hydrogen bonds make the glycoside less flexible compared to M-M and M-G, which can only undergo this interaction in an alternative much less prominent conformation.[80] At the same time, 3-*O*-methylation in MC accelerates hydrolysis[52] and reduces the temperature of thermogelation.[81] Thus, it is of interest, how these higher *O*-methylated hexopyranosyl residues are distributed in the macromolecular dimension.

3.2.2 Oligomer analysis

3.2.2.1 Methyl distribution over the macromolecules

In order to find out, whether the partially *O*-methylated glucosyl and mannosyl units in M-KGMs are distributed randomly over the macromolecules, we analyzed the methyl pattern in oligomeric hydrolysis products. Therefore, M-KGM was fully alkylated with CH_3I-d_3 and then partially hydrolyzed to gluco-manno-oligosaccharides, according to an approach usually applied in order to determine heterogeneities in cellulose ethers by mass spectrometry.[82] This strategy compares the methyl pattern of oligomeric domains with the methyl distribution that is calculated from the monomer composition determined as described above. To obtain a representative mixture of oligosaccharides, hydrolysis must proceed at rather equal rate. This is, however, not the case for mannosyl and glucosyl linkages. Due to angle-dependent field effects axial OH have a less destabilizing effect on intermediate oxocarbenium ion and thus reduces the energy of the preceding transition state compared to an equatorial OH at the same position.[83] Depending on the conditions, rate constant for the cleavage of 1,4-β-M-M linkages is about twice *k* for hydrolysis of corresponding G-G and G-M linkages[84,85] and therefore probably also for M-G, respectively, since both sugars are comparable leaving groups.[85] Assuming similar differences of rate constants for the perdeuteromethylated M-KGM one can estimate that in case of randomly distributed M and G, this will only cause a slight preference of M at the reducing end of generated oligosaccharides. The ratio of M/G will thus decrease with DP, and depending on the degree of hydrolysis, the point of interception with the average M/G ratio (1.68) might even slip between DP 1 and DP 2 with the consequence of underestimation of M in all oligomers. However, since only the terminal residue is concerned, this selectivity is leveled with increasing DP.

Thus, *O*-methyl KGMs were perdeuteromethylated (DM-KGM), partially hydrolyzed, labeled by reductive amination with *meta*-aminobenzoic acid (*m*ABA), and subsequently analyzed in negative mode by means of LC-ESI-MS or direct syringe pump infusion. The three UV chromatograms of the labeled Me/Me-d_3-gluco-manno oligosaccharides and Me/Me-d_3-cellooligomers and Me/Me-d_3-mannooligomers (standards for peak assignment in DM-KGM) are presented in Figure 3.8a, b, and c, respectively. For the cello- and manno-oligosaccharides, a clear oligomer pattern with decreasing intensity with DP is observed. The oligosaccharides from DM-KGM gave a more complex pattern. Due to increasing complexity of possible G-M ratios and sequences with increasing DP, peaks overlap in the chromatogram. By generation of extracted ion chromatograms (EIC) for the *m/z* range of a particular DP, however, sets of oligosaccharides can be separated with respect to DP. By co-injection with the homo-

oligosaccharide standards the retention time of these uniform oligomers can be assigned and in case of no coincidence of a particular peak, its absence can be proved.

Thus, the most abundant oligosaccharides obtained by partial hydrolysis must be mixed oligomers G_mM_n. For DP 2, the four possible combinations, MM, MG, GM, and GG, could be differentiated by HPLC (Figure 3.8a). For DP 3, beside M_3 and G_3 already six mixed oligomers exist (3 M_2G, 3 MG_2), each with various Me/Me-d_3-patterns, which are no longer fully separated. However, as mentioned above, from EIC elution times all constituents belonging to a distinct DP can be recognized. From the LC-ESI-MS runs all signals belonging to a particular DP, i.e. those with the same *m/z*, were summarized and the methyl profile evaluated (Figure 3.8). From the sum of c_i (M) and c_i (G) for the entire sample, normalized to 100% (see Table 3.1, EM-KGM-6, DS 0.80), the substituent patterns of the oligomers for a random distribution of all glycosyl units, making no difference between glucosyl and mannosyl residues, was calculated.

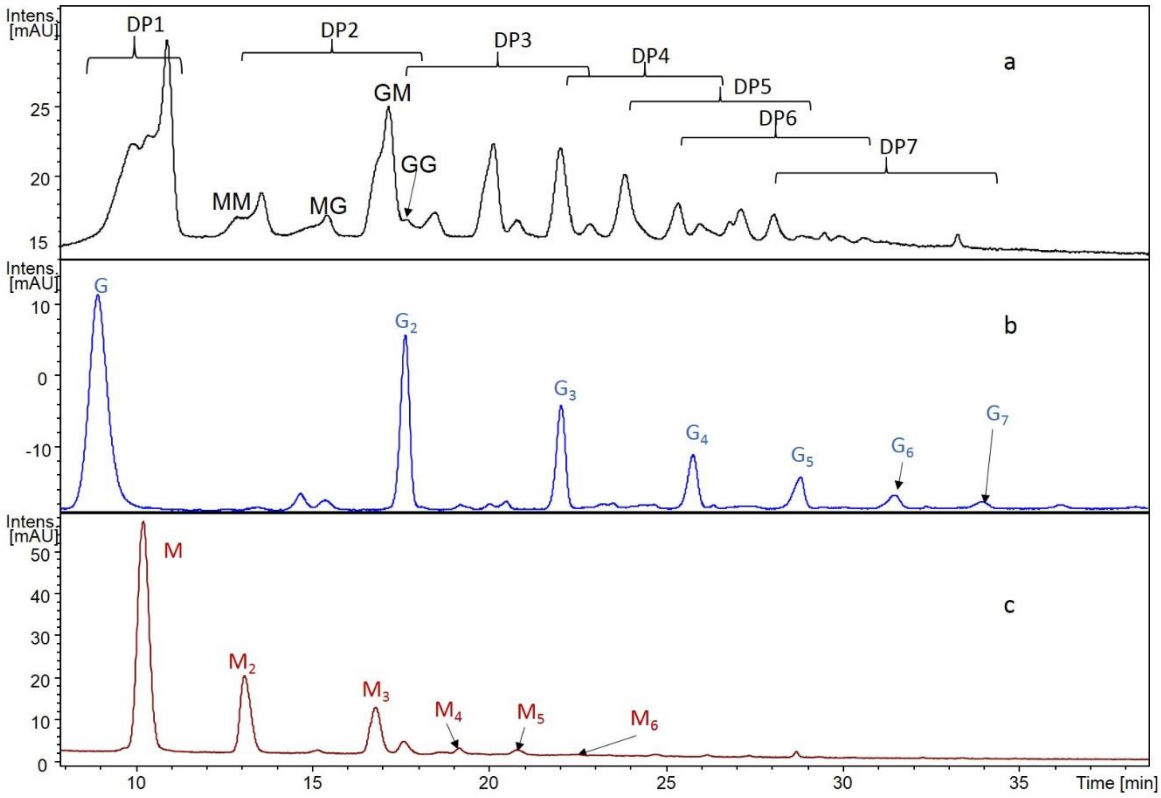

Figure 3.8. HPLC/UV chromatograms (330 nm) of DM-KGM-6 (a), DM-cellulose (b) and DM-mannan (c), partially hydrolyzed and labeled with *m*ABA, using ACN/H_2O/HOAc as mobile phase on RP C_{18}.

In LC-MS of DM-KGM oligomers, the DS evaluated for each DP should match the average DS of the whole KGM, if the cleavage of DM-KGMs had occurred in a random manner (with respect to the methyl pattern in the glycosyl units). The deviation of calculated and

experimental profiles is expressed by the heterogeneity parameter H_i with i = DP.[82] In Figure 3.9, both the calculated and the experimentally determined distribution curves for DP 2 – DP 7 of DM-KGM-6 are shown. For all these oligomer fractions, a nearly perfect coincidence of experimental data and the model curve was observed. DS/DP is between 0.79 and 0.82 and thus representative for the entire material. H_i values are all below 1.0 and thus very small. This means that the non-, mono-, di- and trisubstituted glycosyl units are distributed randomly over and along the macromolecules. The same agreement with a random model was observed for the other M-KGMs of the time course study.

It should be pointed out, that the random model was calculated assuming random hydrolysis which is not fully the case as outlined above. But since the fractions of non-, mono-, di- and tri-substituted sugars do not differ significantly for glucose and mannose and the DS of the mannose part is only about 5% higher than the DS of the glucose fraction, no significant impact on a slight overrepresentation of mannose on DS and methyl profile is expected.

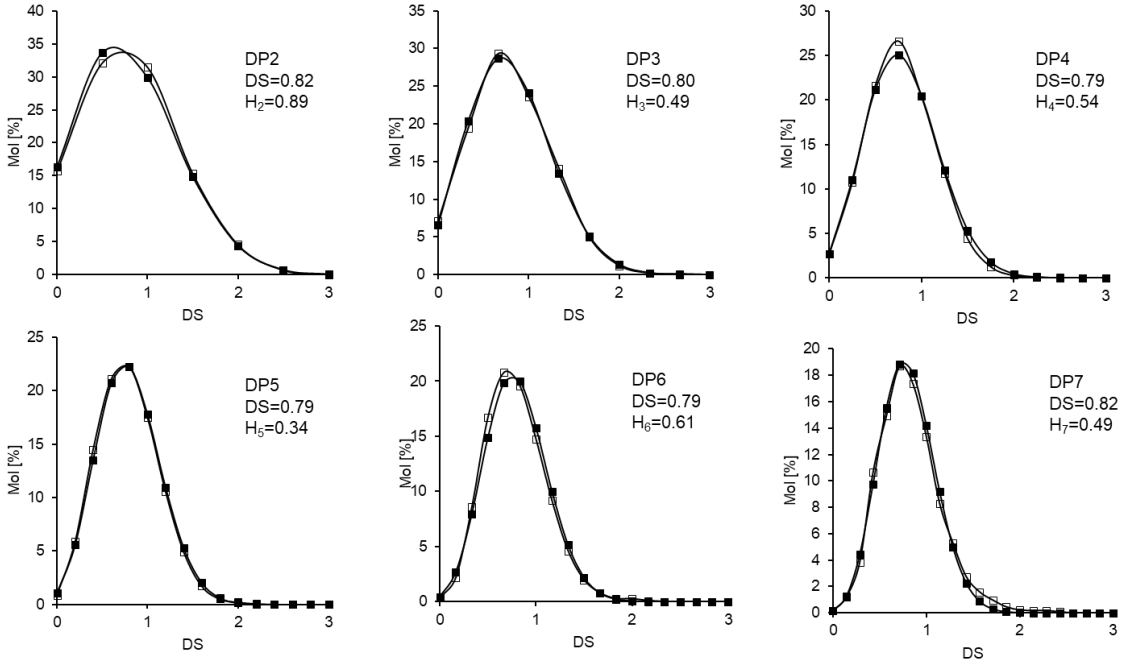

Figure 3.9. Comparison of random (■) and experimentally determined methyl pattern (□) in DP 2 - 7, evaluated from LC-ESI-MS data of DM-KGM-6 (DS_{KGM} = 0.80).

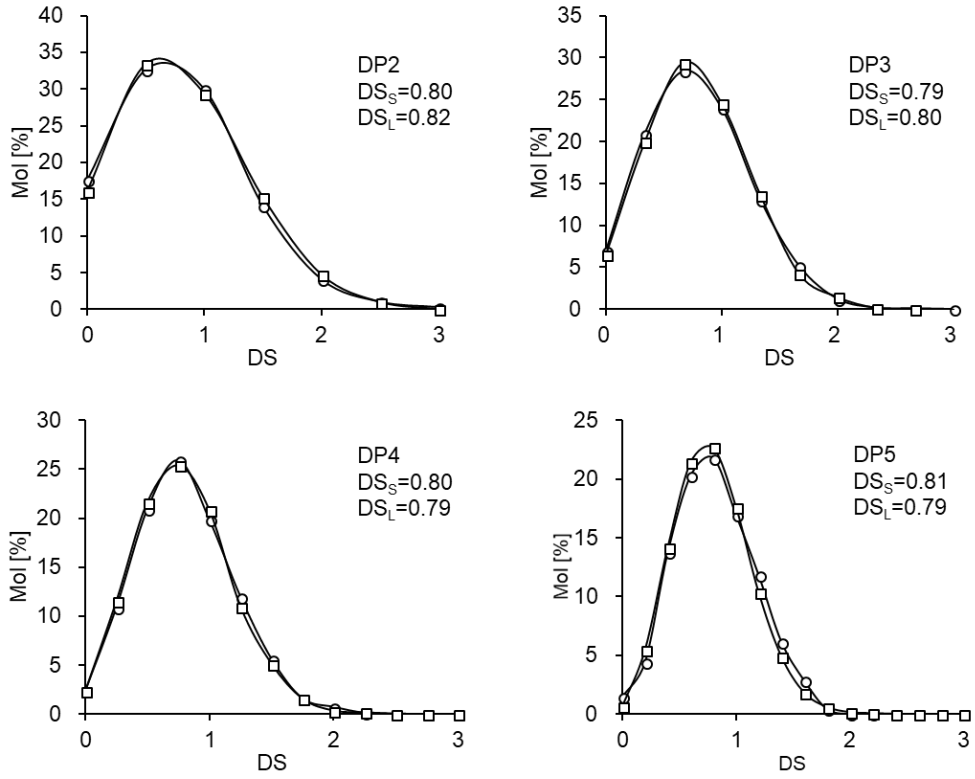

Figure 3.10. Comparison of experimentally determined methyl pattern in DP 2 - 5, evaluated from LC-ESI-MS data (□), and from syringe pump infusion data (○), respectively, of DM-KGM-6 (DS_{KGM} = 0.80). DS values obtained from syringe pump infusion (DS_S) and from LC-MS (DS_L) are presented.

Figure 3.10 shows the comparison of experimentally determined methyl pattern in DP 2-5 of DM-KGM-6, evaluated from LC-ESI-MS data with those from direct syringe pump infusion data, respectively. Results from both sample application methods are in perfect to good agreement. The slight deviation for DP 5 can be explained by the lower intensity for higher DP in syringe pump infusion. Change eluent composition during the gradient HPLC run, might also influence the solvent-dependent ion yields in the ESI process.[82] Nevertheless, due to the similar DS in M and G residues in KGM (DS_{KGM}=0.80, DS_M=0.82, DS_G=0.77), differences with respect to M and G cannot be recognized. The deviating behavior for M-KGM with different DS of G and M is discussed in Chapter 4).

But does this also implicate that also glucose and mannose are distributed randomly in KGM? To check whether the slight differences of non-, mono-, di- and tri-substitution of Man and Glc (see Table 3.1) allows a differentiation of their distribution in the macromolecule, the methyl profile for a di-block-copolymer of methylglucan and methylmannan was calculated for a mixture of M/G ratio of 1.68 (Figure 3.11). This model represents the extreme case, considering mannan and glucan as uniform blocks. The methyl profiles for DP 2 - DP 7 of DM-KGM-6 as a di-block-copolymer are compared with the experimentally found patterns in

Figure 3.11. Obviously, no pronounced differences exist between the di-block model and experimental results neither. In spite of different regioselectivities, the mannose and glucose fraction have nearly identical mol fractions c_i (see Table 3.1) which are the basis for the various model calculations and thus the arrangement of M and G does not play a significant role for the calculation of these oligomer patterns, as long as they are so similar. For further study of the distribution of monomers in KGM, the preparation of methylated KGM with large DS difference in mannosyl and glucosyl residues is required which is the topic of in Chapter 4.

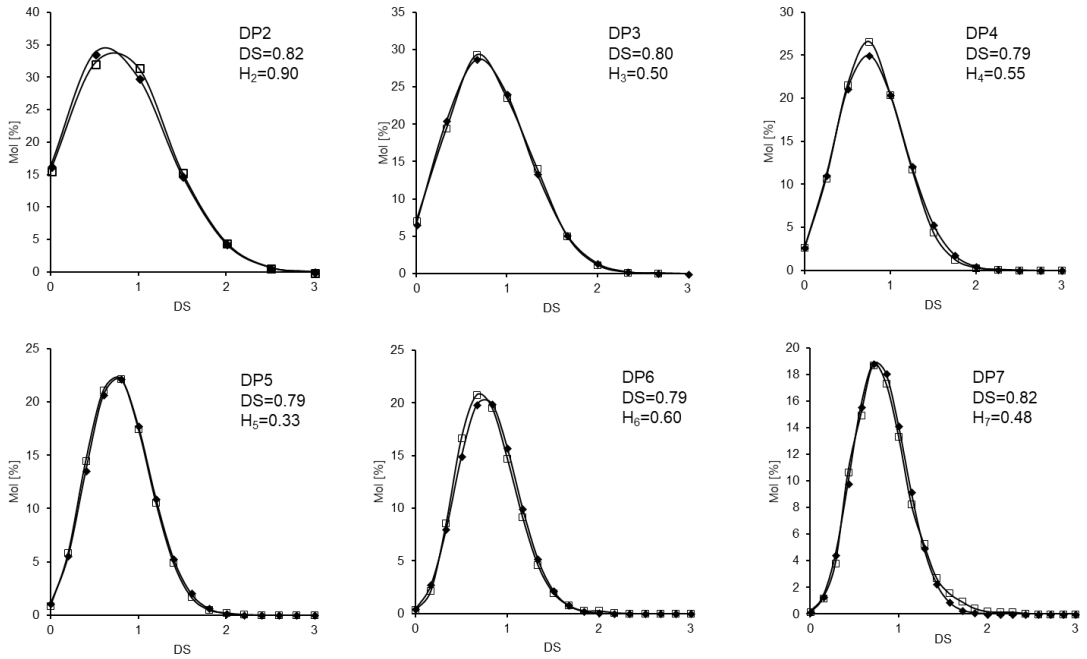

Figure 3.11. Comparison of methyl distribution calculated for diblock gluco/manno copolymer (♦) and determined experimentally (□) in DP 2-7, obtained by LC-ESI-MS of DM-KGM-6.

3.2.2.2 Glucose-mannose distribution pattern

Additional information can be obtained after the different oligomers are separated prior to their mass spectrometric analysis and their ratio is considered. By HPLC-ESI-MS and generation of EIC, the compounds representing various combinations of M and G of the particular DP were differentiated, and first the methyl substitution profile for each component was evaluated and compared with the theoretic profile for the particular MG combination. For instance, by generating the EIC in mass range *m/z* 546 - 564, four peaks were obtained (MM, MG, GM and GG), as shown in Figure 3.12a. The individual methyl substitution profiles were calculated and were all in agreement with the random distribution model, as expected (not shown). GG and MM were assigned by the mannan and cellulose-derived standards. MG and GM were assigned according to their expected ratio: Since mannosidic linkages are faster

cleaved than glucosidic ones, GM should predominate. Since the amount of GG was comparable small the evaluation of its methyl profile is impaired by the overlap with the higher methylated (and less deuteromethylated) components of abundant GM (see Figure 3.12a). Isotopomers with higher number of Me-d_3 are less retained on the RP-phase than those with less Me-d_3 and more Me.

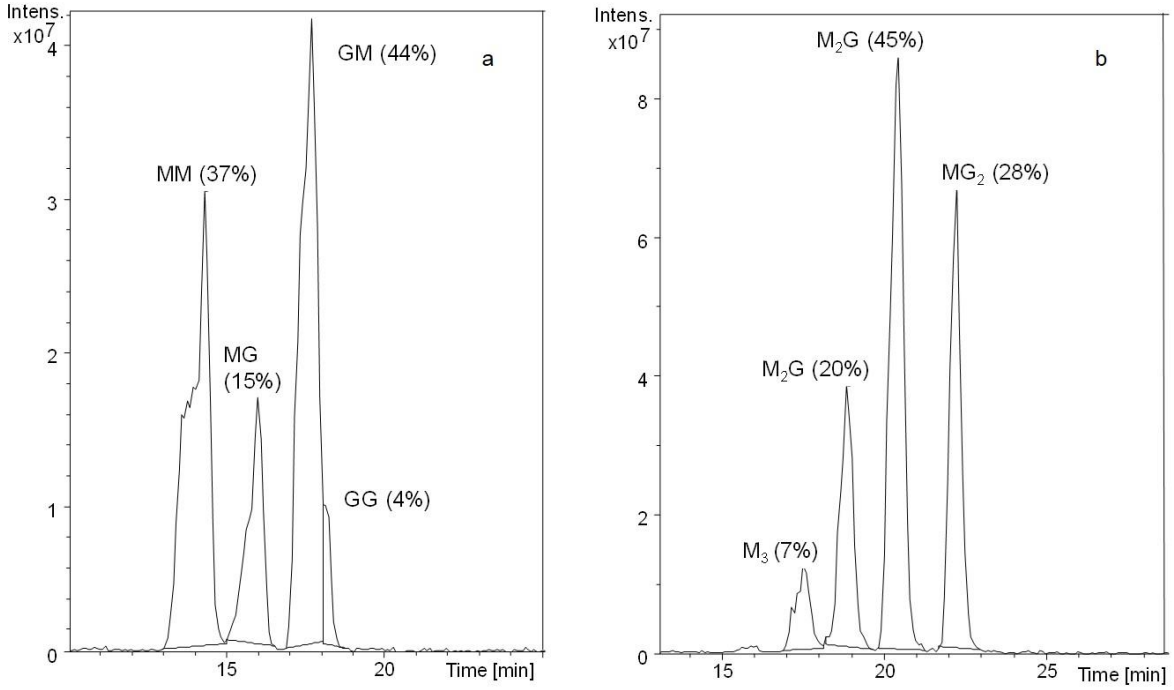

Figure 3.12 Extracted ion chromatogram of *m/z* 546-564 and *m/z* 750-777, corresponding to DP 2 (a) and DP 3 (b), respectively, obtained by LC-ESI-MS of partially hydrolyzed and *m*ABA-labeled DM-KGM-6.

Similarly, by ion extraction in the range *m/z* 750 - 777, four of the eight possible peaks of DP 3 were separated (Figure 3.12b) and evaluated individually. Due to the number of less retained mannosyl units and more retained and less abundant glucosyl units, one can tentatively assign these peaks into M_3, M_2G, M_2G, the latter two comprising MMG, MGM and GMM, and MG_2, also existing in three sequences (GGM GMG and MGG). G_3 was not detected. The peak of M_3 and G_3 could be assigned or excluded, respectively, without doubt by comparison with the standard chromatograms shown in Figure 3.8 in connection with EIC. The three mixed peaks were assigned tentatively according to their expected probability and the chromatographic behavior of G and M (M_2G prior to MG_2). Overlap of isomers of M_2G and MG_2 type cannot be excluded. The methyl distribution profiles of these peaks are again in agreement with those calculated. In contrast, the ratio of the peaks as a measure of the GM distribution in and over the KGM chains gives more insight in the monosaccharide arrangement.

According to the M/G stochastic distribution, 39.3 % of MM, 23.4 % of GM and MG each and 13.9 % of GG should be detected in DP 2 of DM-KGM when the M/G ratio is 1.68. In fact, 37 % of MM, 44 % of GM, 15 % of MG, and 4 % of GG were detected in the DP 2 fraction of DM-KGM-6 experimentally (see Figure 3.12a). Moreover, instead of the theoretic amount (25 % of M_3, 44 % of M_2G, 26 % of MG_2 and 5 % of G_3), only 7 % of M_3, 20+45 % of M_2G, 28 % of MG_2, and no G_3 were obtained for the DP 3 fraction by LC-MS. Supposed the distribution of M and G units in KGM backbone are blocky, especially in small DP (DP 2 and DP 3), larger amounts of MM and GG should be found after partial acid hydrolysis. However, we detected much less MMM (25 %→7 %) and GG (14 %→4 %) than theoretically calculated. In case of random hydrolysis, this oligomer profile would indicate a more regular distribution of G and M than random. Due to the above mentioned faster hydrolysis of M-M and M-G-linkages, this conclusion is, however, not feasible. Due to faster hydrolysis the portion of M_3 might be enhanced or depleted, depending on the degree of depolymerization. The same is true for G_3 which would be underestimated in the beginning of hydrolysis and soon overestimated when M is enriched in smaller DPs. From the lack of gluco- and manno-homo-oligosaccharides above DP 2 and DP 3, respectively, it is concluded that M and G are not organized in larger gluco- and manno-blocks in KGM.

3.2.3 TGA and DSC analysis

The thermal behavior of KGM and all M-KGM (DS 0.27 - 0.80, determined by AAM) were studied by TGA and DSC measurements. The TGA thermograms are shown in Figure 3.13. All samples showed two thermal degradation zones. In the first zone (< 125 °C), all samples underwent around 5 % of the total weight loss. This is attributed to the loss of moisture. The second zone (200-325 °C) of main weight loss presents a complex thermal decomposition region with two main overlapping peaks (the 1st derivative curve as shown in Figure 3.13). The glucosyl residues are thermally more stable than the mannosyl residues. According to the study of Moriana et al.[86] the first of the overlapping peaks at 285 °C- 295 °C in the differential thermogravimetric (TG) curve is assumed to be related to the greater part of the M units, while the larger peak at 300 °C- 310 °C in the differential thermal gravimetry (DTG) curve is correlated with the degradation of the main part of the G units. No TG and DTG curves of M-KGM-2 and M-KGM-3 presented, resulting from the poor resolution of measurements.

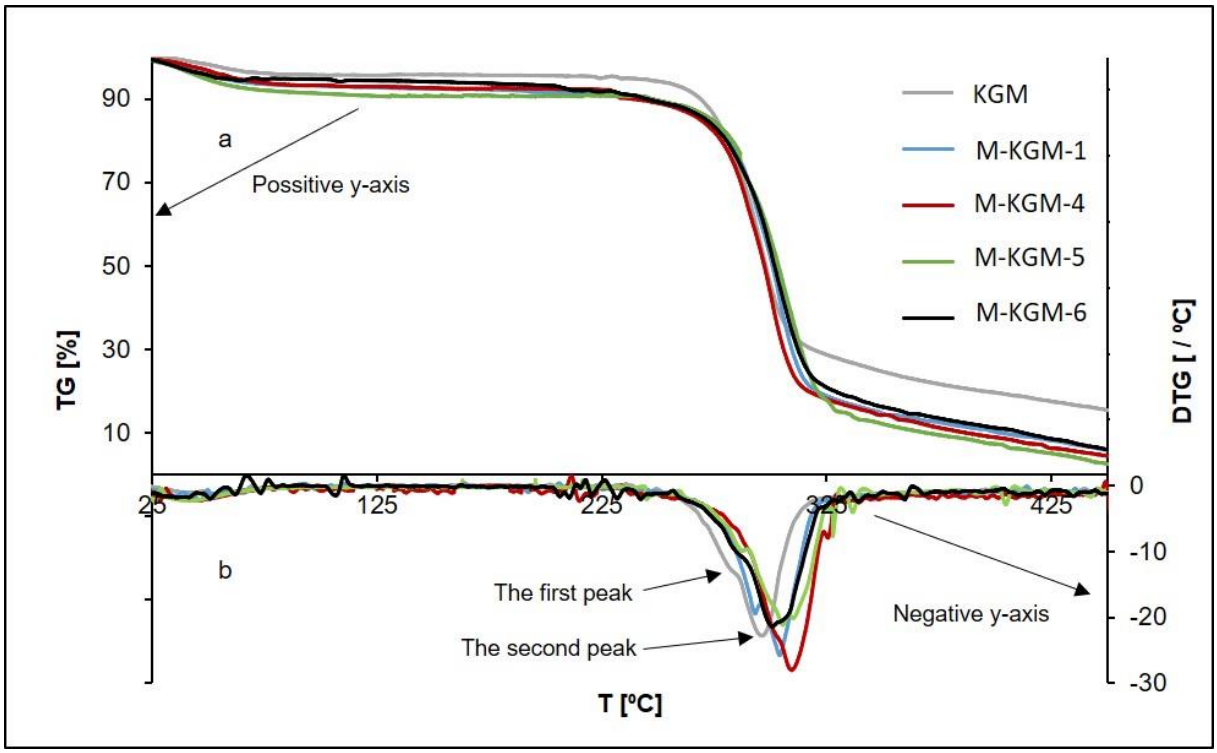

Figure 3.13. Comparison of TG (a) and DTG (b) curves for KGM and M-KGMs (DS 0.27 - 0.80, determined by AAM) at 10 °C/min.

After partial methylation, the TG profile of M-KGM changed compared to original KGM. The chemical modification resulted in a less hydrophilic material with a narrower thermal-decomposition region. An increase of the weight loss (from 67 % to 82 %) was observed in the main thermal decomposition zone as the DS increased. The initial decomposition temperature (i.e., its onset temperature) at 80 % weight loss for the M-KGM-1 (DS 0.27) with 283.4 °C was higher than that of native KGM (277.0 °C). Decomposition temperatures at 80 % weight loss of 283.5 °C (DS 0.30), 284.0 °C (DS 0.40), 285.0 °C (DS 0.51), 286.2 °C (DS 0.77), and 287.0 °C (DS 0.80) were measured. Similar results were reported by other researchers, e.g. for a methylated KGM with DS 1.07 the onset decomposition temperature was found to be 287.2 °C at heating rate of 10 °C/min (the same as in this study).[86] Thus, as expected, the thermal stability of KGM was improved by methylation. From M-KGM-1 (DS 0.27) to M-KGM-6 (DS 0.80), the partial DS value at position 6 in glucose residues increased from 0.14 to 0.37, and from 0.12 to 0.34 in mannose residues. Thus, there are less free 6-OH available for intramolecular attack at C-1 and subsequent chain scission under formation of 1,6-anhydro sugars.[87]

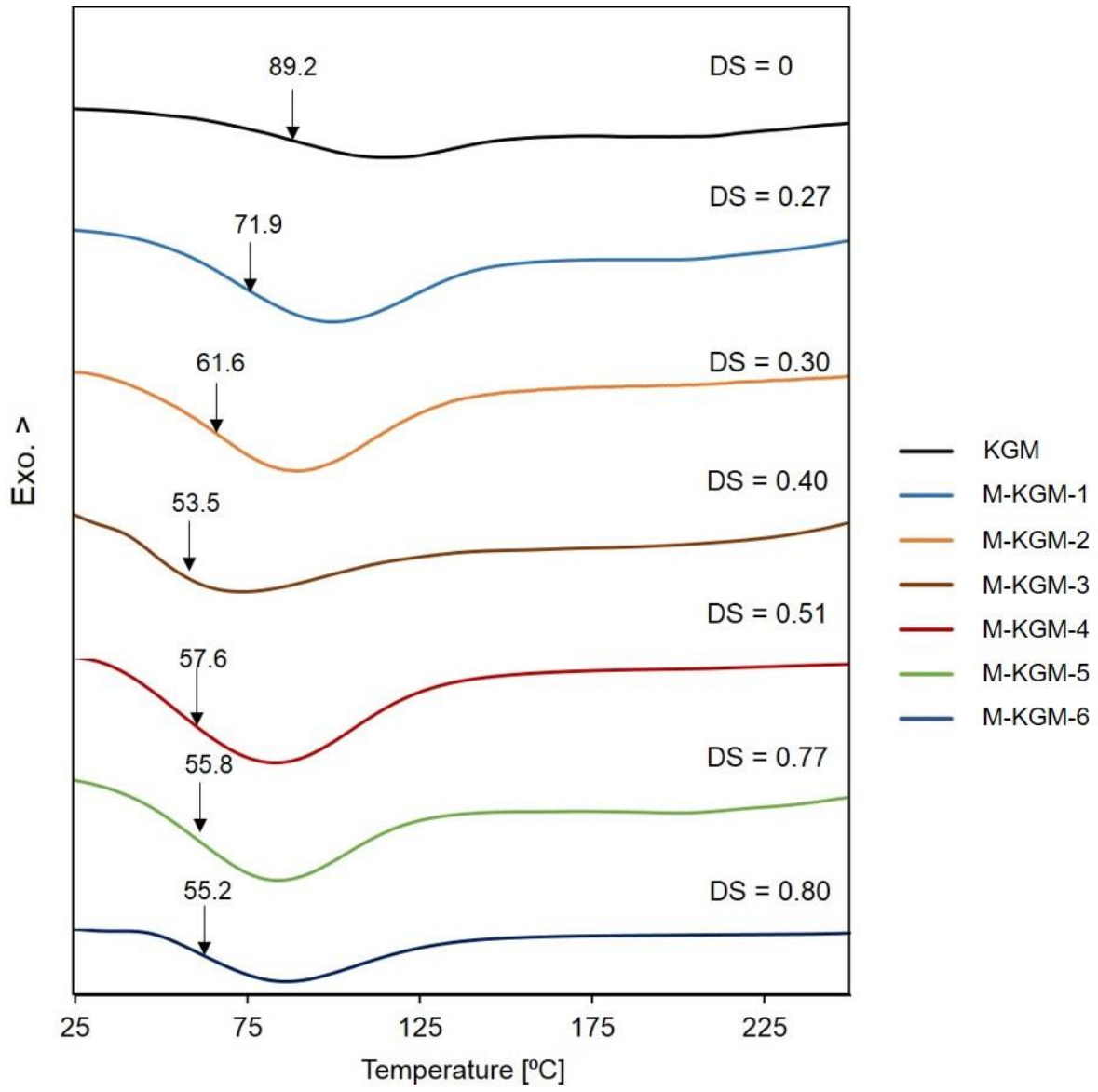

Figure 3.14. Comparison of DSC thermograms for KGM and M-KGM entry at 30 °C /min.

In the differential scanning calorimetry (DSC) test, a first temperature-raise was conducted to erase the thermal history of the material. Then the DSC thermograms of KGM and M-KGMs were recorded in the second heating cycles, as shown in Figure 3.14. No melting point was found in all thermograms, indicating that KGM and M-KGMs are amorphous. In contrast to the midpoint temperature of the endothermic capacity change of the starting material KGM (T=89.2 °C), all M-KGM exhibited lower temperatures decreasing from 71.9 to 55.2 °C in the DS_{KGM} range of 0.27 to 0.80. A corresponding trend had been found for the glass transition temperature (T_g) of glucomannan acetates, where T_g dropped from 219 °C at DS_{Ac} 1.3 to 172 °C at DS 3.0.[33] According to the literature, it is difficult to measure absolute values for T_g of polysaccharides and their derivatives. Barros et al.[88] reviewed the literature of T_g measurements of chitosan and HPMC and found T_g for the latter being in the range of 55-

167 °C. Values below 100 °C[89] were measured for HPMC stored at defined humidity, but also non-processed HPMC showed T_g at 84.9 °C. From this Barros concluded that T_g might be masked by water evaporation peaks and is not well measurable by DSC. Zohuriaan and Shokrolahi reported on thermal characterization of several gums and polysaccharide derivatives,[90] among which MC is most similar to our M-KGM, but probably with a higher DS. They do not observe a glass transition for MC and reason that this is due to interference of heat capacity change at T_g by the moisture endothermic peak. They also take into consideration that T_g for the MC studied might be below 30 °C. Thus, it is difficult to judge whether in our case the temperatures calculated from the capacity change describe T_g of M-KGM.

However, the DSC measurements for all samples presented in the manuscript were measured under the same conditions. Thus, although the observed temperature as T_g of methylated KGM cannot undoubtedly be interpreted, the relationship between endothermic change of heat flow and the different degree of KGM methylation are obtained. There is a trend visible that this temperature decreases with increasing DS which means decreasing polarity and less intramolecular hydrogen bonds. Thus the shift of this temperature visible in the DSC curves in Figure 3.14 seems plausible.

Above all, the relatively high initial decomposition temperature and amorphous structure makes methylated KGM an interesting material due to its ability to withstand high-temperature processing operations or for applications in thermally stable biomaterials (e.g., as a promising candidate bio-based thermoplastic materials in industry).

3.3 Conclusion

The relative reactivities of OH in stereoisomeric glucosyl and mannosyl units in KGM with a molar ratio of M to G of 1.68 were investigated by partial methylation at constant pH 13.6 in an aqueous NaOH/CH_3I system. In a time course study, M-KGM with DS between 0.27 and 0.80 were obtained, with average DS_M being only slightly higher than DS_G. Both the methyl pattern in glucosyl and mannosyl units and the methyl distribution along and over KGM chains were studied and presented in this study. For both glucose and mannose, the primary OH was the most reactive under the conditions applied. While the relative rate constant k_2 was equal for mannose and glucose, the lowest reactive position 3-OH was methylated to a much higher extent in mannose than in glucose. Due to the *cis*-2,3-diols configuration in M units, the acidity of O-3 profited from adjacent O-2, resulting in 2.4 times larger M-k_3 compared to G-k_3. In conclusion, in one series of M-KGMs with DS_{KGM} from 0.27-0.80, the order of the

six hydroxyl groups in KGM is G-k_6 > M-k_6 > G-k_2 ≈ M-k_2 > M-k_3 > G-k_3 (k_2: k_3: k_6 = 4.1 : 2.3 : 4.9 for M and k_2: k_3: k_6 = 4.2 : 1.0 : 5.5 for G).

Second, the methyl and the GM distribution was analyzed by LC-ESI-MS measurements of *m*ABA-labeled partially hydrolyzed *O*-methyl/methyl-d_3-KGM samples. Comparison of the experimental data with calculated random distribution of all glycosyl units present showed full agreement. Therefore, the methyl groups are distributed randomly over the KGM chains which is expected from a reaction in water. Due to very similar molar ratios of non-, mono-, di- and tri-*O*-methylated units of glucose and mannose, their distribution along the KGM macromolecules could not be deduced from the methyl pattern in oligosaccharide fractions in this case. However, LC-ESI-MS in combination with the extracted ion chromatograms for a particular DP allowed to quantify the ratio of MM, MG, GM and MM disaccharides and also groups of trisaccharides (M_3, M_2G, MG_2). No (e.g. G_3) or only small amounts (M_3) of higher uniform oligosaccharides were detected. Consequently, along the long KGM chains, M and G residues seem to be randomly distributed in general, rather than in big M and G blocks. Whether G and M are distributed even more regular than random cannot be decided so far due to faster acid hydrolysis of mannosidic than glucosidic linkage which restricts quantitative evaluation of the GM distribution in the oligosaccharides. To gain more insight in stereochemically controlled methylation of the GM chains, a type of chemical modification giving larger differences in DS values for glucose/mannose residues is prepared and the results are presented in Chapter 4. Thermal stability was improved by methylation and a temperature, where a heat capacity change was observed, probably T_g, decreased with increasing DS.

4 Borate-mediated Stereo- and Topo-selective Methylation of KGM

4.1 Introduction

As a stereoisomer of cellulose, KGM only differs with respect to the orientation of OH at C-2 in mannose, i.e. axial (ax) in M and equatorial (eq) in G. Due to this difference in stereochemistry the relative reactivities of the hydroxyl groups of glucose and mannose are expected to be different, as is known for the monosaccharides.[60,76] In the previous chapter, we found G-k_6 > M-k_6 > G-k_2 ≈ M-k_2 > M-k_3 > G-k_3 for a series of partially methylated KGM (M-KGM) obtained in NaOH/CH_3I in an aqueous system at constant pH 13.6.[12] As discussed there, M-KGM with large difference of DS in M and G residues is required, in order to identify the M/G arrangement pattern in KGM polysaccharide chains. Furthermore, such a methyl pattern might induce interesting properties. Therefore, the question arose how to prepare such a KGM derivative. In contrast to uniform cellulose, KGM contains 2,3-*cis* (M) and 2,3-*trans*-diol (G) features. This difference shall be used to control the reactivity and selectivity of modification in M and G, respectively, thus generating a non-uniform methyl pattern controlled by the G,M-distribution in the polysaccharide. In general, protecting or activating groups selective to position and/or stereochemistry can serve for efficient control of the reactivities of OH groups. In contrast to monosaccharides, to achieve regioselective and topochemical modification of polysaccharides is a more complex task. Due to the small reactivity differences between the KGM hydroxyl groups, G/M-selectivity of etherification of KGM is not very pronounced in conventional reactions. As a transient protecting or activating group, boronic acids and dibutyltin oxide have been applied in monofunctionalization of *cis*-diols. Using an ethanolamine ester of diphenylboronic acid to generate a tetra-coordinated boronate complex with the carbohydrates, Chudzinski et al. proposed an interesting way to selectively activate the benzoylation of equatorial over axial OH groups of *cis*- and *trans*-diol.[91] In their study, in the BzCl/DIPEA/ACN system in the presence of 5 Mol% of organoboron catalyst, a *cis/trans* ratio of 11:1 of 2-*O*-benzoates of *cis*-cyclohexane-1,2-diol (ax-eq) and *trans*-cyclohexane-1,2-diol (eq-eq) was found. Dibutyltin oxide (Bu_2SnO) in methanol under reflux preferentially reacts with *cis*-diols to obtain a thermodynamically stable stannylene acetal which selectively reacts in further modifications as will be outlined in more detail in the next chapter.[92] Haque et al. reported that mainly 2-*O*-benzyl-*α*-D-glucopyranoside was obtained from a stannylene intermediate, whereas they observed preferential benzylation at position 3 for *α*-D-mannopyranosides.[93] Another approach aims to

prevent 1,2-*cis*-diol from derivatization by the use of isopropylidene acetal as protecting group.[94] Copper ions can be used for selective deactivation. Eby et al. found that disubstitution was absent for methyl 4,6-*O*-benzylidene-*α*-D-glucopyranosides and mannopyranosides when alkylating their copper chelates.[95] Moreover, they reported that monosubstitution of O-3 dominated over that of O-2 under the conditions applied.

Using lipase as bio-catalyst, Chen et al. synthesized regioselectively acylated KGM in a solvent mixture of ionic liquid and *tert*-butanol, favoring reaction of 6-OH.[96] From ^{13}C-NMR spectroscopic studies they reported a slight preference for M. Furthermore, 1,2- and 1,3-diols form dynamic complexes with borate in aqueous solution (Scheme 4.1). Making use of this phenomenon in chromatography or electrophoresis for the separation of polyhydroxy compounds including carbohydrates is well known.[97] At pH ≥ 12, all boric acid is converted to borate and also polyborate ions should no longer occur.[98,99] Higher stability of *cis*- compared to *trans*-1,2-diols is well known. Makkee et al. studied the species formed and the stability constants of carbohydrate-borate esters depending on concentration, ligand : borate ratio and pH by ^{11}B- and ^{13}C-NMR spectroscopy. For the model compounds *cis*- and *trans*-1,2-cyclohexanediol, resembling manno- and glucopyranose, they reported stability constants of 1.2 L/Mol (*cis*) compared to <0.1 L/Mol (*trans*) for a 1:1 mixture of diol and borate, both 0.1 M, at pH 12 in D_2O.[100] Therefore, it was expected that addition of borate should block the *cis*-2,3-diol in mannose to a much higher extent than the *trans*-2,3-diol in glucose and thus prevent its methylation more efficiently.

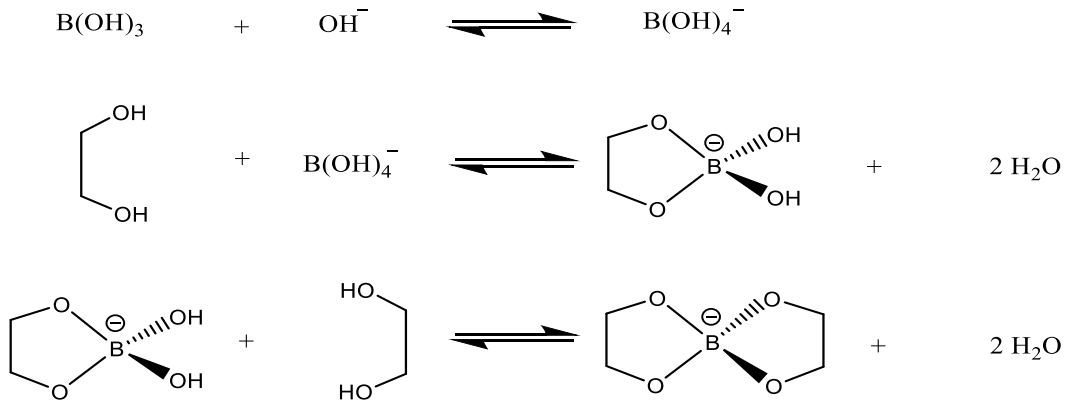

Scheme 4.1 Equilibria between boric acid, borate, and between diols and borate esters in water.

Studies of GGM and KGM in the presence of borate display a more complex behavior.[101–104] Beside *cis*-diol borate esters, 6-membered cyclic complexes involving 6-OH have been described for galactomannan from guar, probably formed via the galactosyl side chains.[102] Monocomplexes (1:1) are favored, if stabilized by hydrogen bonding through an appropriately located sugar OH, while the lack of such a possibility favors crosslinking.[105] However, pH,

ratio of diol to borate, and total concentration naturally also play important roles. The properties of borate mediated gels of KGM and related glycans have been studied by Gao et al.[98] The authors assumed the reversible crosslinking of 2,3-diol of M by borate. Cooperative effects of M sequences were not addressed. In contrast, Jian et al. performed dynamic simulations of acetyl containing KGM and borate under neutral conditions or at least without any base addition. This study resulted in a helical Ac-KGM with hydrogen bonding of borate to 6-OH of M and G and ring O-5 of M, thus stabilizing the helical conformation of Ac-KGM and gel formation by chain-chain aggregation.[104] The authors did not perform chemical reactions in the presence of borate, and to the best of our knowledge, no other modifications of KGM with large DS differences on M and G residues on the KGM backbone have been reported. In this chapter an approach for M/G-selective methylation of KGM by use of borate as an transient protecting group with a preference for 2,3-*cis*-diols in M residues is described. Beside the analysis of the methyl patterns of glucosyl and mannosyl residues,[12,36] all free OH in M-KGM were perdeuteromethylated, and subsequently, submitted to oligomer analysis by (LC)-ESI-MS in order to discuss the methyl pattern in M and G and the distribution of M and G units over the polysaccharide chains.[82] Thermal properties of M-KGM with large DS-differences were measured.

4.2 Results and discussion

4.2.1 Methylation of KGM in the presence of borate

Methylation of KGM was performed with NaOH/CH_3I in water or water/acetone in the presence of various amounts of borate at temperatures between 20 and 40 °C. Due to the higher stability of 1,2-*cis*-diols compared to 1,2-*trans*-diols, it was expected that methylation of O-2 and O-3 in mannose could be more efficiently suppressed in mannose than in glucose. Such a toposelective modification is not possible in homoglycans since protecting groups are only selective with respect to the OH-position in the glycosyl units, not for their position in the polymer chain. By a derivatization process which is selective with respect to G and M, the methyl distribution over the polymer chains will additionally be controlled by the G-M distribution. To facilitate a direct comparison and evaluation of the borate effect, experiments were performed in parallel with and without borate while, apart from this, keeping the conditions constant. Products were analyzed with respect to their methyl pattern in G and M as described.[12] Table 4.1 gives an overview over all entries.

Table 4.1. Methylation conditions of M-KGM with or without addition of borate. M-KGM-8 was prepared by adding 0.2 g of NaOH and 1 mL of CH_3I. All other M-KGMs were prepared by adding 0.4 g of NaOH and 2 mL of CH_3I.

M-KGM	Solvent H_2O/acetone mL/mL	Borate equiv./ KGM[2]	T[3] [°C]	DS_{KGM}	DS_G	DS_M	DS_G/DS_M	$x_6/(x_2+x_3)$[4] in M	$x_6/(x_2+x_3)$[5] in G	Diversity H_c[6]
8	5 / -	2	25	1.00	1.06	0.96	1.10	0.80	0.75	4.1
9	10 / -	4	30	1.33	1.38	1.29	1.07	0.74	0.83	4.1
10[1]	10 / -	-	30	1.56	1.48	1.61	0.92	0.62	0.78	3.7
11	10 / -	8	20	0.73	0.86	0.64	1.34	0.95	0.64	7.7
12	10 / -	20	20	0.51	0.69	0.40	1.73	1.39	0.59	9.7
13	10 / -	40	20	0.45	0.64	0.33	1.94	1.99	0.78	12.4
14[1]	10 / -	-	20	0.99	0.91	1.04	0.88	0.69	0.97	3.5
15	10 / -	40	40[b]	0.75	1.07	0.55	1.95	1.25	0.50	16.7
16[1]	10 / -	-	40[b]	1.91	1.91	1.92	1.00	0.58	0.57	4.0
17	10 / 5	40	20	0.81	1.18	0.59	2.00	1.63	0.53	18.0
18[1]	10 / 5	-	20	1.71	1.62	1.76	0.92	0.56	0.59	5.6
19	10 / 5	40	50	0.76	1.18	0.50	2.36	2.52	0.51	20.9
20	10 / 5	-	50	2.52	2.38	2.61	0.91	0.54	0.60	10.7

[1]Borate-free reference for M-KGM-9, -13, -15, and 17, respectively
[2]First addition of borax, calculated as borate
[3]Estimated room temperature.
[4]The ratio of partial DS-values $x_6/(x_2+x_3)$ in M residues.
[5]The ratio of partial DS-values $x_6/(x_2+x_3)$ in G residues.
[6]The diversity parameter H_c from the deviations Δc_i between M and G residues. $H_c=\sqrt{\frac{\sum(ci(G)-ci(M))^2}{4}}$ i=0,1,2,3 (4.1)

In Chapter 3, the study on methylation of KGM in aqueous NaOH/CH_3I at constant pH (13.6), methyl distribution was found to be random in both mannosyl and glucosyl units, but they reacted with different rate constants k_i (i = position 2, 3, 6 of G and M, respectively), i.e. random in a way that all OH reacted independently from each other. By the analysis of oligomeric domains, the methyl pattern along and over the polymer chains was also found to be random.[12] Whether this means that also G and M are randomly distributed in KGM chains could not be concluded from the analysis of the methyl pattern. In spite of different regioselectivities for G and M, average DS and the molar fractions of un-, mono-, di- and trisubstituted glycosyl units (c_0 - c_3) were nearly equal in G and M. Thus, they could not be differentiated by their mass in MS analysis of oligomer domains. In the presence of borate, however, larger DS values were gained for G than for M with a ratio DS_G/DS_M up to 2.4 (see Table 4.1), while the overall DS decreased. Figure 4.2a shows this decrease differentiated for mannosyl and glucosyl units for the reactions performed at approx. 20 °C in the presence of various amounts of borate. As expected, the inhibition of alkylation was much more pronounced in mannosyl than in glucosyl units. Monomer data for all M-KGM are summarized in Table 9.7 in appendix. IR spectra of all M-KGM were measured and that of M-KGM-15 and M-KGM-16 are shown in 9.1 as an example.

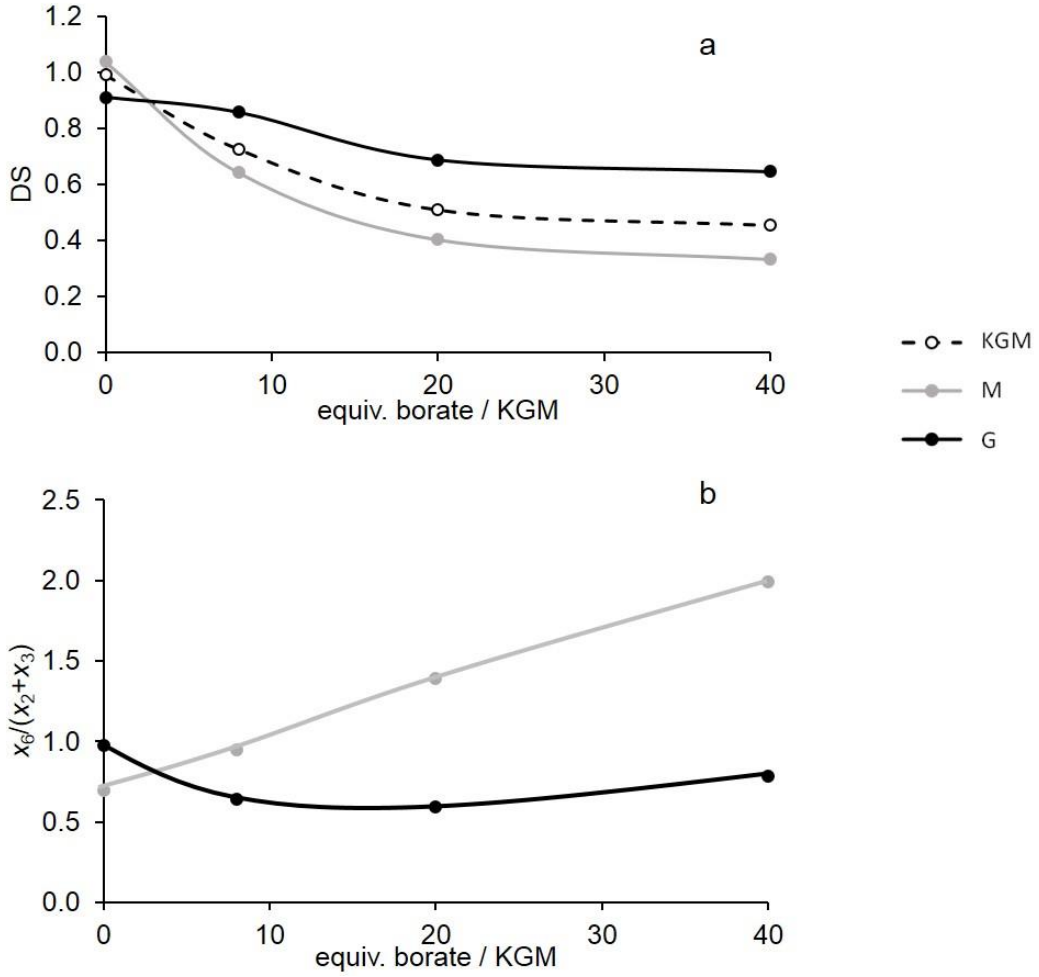

Figure 4.2. (a) Change of DS of M, G and KGM with equiv. borate/KGM present during methylation. For comparability, only M-KGM-11, 12, and 13, and 14, all prepared at ca. 20 °C are presented (for further data see Table 9.7 in appendix). (b) Ratio of the partial DS values $x_6/(x_2+x_3)$ in M and G of M-KGM prepared in the presence of various equiv. of borate/KGM at approximately 20 °C (M-KGM-11, 12, 13, and 14).

In order to visualize the effect of borate on the regioselectivity of methylation, the ratio of partial DS values $x_6/(x_2+x_3)$ is presented in Figure 4.2b for M and G residues of the same M-KGM series. (This selectivity parameter is included in Table 4.1 for all entries). For mannose, this ratio linearly increases with the amount of borate added, while for the glucosyl units in KGM only slight changes are observed.

For a more detailed consideration, the molar portions of all methyl patterns of G and M for M-KGM-13 (40 equiv. borate/KGM; $NaOH/H_2O/CH_3I$, 20 °C) and its direct reference sample prepared in parallel without borate (M-KGM-14) are shown in Figure 4.3.

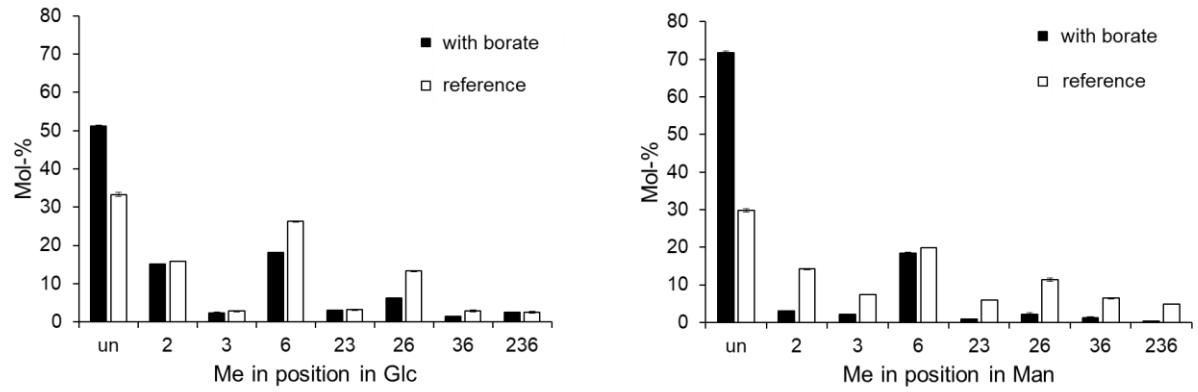

Figure 4.3. Comparison of methyl distribution in G and M of M-KGM-13, prepared in the presence of borate (40 equiv./KGM), and M-KGM-14 prepared in parallel without borate in $NaOH/H_2O/CH_3I$ at ca. 20 °C. G (left) and M (right) were both normalized to 100%.

Obviously, methylation in the presence of the large excess of 40 equiv. of borate strongly inhibited methylation of O-2 and O-3 in mannose units causing nearly complete suppression of two- and threefold methylation, while in glucose units, reactivity of O-6 was mostly affected, and as a consequence the portions of 2,6- and 3,6-di-*O*-methyl-glucose were also reduced. Compared to the borate-free reference sample, the overall DS_{KGM} was reduced by 2/3 for mannose and by 1/3 for glucose. The partial DS x_2 and x_3 of M in M-KGM-13 was only 1/5 of that in reference M-KGM-14. Preferential inhibition of 6-*O*-methylation in glucose suggests that here a borate complex which involves 6-OH (and perhaps the ring oxygen O-5) is the most stable, rather than the complex with the 2,3-*trans*-diol, as has been discussed.[104] Thus, M-KGM with DS values of G twice that of M units could be obtained in a one-pot reaction by applying excess of borate as a stereo- and hence regioselective transient protecting agent. However, when applying a sufficient amount of borate to achieve a large difference in DS of M and G, the overall DS was finally comparatively low (M-KGM-13: DS_M 0.33, DS_G 0.64). To enhance overall reactivity of M and G, while hopefully maintaining the selectivity with respect to M and G, the reaction temperature was increased, and alternatively an aprotic co-solvent (acetone) was added.

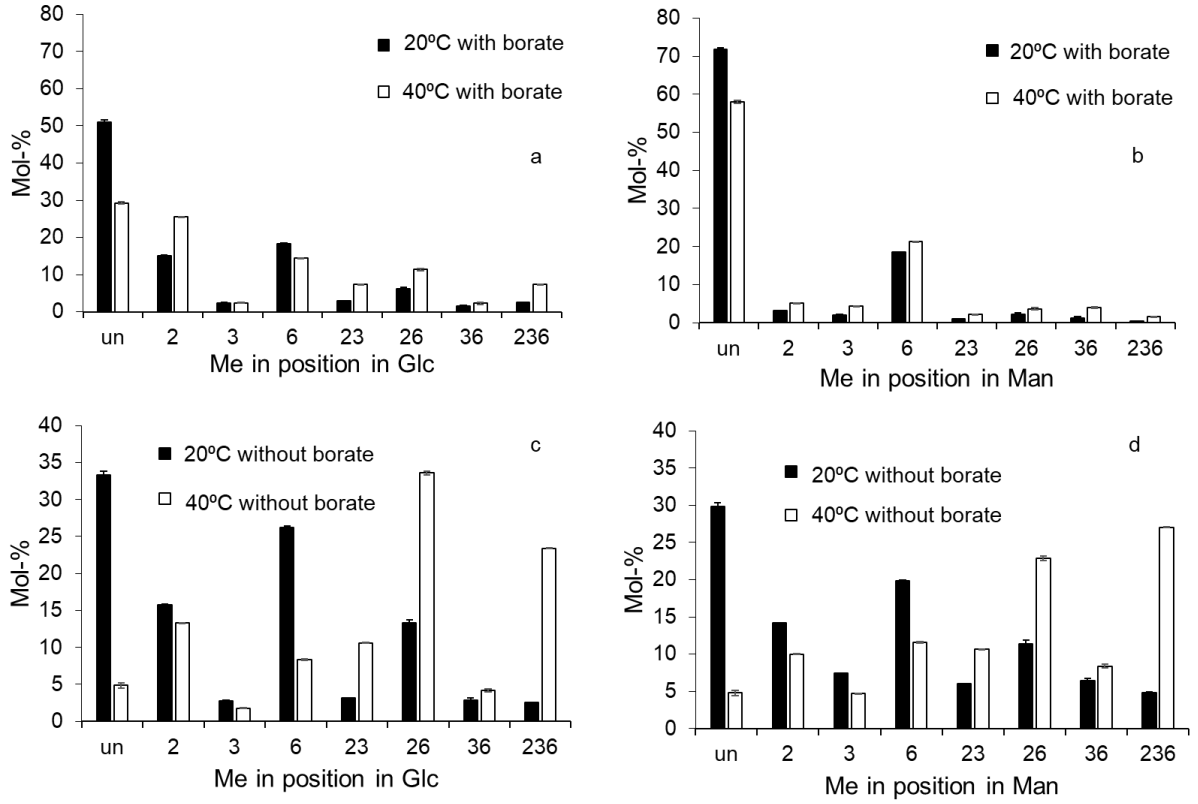

Figure 4.4. Comparison of methyl distribution in G (a) and M (b) in M-KGM, prepared in NaOH/H_2O/CH_3I in the presence of 40 equiv. borate/(KGM) at ca. 20 °C (M-KGM-13, DS_{KGM}=0.45, DS_M 0.33, DS_G 0.64), and at 40 °C (M-KGM-15, DS_{KGM}=0.75, DS_M 0.55, DS_G 1.07), respectively, and of methyl distribution in G (c) and M (d) in M-KGM, prepared in NaOH/H_2O/CH_3I at 20 °C (M-KGM-14, DS_{KGM}=0.99, DS_M 1.04, DS_G 0.91) and at 40 °C (M-KGM-16, DS_{KGM}=1.91, DS_M 1.92, DS_G 1.90), without borate. M and G are both normalized to 100%.

Figure 4.4 compares the methyl pattern of glucose and mannose residues in M-KGM obtained from methylation at 40 °C and 20 °C, both in the presence of borate, and as a reference, without borate addition (entries M-KGM-13/14 (20 °C) and M-KGM-15/16 (40 °C)). In the reference samples, the DS was doubled, with glucose profiting somewhat more from the elevated temperature than mannose (DS_{KGM} +93%, DS_M +84% and DS_G +109%). In accordance with the progress of the reaction, the regioselectivity of methylation (at 20 °C $x_6 > x_2 > x_3$) is leveled. The strongest relative increase but still lowest absolute degree of methylation is observed for O-3, followed by O-2 and O-6. In the presence of borate, the overall DS increased by only 65% for both M and G when the temperature was raised to 40 °C. When elucidating the methyl pattern in more detail (Table 9.7 in appendix), it becomes obvious that regioselectivity is reduced for M, and shifted in favor of O-2 for G. Compared to M-KGM-13 (20 °C), x_2, x_3 and x_6 of M in M-KGM-15 (40 °C) are enhanced by 92, 157 and 37%, respectively. Thus the selective diol-blocking by borate is less efficient at elevated

temperature. Consequently, the ratio of $x_6/(x_2+x_3)$ in mannosyl residues, used as regioselectivity parameter, dropped from 1.99 in M-KGM-13 to only 1.25 in M-KGM-15 (see Table 9.7 in appendix). For G, the 65% average increase of DS is the result of +93% for O-2, +108% for O-3, and only +25% for O-6. Previous studies have shown that crosslink density depends on temperature, since the complex formation between polysaccharide and $B(OH)_4^-$ in water is exothermic and the equilibrium constant decreases with increasing temperature.[98,102] From the results of their molecular dynamic simulation study of the KGM-borate complex in water, Jian et al. proposed that at elevated temperature the crosslinking site between 6-OH at G and $B(OH)_4^-$ is maintained.[104] In conclusion, the comparison of reactions performed with or without borate at elevated temperature indicated that enhanced reactivity was only possible at the expense of regioselectivity. However, the DS_G/DS_M ratio was maintained at ca. 2.4 (see Table 4.1), which nevertheless is of high value for the goal of products with pronounced local differences of methylation along the chain. The overall diversity with respect to c_i (molar fractions of *i*-fold substituted glycosyl units in Mol %) was expressed as follows

$$H_c=\sqrt{\frac{\sum(ci(G)-ci(M))^2}{4}} \qquad i=0,1,2,3 \qquad (4.2)$$

This diversity parameter H_c is given for all M-KGM in Table 4.1. For all borate free reactions, H_c was 3-4, while for M-KGM-13 (40 equiv. borate, 20 °C) it was 12.4, and 16.7 for M-KGM-15 (40 equiv. borate, 40 °C).

When M-KGM was prepared in water/acetone (1:2, v/v), also higher DS values were achieved compared to the entries in water under otherwise same conditions. The aprotic co-solvent enhances the nucleophilicity of the deprotonated glycan, and might improve the availability of the methyl iodide. For instance, Viera et al. reported that in $NaOH/H_2O$, the DS of MC was 0.7, while a DS of 1.2 was achieved when adding acetone as co-solvent.[106] On the other hand, acetone causes coagulation of KGM, so that it is not clear whether all KGM chains are equally accessible. As shown in Figure 4.5, at 40 equiv. of borate, the overall DS increased by 80% from 0.45 (M-KGM-13) to 0.81 (M-KGM-17) and in the corresponding reference experiments by 72% from 0.99 (M-KGM-14) to 1.70 (M-KGM-18). The individual increase for M and G was nearly the same: for DS_M from 0.33 to 0.59 (+79%), and for DS_G from 0.64 to 1.18 (+84%).

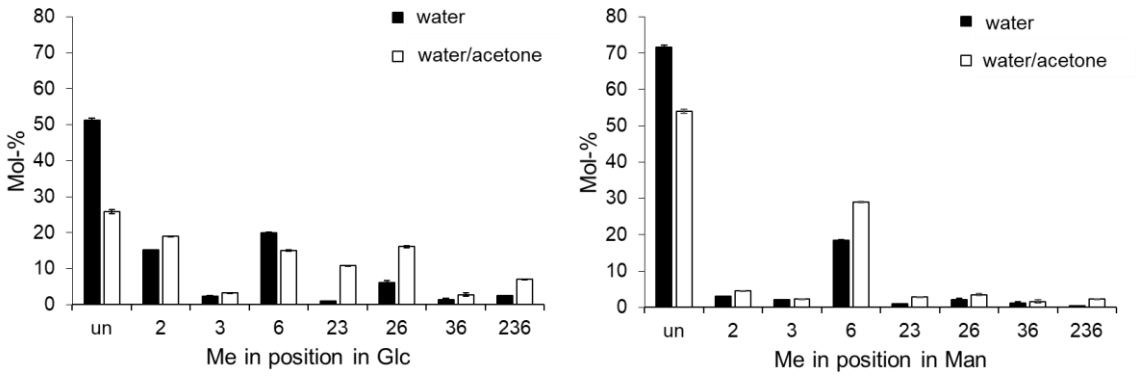

Figure 4.5. Comparison of methyl distribution in G and M in M-KGM, prepared in the presence of 40 equiv. borate at 20 °C with NaOH/CH_3I in water (M-KGM-13, DS_{KGM}=0.45, DS_M 0.33, DS_G 0.64), and in water/acetone (M-KGM-17, DS_{KGM}=0.81, DS_M 0.59, DS_G 1.18), respectively. G and M both are normalized to 100%.

Due to the coagulation of KGM in the presence of acetone, a slightly heterogeneous methyl distribution was obtained for the M-KGM prepared in water/acetone mixture. Figure 4.6 shows the comparison of methyl distribution in G and M in M-KGM, prepared in water (M-KGM-13) and in water/acetone (M-KGM-17) with the substitution pattern calculated according to the models by Spurlin. Beside H_1 values, the still higher amount of unsubstituted glycosyl units and the already significant amount of trisubstituted residues is characteristic for a DS gradient in the material. (Data are given in the appendix; H_1 2.3 (M), 3.1 (G) for M-KGM-17, H_1 1.3 (M), 1.9 (G) for M-KGM-13).

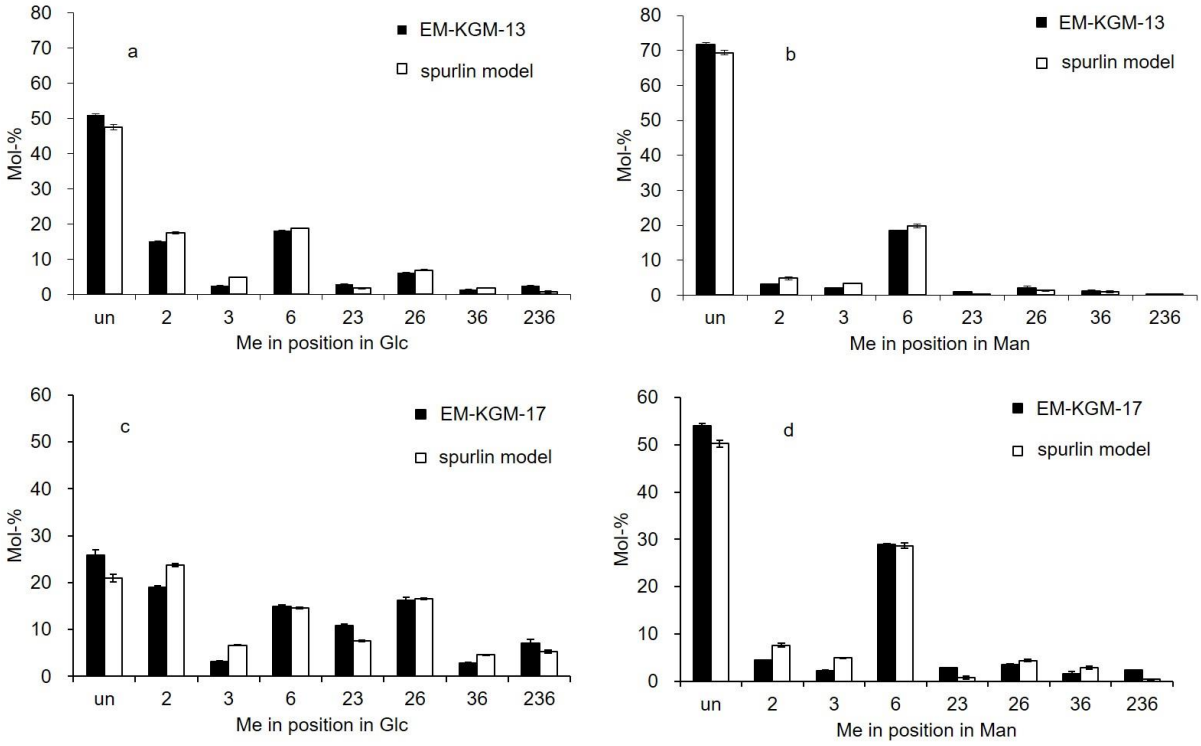

Figure 4.6. Comparison of methyl distribution in G (a) and M (b) in M-KGM-13, prepared in the presence of 40 equiv. borate at 20 °C with NaOH/CH_3I in water (DS_{KGM}=0.45, DS_M 0.33, DS_G 0.64) and the corresponding methyl pattern based on the model of Spurlin. Comparison of methyl distribution in G (c) and M (d) in M-KGM-17, prepared in the presence of 40 equiv. borate at 20 °C with NaOH/CH_3I in water/acetone (DS_{KGM}=0.81, DS_M 0.59, DS_G 1.18) and the corresponding methyl pattern based on the model of Spurlin. G and M both are normalized to 100%.

Again, the regioselectivity for M, expressed as $x_6/(x_2+x_3)$ decreased, but with a drop from 1.99 to 1.63 less than at elevated temperature at about the same DS (see Table 4.1). DS ratio of G and M was even slightly higher (2.0 compared to 1.94), and H_c increased from 12.4 to 18.0. Therefore, applying an organic co-solvent raised reactivity which, however, has to be paid by a penalty for the selectivity, and unfortunately loss of homogeneity. It is, though, superior to raising the temperature.

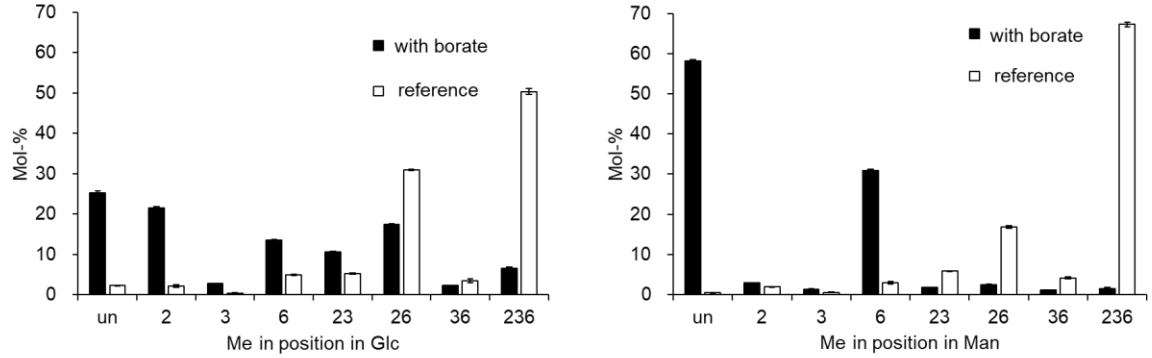

Figure 4.7. Comparison of methyl distribution in G and M of EM-KGM-19, prepared in the presence of borate (40 equiv./KGM), and M-KGM-20 prepared in parallel without borate in NaOH/acetone/H_2O/CH_3I at ca. 50 °C. G (left) and M (right) were both normalized to 100%.

Although a loss of regioselectivity is observed when raising the reaction temperature, we were still interested of whether excellent region- and topo-selectivity in KGM via borate-intermediates is maintained when we combine these two factors (adding acetone and elevating temperature). As shown in Figure 4.7, with 40 equiv. of borate and at elevated temperature in the acetone/water mixture M-KGM-19 was prepared, and the individual methyl distribution in M and G is compared to that of M-KGM-20 as reference, prepared in parallel without addition of borate. The average DS value of M-KGM-19 was only 0.76, while that of M-KGM-20 was 2.52. DS ratio of G and M was much higher in M-KGM-19 (2.36 compared to 0.91), and so was H_c (20.9 compared to 10.7 in the reference entry, see Table 4.1). On the other side, with respect to O-6 selectivity, the ratio of $x_6/(x_2+x_3)$ increased for mannose units (from 0,54 to 2.52), while no significant difference was observed for glucose units (0.50 and 0.51). This result show that with acetone as co- solvent and at elevated temperature, the substitution of 2-OH and 3-OH were sufficiently decreased in M while no such change in G was observed. However, since the reaction mixture was heterogeneous under these conditions, visible also from the relative large H_c of the borate free sample, more experiments are required as basis for further conclusions.

In summary, the G/M-selectivity and the regioselectivity of the methylation of KGM was controlled by borate complexation. In contrast to the reference sample with similar DS of glucose and mannose, the presence of 40 equiv. borate leads to a product with twice the DS value for glucosyl compared to mannosyl residues at an average DS of 0.45. Furthermore, at elevated temperatures or in the presence of an aprotic co-solvent, the overall reactivity of OH groups in KGM could be enhanced. The DS ratio of G and M could be kept at about 2 at an average DS of 0.8. The regioselectivity in the mannosyl residues, favoring O-6 was reduced, however. This loss in regioselectivity was more pronounced at elevated temperature than by adding acetone.

In spite of the loss in regioselectivity, the diversity with respect to the molar fractions c_i in M and G, expressed as H_c (Table 4.1) could be further enhanced by temperature and solvent effects.

4.2.2 Oligomer analysis

In Chapter 3 which dealt with methylation of KGM in an aqueous system, we demonstrated that methyl groups were randomly distributed in the glycosyl units, and these partially methylated glycosyl units were randomly distributed over the polysaccharide chains.[12] The analytical strategy was to compare the methyl pattern of oligomeric domains with those calculated from the monomer composition (c_i).[82] Methyl glycans were fully alkylated with CH_3I-d_3 (→ DM-KGM), partially depolymerized to oligosaccharides, subsequently labeled with *m*ABA and then submitted to (HPLC-)ESI-MS to determine the methyl pattern in oligosaccharide fractions of various DP. Whether M and G are also randomly distributed along and over the KGM chain, could, however, not be established, since both, despite differences in regioselectivity, had similar molar fractions of un-, mono-, di- and trisubstituted units (c_i) which are the basis for the *m/z*-distribution in oligomers obtained from the MS analysis.[12,82] Thus, preparation of M-KGMs with largely different DS values for M and G units was not only of interest with respect to properties, but also for gaining some information on the distribution of M and G residues in the polymer. In any case, MS analysis of DM-KGM shall give insight how methyl groups are distributed over the polysaccharide chains.

M-KGM-13 and M-KGM-15 with DS_G/DS_M for both close to 2 at increasing average DS, and c_i diversity H_c of 12.4 and 16.7, respectively, were chosen for additional oligomer analysis. M-KGM-17, showing even larger differences in G and M (H_c 18.0) is also considered here in spite of the coagulation in the presence of acetone which might have caused additional heterogeneity. Methyl distributions in M and G were compared with the Spurlin[73] model for weighted randomness (i.e. considering various x_i). In contrast to the previous study,[12] there was a significant deviation (heterogeneity parameter H_1 0.8 – 3.1, see appendix), especially for M-KGM-15 and 17 ($H_1 > 2$). Since one prerequisite of the Spurlin model, that the reaction of all OH is independent from each other, is no longer fulfilled in the presence of borate, we also compared the methyl pattern of G and M to the model of Reuben[107] which considers an interdependence of the reactivity of positions 2 and 3. H_1 was reduced to values between 0.3 and 2.1 with values below 1 for M-KGM 13, 1.7 (M) and 1.5 (G) for M-KGM-15 and 0.7 (M) and 1.3 (G) for M-KGM-17. At highly selective reaction of one OH position (as here in M), no large deviation from statistics is possible, however, since there are nearly no products of consecutive reactions (no 23, 26 etc). So heterogeneity of M-methylation is not well estimated

in this case. That there is some heterogeneity over the material has to be kept in mind when discussing the results for the oligomeric domains.

Deuteriomethylated M-KGM (DM-KGM-13, 15 and 17) were partially depolymerized. ESI-MS spectra of *m*ABA-labeled *O*-Me/*O*-Me-d_3-oligosaccharides from DM-KGM were measured by direct syringe pump infusion, and the methyl patterns were evaluated for individual DPs separated according to their *m/z*. Results for DP 3 to DP 5 of M-KGM-13, (DS_{KGM} 0.45, DS_M 0.33, DS_G 0.64) and M-KGM-15, (DS_{KGM} 0.75, DS_M 0.55, DS_G 1.07) are illustrated in Figure 4.8 and compared with the random methyl pattern corresponding to randomly distributed M and G units, calculated from the molar fractions c_i (M) and c_i (G) for the entire M-KGM sample at the ratio of M/G 1.6 (for c_i see appendix).

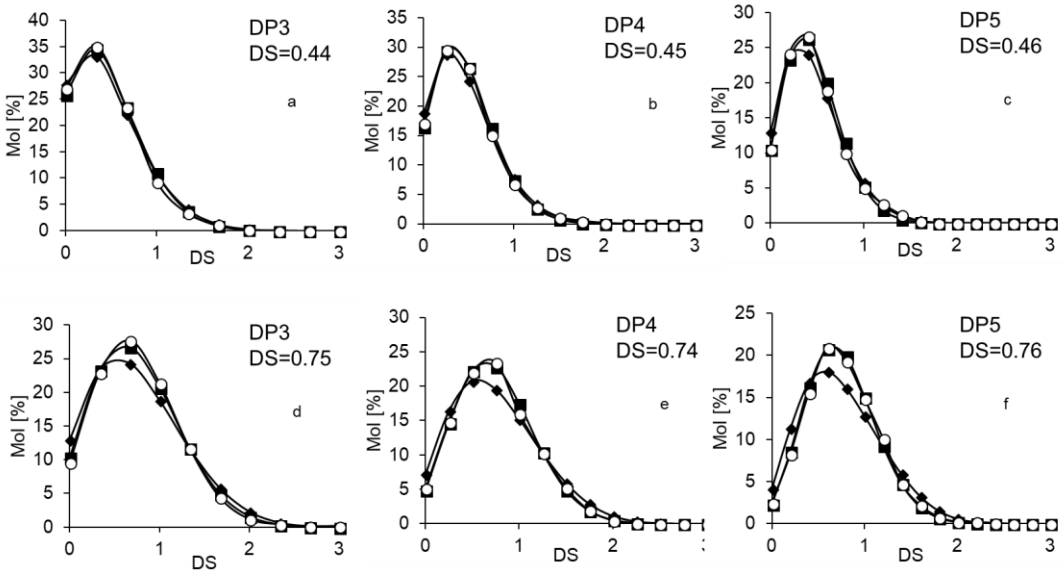

Figure 4.8. Comparison of theoretical methyl pattern of random GM (■) and di-block GM copolymer (♦), and experimentally determined methyl pattern (○) of DP 3-5 of: (a-c) DM-KGM-13 (DS_{KGM} 0.45, DS_M 0.33, DS_G 0.64; H_c 12.4), and (d-f) of DM-KGM-15 (DS_{KGM} 0.75, DS_M 0.55, DS_G 1.07, H_c 16.7), evaluated from syringe pump infusion ESI-MS data. M/G ratio of 1.60 and 1.62 (average value from monomer analysis) were used for the calculation of random and di-block model for DM-KGM-13 and 15, respectively.

It is known, that hydrolysis of mannosidic linkages is faster than that of glucosidic linkages ($k_M : k_G \approx 2$),[12,14,85]. However, since the DS obtained from the MS profile of a particular DP was equal or close to the expected DS for the natural M/G ratio (except DP 2), this ratio was taken for the model calculations. In addition to a random M-G distribution, the methyl distribution profile for a di-block copolymer of methyl-glucan and methyl-mannan was calculated. This is referred to the theoretical border case that one long mannan block and one long glucan block are linked to each other. Therefore, the profiles were calculated for the mannan part and for the glucan part and then these two were combined considering their

relative portions. The same trend is found for M-KGM-13 (Figure 4.8a-c) and M-KGM-15 (Figure 4.8d-f), but due to the larger absolute DS difference, the agreement with the random model rather than the block model is better visible for the latter.

Since M and G have different c_i portions and DS values, profiles calculated for random and di-block distribution of the two stereoisomeric sugar constituents differ from each other. As particularly visible for M-KGM-13 (Figure 4.8a-c) the theoretical profiles for these two extreme cases of G-M distribution do not differ much at low DP. When the DP increases, homo-glyco sequences would enhance the probability of low and high DS sequences and thus make the profiles more flat, while they become narrower in case of random distribution of M and G.

Obviously, methyl distribution profiles determined experimentally are in relative good agreement with the random model. Random means, random distribution of methyl groups in M and in G, and furthermore random arrangement of the M and G residues along and over the polymer chains. Due to the difference in DS related to the diversity in c_i, random and di-block distribution of M and G can now be differentiated. With increasing H_c and DP, the profiles (progressively) diverge. Therefore, differences are better visible for M-KGM-15 (H_c 16.7) and better for DP 5 than for DP 3. Since the glucomannan is a product of biosynthesis, the presence of alternating GM should also be considered. E.g. in alginates which are produced by the action of C5-epimerases on a primary formed β-1,4-D-mannuronate,[108] depending on the specificity of the enzyme, alternating and homogeneous blocks are formed. A more regular distribution of M and G in KGM, closer to alternating, would give a more narrow profile than a random distribution, because the variance of GM-sequences/DP is very low. A combination of alternating and block structures like in alginate would produce a more complex pattern with contributions of narrow and broad methyl profiles. Whether the resulting methyl profile could be distinguished from other patterns would again depend on H_c, DP and length of such blocks. Therefore, not only the methyl profile but the GM-composition should be considered which is available by LC-ESI-MS (see below). The di-block model is, however, an extreme and, in case of KGM, only theoretical case. Thus, the question arises whether shorter blocks could also be distinguished from a random M-G distribution. Therefore, MM and GG diades were considered as ‘macromonomers’ and a random distribution of DP 4 was calculated from these building blocks. Within these MM and GG units, methyl groups were assumed to be distributed randomly. In the same way, methyl profiles of DP 6 were calculated from homo-triades. These calculations show that for M-KGM-15 with H_c 16.7 and for M-KGM-17 with H_c 18, random and short blocks can be

differentiated by their methyl pattern in the oligosaccharides at ≥ DP 4, while for M-KGM-13 with H_c 12.4 this is only possible for ≥ DP 6, if the quality of experimental data is sufficient (see Figure 4.9). The experimental data are closer to random M-G distribution than to randomly distributed short M and G blocks.

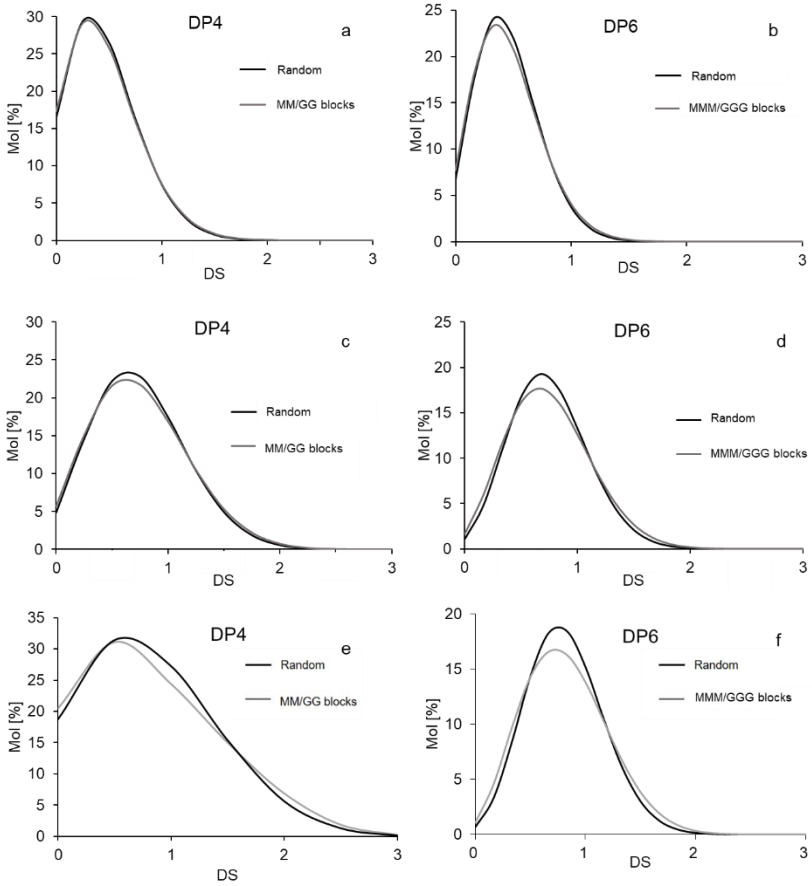

Figure 4.9 Comparison of random G-M (—) and short GG-MM/GGG-MMM blocks (—) in DP 4 and 6 of DM-KGM-13 (DS_{KGM} 0.45, DS_M 0.33, DS_G 0.64, H_c 12.4, a and b), of DM-KGM-15 (DS_{KGM} 0.75, DS_M 0.55, DS_G 1.07, H_c 16.7, c and d), and that of DM-KGM-17 (DS_{KGM} 0.81, DS_M 0.59, DS_G 1.18, H_c 18, e and f).

The experimentally determined methyl profile of DM-KGM-17 (DS_{KGM}=0.81, DS_M=0.59, DS_G=1.18) is broader than the random methyl distribution (as shown in Figure 4.10). This observation is different from the results obtained for DM-KGM-13 and 15. However, this does not mean that GM are arranged in a non-random manner that to in KGM backbone. As mentioned in the previous section, a heterogeneous methyl distribution of was obtained for the M-KGM prepared in water/acetone (H_1 2.3 (M), 3.1 (G) for M-KGM-17, as shown in Figure 4.6). Thus, a prerequisite to conclude the G-M arrangement from the methyl pattern in oligosaccharide sequences, a uniform methylation in both types of sugars, is not fulfilled. Therefore, one should be careful to compare this experimentally determined methyl distribution oligomer profile with the corresponding theoretical random distribution model calculated from the monomer composition determined from GLC (the model was calculated

based on the homogeneous substitution situation). Thus, the further discussion regarding the M/G distribution over the KGM chains is focused on the samples prepared in water with homogeneous substitution (M-KGM-13 and 15).

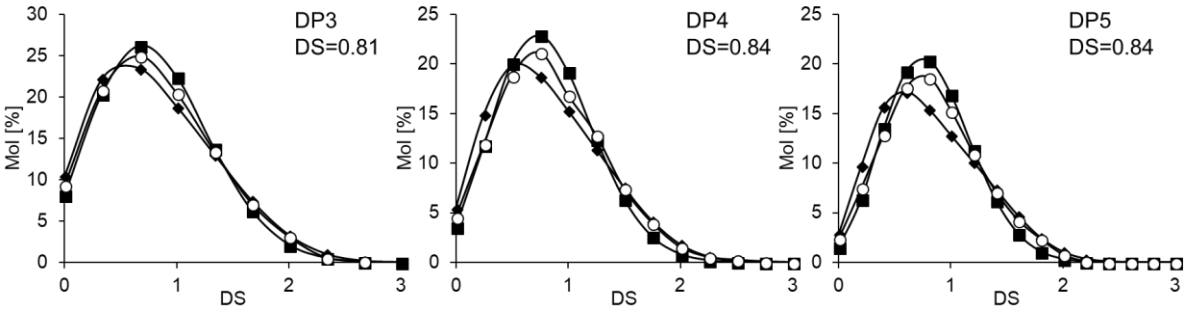

Figure 4.10. Comparison of experimentally determined methyl pattern (○) with the random methyl pattern of random GM (■) and with di-block GM copolymer (♦) and in DP 3-5 of DM-KGM-17 (DS_{KGM} 0.81, DS_M 0.59, DS_G 1.18; H_c 18), evaluated from syringe pump infusion ESI-MS data. M/G ratio of 1.64 (average value from monomer analysis) was used for the calculation of random and di-block model for DM-KGM-17.

The experimental data used in Figure 4.8 were obtained from ESI-MS measurements in which the samples were applied by syringe pump infusion. To analyze the hetero-oligosaccharide derivatives in more detail, LC-ESI-MS was applied to separate the constituents belonging to one DP prior to ESI-MS as has been described in Chapter 3. The chromatograms did not show peaks of homo-oligosaccharides above DP 2 (gluco-) or DP 3 (manno-), while at higher DP the most abundant oligosaccharides were of mixed type G_mM_n (n, m = 0, 1, 2... n+m = DP). This already indicates that the two sugar constituents are not organized in large blocks in the KGM chains. In spite of overlapping of peaks belonging to various DP,[12] retention times of all constituents of a particular DP can be assigned by generating extracted ion chromatograms (EIC) from the LC-ESI-MS run. The integrated areas of all peaks belonging to one particular DP were summed up, and the methyl distribution profile was evaluated. By this evaluation, the same methyl profile should be obtained as from syringe pump infusion ESI-MS, as shown in Figure 3.10 in Chapter 3 (DM-KGM-6, DS_{KGM} 0.80, DS_M 0.82, DS_G 0.77). This was not the case, however, methyl distribution determined by LC-MS occurred to be narrower compared to that obtained by MS with syringe pump infusion (as shown in Figure 4.11), while the average DS/DP does not differ much from syringe pump infusion data. How can this be rationalized? – Among other factors, ion yield in ESI-MS is influenced by the solvent composition and analyte concentration. In the reverse phase liquid chromatography separation (RP-LC-separation) of methylated oligosaccharides, the solvent composition (ACN/H_2O) necessarily changes with time as does the compound concentration over the peak elution time. This is usually no problem in the analysis of MCs, where the constituents of one DP elute in

one peak, with the higher deuteriomethylated representatives at the front and the higher methylated ones at the back.[82] In case of glucomannan, mixed isomers G_mM_n exist which elute over a wider range at various ACN/water ratio[12] and are thus measured under different spray conditions (for the gradient profile see Figure 4.12).

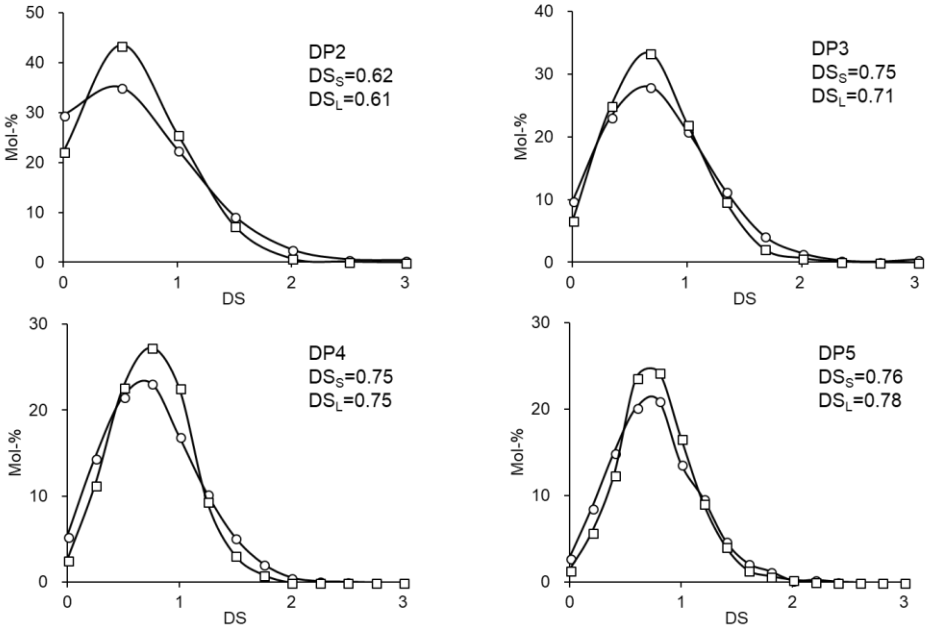

Figure 4.11. Comparison of experimentally determined methyl pattern in DP 2 - 5, evaluated from LC-ESI-MS data (□) or from syringe pump infusion data (○) of DM-KGM-15 (DS_{KGM} 0.75, DS_M 0.55, DS_G 1.07). DS values obtained from syringe pump infusion (DS_S) and from LC-MS (DS_L) are presented.

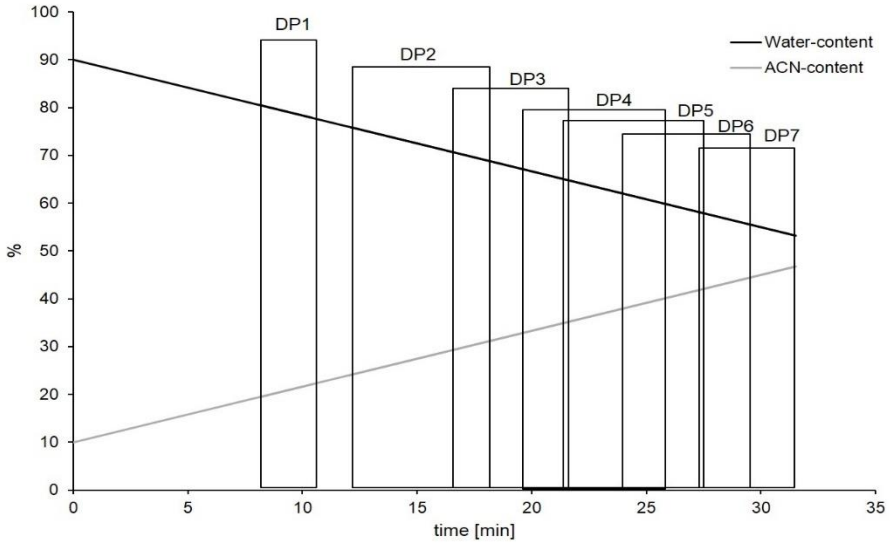

Figure 4.12. Gradient of HPLC-ESI-MS runs for DM-KGM-13, and 15.

Applying the samples by LC but at an ACN/water ratio prompting elution into the ESI source with nearly no separation showed a profile closer to that from syringe pump infusion. Beyond spray conditions, the ion yield of oligosaccharides of interest is important, but is assumed to

be comparable in negative mode, since the charge is located at the *m*ABA label. It should be mentioned here that mass spectra were also recorded in the positive mode during LC-MS and showed a different intensity profile for the disaccharides MM, MG, GM and GG. The constituents with terminal G-*m*ABA showed preferential sodiation, while for those with M-*m*ABA, $[M+H]^+$ dominates. While protonation most probably occurs at the nitrogen of *m*ABA, sodiation requires the interaction with several oxygens of the carbohydrate and thus also depends on the energy of appropriate conformations and thus from stereochemistry.[109] In contrast, all parameters are constant in syringe pump infusion, where spectra recorded under identical conditions are accumulated and averaged. In conclusion, the results from direct infusion and of negative ions are considered to be more reliable to reflect the actual methyl distribution and M and G arrangement in the polysaccharide chains.

In order to investigate the influence of the solvent on the quality of the mass spectra, DM-KGM-15 was measured in different solvent mixtures by syringe pump infusion. Depending on the quality of the spectra, the data from various measurements in different solvents of sufficient quality (referred to a certain DP) were averaged for the comparison with a calculated pattern for a random/di-block distribution (see Figure 4.8).

While the change of eluent composition with time could cause bias of ion yields for consecutive peaks and thus influence their relative ratio, such an effect can be neglected for the isotopomers belonging to a particular peak with defined M/G ratio, e.g. MM, MG, GM and GG which is only broadened due to less retention of deuteromethyl than methyl. Keeping this in mind, peaks of EICs generated from LC-ESI-MS runs and representing various M/G combinations of a particular DP were evaluated and compared with the corresponding theoretic model. For instance, by generating the EIC in the mass range *m/z* 546 – 564 (DP 2), four peaks were obtained (MM, MG, GM and GG), and the signals of mass spectra of these four peaks were evaluated to generate individual methyl substitution profiles as shown in Figure 4.13. GG and MM were assigned by the standards derived from cellulose and mannan. Since the mannosidic linkages are hydrolyzed faster than the glucosidic linkages, MG should be less than GM.[12]

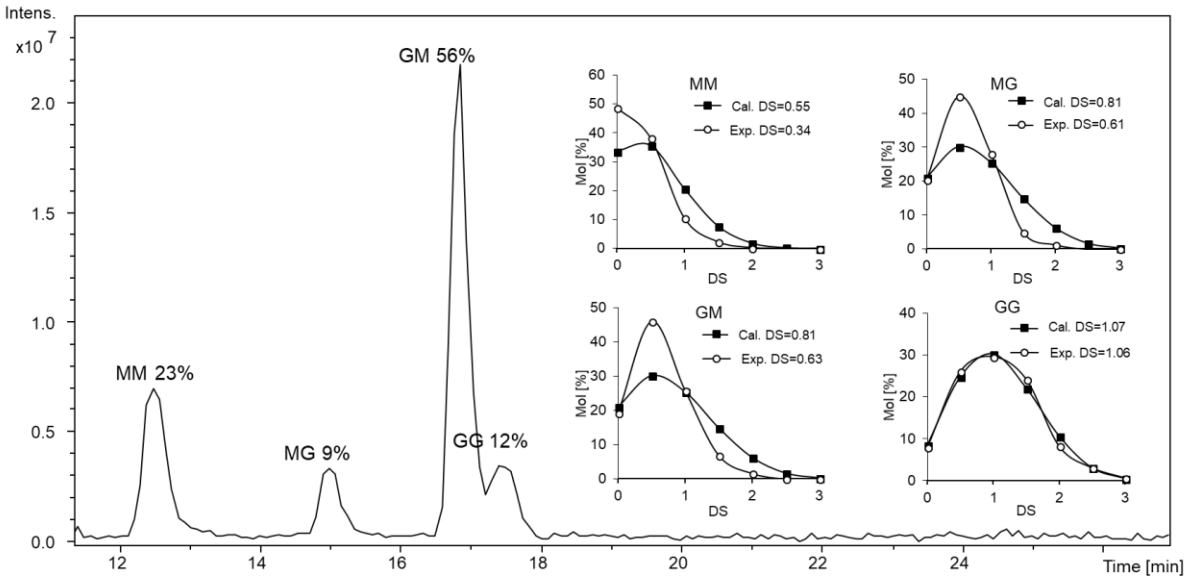

Figure 4.13. Comparison of experimentally determined (○) and calculated random (■) methyl pattern of four separated peaks (MM, MG, GM and GG) of DP 2, evaluated from the EIC (*m/z* 546 – 564) generated from LC-ESI-MS run of DM-KGM-15.

For randomly distributed M and G (M/G 1.62, determined by the alditol acetate method refer to EM-KGM-15), 38 % of MM, 24 % of MG and GM each, and 14 % of GG would be obtained in DP 2 if glucosidic and mannosidic linkages would be cleaved at the same rate. From the integrated areas of the individual peaks in EIC and in relative good agreement with the peak areas of the UV-chromatogram, portions of 23 % (MM), 9 % (MG), 56 % (GM) and 12 % (GG) were obtained in the DP 2 fraction of DM-KGM-15, as shown in Figure 4.13. For DP 3, four peaks were observed of which a very tiny one co-eluted with M_3 but none with G_3. For larger DP, due to peak overlapping, it becomes difficult to clearly distinguish and assign the individual peaks, but few mixed G_mM_n peaks always dominated. These results also support the assumption of a random M-G arrangement while a block-like structure can be excluded.

As discernable from Figure 4.13, however, the DS values experimentally determined for individual disaccharides with a defined composition of M and G did not agree with those calculated using the average DS of M and G. Only the DS and the methyl profile of GG was in agreement with theory, while the DS of all M-containing disaccharides was lower than expected. This was also the case for larger DPs which did not show distinct DS values in accordance with their particular number of M and G, but something in between. Therefore, the DS obtained from the methyl profile of a certain peak could not be used for reliable peak assignment. From comparison with oligosaccharides obtained from a permethylated β-1,4-

mannan and cellulose, only the retention time of M_n and G_m oligomers were known, and that elution of mixed G_mM_n occurs in the order of decreasing n and increasing m.

What is the reason behind these unexpected deviations from the calculated DS? All OH of M-KGM were methylated or deuteromethylated and the ratio of Me and Me-d_3 for a particular DP can be determined without discrimination in MS. Secondly, kinetic selectivity only refers to the manno or gluco configuration, but not to the methyl/deuteromethyl pattern. Thus, the MM disaccharides should, independent of their amount, exhibit the average DS of M. Therefore, the measured DS should be the real DS of the individual oligosaccharides. To find out what the reason for this DS deviation is, we estimated the DS of all individual G_mM_n oligosaccharides for each DP, as far as possible. This ascribed composition of the oligosaccharide peaks eluting between the known retention times of M_n and G_n is shown in Figure 4.14. Supposed DS values of M in G_mM_n were calculated on the basis of the DS found for the particular peak and the average DS of G. These are listed in detail in Table 4.2.

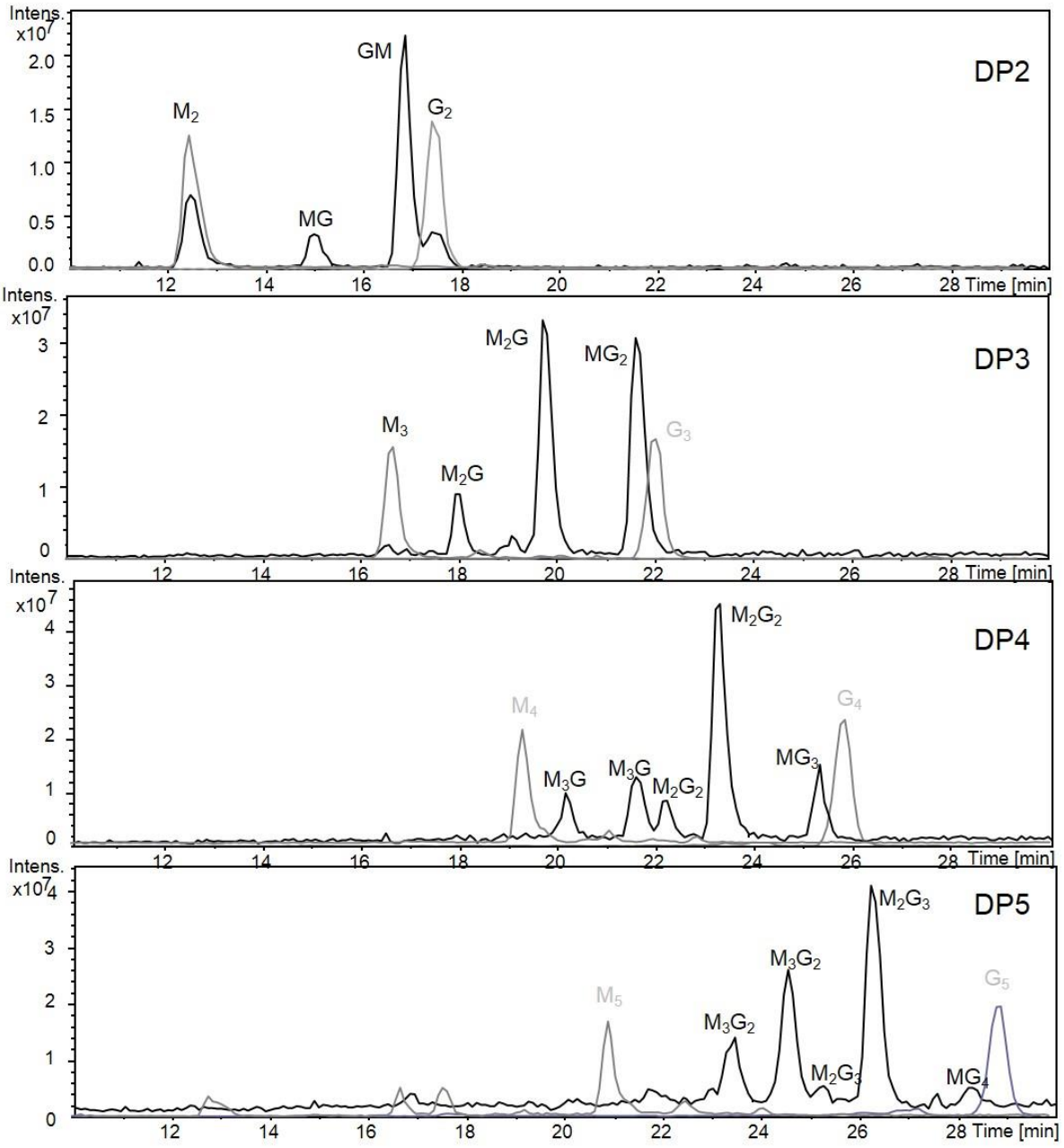

Figure 4.14 Extracted ion chromatograms of DP 2 (*m/z* 546 – 564), DP 3 (*m/z* 750 – 777), DP 4 (*m/z* 954 – 990) and DP 5 (*m/z* 1158 – 1203) generated from LC-ESI-MS run of DM-KGM-15, compared with the homo-oligosaccharides of DP 2 to DP 5 (manno- / gluco-) from LC-ESI-MS runs of DM-mannan and DM-cellulose, respectively.

Table 4.2. Peak assignment, the theoretic calculated DS based on the average DS_M and DS_G (from monomer analysis), and the calculated DS_M for each separated peak based on total DS (as determined from the EIC of the LC-ESI-MS run) and the average DS_G for DP 2 to DP 5 of DM-KGM-15.

DP	**Peak assignment**	**DS_{theory}**	**DS_{LC-MS}**	**n/(n+m) in G_mM_n**	**DS_M**
2	M_2	0.55	0.34	1.00	0.34
	MG	0.81	0.61	0.50	0.14
	GM	0.81	0.63	0.50	0.19
	G_2	1.07	1.06	-	-
3	M_3	0.55	0.31	1.00	0.31
	M_2G	0.72	0.57	0.67	0.32
	M_2G	0.72	0.62	0.67	0.40
	MG_2	0.90	0.84	0.33	0.37
4	M_3G	0.68	0.52	0.75	0.33
	M_3G	0.68	0.47	0.75	0.27
	M_2G_2	0.81	0.72	0.50	0.36
	M_2G_2	0.81	0.74	0.50	0.42
	MG_3	0.94	0.95	0.25	0.59
5	M_3G_2	0.76	0.66	0.60	0.39
	M_3G_2	0.76	0.67	0.60	0.41
	M_2G_3	0.86	0.85	0.40	0.51
	M_2G_3	0.86	0.82	0.40	0.44
	MG_4	0.97	0.96	0.20	0.50

Figure 4.15 shows the results for all peaks of DP 2 – DP 5. A trend is observed: The DS of M in G_mM_n decreases with n/(m+n), i.e. with the amount of M. How can this be explained?

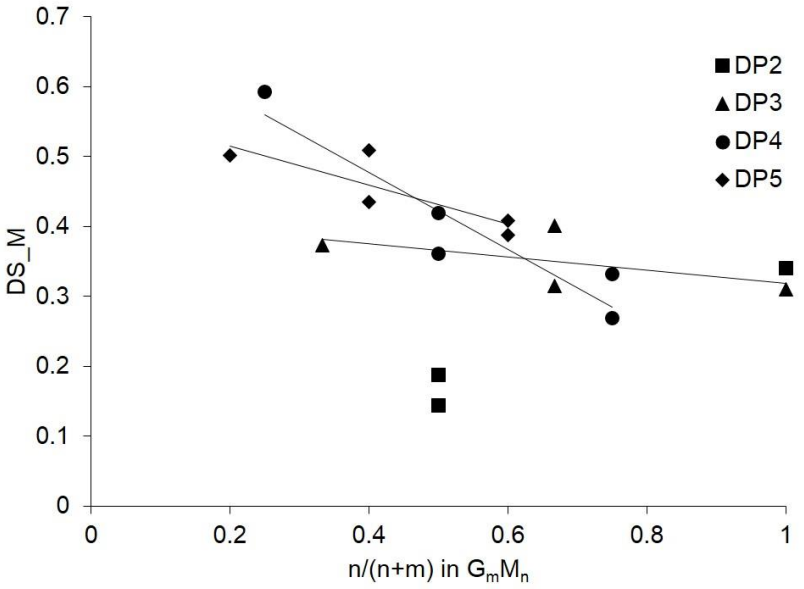

Figure 4.15. Calculated DS_M for each separated peak, based on total DS_{KGM} (as determined from the EIC of the LC-ESI-MS run) and the average DS_G (from monomer analysis) for DP 2 to DP 5 of DM-KGM-15.

Assuming a random M-G distribution for M/G=1.6, a certain probability of M blocks can be calculated (M_4: 14.3 %, M_5: 8.8 %, M_6: 5.4 %, M_7 3.3 %). These M blocks are called M-rich areas here. When borate was added to the aqueous solution of KGM, it formed a gel due to crosslinking by borate. When NaOH was added, viscosity decreases. Due to the chain-chain interaction,[110] borate-*cis*-diols crosslinks are assumed to be more favored with M from M-rich areas than with M adjacent to G.[32] Borate complexation (B) is a dynamic process. The probability to form a M-B-M crosslink is expected to be enhanced adjacent to another M-B-M crosslink, since the chains are already close to each other. Therefore, a cooperative effect, well known from the formation of junction zones in gel formation, is assumed which finally might cause a more efficient inhibition of methylation in mannose-rich domains compared to isolated mannosyl residues.

Furthermore, kinetics of hydrolysis has an impact on the DS gradient with DP (DP 2 to DP 6 for M-KGM-15, 0.64 → 0.75, data from direct infusion ESI-MS measurements, 0.61 → 0.78 from LC-ESI-MS). DS of DP 2 is always significantly lower than average. This might be caused by higher mannosyl content or more mannosyl units from M-rich areas, since mannosidic linkages are hydrolyzed faster. On the other hand, no such effect was found for G, where the DS of GG is in accordance with the average DS_G. One could argue that, if the lower DS values are found in small oligomers, higher DS are expected for higher oligomers to compensate the average DS in the entire sample (DS_{KGM}=0.75). This is what has been

observed. In contrast, in our previous studies on M-KGM prepared without borate, the DS of particular peaks was in agreement with theory.[12]

As mentioned in the introduction, literature data on the distribution of M and G in KGM is not in full agreement, although there is more evidence that points to a random distribution.[14,16] Nothing has been reported about the biosynthesis in KGM, however, more knowledge is available about the biosynthesis of glucomannans in gymnosperms[111] or legumes like mung beans[112] or peas.[113] Membrane located glycosyltransferases producing β-1,4-glucomannans accept GDP-mannose and GDP-glucose as well and link them in a random manner. In some cases[111,114] an additional 2-epimerase was observed which can invert GDP-mannose in GDP-glucose, but no post-modification of a primarily formed β-1,4-mannan has been described. Thus, at least for these related glucomannans, a random distribution of M and G in various ratios is feasible. From our studies, there is also a strong indication to a random distribution of M and G in KGM. However, due to a number of restrictions, comprising kinetics of hydrolysis, non-randomness of methylation due to no longer independent reaction of O-2 and O-3 of M in the presence of borate, and perhaps a more efficient suppression of methylation in M-rich domains, methyl profiles cannot be easily compared to model profiles based on random methylation to decide this question. It will be the subject of further studies, how the stereochemistry of the glycosyl units adjacent to mannosyl residues influences the inhibition of methylation by borate complexation.

4.2.3 TGA and DSC analysis

In order to investigate the relationship between the thermal behavior of M-KGMs and the methylation of M and G residues, KGM and M-KGM-13 (DS_{KGM}=0.45, DS_M=0.33, DS_G=0.64) and M-KGM-17 (DS_{KGM}=0.81, DS_M=0.59, DS_G=1.18) were studied by TGA and DSC measurements. For comparison, a partially methylated KGM prepared without borate in Chapter 3 (M-KGM-6, DS_{KGM}=0.80, DS_M=0.82, DS_G=0.77)[12] had been analyzed in the same way. The TGA thermograms are shown in Figure 4.16. All measurement involved two thermal degradation zones. In the first zone (< 125 °C), all samples lost the moisture with around 5 % to 10 % of the total weight loss. In the second zone (225 °C – 350 °C) (Figure 4.16a), a complex thermal decomposition region with two main overlapping peaks is visible in the 1st derivative curve as shown in Figure 4.16b. The D-glucosyl residues are more resistant to heat than the D-mannosyl residues.[86] According to the study of Moriana et al.,[86] in the DTG curve (Figure 4.16b), the first overlapping peak at 275 °C to 295 °C is considered to be associated to the M residues, and the second peak at 300 °C to 320 °C in the DTG curve is interpreted as the degradation of G units.

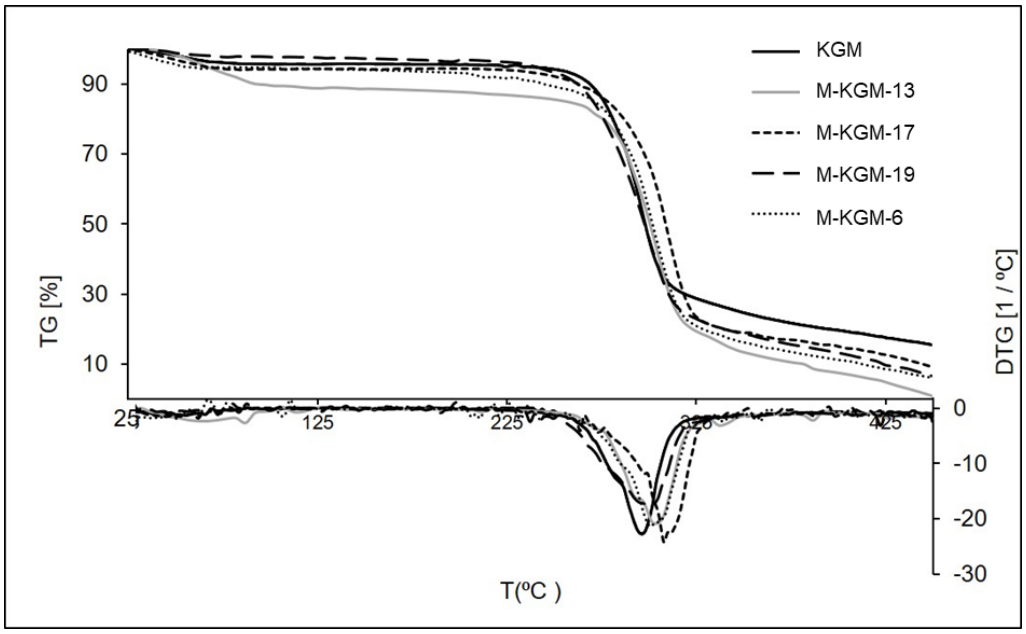

Figure 4.16. Comparison of TG (a)and DTG (b) curves for KGM and M-KGM-13 and M-KGM-17 and M-KGM-19 at 10 °C/min

TG profiles of M-KGM were changed compared to the starting material KGM. The chemical modification resulted in a less hydrophilic material. An increase of mass loss was observed in the main thermal decomposition zone (from 67 % to 76 %) as the DS increased. The decomposition temperature (i.e., its onset temperature) at 76 % of total weight loss for the M-KGM-13 (DS_M= 0.33, DS_G= 0.64) with average DS 0.45 was 284.9 °C was higher than that of KGM (277.0 °C). When the DS difference between M and G residues of M-KGM increased (DS_M=0.59, DS_G=1.18), as well as the average DS of the entire sample as for M-KGM-17 (DS 0.81), decomposition temperature increased to 290.6 °C. Similar results have been reported for a methylated KGM sample with DS 1.06 which had an onset decomposition temperature of 287.2 °C at a heating rate of 10 °C/min (the same as in this study).[86] For a M-KGM with the overall DS 0.80 and no significant difference in DS of M and G residues (DS_M=0.82, DS_G=0.77), the decomposition temperature was 287 °C (80 % weight loss).[12] Thus, the M-KGM with a higher DS_G (1.18) and a lower DS_M (0.59) (M-KGM-17), is thermally more stable than M-KGM-6 with the same DS but no difference in M and G units. Furthermore, the temperature of the first peak in DTG increased from 286 °C (M-KGM-6) to 300 °C (M-KGM-17), and for the second peak increased from 300 °C to 308 °C, as shown in Figure 4.16 b. This can be attributed to the higher thermal stability of higher methylated G residues. Moreover, the partial DS at position 6 (x_6) in M residues increased from 0.34 to 0.36, and from 0.37 to 0.41 in G residues (M-KGM-6 → M-KGM-17).

Thus, there are less free 6-OH available for intramolecular nucleophilic attack at C-1 and subsequent chain breaks under formation of 1,6-anhydro sugars.[87]

DSC test for KGM, M-KGM-13, and 17 were performed as well. Unfortunately, no clear glass transition temperature (T_g) was visible in DSC thermograms. During the heating and cooling process, these samples showed similar DSC curves.

4.3 Conclusions

Borate was successfully applied as a stereo- and consequently topo-selective reagent to control the methylation of KGM in water or water/acetone with NaOH/CH_3I. Borate forms reversible complexes with diols in KGM, with higher stability for *cis*-2,3-diols (M) compared to *trans*-2,3,-diols (G). With increasing equivalents of borate/KGM, the overall DS decreases compared to borate-free reference samples, predominantly at O-2 and O-3 of M, but also, but to a lower extent at O-6 of G residues. M-KGMs with a DS difference up to 100 % between M and G at an average DS of 0.81 were obtained. From the ESI-MS measurements of *m*ABA-labeled partial hydrolysate of DM-KGMs, best agreement of the experimental data with random M-G distribution was found, while large blocky structures and strictly alternating arrangement could be excluded. From LC-ESI-MS analysis of oligosaccharides with defined composition (G_mM_n), it was concluded that borate-mediated inhibition might have caused a lower degree of methylation in M-rich areas compared to isolated M (cooperative effect).

5 Stannylene-acetal-mediated Regioselective *O*-Methylation of KGM

5.1 Introduction

In polysaccharides different relative reactivities of the OH groups are expected. For instance, the regioselectivity follows acidity of OH (2 > 6 > 3 in cellulose) and in addition sterical requirements (primary alcohols are better accessible for the nucleophiles). In Chapter 3 of this thesis, an order of relative reactivities, G-k_6 > M-k_6 > G-k_2 ≈ M-k_2 > M-k_3 > G-k_3 was described for a series of partially methylated KGM (M-KGM), obtained in NaOH/CH_3I in an aqueous system while maintaining a constant pH 13.6.[12] However, the average DS of the two epimeric constituents was very similar. Since the distribution of substituents along the macromolecule chains would also influence the properties of polysaccharide derivatives (besides the average DS of the polymer), we were interested to make use of the difference in stereochemistry (*cis*/*trans*-diols in M/G residues) to achieve higher and lower methylated regions in KGM chains. Such a toposelective derivatization is not possible for a homoglycan like cellulose. In Chapter 4 of this thesis, the employment of borate for the selective protection of the *cis*-diol in M and thus preferred methylation of G in KGM was presented. M-KGM with an average DS up to 0.8 and a DS ratio for G and M of 2 were obtained.

In the field of carbohydrate chemistry, dibutyltin oxide and bis(tributyltin) oxide have been widely used for regioselective derivatizations, mainly benzylation and acylations for intermediate protection in oligosaccharide synthesis.[115,116] The advantage of regioselective activation as compared to classical regioselective derivatizations is the more convenient manipulation without deprotection step, and the high regioselectivities achieved.[115,117] Dibutyltin oxide reacts with *cis*-diols to dibutylstannylene acetals, often performed *via* the tin dimethoxide acetal formed from Bu_2SnO in refluxing methanol.[118] Afterwards, this five-membered ring carbohydrate intermediate (2,2-dibutyl-1,3,2-dioxastannolanes) usually reacts with alkyl-, aryl- or acyl halides in an aprotic solvent (such as *N*,*N*-dimethylformamide (DMF), ACN or dioxane) to form ethers or esters, respectively.[92] Which of the two oxygens involved in the stannylene preferentially reacts, depends on the stereochemistry and stability of the formed stannylene derivatives.

Dibutyltin oxide and bis(tributyltin) oxide are toxic and harmful for the environment as well as for humans. For instance, dibutyltin oxide is a powder, therefore, it can easily be transported through the air, and can be absorbed by the skin, or the respiratory mucosa.

Damage of the central nervous system results upon absorption of large amounts, yielding to symptoms such as headaches, earaches, dizziness and loss of orientation. Furthermore, repeated exposure leads to liver damage and genetic material.[119] Interestingly, despite the high-toxic feature of tin derivatives making the industrial applications difficult, there is still some research done with respect to their use in carbohydrate chemistry.[120–122] However, the advantage of this method should not be neglected. The tin intermediates are easily prepared, and the regioselective alkylation methods are reliable and high-yielding.[123] Moreover, it can be carried out under mild reaction conditions (e.g. without the addition of a strong base) and subsequently yields less side reactions. The reaction sequence of diols with dibutyltin oxide is shown in Figure 5.1.

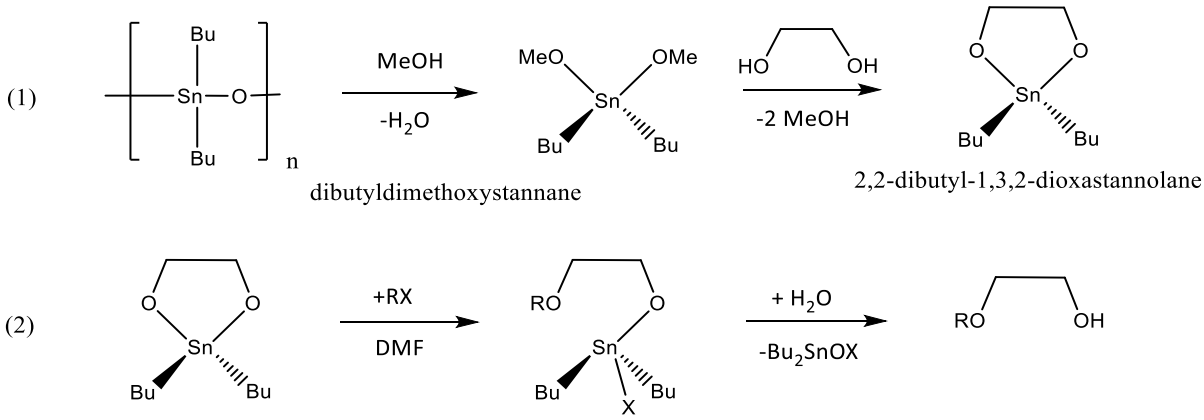

Figure 5.1 Monoalkylation of diols via transient dibutyl stannylene

The mechanism of regioselective substitution by means of bis(tributyltin) oxide is different from that of dibutyltin oxide. By refluxing of an alcohol mixture with hexabutyldistannoxane in benzene or toluene and azeotropic removal of water, tributylstannyl ethers are formed.

Dibutyltin oxide

We therefore were interested in the influence of dibutyltin oxide on the regioselectivity of methylation of KGM and whether we can obtain a methylated KGM with large difference of DS in M and G units. Application of tinoxides to polysaccahrides has not been reported in the literature. Due to the regioselective activation of mannosyl units with its *cis*-diol features, higher substitution is expected in M while low substitution in G (no *cis*-diols exist).

In 1974 Wagner et al. reported the application of dibutylstannylene acetals for regioselective derivatization (e.g. benzoylation or tosylation)of ribonucleosides (as shown in Figure 5.2).[92] Obviously, with different reagents (benzoyl chloride or tosyl chloride), opposite activation of 2'- or 3'- oxygen was observed. No explanation of this behavior was provided at that time.

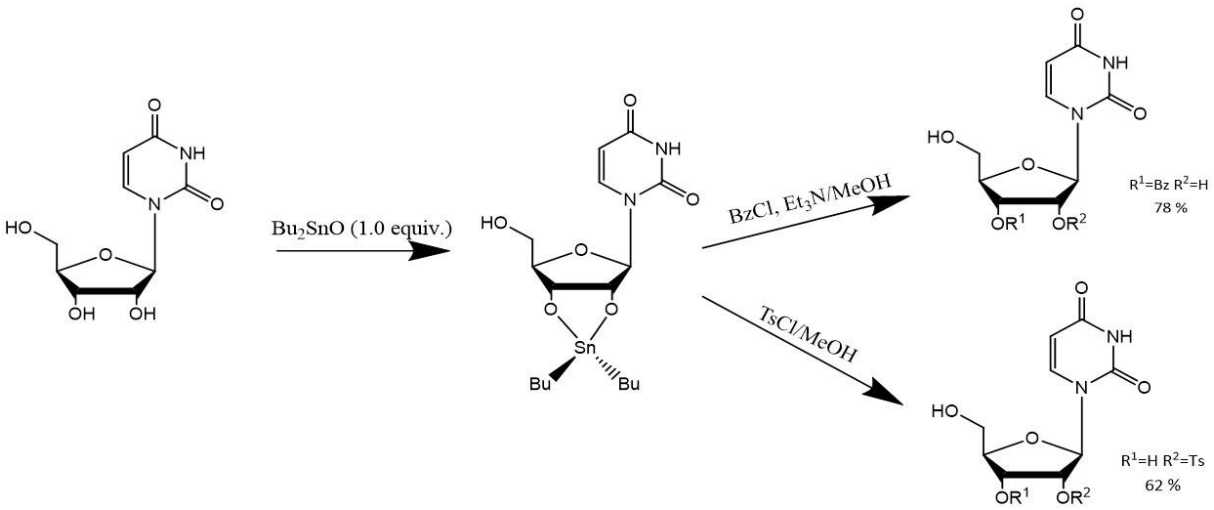

Figure 5.2 The first use of dibutyltin oxide for regioselective esterification (modified after ref. 124).

Haque et al. applied this method for the derivatization of non-protected glycopyranosides (methyl α-D-galactopyranoside, methyl α-D-mannopyranoside, methyl α-D-glucopyranoside and methyl β-D-glucopyranoside) and obtained monoalkylated and monoacylated products, respectively.[93,125] Some examples of selective reactions are listed in Table 5.1. A preferential formation of dioxastannolanes with *cis*-vicinal diols was observed, followed by alkylation or acylation, respectively. The introduced substituent was more likely located at the equatorial than at the axial position involved in the stannylene acetal). For instance, O-3 was substituted with high selectivity in both, Me-Gal (*cis*-3,4- diol) and Me-Man (*cis*-2,3- diol). The steps of regioselective alkylation of some non-protected glycopyranosides are presented in Figure 5.3. One can clearly see improved selectivity in dioxane compared to DMF in Table 5.1. Here four parameters need to be considered: stereochemistry of the substrate, solvent, derivatizing reagent, and equiv. of Bu_2SnO used. Table 5.1 shows that in methyl α-D-glucopyranoside O-2 substitution is preferred, whereas in the β-anomer O-6 dominates. In methyl α-D-glucopyranoside, the glycosidic methoxy group is in *cis*-relationship to the 2-OH group (as shown in Figure 5.3 (3)) and thus can stabilize the stannylene and promote functionalization at O-2. In contrast, the corresponding β-D-glucopyranoside lacks such an anomeric stabilization (Figure 5.3 (4)). Instead, a stannylene is formed involving the primary OH group and the ring oxygen, yielding mainly 6-*O*-substituted products. In methyl α-D-mannopyranoside, O-3 is preferentially activated and subsequently substituted due to its *cis*-2,3-diol structure (as shown in Figure 5.3 (2) and Table 5.1).

Table 5.1 Molar composition of the products obtained from methyl glycopyranosides in alkylations and acylations of their dibutylstannylene acetals with various alkyl, aryl or acyl halides in various solvents.[93,125] 1.5 Equiv. of Bu_2SnO/glycoside were used in all entries.

	Solvent/	Monosubst./%			Disubst./%	DS
Substrate	Reagent (equiv.)	O-2	O-3	O-6		
Me-α-D-Glc[1]	Dioxane / BnBr (6)	55	18	-	23 [mix]	1.19
Me-α-D-Gal[1]	Dioxane / BnBr (6)	-	71	-	-	0.71
Me-α-D-Glc[1]	Dioxane / CH_3I (18)	41	32	-	20 [2,3]	1.13
Me-α-D-Glc[1]	DMF / BnBr (6)	-	-	-	32 [mix]	0.64
Me-α-D-Glc[1]	ACN / BnBr (6)	56	6	-	9 [mix]	0.80
Me-α-D-Glc[1]	Dioxane / AcCl (1.5)	61	15	-	10 [2,3]	0.96
Me-α-D-Glc[1]	ACN / AcCl (6)	36	-	-	14 [mix]	0.64
Me-α-D-Glc[2]	Dioxane / BzCl (1.1)	76	-	-	6 [2,6]	0.88
Me-β-D-Glc[2]	Dioxane / BzCl (1.1)	-	-	86	-	0.86
Me-β-D-Glc[1]	Dioxane / BnBr (6)	30	8	24	-	0.62
Me-β-D-Glc[1]	Dioxane / CH_3I (18)	6	10	41	-	0.57
Me-α-D-Man[1]	DMF / BnBr (6)	12	47	-	18 [mix]	0.95
Me-α-D-Man[1]	Dioxane / AcCl (1.5)	30	47	-	21 [2,3+3,6]	1.19

[1]Data refer to ref.93
[2]Data refer to ref.125.

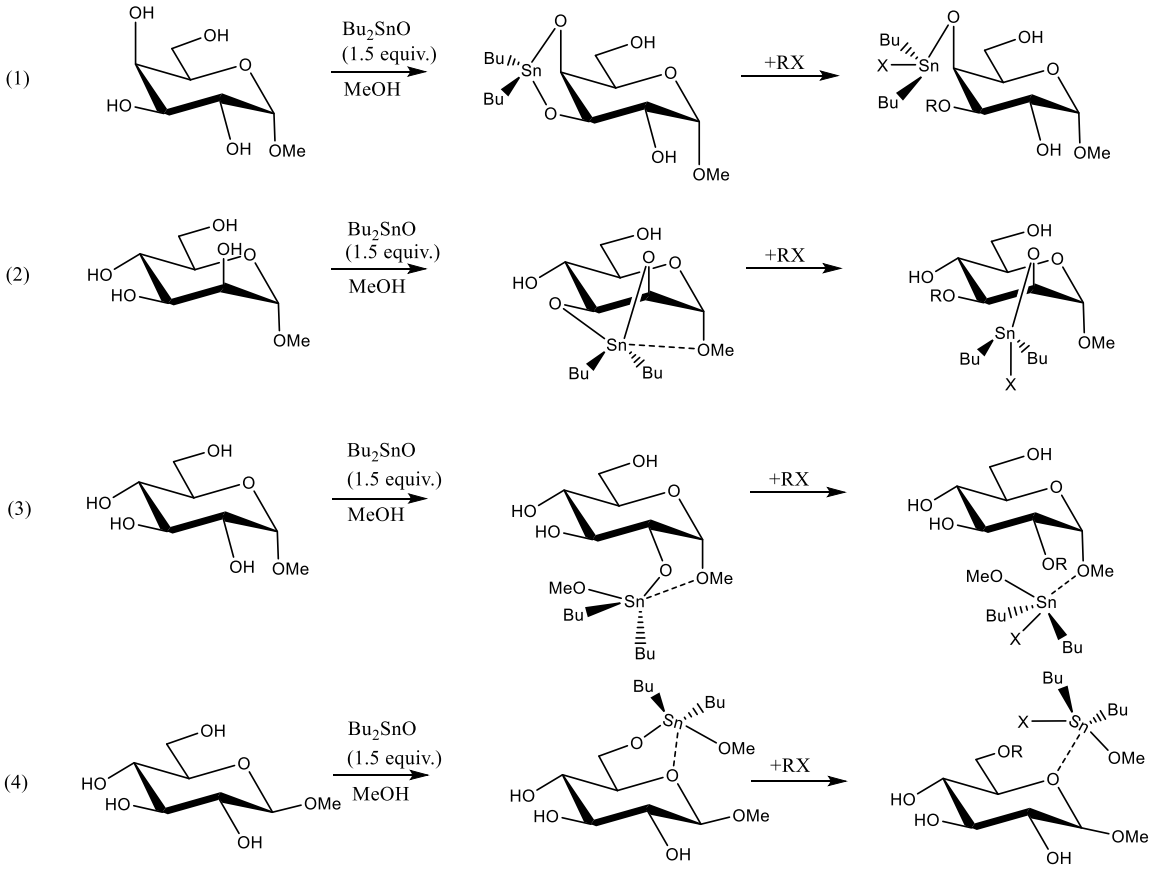

Figure 5.3 Regioselective alkylation of various methyl D-glycopyranosides *via* reactive stannylene intermediates: (1) methyl α-D-galactopyranoside, (2) methyl α-D-manno-pyranoside; (3) methyl α-D-glucopyranoside; (4) methyl β-D-gluco-pyranoside (modified after ref. 72.

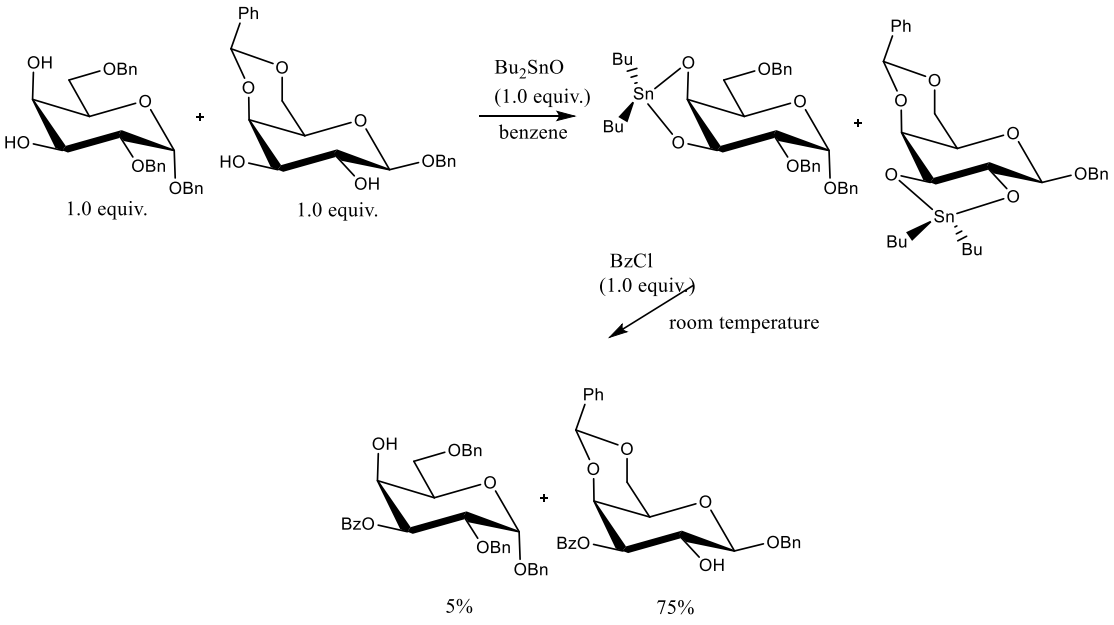

Figure 5.4 Competition experiment: equatorial O-3 of dibutylstannylene acetal of Gal-3,4-*cis*-diol is less reactive than of the Gal-2,3-*trans*-diols (modified after ref. 126).

While formation of stannylenes from *cis*-diols is usually found to be preferred to that of *trans*-diols, a competition experiment reported by David et al.[15] showed a contrary behavior. They observed that subsequent stannylation and benzoylation of 2,6-*O*-protected α- and 4,6-*O*-protected β-D-galactopyranosides preferentially yielded the 3-*O*-benzoate of the 4,6-*O*-benzylidene derivative where only a *trans*-diol group had been available (product ratio 1:15), as can be seen in Figure 5.4.[126]

Beside transformations with stoichiometric amounts,[93,125,127] catalytic methods have also been developed to facilitate the purification of the products. Xu et al. obtained 70-94% isolated yields for equatorial-benzylation products of *cis*-diol using 0.1 equiv. Bu_2SnO in stannylation of the diols and polyols containing *cis*-vicinal diol units.[128] When an excess of Bu_2SnO (2-3 equiv.) was used in regioselective benzoylation of carbohydrates, di- and tri-*O*-benzoylated glycosides were obtained in high yield at room temperature (i.e. 22 ºC, 93% yield of 3,6-di-*O*-Bz) or at a higher reaction temperature (100 °C, 93% yield of 3,4,6-tri-*O*-Bz) including galactosides, glucosides, mannosides and lactosides.[129] The authors found that a fast migration of Bz from position O-3 to O-4 occurred in the presence of excessive amount of Bu_2SnO and BzCl.[129]

Zhang et al. reported that the equatorial OH group, which was *cis* to an adjacent axial OH group, was much more reactive than another equatorial OH which was *trans* to an adjacent equatorial OH group (e.g. O-3 > O-2 in galactoside, O-3 > O-4 in mannoside).[129] The low reactivity of the axial oxygen in the *cis*-dioxastannolanes can be further explained by their steric shielding of the butyl groups. As opposed to this, the equatorial positions are easily accessible for possible reaction partners. It can be assumed that the size of the electrophile used is also important for regioselectivity, i.e. the less bulky the reagent, the better it can react with the equatorial positions.

Besides the application of Bu_2SnO to monosaccharides, work on some partly protected disaccharides[120,130–132] and short oligosaccharides[133] (up to DP 4) has been reported. Conversion of methyl β-lactoside is displayed in Figure 5.5.[131,132] Another interesting experiment was reported by Ballell et al.[120] They applied microwave irradiation (MW) to both, the stannylation and alkylation step and obtained efficiently a 3'-*O*-alkylated lactoside in 80% yield, as shown in Figure 5.6. Obviously, reactivity of the unique and well-accessible *cis*-diol is superior in allowing selective benzylation of the galactosyl side (compare Figure 5.4) Xia and Lowary reported that a certain extent of methylation at O-2 was observed in the derivatization of octyl 6,6'-di-*O*-benzyl-mannobioside and the homolog trisaccharide with Bu_2SnO.[133] They assumed that the steric hindrance mainly caused by

bulky substituents at the terminal O-4' reduces the expected 3-*O*-selectivity. The 2-*O*-selectivity was most pronounced in the case of tosylation.[133]

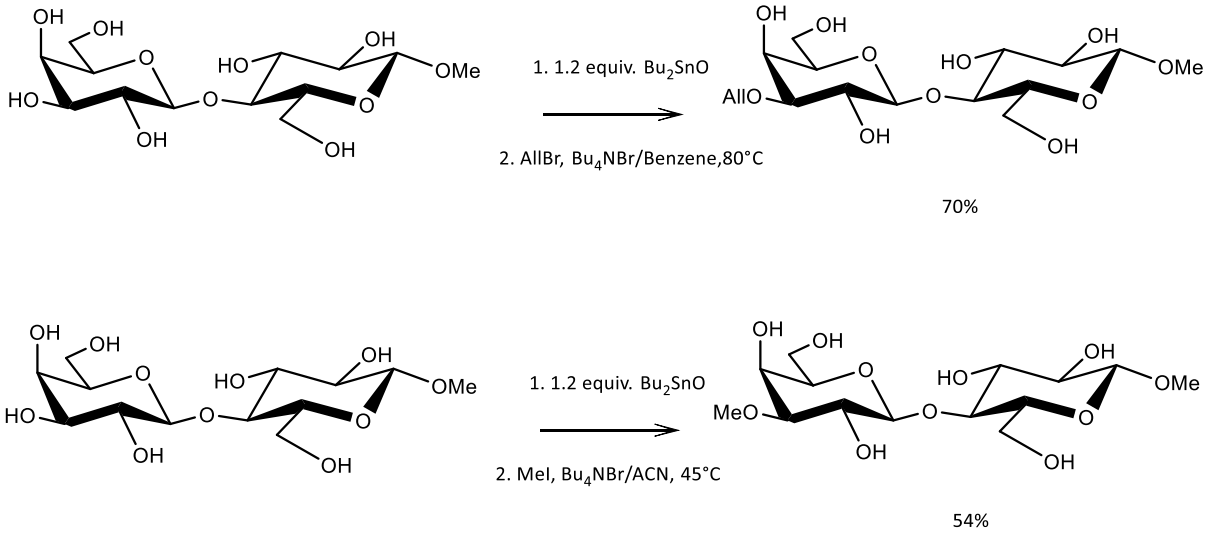

Figure 5.5 Regioselective reactions of methyl β-lactoside in stannylene-mediated alkylations (modified after ref. 124).

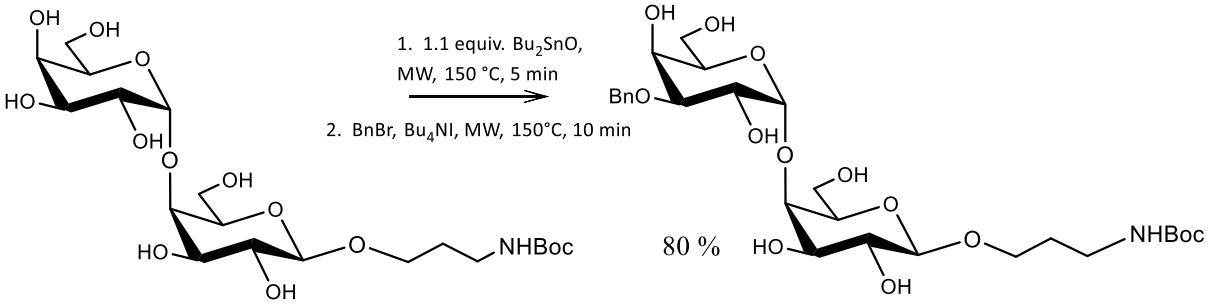

Figure 5.6 Regioselective reaction of an α-1,6-linked digalactoside in $SnBu_2O$-mediated benzylation under microwave irradiation (modified after ref. 120).

Mechanism of selective acylation or alkylation in tin-promoted reactions is complex and has so far not been fully clarified. By means of ^{119}Sn NMR-spectroscopy, Grindley et al. investigated and characterized dimers and larger oligomer associates of the dibutylstannylene acetals derived from *trans*-1,2-diols on six-membered rings in solutions.[134] In a dimer, two oxygen atoms of the stannylenes are di-coordinated and two are tri-coordinated. The tin atoms are arranged in a distorted trigonal bipyramidal geometry with the butyl groups being arranged equatorially. The tri-coordinated oxygen atoms are equatorially to one and axially to the other tin atom, while the di-coordinated oxygens are arranged apically. Since the two OH groups in a *trans*-diol of a carbohydrate are more likely to be both equatorially oriented, the formation of several dimers is possible. Thus, according to this theory, the result of the

reaction also depends in a complex manner on the equilibria of these dimerizations or oligomerizations, and relative rate constants of all the reactions involved.[135] In contrast, Ramström et al. reported that the ax/eq selectivity usually obtained is only controlled by the stereoelectronic effects of the parent diol structure, showing the similarity to the participation of adjacent groups, ester migration, or Sn-catalyzed transesterification of orthoesters.[123]

On the other hand, enhancement of nucleophilicity of the oxygen by the addition of nucleophiles (e.g. tetrabutylammonium iodide) to stannylene acetal solutions in non-polar solvents has been reported to significantly enhance the degree of conversion with electrophiles.[136] In the presence of catalytic amounts of tetrabutylammonium bromide (TBAB, 0.1 equiv.), and potassium carbonate (K_2CO_3, 1.5 equiv.) in Bu_2SnO/ACN/DMF/BnBr, very good yields for the benzylation of the equatorial OH groups in *cis*-diols (85% 3-O-Bn for methyl α-D-mannoside, and 87% 3-O-Bn for methyl α-D-galactoside) were achieved.[128] The proposed mechanism of this catalytic regioselective benzylation is presented in Figure 5.7. In the dibutylstannylene acetal with two adjacent OH groups of the carbohydrates, a catalytic amount of TBAB (0.1 equiv.) was applied to brominate and thus penta-coordinate the tin atom. The selective Sn-O bond cleavages and consequently 3-*O*-benzylation is favored by this penta-coordination. Therefore, a moderate amount of K_2CO_3 (1.5 equiv.) was applied as proton scavenger, promoting the nucleophilic attack of the activated oxygen species to an electrophile to generate a benzyl substitution and transfer the stannylene group to a new substrate molecule for the next reaction cycle. Furthermore, regioselective *O*-benzylation of primary positions have successfully been performed with catalytic amounts of Bu_2SnO under solvent free conditions (DIPEA/BnBr/TBAI).[137]

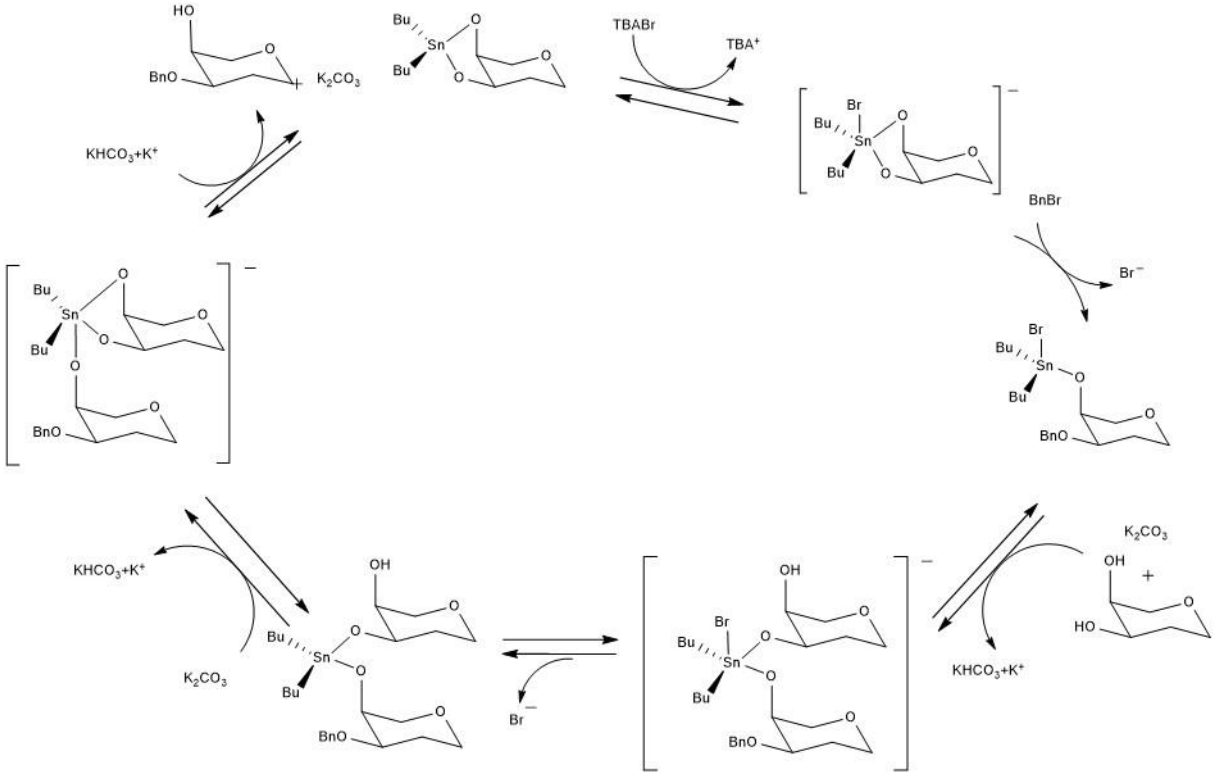

Figure 5.7 Proposed mechanism for the benzylation of a dibutylstannylene acetal intermediate (*cis*-diol) formed by dibutyltin oxide (modified after ref. 128). TBAB and K_2CO_3 were added as additive.

Bis(tributyltin) oxide

Regarding the regioselective substitution *via* tributylstannyl ethers, there is a similar influence on the subsequent substitution reaction by the stereochemistry of substrates and some of the results are listed in Table 5.2.[138,139]

Table 5.2 Overview of the product composition after formation of tributylstannyl ether intermediates with listed methyl aldohexopyranosides and benzylbromide as reagent.[138,139] Yields in % of theory are given.

Substrate	Solvent/ Reagent	Monosubst.			Disubst.	Trisubst.
		2	3	6		
Me-α-D-Glc[1]	BnBr	-	-	49	31[2,6][2]	-
Me-β-D-Gal[3]	BnBr	-	-	24	49 [3,6]	-
Me-α-D-Man[3]	BnBr	-	-	-	81 [3,6]	11 [3,4,6]

[1]Data refer to ref.138.
[2]As minor products, methyl 3,6-di-*O*-benzyl-α-D-Glc and methyl 4,6-di-*O*-benzyl-α-D-Glc were isolated in 4.5% and 6.0% yield, respectively.[138]
[3]Data refer to ref.139.

As shown in Table 5.2, the presence of bis(tributyltin) oxide led to a strong activation of O-6. Moreover, large amounts of di-substituted methyl glycosides were detected whose

substitution patterns were influenced by the stereochemistry of the OH groups involved in the tin-intermediate. Transformation of the methyl manno- and galactopyranosides resulted in an activation of the 3-OH and thus to a similar regioselectivity as in the case of the dibutyltin oxide method. If no *cis*-diol is present as in methyl α-D-glucoside, the *cis*-relationship of the methoxy group at the anomeric center also favored reactivity at O-2, e.g. in case of methyl 4,6-*O*-benzylidene-α-D-glucopyranoside.[140] When tributylstannyl ethers were formed from the compound containing more free OH groups (especially free 6-OH), the primary OH groups were preferably substituted (the 6-*O*-tin ether formed from a hexopyranoside was stabilized by coordination with the ring oxygen)[139], similar to dibutylstannylene acetals mentioned above (Figure 5.3(4)).

Ogawa et al. suggested that the formation of the butyltin ethers was related to their stabilization by neighboring oxygen atoms in appropriate arrangement.[139] A stability order is shown in Figure 5.7, for the example of methyl α-D-mannopyranoside. By employing bis (tri-*n*-butyltin) oxide, Migdal et al. prepared tributyltin ester of CM-KGM by attaching the organotin group to the side chain of the polymer.[141] The resulting products were proved to inhibit the in vitro growth of some yeasts and fungi varied directly with the Sn content (e.g. *Candida albicans, Cryptococcus neoformans A*).

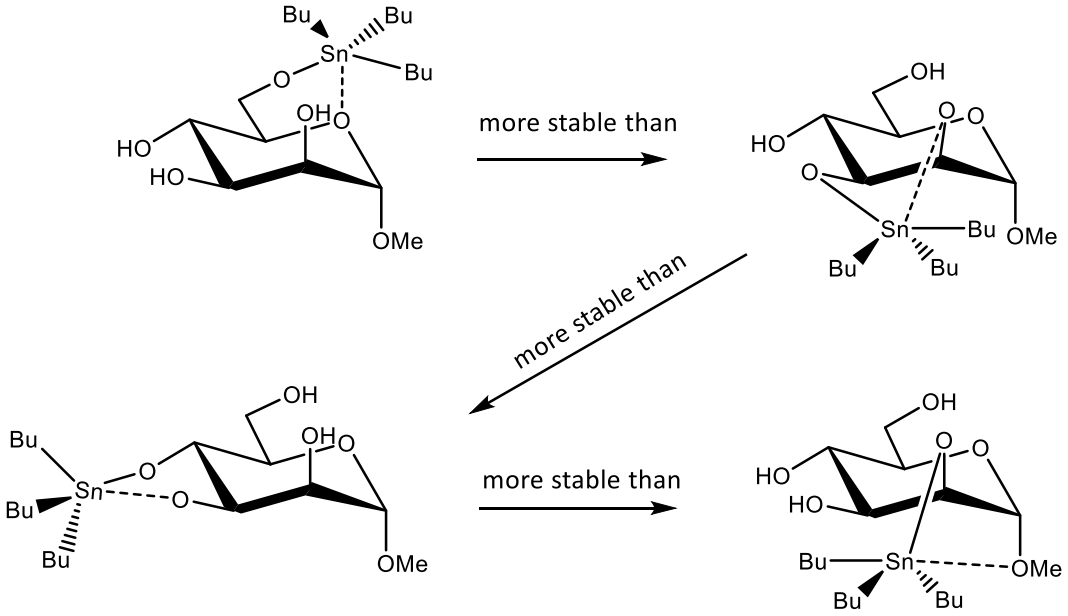

Figure 5.7 Order of stability of the tributyltin ethers of methyl α-D-mannopyranoside (modified after ref. 142).

As described above, dibutyltin oxide and bis(tributyltin) oxide have been well-studied with respect to their regioselective etherification or esterification of monosaccharides and their derivatives, while the reactions of stannylene acetals have attracted more attention than those of tributylstannyl ethers. The two tin-intermediates induce different reactivities of the OH

groups in carbohydrates which in addition are affected by the particular reaction conditions. However, all the results on the reactions of organotin compounds with carbohydrates described above are related to monosaccharides or short oligosaccharides. To the best of our knowledge, no application of Bu_2SnO to a polysaccharide has been reported so far. Therefore, we were interested in the influence of dibutyltin oxide on the regioselectivity of methylation of KGM and whether we can obtain a methylated KGM with large difference in DS of M and G units. Due to the regioselective activation for mannose units with their *cis*-diol feature, higher substitution is expected in M than in G (*trans*-diol) in the entire KGM polymer chains as demonstrated in Figure 5.8. Consequently, an uncommon pattern compared to Williamson alkylation should be generated.

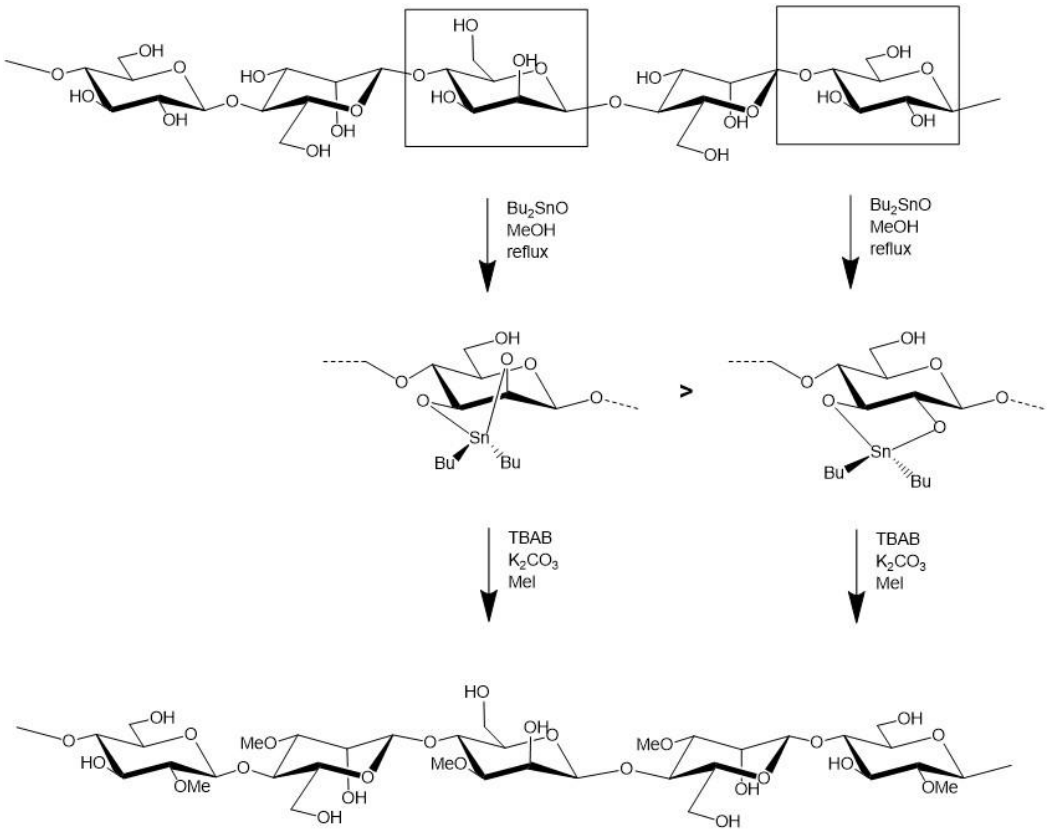

Figure 5.8 Possible stannylene acetals of KGM with that of the *cis*-diol in mannosyl residues being more stable than that of the *trans*-diol in glucosyl units, and preferred methylation in M-KGM.

However, the methods and reaction mechanisms for the mono- and disaccharides cannot be directly transferred to polysaccharides (such as KGM) due to the poor solubility of the polymers in commonly applied solvents. H-bonds between polysaccharide chains and sterical requirements will cause different behavior and lower reactivities. The following study on alkylation of KGM after treatment with dibutyl tin oxide was carried out to answer the following questions: (1) Can the polysaccharide KGM be converted to stannylene-KGM? (2)

Does stannylation of KGM allow subsequent methylation? And if so, (3) to which extent and in which positions does methylation occur?

Most of the experiments of the studies presented and discussed in the this chapter have been performed by Janick Raßloff in his diploma work.[72,143]

5.2 Results and discussion

5.2.1 Outline

In this study, we focus on the application of dibutyltin oxide in the methylation of KGM. To monitor the degree and regioselectivity of methylation in *O*-methyl-KGM, the products of stannylation and methylation sequences will be depolymerized and the constituents analyzed by GLC/FID as has been described earlier (see Chapter 3). An overview of the steps of preparation and analysis of M-KGM is shown in Scheme 5.1.

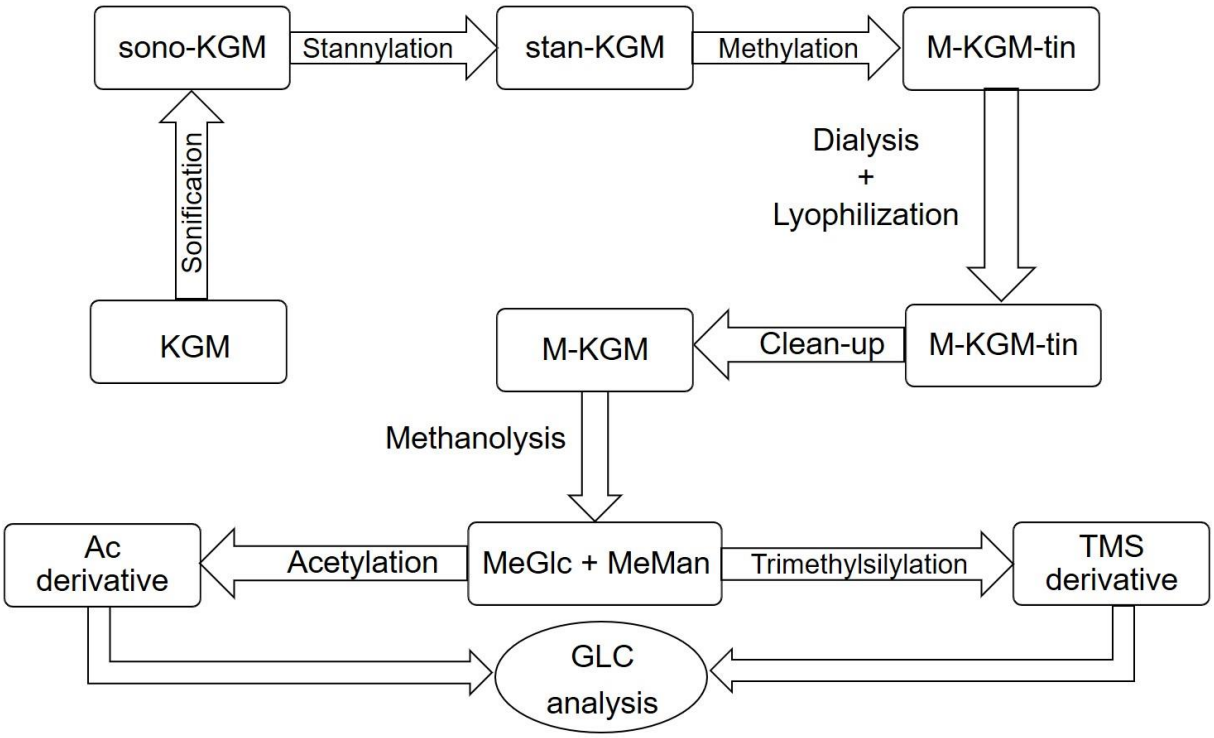

Scheme 5.1 Procedures applied to the preparation of regioselective methylated KGM and analysis of methyl patterns in M-KGM.

In the first step, as discussed in chapter 3, the high average molar mass of the starting material was reduced by ultrasonic treatment, thereby reducing the dispersity and improving the solubility.[144] The resulting material is called sono-KGM, which subsequently was boiled with dibutyltin oxide in various solvent systems under reflux with the goal to form dibutylstannylene acetals. Subsequently, the solvents and the generated water were removed by a rotary evaporator. AT-IR spectroscopy was applied in order to check the degree of stannylation of KGM (stan-KGM) by shift of the maximum of the OH vibration to higher

wave numbers, usually observed when H bonding is interrupted by protection of OH. However, shifts were so small that not consistent results were obtained. Hereafter, the stan-KGM was reacted with methyl iodide in different solvent. The product, M-KGM-tin (still containing tin reagent) was purified by dialysis, followed by lyophilization. Since the non-soluble dibutyltin oxide cannot be removed by dialysis, an additional clean-up step was performed, an extraction by repeated boiling the raw product in MeOH and removing the solution of $Bu_2Sn(OMe)_2$ from the non-soluble M-KGM. From the purified M-KGM ATR-IR spectra were recorded to check whether methylation has occurred.

For the analysis of the methyl pattern in glucosyl and mannosyl constituents, M-KGM was completely methanolized to methyl glucosides and mannosides, a portion of which was subsequently acetylated and trimethylsilylated for GLC analysis, respectively.

5.2.2 Monomer analysis by methanolysis method

As described in chapter 3, for methyl substitution pattern analysis, the alditol acetate method (AAM) is often applied.[36] The advantage of AAM is that this method could halve the number of peaks in GLC chromatograms by reduction of the anomeric position. It has been successfully applied in previous two studies.[12,145] However, to avoid side reaction during the hydrolysis and subsequent work-up, perethylation of the remaining free OH groups needs to be performed prior to depolymerization, especially at very low DS. Moreover, AAM is very time-consuming. Here we were interested to monitor a huge number of entries, varying several parameters of synthesis. Therefore, we needed a faster procedure and decided to apply methanolysis, sufficient for getting a first impression on the influence of the dibutyltin oxide on methylation of KGM. As presented in Chapter 3, there are two types of derivatization for the depolymerized KGM, trimethylsilylation (TMS) and acetylation (Ac). During the analysis of the monomer composition by the evaluation of the gas chromatograms of these two derivatives, it turned out that nor TMS-ethers nor acetates of *O*-methylated α- and β-gluco- and mannosides are fully separated. But fortunately, different types of peaks are overlapping (see Figure 3.4 in Chapter 3). Thus, it was possible to make a full evaluation by using the information from TMS to evaluate the ratio of unseparated Ac derivatives and vice versa.

Both methods showed similar average DS and methyl distribution.[72] However, among TMS derivatives the peak of 3-*O*-methyl mannoside co-eluted with 3,6-Me-Mann whereas this important constituent was fully separated in case of acetyl (see Figure 3.4b in Chapter 3). Thus, these data are used and the ratio of non-separated glycoside acetates (α-G2 and α-G3, α-G6 and β-M6, α-G23 and α-M23, and β-G23 and α-M26) were taken from the GLC

evaluation of the TMS derivatives (Figure 3.4b in Chapter 3) for the GLC evaluation of Ac derivatives (Figure 3.4a in Chapter 3).

5.2.3 Starting condition for stannylation and methylation of sono-KGM

5.2.3.1 Ultrasonic treatment of KGM to increase the solubility in organic solvent

To obtain an efficient reaction, the solubility of the substrate is an important parameter for accessibility and thus a successful reaction. As mentioned in the introduction, due to the polymer character (M_w = 1 ×10^4 to 1.9 ×10^6)[8] and the H-bonds between the polysaccharide chains, KGM is hardly soluble in water, where it forms a homogeneous viscous gel, while it is even less soluble in polar aprotic organic solvents commonly used for carbohydrates, e.g. DMSO or DMF.[9,59] As mentioned in the introduction, stannylation of diols with Bu_2SnO requires water-free conditions. Methanol has often been used due to the formation of the less stable but soluble dibutyltin dimethoxide as intermediate.[92] Furthermore, toluene and benzene have often been used, however, these procedures require significantly longer reaction times and are associated with azeotropic distillation (or adding molecular sieves towards the end of the reaction to remove the generated water).[124,134] These solvents are neither appropriate for polysaccharides. Therefore, to improve its solubility, KGM was partially depolymerized by sonification (sono-KGM). In contrast to alternative partial deploy-merization by enzymes or acid hydrolysis, ultrasound causes disruption in the middle of sufficiently long polymer chains, thus avoiding the formation of low DP degradation products like in random processes. Moreover, ultrasonication reduces the molecular weight of polysaccharides without resulting any change in the chemical structure of the polysaccharides during cavitation.[146]

After the ultrasonic treatment of a stirred aqueous KGM suspension in a vial, a clear solution was obtained (not viscous as before). After dialysis and lyophilization, white, cotton-like material is obtained which can easily be re-dissolved in water or even DMSO.

The amounts of the native KGM and the recovery of the sono-KGM are listed in Table 5.3. Due to a MWCO of 14 kDa the molecular weight of the sono-KGM should be at least 14 kDa (DP ~ 86), even it will be much higher. Schittenhelm et al. reported that a limiting molar mass of 40000 g/mol was obtained after they sonicated hydroxyethylsulfoethyl celluloses (DS_{SE} 0.27) for four hours.[147] The lost weight after lyophilization could be attributed to be the loss of moisture.[148]

Table 5.3 The weight of native KGM (not dried) and sono-KGM (lyophilized) and the recovery after ultrasonic degradation.

Batch	KGM [g]	Sono-KGM [g]	Recovery yield [%]
1	1.919	1.738	91
2	0.36	0.33	92

5.2.3.2 Stannylation of KGM

As mentioned in the introduction of this chapter, polysaccharides are not soluble in any of the common solvents used for stannylation (i.e., MeOH, benzene or toluene[124,134]). This would not matter if the reaction would start under heterogeneous conditions and solubility thus would increase over the course of the reaction. Various solvents and solvent mixtures were tested for solubility of sono-KGM. An overview of these tests is given in Table 5.4.

Table 5.4 Solubility tests with sono-KGM in different solvents under stirring and the behavior after adding Bu_2SnO. Test 1 - 5 was performed in 100 mL round flasks and test 6 to 11 in 4 mL V-vials.

Test	Sono-KGM [mg]	Solvent (mL)	Solubility after 24 hours	Solubility after adding Bu_2SnO[1]
1	20	MeOH (15)	white coarse suspension	no change
2	10	ACN (10)	white coarse suspension	no change
3	11	DMSO+MeOH 2:1 (15)	sedimentation	white layer on the surface of the mixture
4	10	DMSO+MeOH 1:1 (10)	sedimentation	white layer on the surface of the mixture
5	11	DMSO+ACN 1:1 (10)	sedimentation	white layer on the surface of the mixture
6[2]	2	Dioxane (2)	turbid fine suspension	-
7	2	t-BuOH + MeOH (2)	turbid coarse suspension	-
8	2	t-BuOH + Dioxane (2)	white coarse suspension	-
9	2	t-BuOH + n-BuOH (2)	white coarse suspension	-
10	2	toluene (2)	virtually no solubility	-
11	2	pyridine (2)	clear solution	-

[1]The situation of the mixture which was directly adding Bu_2SnO.
[2]Test 6 to 11 was carried out by Janick Raßloff.[72]

With respect to the solubility of sono-KGM, methanol is not a good option. From our experience, DMSO is a better solvent for sono-KGM than methanol as well as ACN, however,

it could not dissolve Bu_2SnO at all, even after adding some methanol. In contrast to small carbohydrate substrates, the solubility of KGM from the beginning is more important since otherwise it is not accessible and will not undergo any reaction (no formation of KGM-tin intermediates). Thus, a suitable solvent need to be found to make the structure of KGM accessible and undergo dissolution during the stannylation reaction. From our tests in Table 5.4, all solvent except pyridine did not dissolve but in the best case disperse KGM. To judge the success of the reaction, DS of each M-KGM was analyzed after subsequent treatment with CH_3I in different solvent with or without catalyst. As will be seen from the results in Table 5.5 given below, pyridine was indeed the best solvent to achieve any reaction.

After stannylation, stan-KGM was obtained by removing the solvent (e.g. methanol, pyridine, etc). Figure 5.9 shows the ATR-IR spectra of the starting materials, sono-KGM and dibutyltin oxide, while Figure 5.10 shows the spectra of the products. The strongly enhanced C-H stretching vibration between 2850 and 2960 cm^{-1} in the spectrum of stan-KGM is mainly caused by the butyl groups in dibutyltin oxide still present. Stannylation should cause a shift of the maximum of OH absorption at 3347 cm^{-1} for the starting material to higher wave numbers due to the decrease of H-bonds between OH. A slight shift was observed as can be seen for stan-KGM-21 at 3363 cm^{-1}, however shifts were small and not consistent with DS of methylation finally obtained.

The excess of Bu_2SnO remained in the products of stan-KGM after the methylation, even after dialysis against water. Since Bu_2SnO will form dibutyltin dimethoxide in hot methanol, raw M-KGM was suspended in methanol in a pressure-sealed V-vial and heated in an oil bath (80 ^{0}C) for 30 min. Afterwards, the supernatant was carefully removed by a syringe from the solid polysaccharide. As depicted in Figure 5.11, successful purification could be confirmed by the significant decrease in the C-H stretching vibration between 2850 and 2960 cm^{-1}.

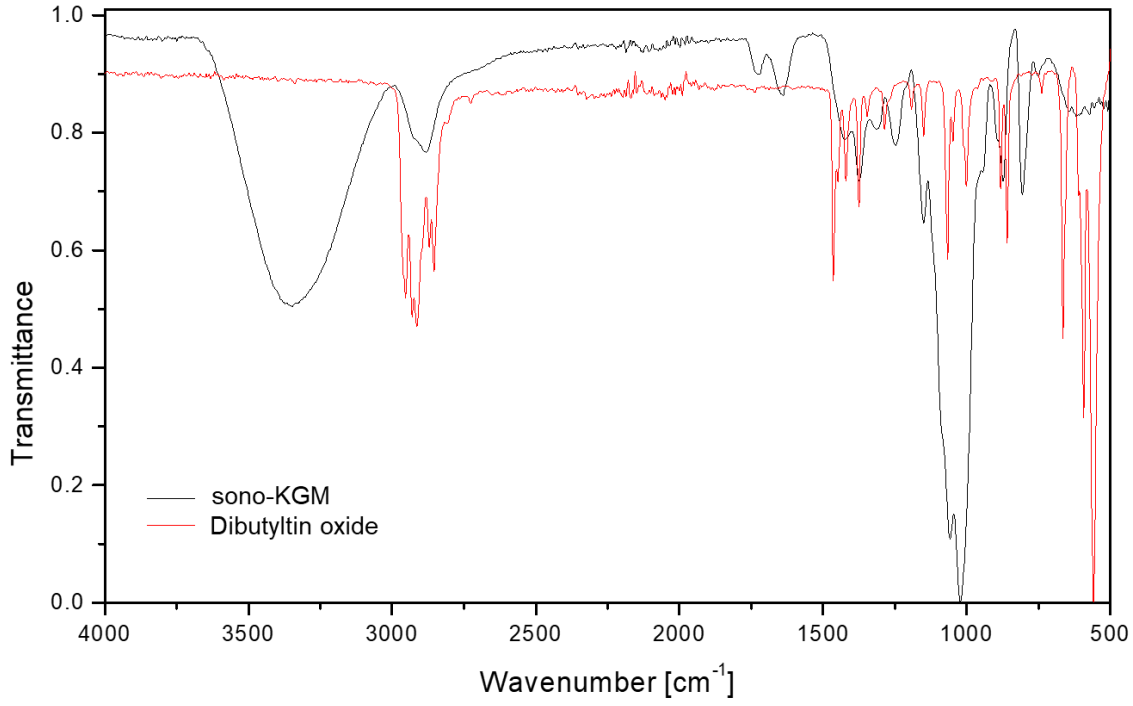

Figure 5.9 IR spectra of sono-KGM and dibutyltin oxide (max (OH) = 3347 cm^{-1})

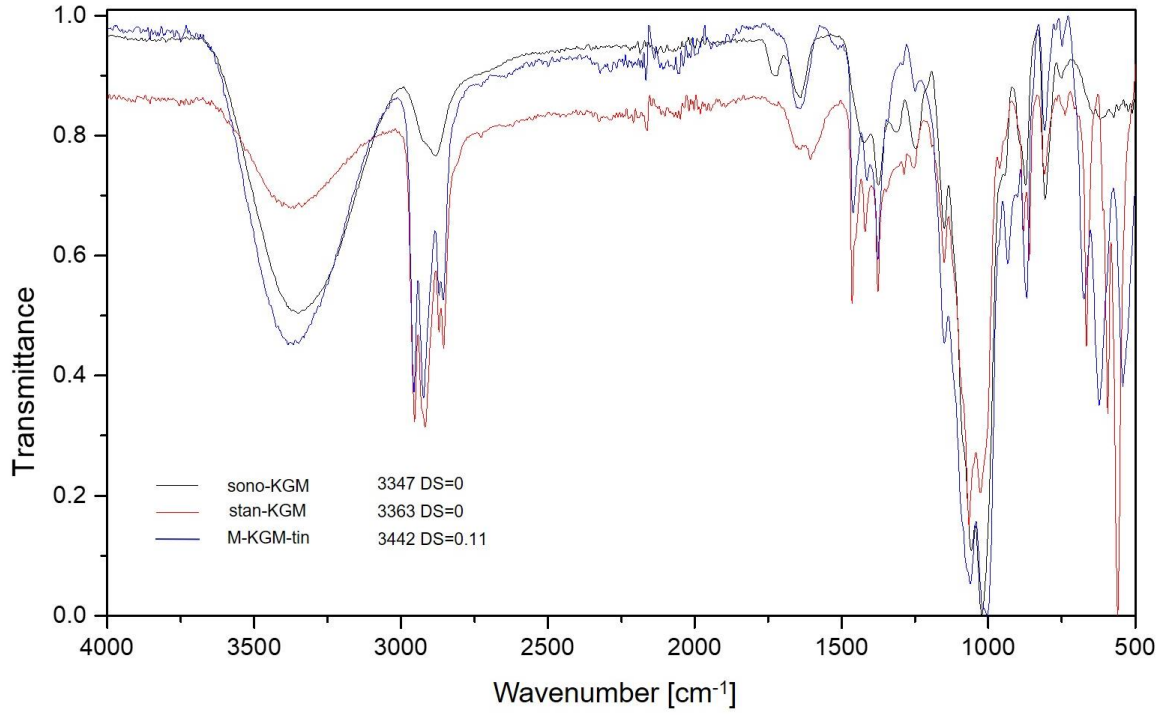

Figure 5.10 IR spectra of sono-KGM, stan-KGM-21 and M-KGM-21 (dialyzed raw product including Bu_2SnO. DS values were determined by MeOH/Ac method. Samples preparation was carried out by Janick Raßloff.[72] (max (OH) = 3442 cm^{-1})

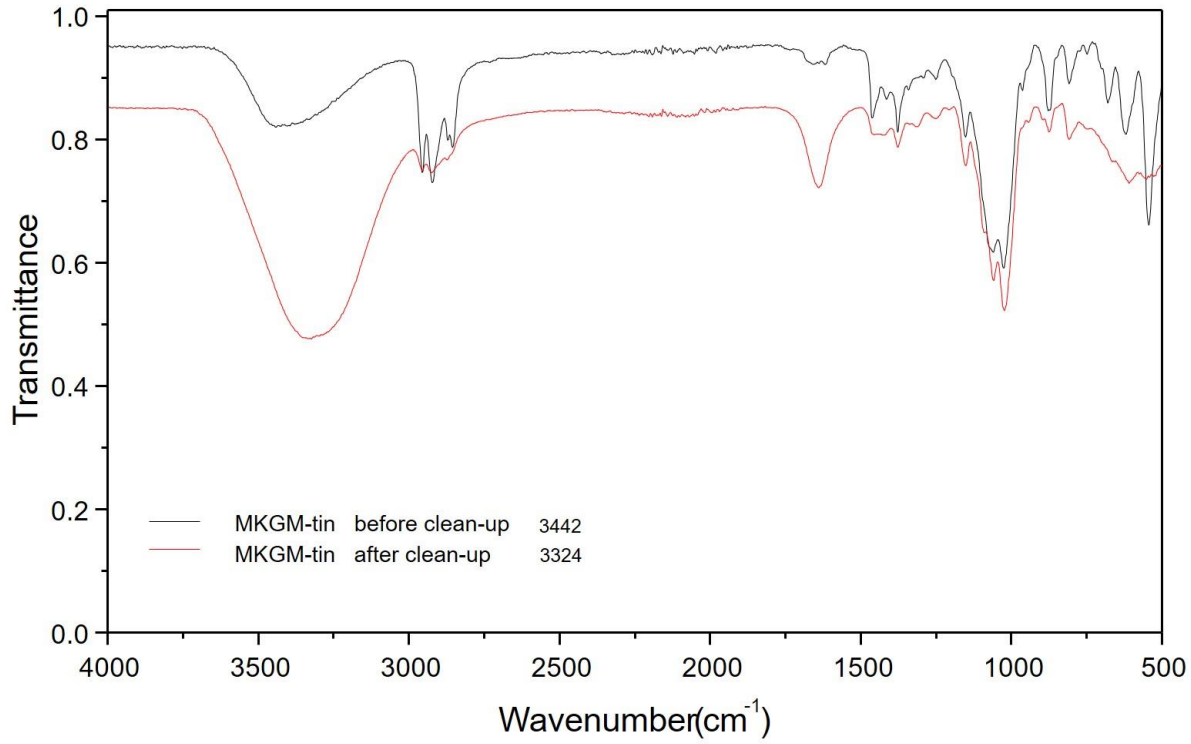

Figure 5.11 IR spectra of M-KGM-21 before and after purification by extraction with hot methanol. Experiments were carried out by Janick Raßloff.[72]

5.2.3.3 Methylation of stan-KGM

ATR-IR spectra of stan-KGM samples from various entries indicated that reaction has happened, but probably only to a very low extent. Therefore, it was important to perform methylation of stan-KGM in a subsequent step, and further apply methanolysis on the products (MKGM-tin) to check whether regioselective methylation *via* stannylene acetals was successful. In the preliminary experiments, some parameters have been studied, for instance, solvent for stannylation, application of Bu_2SnO (as powder or partly of transformed to dibutyltin dimethoxide in methanolic suspension), and methylation conditions (solvent, reaction temperature, time). However, all entries showed very poor reactivity with DS_{KGM} in most cases below 0.06. With 0.11 the best result was obtained (M-KGM-21) when KGM was dissolved in pyridine for stannylation. In many cases the solvent used for stannylation would also be used in the subsequent alkylation step (benzene,[126] benzene/ACN mixture (5:1)[120]). However, some researchers performed alkylation in a different solvent , for instance in DMF,[149,150] dioxane[151] or a mixture of DMF/ACN[128]. Thus, for methyl α-D-glucopyranoside a much higher substitution was obtained in dioxane (DS 1.19) compared to DMF (DS 0.64)[93] as has been mentioned in Table 5.1 in the introduction of this chapter. David et al. had suggested that addition of nucleophiles promotes the reaction of stannylenes with electrophiles.[136] Therefore, tetrabutylammonium bromide (TBAB) and K_2CO_3 were

added as described by Xu et al.[128] The coordination of bromide to the tetracoordinated tin atom polarizes the linkage to the equatorial oxygen in the *cis*-stannylene, enhancing the nucleophilicity of this oxygen. The contribution of K_2CO_3 to the reaction is its water binding ability and weak basic character (new formation of stannylenes in cycles as shown in Figure 5.6).[152]

As mentioned in the introduction of this chapter, no regioselective alkylation of polysaccharides mediated by Bu_2SnO has been reported so far. Therefore, to see whether in spite of the very low DS achieved, any influence of the stannylation step can be detected in the methyl pattern, we performed a control experiment without addition of Bu_2SnO under otherwise same conditions. Results are presented in Figure 5.12. The average DS of M-KGM-22 (0.13) is very close to that of M-KGM-21 performed with stannylation (0.11), however, there is a huge difference between Glc and Man with respect to reactivity and regioselectivity of methylation. A significant difference between DS values for M and G residues in M-KGM-21 (DS_M/DS_G=2.1) was obtained. As expected, in the case without Bu_2SnO addition (M-KGM-22), due to the highest acidity of 2-OH and the best accessibility of 6-OH,[12] 2-OH in G and 6-OH in M were preferentially methylated under these mild basic conditions (2 equiv. K_2CO_3) (G-x_2=0.06 and M-x_6=0.06), followed by O-2 in M and O-6 in G, and the least active position being O-3 in both M and G, as shown in Table 5.5. DS is in the order of methylation under slight basic conditions as reported by An et al. By methylation of KGM in aqueous NaOH/CH_3I (pH=10) they obtained *O*-methyl-glucomannans with DS values of 0.09-0.18.[153] In contrast, in the case of M-KGM-21, the order of reactivity in M was clearly changed in favor of the secondary OH of the *cis*-diol ((x_2+x_3)/x_6 in M increased from 1 to 9). However, among these two secondary OH in M, O-3 was only slightly preferred (x_3/x_2 increased from 1 to 1.2). Moreover, with stannylation the preference of O-3 in M was much more pronounced compared to that of in G ((M-x_3/G-x_3 increased from 1.2 to 4.3). So, with respect to overall reactivity, it can be stated: While without Bu_2SnO addition, the order in KGM was G2 ≥ M6 ≥ G6 > M2 ≥ M3 ≥ G3, it was M3 > M2 ≥ G2 >> G3 ≥ M6 = G6 with stannylation. Thus, Bu_2SnO was clearly affecting the absolute and relative reactivities in KGM towards methylation.

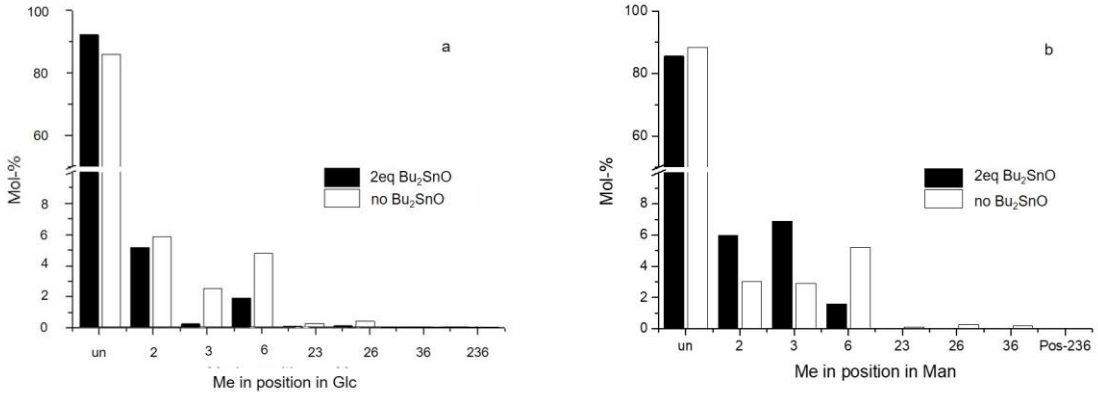

Figure 5.12 Comparison of methyl distribution in G (a) and M (b) of M-KGM-21, prepared after stannylation in pyridine in the presence of Bu_2SnO methanolic suspension (2 equiv./KGM) by methylation ACN/DMF/TBAB/K_2CO_3 at 70 ^{0}C, and M-KGM-22 prepared without Bu_2SnO under otherwise same conditions. M and G both were normalized to 100%. Experiments were carried out by Janick Raßloff.[72]

Table 5.5 Results for M-KGM-21 and M-KGM-22, including the ratio of partial DS-values x_i for individual OH group in position *i* in M/G residues and the ratio of DS_M/DS_G. DS values were determined by MeOH/Ac method. Experiments were carried out by Janick Raßloff.[72]

M-KGM	DS_{KGM}	DS_M	DS_G	DS_M/DS_G	$(x_2+x_3)/x_6$ in M	x_3/x_2 in M	M-x_3/G-x_3
21	0.11	0.14	0.07	2.1	8.8	1.2	4.3
22	0.13	0.12	0.14	0.9	1.2	0.9	1.2

Moreover, stannylation reaction time and temperature are also important. Stannylation was always performed at elevated temperature given in Table 5.6. It needs to be mentioned that all reactions in Table 5.6 were carried out in flask with a condenser, however, from M-KGM-37, reactions were performed in pressure-sealed V-vials. Best results were obtained for reactions performed with the addition of TBAB and K_2CO_3 (entry 32 in dioxane/MeOH and 34 in pyridine). For all other entries, reactivity was very low, probably due to poor solubility and thus accessibility of KGM, but also due to the lack of the reactivity enhancing nucleophile.

Table 5.6 Overview of some methylation experiments of stan-KGM. M-KGM-tin-30 - 34 were prepared by Janick Raßloff.[72]

MKGM (mg)	Solvent for Stan. (mL)	Bu_2SnO equiv./ glycosyl unit[1]	Stannylation *t* (h)/T (^{0}C)	Solvent for Me (mL)	Methylation *t* (h)/T (^{0}C)	DS_{KGM}
23 (20)	MeOH (15)	2	6 / 75	ACN (7)	24 / 25	0.07
24 (17)	MeOH (10)	1.5	6 / 78	DMF (10)	048 / 56	0.04
25 (10)	ACN (10)	2	24 / 80	DMF (10)	072 / 40	0.03
26 (11)	DMSO + MeOH 2:1 (15)	2	24 / 72	DMSO (10)	0 24 / 45	0.02
27 (10)[2]	DMSO + MeOH 2:1 (15)	5	24 / 80	DMSO (10)	48 / 10	0.03
28 (10)[2]	DMSO + MeOH 1:1 (10)	2	24 / 80	DMSO (5)	30 / 25	0.02
29 (11)	DMSO + ACN 1:1 (10)	5	20 / 110	DMSO (5)	0 20 / 32	0.02
30 (11)	Dioxane (15)	5	6 / 110	Dioxane (10)	024 / 36	0.01
31 (8)	*t*-BuOH (8)	2	24 / 100	ACN+DMF 10:1 (8)	0 48 / 60	0.06
32 (5)[3]	Dioxane + MeOH 1:1 (5)	2 Sus.[5]	24 / 80	ACN+DMF 10:1 (5)	66 / 60	0.09
33 (10)[3]	Toluene (20)	2 Sus.	24 / 120	ACN+DMF 10:1 (10)	39 / 70	0.02
34 (10)[4]	Pyridine (10)	2 Sus.	24 / 115	ACN+DMF 10:1 (8)	48 / 70	0.11

[1]Glycosyl unit = anhydro glucose unit / anhydro mannose unit in KGM.
[2]In methylation step, 10 (for M-KGM-27) or 15 µL (for M-KGM-28) of 1-methylimidazole was added as catalyst.
[3]In methylation step, 0.5 equiv. of TBAB and 1.5 equiv. of K_2CO_3 / glycosyl unit were added.
[4]In methylation step, 1 equiv. of TBAB and 2 equiv. of K_2CO_3 / glycosyl unit were added.
[5]Sus. means Bu_2SnO boiled in MeOH at 50mg/mL yielding a methanolic suspension of $Bu_2Sn(OMe)_2$ and Bu_2SnO.

As mentioned before, it is difficult to find a solvent which can dissolve KGM and Bu_2SnO at the same time (in one step). Therefore, to improve their solubility and reactivity, Bu_2SnO was separately refluxed in MeOH and subsequently added to the dispersion or solution of KGM. Bu_2SnO could be fully dissolved under transformation to dibutyltin dimethoxide, but to keep the volume of MeOH small in order to avoid later precipitation of KGM, concentration of 50 mg of tin reagent/mL MeOH was taken which did not allow full dissolution. This Bu_2SnO suspension was denoted by Sus. and is included in Table 5.6. After generating the organotin intermediate by stannylation, solvents were removed and etherification with methyl iodide

was performed in ACN/DMF (10:1).[128] Results for three entries under these conditions but various amounts of the additives TBAB and K_2CO_3 are shown in Table 5.7.

Table 5.7 Overview of methylation experiments performed under various conditions. 2 Equiv. of Bu_2SnO (methanolic suspension) was used for stannylation of sono-KGM dissolved in pyridine. All methylations were performed in ACN:DMF (10:1) mixture and in the presence of various amount of TBAB and K_2CO_3. DS values were determined by MeOH/Ac method. Experiments were carried out by Janick Raßloff.[72]

M-KGM	DS_{KGM}	DS_M	DS_G	DS_M/DS_G	x_3/x_2 in M	x_3/x_2 in G	$(x_2+x_3)/x_6$ in M	$M\text{-}x_3/G\text{-}x_3$
34[1]	0.11	0.12	0.08	1.5	1.0	0.7	5.7	2.1
35[2]	0.08	0.10	0.06	1.7	1.6	1.5	3.9	1.8
36[1]	0.13	0.15	0.10	1.4	1.1	0.3	4.6	3.4

[1]In the methylation step, 1 equiv. of TBAB and 2 equiv. of K_2CO_3 and excess (≥ 65 equiv.) of CH_3I were added.
[2]In the methylation step, 1.5 equiv. of TBAB and excess (91 equiv.) of CH_3I were added.

M-KGM-34, 35 and 36 were obtained from the same stannylene acetals, but with different amount of TBAB and with or without addition of K_2CO_3. In the presence of K_2CO_3 (entry 34 and 36), a higher DS was obtained. The regioselectivity regarding the two secondary positions in M (x_3/x_2), however, was leveled to about 1:1 compared to M-KGM-21.2 (x_3/x_2 =1.6) which was prepared without the mild base. On the other hand, the preference for the secondary (2 and 3) over the primary position 6 in M slightly increased. Since in the presence of base, the regioselectivity in G was significantly shifted in favor of the most acidic 2-OH, finally the M/G selectivity for position 3 M-x_3/G-x_3 was superior when K_2CO_3 was added. This result brings us to the question, whether the slightly larger reactivities of M-KGM-34 and 36 was caused by the presence of weak base? This issue will be discussed in section 5.2.5.

In summary, pyridine was the most suitable solvent to dissolve KGM, as well as for the stannylation with Bu_2SnO. The mixture of KGM suspension and Bu_2SnO methanolic suspension became clear after heating at 115 ^{0}C for 16 hours. From this intermediate, a M-KGM with DS of 0.13 was obtained by subsequent methylation, higher than with other solvents. Therefore, pyridine showed significant advantage in the preliminary test. Moreover, the application of methanol in the pre-reaction of dibutyltin dimethoxide formation was also supporting. Furthermore, to avoid the reaction mixture turning to black, CH_3I was added in portions to the mixture and reaction time was extended to at least 48 hours to gain higher degree of methylation.

The sample with the highest DS_{KGM} and good regioselectivity achieved so far, M-KGM-21 with an average DS of 0.11 (stannylation in pyridine), was considered for further systematic

studies. Various solvent systems for methylation were tested (as shown in Table 5.5), but finally ACN/DMF (10:1, v/v) was used,[128] since the DS values of the products obtained in this solvent mixture were highest. While products of benzoylation of methyl α-D-glucoside showed nearly two times higher DS in dioxane than in DMF as reported by Haque et al.[93], dioxane was not suitable in our case (DS_{KGM} 0.01, see Table 5.6). Thus, the mixture ACN/DMF (10:1) was selected as the solvent for future methylation.

Since pyridine used in stannylation of M-KGM-21 usually is not a common solvent for stannylation, we proved in a reference experiment with monosaccharides (methyl α-D-mannoside and methyl α-D-glucoside) that the chosen conditions principally work. Thus, methyl α-D-mannoside (M-Man) and methyl α-D-glucoside (M-Glc) were performed under the elaborated reactions conditions (stannylation in pyridine, methylation in ACN/DMF (10:1), TBAB/K_2CO_3 (1 equiv./2 equiv.), excess of CH_3I, 48 hours/70 ºC)). The methyl substitution of M-Man and M-Glc obtained from regioselective methylation are displayed in Table 9.8 in appendix. In case of M-Man, DS 1.35 was achieved and selectivity for the secondary OH was in favor of O-3 (64%) followed by O-6 (20%), O-2 (14%) and O-4 (2%). For M-Glc, the DS was 1.73 and the order for OH groups was O-3 > O-2 > O-6 > O-4. This control experiment proved that the conditions applied above allow efficient methylation of common substrates, however, low DS values of M-KGM were a consequence of the macromolecular character (i.e. poor solubility and accessibility). Moreover, one should keep in mind, the difference in configuration of the glycosidic bond, α in the methyl mannoside (the reference monosaccharide used) and 1,4-linked β-D-mannosyl residues in KGM, which can also influence the formation of dibutylstannylene acetals (as shown in Figure 5.3 (entry 3 and 4) in the introduction of this chapter), and thus regioselectivity. However, the main purpose was to prove that pyridine is principally appropriate for stannylation.

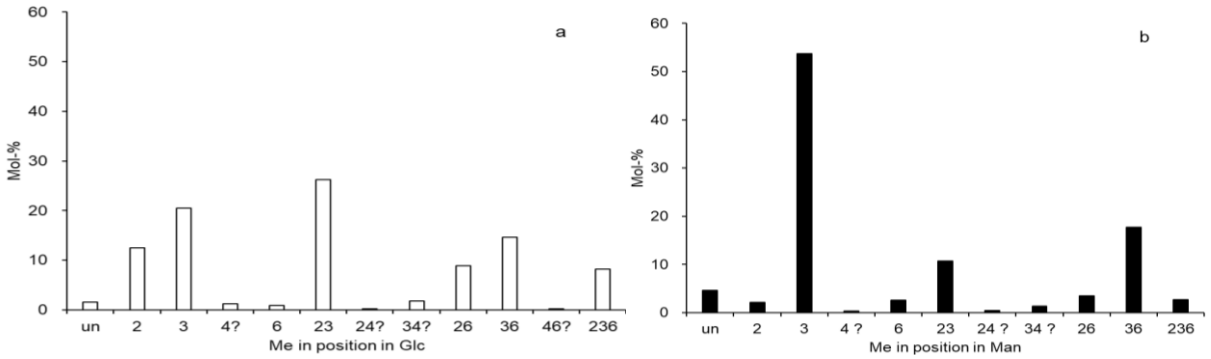

Figure 5.13 Methyl distribution methyl α-D-mannoside (a) and α-D-glucoside (b) (M-Glc and M-Man), prepared in pyridine (stannylation) in the presence of 2 equiv. of Bu_2SnO suspension, and subsequently in ACN/DMF (methylation) at 70 ºC in the presence of 1 equiv.

of TBAB and 2 equiv. of K_2CO_3 and an excess of CH_3I (DS_M=1.35, DS_G=1.73). Sample were prepared by Janick Raßloff.[72]

According to the above presented results, a standard method for regioselective methylation of KGM via dibutylstannylene acetal intermediate has been established which can be summarized as follows:

15 mg of sono-KGM were dissolved in 3 mL of pyridine in a pressure-sealed 5 mL V-vial and 2 equiv. of methanolic Bu_2SnO suspension was added. The stannylation was carried out at 115 ^{0}C for 16 hours. After removal of the pyridine, stan-KGM was suspended in ACN:DMF (10:1), 1 equiv. of TBAB and 2 equiv. of K_2CO_3 were added and the mixture was methylated at 70 ^{0}C for 48 hours with an excess of CH_3I. The reaction mixture was submitted to dialysis and freeze drying to obtain M-KGM. Subsequently, dialyzed M-KGM were submitted to a purification step with hot methanol to remove the dibutyltin oxide (dibutyltin oxide dissolves under reaction in methanol while M-KGM does not) and purified M-KGM was obtained.

An important point to notice is that ultrasonic treatment was applied to the solution of sono-KGM in pyridine (30 min, 15% amplitude) due to the slow dissolving process. Based on these conditions, the effects of the amount of Bu_2SnO and K_2CO_3 on the reactivity of KGM and the regioselectivity of methylation were further investigated, including the average DS, the reactivity of different OH groups, the DS in M/G residues of KGM and the ratio of partial DS-values $(x_2+x_3)/x_6$ in M/G residues and M-x_3/G-x_3.

5.2.4 Effect of the amount of Bu_2SnO applied in stannylation upon methylation

In the introduction it was mentioned that various amounts of Bu_2SnO have been applied in regioselective substitutions.[125,128,129] Furthermore, due to the observed poor reactivity of KGM, an excess of reagent might be helpful to promote the yield of stannylation. Therefore, under the standard conditions just mentioned, various amounts of Bu_2SnO (0 → 4 equiv., as $Bu_2Sn(OMe)_2$/Bu_2SnO suspension in MeOH) were applied for the formation of stannylene acetals, and subsequently methylated as described above.[72] The average DS (DS_{KGM}), DS in M and G units, the ratio of DS_M/DS_G, the ratio of partial DS-values $(x_2+x_3)/x_6$ in M/G residues, and M-x_3/G-x_3 are listed in Table 5.8.

Table 5.8 Results for M-KGM, prepared in the presence of different equiv. (calculated per glycosyl units of KGM) of Bu_2SnO in methanolic suspension, 1 equiv. of TBAB, and 2 equiv. of K_2CO_3 at 70 ^{0}C, including the average DS_{KGM}, DS in M and G units, the ratio of DS_M/DS_G, the ratio of partial DS-values $(x_2+x_3)/x_6$, x_2/x_3 of M residues and M-x_3/G-x_3. DS values were determined by MeOH/Ac method. Experiments were carried out by Janick Raßloff.[72]

M-KGM	Bu_2SnO equiv./ KGM	DS_{KGM}	DS_M	DS_G	DS_M/DS_G	x_3/x_2 in M	$(x_2+x_3)/x_6$ in M	M-x_3/G-x_3
37	0.0	0.099	0.095	0.104	0.9	1.2	1.2	1.3
38	0.5	0.056	0.069	0.039	1.7	1.2	4.1	2.7
39	1.0	0.071	0.081	0.051	1.6	1.2	6.0	3.8
40	1.5	0.111	0.135	0.076	1.8	1.2	3.8	3.3
41	2.0	0.124	0.149	0.085	1.8	1.2	5.4	3.4
42	2.5	0.095	0.113	0.066	1.7	1.3	5.6	3.2
43	3.0	0.095	0.111	0.065	1.7	1.3	5.6	3.9
44	4.0	0.087	0.107	0.054	2.0	1.4	5.5	3.8

In order to enable recalculation of selectivity parameters given in Table 5.8, the average DS of KGM, DS in M and G units were displayed with three decimals although accuracy is lower (in Table 5.8). One thing needs to be pointed out, that M-KGM-38 and 39 (in Table 5.8) are not fully comparable to the other samples, since stannylation and methylation were performed in a round-bottom flask with larger volume (150 mg KGM/30 mL pyridine) instead of in a vial (15 mg KGM/3 mL pyridine) under pressure. Nevertheless, the proportion of the KGM and pyridine were consistent in stannylation step for those same eight samples. The average DS and DS in M and G units were plotted against the amount of dibutyltin oxide used (presented in Figure 5.14).

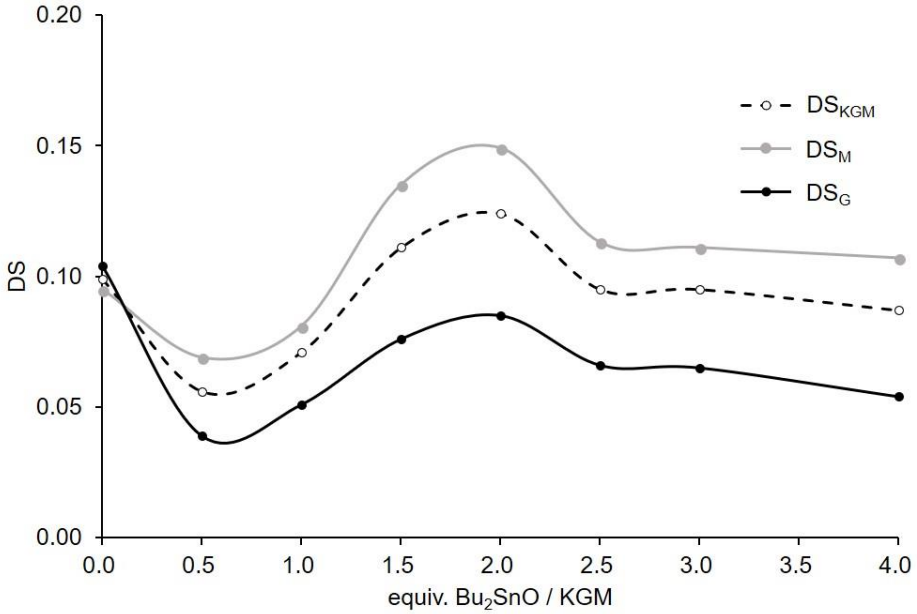

Figure 5.14 Change of DS of M, G and KGM with equiv. Bu_2SnO/KGM present during stannylation. All samples were methylated in the presence of TBAB/K_2CO_3/ACN/DMF/CH_3I at 70 ^{0}C (M-KGM-37, 38, 39, 40, 41, 42, 43 and 44 from Table 5.8).

Figure 5.14 displays the DS development for M and G units and average DS of M-KGM with increasing amount of Bu_2SnO. In comparison to the parallel tin-free reference experiment (M-KGM-37), DS_M/DS_G increased from 0.9 to 1.7-1.8 (see Table 5.8). With increasing equiv. of Bu_2SnO (0.5-2 equiv.), the DS values increased for both M and G residues. A maximum of DS values (including average DS and individual DS in M/G) is observed at 2 equiv. Bu_2SnO, and reactivity of M residues increase to a higher extent than that of G. Regioselectivity regarding 3-OH in *cis*-diol in M residues (x_3/x_2) increased from 1.1 to about 1.2-1.3 after stannylation independent of the amount of Bu_2SnO. However, the preference of secondary over primary OH in M ($(x_2+x_3)/x_6$ in M) increased to a value of about 5.4 and the ratio of M-x_3/G-x_3 also increased to a value of about 3.9. For glucose the DS generally decreased in the presence of Bu_2SnO from the maximum value of 0.10 obtained without stannylation (Table 5.8).

Figure 5.15 shows the development of the partial DS (x_i) in individual positions i of M and G residues. In conclusion, the optimum with respect to total DS and DS_M/DS_G ratio was found to be ca. 2 equiv. Bu_2SnO.

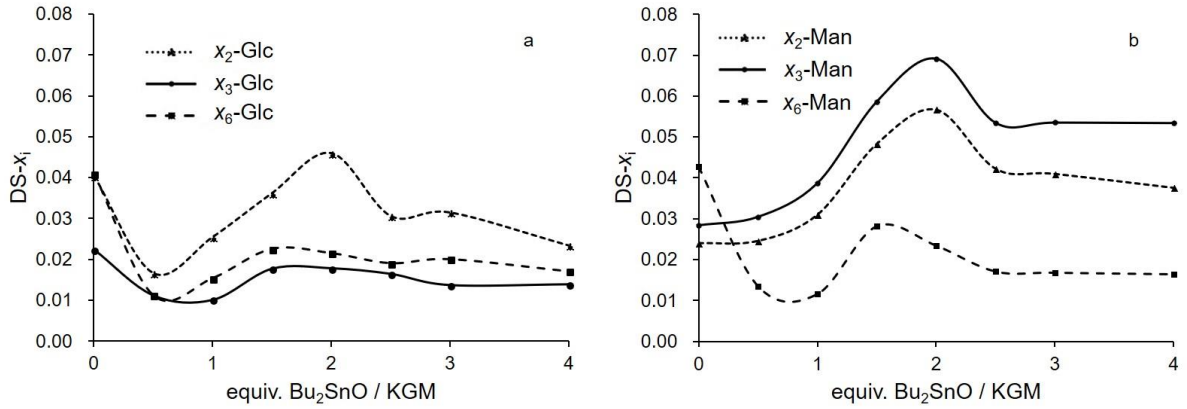

Figure 5.15 Change of partial DS value x_i of G (a) and M (b) in KGM with various equiv. Bu_2SnO/KGM applied in the stannylation step. Corresponding data are presented in Table 9.8 in the appendix.

5.2.5 Effect of the amount of K_2CO_3 applied in methylation

It has already been shown that the addition of TBAB and K_2CO_3 promotes methylation of stannylene acetals.[128] Thus, a stoichiometric amount of tetrabutylammonium bromide was applied in our experiment. Here we report on the effect of the amount of K_2CO_3 on the outcome of methylation under the standard conditions established. For this purpose, the amount of K_2CO_3 was varied in the range of 0-2 equiv./glycosyl unit.[72] The results are listed in Table 5.9. With increasing amount of K_2CO_3, the overall DS increased from 0.07 to 0.12, from 0.08 to 0.15 for Man and from 0.05 to 0.09 for Glc. At the same time, the ratio of partial DS-values $(x_2+x_3)/x_6$ in Man increased from 2.8 to 5.4 (Table 5.9).

Table 5.9 Results for M-KGM prepared in the presence of 2 equiv. (calculated with respect to glycosyl units in KGM) of Bu_2SnO (applied as methanolic suspension), and with 1 equiv. of TBAB at 70 ^{0}C for methylation, including the average DS, DS in M and G units, the ratio of DS_M/DS_G, the ratio of partial DS-values $(x_2+x_3)/x_6$ in M residues and M-x_3/G-x_3. DS values were determined by MeOH_Ac method. Experiments were carried out by Janick Raßloff.[72]

M-KGM	K_2CO_3 equiv./	DS_{KGM}	DS_M	DS_G	DS_M/DS_G	M-3/ M-2	$(x_2+x_3)/x_6$	M-x_3/ G-x_3
45	0.0	0.07	0.08	0.05	1.7	2.1	2.8	2.1
46	0.5	0.09	0.11	0.06	1.8	1.5	5.3	4.0
47	1.0	0.10	0.11	0.07	1.6	1.4	5.2	2.8
41	2.0	0.12	0.15	0.09	2.1	1.4	5.4	3.9

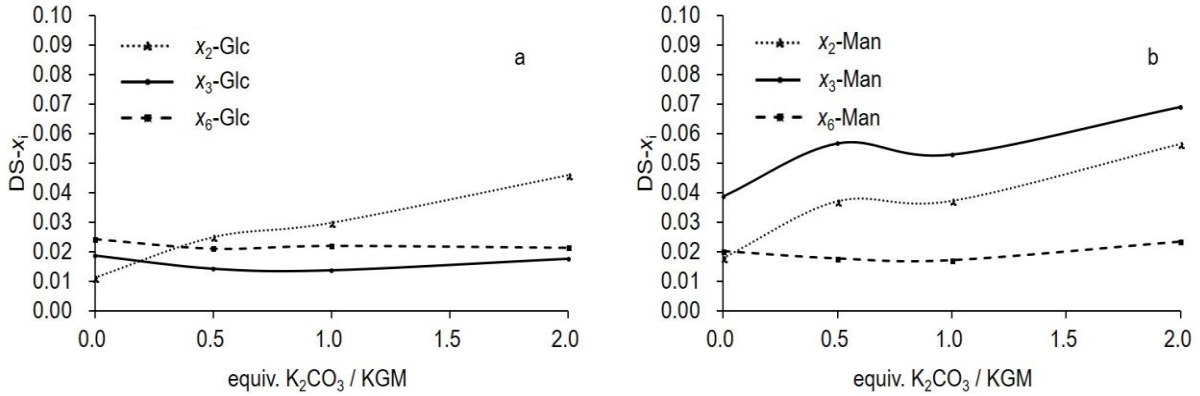

Figure 5.16 Change of partial DS value x_i of G (a) and M (b) in M-KGM with equiv. of K_2CO_3/KGM present during methylation. For corresponding data see Table 9.8 in appendix.

It must be pointed out that the connecting line through the data points in Figure 5.16 are only added for better visualization of trends. Looking at the three different OH in M and G, respectively (Figure 5.16a and b), it is obvious that with increasing amount of K_2CO_3 the two secondary OH groups in M both profit significantly (with 0→2 equiv. of K_2CO_3, $(x_2+x_3)/x_6$ increased from 2.8 to 5.4), while in G only methylation at the most acidic position 2 is favored. In contrast, the reactivity of the OH groups at O-3 and O-6 were not much affected (slight decrease). The ratio of 3- and 2-*O*-methyl slightly drops for Man and Glc as well, while M-3/G-3 increases from about 2 to 4 (see Table 5.9). In case of Glc, the enhancement of 2-*O*-methylation might be explained by better deprotonation of this most acidic position with increasing amounts of base.

5.2.6 Repeated stannylation/methylation

Beside obvious influence of stannylation on manno/gluco- and regioselectivity of methylation, the overall DS achieved was relatively low. Since poor solubility hampered stannylation it was expected that this problem might be reduced after initial methylation. Alais et al reported that mono-3-*O*-alkylation of methyl lactoside has been achieved by means of repeated stannylation/alkylation sequences without significant formation of other substitution patterns.[131] Thus, repeated methylation might probably increase DS while maintaining selectivity.

The starting material (e.g. M-KGM-21, DS_{KGM}=0.11, DS_M=0.14, DS_G=0.07) should be better soluble in pyridine due to less intermolecular interactions between polysaccharide chains (H-bonds). Considering the amount of Bu_2SnO in M-KGM-21 arising from the first reaction, the real amount of Bu_2SnO in M-KGM-48 and 49 was higher than the added 1 or 2 equiv. (in the range of 4-5 equiv.). The results are listed in Table 5.10.

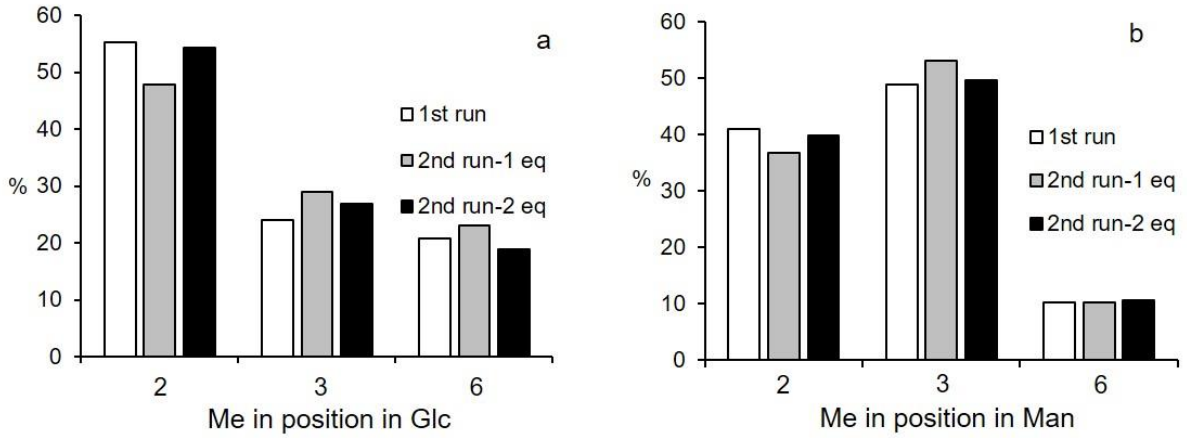

Figure 5.17 Distribution of methyl groups (%) on position 2, 3 and 6 in glucose (a) and mannose (b) after one stannylation/methylation step under standard conditions, and after a second step with 1 or 2 equiv. dibutyltin oxide. Samples were prepared by Janick Raßloff.[72]

Table 5.10 Results for the first (M-KGM-21) and the second step with 1 equiv. (M-KGM-48) or 2 equiv. Bu_2SnO (M-KGM-49, see appendix Table 9.8), including the average DS, individual DS of M and G residues, DS_M/DS_G, the ratio of partial DS-values $(x_2+x_3)/x_6$ in M residues and M-x_3/M-x_2. DS values were determined by MeOH/Ac method. Experiments were carried out by Janick Raßloff.[72]

M-KGM	DS_{KGM}	DS_M	DS_G	DS_M/DS_G	$(x_2+x_3)/x_6$ in M	x_3/x_2 in M
21(1st run)	0.11	0.14	0.07	2.1	8.8	1.2
48(2nd run-1 eq)	0.23	0.27	0.17	1.6	8.4	1.3
49(2nd run-2 eq)	0.28	0.36	0.20	1.8	8.9	1.4

The average DS could be enhanced from 0.11 (first step) up to 0.23 (1 equiv. Bu_2SnO) or 0.28 (2 equiv. Bu_2SnO) in the second step, especially DS_M increased up to 0.36. Figure 5.17 shows the absolute increase in mono-substitution for glucose (a) and for mannose (b). The ratio of DS_M/DS_G slightly decreased, but with 1.8 after the 2nd stannylation/methylation with 2 equiv. Bu_2SnO, the absolute DS difference between M and G residues increased (0.07→0.10 / 0.16). Moreover, there was no loss in regioselectivity with respect to OH in M as illustrated by the nearly constant ratio of x_3/x_2 in M (1.2 → 1.4) and the preference of secondary over primary groups in M and G (Table 5.10). The ratio $(x_2+x_3)/x_6$ in M was more or less constant between 8 and 9. Therefore, repetition of reaction is presently the most promising strategy to profit from the directing effect of stannylenes. Thus, M-KGM-tin with an average DS 0.28 and a DS ratio for M and G 1.8 were obtained. Moreover, an uncommon methyl pattern with high 3-OH substitution in M residues was achieved compared to base-promoted methylation.

5.2.7 Solvent-free stannylation

Due to the poor solubility of KGM, we also considered solvent-free stannylation. Giordano et al. reported on stannylation of polyols including many monosaccharides by applying catalytic amounts of dibutyltin oxide (0.1 equiv.) and TBAB (0.3 equiv.), followed by benzylation or allylation in a single-step solvent-free process.[121] They obtained 64% yield of methyl 3-*O*-benzyl-α-D-manno-pyranoside in the presence of benzyl bromide and diisopropylethylamine (DIPEA) at 70 °C. In our experiments, we added 1 equiv. of Bu_2SnO, solid or as methanolic suspension, and beside CH_3I, 1 or 0.5 equiv. of TBAB, and 4 or 6 equiv. DIPEA to KGM. In addition, we performed two experiments with 2 equiv. of K_2CO_3 instead of DIPEA. An excess of CH_3I was added in portions and the mixture was heated in a pressure-sealed vial to 90 or 100 °C for 12 or 24 hours. Methyl substitution pattern of obtained samples are listed in Table 9.8 in appendix. Unexpectedly, high average DS values in the range of 0.13 to 0.30 were observed by this procedure. However, no significant DS difference between M and G residues was found and the preference of methylation switched to primary OH. For both, G and M, 50 - 71% of methyl groups were located at O-6, followed by position 3 and 2 (see Figure 5.18), even for G in all DIPEA entries (with K_2CO_3 x_3/x_2 in G is about 1). These results indicate a better accessibility of the primary OH dominating the reactivity in the solvent-free mixture. Preferred reaction at primary 6-OH in a tin-promoted reaction has been reported by Munavu et al. for acylation of methyl β-D-glucopyranoside, while O-2 was the preferred position for the α-anomer.[151] This different behavior of methyl α- and β-glucosides was explained with the coordination between the axial OCH_3 at C-1 and the 2,3-stannylene acetal in α-, whereas such an interaction is not possible for the equatorial OCH_3 in the β-anomer. However, intramolecular migration of acyl group could occur in this case since the product was an ester. In case of KGM, H-bonds pattern and steric effects are probably more important for the change in regioselectivity. In contrast to our observations for KGM, Sethi et al. reported no change in common regioselectivity for the reaction of lactoside and Bu_2SnO in MeOH.[154] They obtained 3'-*O*-benzyl-lactoside in 83% yield when reacting the prepared stannylene acetal with BnBr and TBAB under solvent-free conditions in a ballmill.

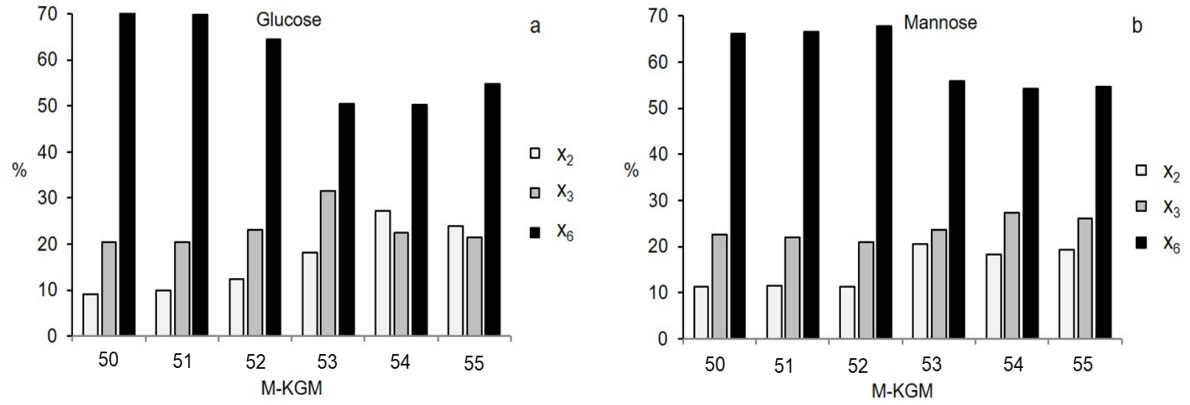

Figure 5.18 Distribution of methyl groups in M-KGM under solvent-free conditions in % in glucose (a), and mannose (b), each normalized to 100%. M-KGM 50-53: with DIPEA, M-KGM 54-55: with K_2CO_3; 50 and 51: 1 equiv. TBAB, 52-55: 0.5 equiv. TBAB; 50-52, 54: 90 ºC, 53 and 55: 100 ºC. x_i = portion of i-*O*-substitution in %; Σx_i = 100%. Experiments were carried out by Janick Raßloff.[72]

Although the results of this reaction on KGM are contrary to the intended pattern, the observation is very interesting. To the best of our knowledge these are the only methylation conditions leveling the differences in reactivity and selectivity of glucose and mannose nearly completely. Furthermore, the usually most reactive 2-OH (in kinetically controlled reactions at low base concentration) was strongly suppressed under these conditions for both glycosyl units. Since this most acidic position shows the lowest degree of methylation (see Figure 5.18), the added base (K_2CO_3) cannot be responsible. Whether, and if which role Bu_2SnO plays for the order of reactivity must be the object of further investigations.

5.3 Conclusion

Stereochemistry at O-2 of mannosyl residues and glucosyl residues and thus relation of the two adjacent secondary OH at C-2 and C-3 are different in the β-1,4-linked Konjac glucomannan KGM. In this chapter, it has been investigated whether advantage could be made of this structural difference for generating various degrees and patterns of *O*-methylation in these two glycosyl units belonging to the same macromolecule by regioselective activation with Bu_2SnO. Due to the poor solubility of the polysaccharides, the stannylation step was hampered by insufficient accessibility and thus reactivity of OH. Pyridine as the solvent for KGM, in combination with pretreatment of Bu_2SnO in a small volume of MeOH allowing partial dissolution as $Bu_2Sn(OMe)_2$ and thus better dispersion were found to be the best compromise.

Best results for the subsequent methylation step with CH_3I were achieved in ACN/DMF (10:1, v/v) but average DS was only about 0.1. Addition of TBAB and K_2CO_3 slightly enhanced the

DS, but O-2 in both, Glc and Man, was the position that profited most from the addition of the mild base. Typically, the DS of Man was about 2 times that of Glc, methylation was preferred at secondary OH over primary OH in Man by factor 6-10 and in Glc by factor 2-4. O-3/O-2-Selectivity was weak, probably due to steric hindrance by 4-*O*-substitution as has been described in the literature.[133] In the *cis*-diol, position 3 was slightly preferred, while among the OH of the *trans*-diol, position 2 was preferentially methylated in most cases. Optimum of Bu_2SnO equiv. with respect to DS and selectivity was found to be at 2 equiv./glycosyl unit. Reference experiments without Bu_2SnO under otherwise same conditions resulted in similar average DS of 0.09 - 0.15, but with completely different methyl pattern, clearly indicating the influence of stannylene acetal formation as transient protecting groups (Glc) and selectively activating group (Man).

Single-step reaction under solvent-free conditions gave higher DS values (0.13 - 0.30), but selectivity with respect to Glc and Man was completely lost. Surprisingly, now the primary 6-OH became strongly preferred while 2-OH showed least conversion for Man and Glc as well. The most promising approach which enhanced the DS while maintaining selectivity turned out to be the repeated stannylation and methylation in the optimized system.

Thus, application of Bu_2SnO in the methylation of KGM gives access to very uncommon methyl pattern in glucomannan with about twofold conversion of Man compared to Glc which is just the reverse to the outcome of borate-affected methylation.[145] Depending on the conditions, preferential methylation at O-3 and secondary OH in general can be achieved with high manno/gluco selectivity, while under solvent-free conditions according to Giordano and Iadonisi[137], rather 6-OH dominated followed by O-3 and O-2 with no difference for Glc and Man.

6 Summary

The relative reactivities of OH in stereoisomeric glucosyl (G) and mannosyl (M) units in KGM with a molar ratio of M to G of 1.68 were investigated by partial methylation at constant pH 13.6 in an aqueous NaOH/CH_3I system. In a time course study, M-KGM with average DS_{KGM} values in the range of 0.3 - 0.8 were obtained. For both glucose and mannose, the primary OH was the most reactive under the conditions applied. While the relative rate constant k_2 was equal for mannose and glucose, the lowest reactive position 3 was methylated to a much higher extent in mannose than in glucose. Due to the *cis*-2,3-diol (ax-eq) configuration in M units, the acidity of O-3 profited from adjacent O-2, leading to 2.4 times larger M-k_3 compared to G-k_3. In conclusion, in one series of M-KGMs with DS_{KGM} from 0.3 - 0.8, the order of the six hydroxyl groups in KGM is G-k_6 > M-k_6 > G-k_2 ≈ M-k_2 > M-k_3 > G-k_3 (k_2: k_3: k_6 = 4.1 : 2.3 : 4.9 for M and k_2: k_3: k_6 = 4.2 : 1.0 : 5.5 for G).

To enhance the difference in alkylation of M and G, KGM was methylated with NaOH/CH_3I in water in the presence of borate, and as a reference without this additive. Borate was successfully applied as a stereo- and consequently topo-selective reagent to control the methylation of KGM in water or water/acetone. Borate forms reversible complexes with diols in KGM, with higher stability for *cis*-2,3-diols (M) compared to *trans*-2,3-diols (G). With increasing equiv. of borate increasing suppression of 2- and 3-*O*-methylation of M residues was observed while G residues were mainly affected at O-6, but to much lower extent. Elevating the temperature and addition of aprotic acetone as a co-solvent enhanced reactivity but on the penalty of M/G regioselectivity. M-KGMs with a DS difference up to 100 % between M and G at an average DS of 0.81 (DS_M 0.59, DS_G 1.18) were obtained. Oligosaccharides obtained by partial hydrolysis after full protection of M-KGM with CH_3I-d_3 were labelled with *m*-ABA and measured by LC-ESI-MS. DS/DP profiles were in full agreement with random distribution of methyl groups. Moreover, an agreement of the experimental data with random M-G distribution was found, while blocky structures could be excluded. From LC-ESI-MS analysis of oligosaccharides with defined composition (G_mM_n), it was concluded that borate-mediated inhibition might have resulted in a lower degree of methylation in M-rich areas compared to isolated M (cooperative effect).

In a second approach, the difference of the stereochemistry at O-2 of M and G residues was used to generate various degrees and patterns of *O*-methylation in these two glycosyl units belonging to the same macromolecule by regioselective activation with Bu_2SnO. Under optimized conditions, M-KGM with the DS of M about 2 times that of G was obtained, even at a very low overall DS (DS_{KGM} 0.11, DS_M 0.14, DS_G 0.07). Methylation was preferred at

secondary OH over primary OH in M by factor 6-10 and in G by factor 2-4. In the *cis*-diol, position 3 was slightly preferred, while for the *trans*-diol, position 2 was preferentially methylated in most cases. Reference experiments without Bu_2SnO under otherwise same conditions caused similar average DS of M-KGM, but with completely different methyl pattern, indicating the influence of stannylenes acetal formation as transient protecting groups for G and selectively activating groups for M. One-pot reaction under solvent-free conditions produced M-KGM with higher DS values, but selectivity with respect to G and M was completely lost. Surprisingly, now the primary 6-OH became strongly preferred while 2-OH showed least conversion for M and G as well. The most promising approach which enhanced the DS while maintaining selectivity turned out to be the repeated stannylation and methylation in the optimized system.

KGM derivatives showed interesting chemical and physical properties, for instance thermal stability was improved by methylation. Moreover, oligomer pattern analysis indicates that blocky structures in KGM backbone can be excluded and a random G-M pattern being the most probable. Furthermore, stereo- and thus also topo-selective methylation in the presence of borate as temporary protecting groups, or via stannylenes acetal intermediates of KGM can be used to modify the polymers' properties for specific applications.

6 Zusammenfassung

Die relativen Reaktivitäten von OH in stereoisomeren Glucosyl- (G) und Mannosyl-(M) Einheiten in Konjak Glucomannan (KGM) mit einem Molverhältnis von M zu G von 1,68 wurden durch partielle Methylierung bei konstantem pH 13,6 in einem wässrigen NaOH/CH_3I-System untersucht. In einer Zeitstudie wurden M-KGM mit durchschnittlichen DS_{KGM}-Werten im Bereich von 0,3 - 0,8 erhalten Sowohl bei Glucose als auch bei Mannose war die primäre OH-Gruppe unter den gewählten Bedingungen das reaktivste. Während die relative Geschwindigkeitskonstante k_2 für Mannose und Glucose gleich war, war die am wenigsten reaktive Position 3 in Mannose deutlich stärker methyliert als in Glucose. Aufgrund der *cis*-2,3-diol (ax-eq)-Konfiguration in M-Einheiten profitierte die OH-Grupp an C-3 von der Acidität der benachbarten 2-OH, was zu einem 2,4-fach größeren M-k_3 im Vergleich zu G-k_3 führte. In einer Serie von M KGMs mit DS_{KGM} von 0,3 - 0,8 ist die Reihenfolge der sechs Hydroxylgruppen in KGM G-k_6 > M-k_6 > G-k_2 ≈ M-k_2 > M-k_3 > G- k_3 (k_2: k_3: k_6 = 4,1 : 2,3 : 4,9 für M und k_2: k_3: k_6 = 4,2 : 1,0 : 5,5 für G).

Um den Unterschied in der Alkylierung von M und G zu verstärken, wurde KGM mit NaOH/CH_3I in Wasser in Gegenwart von Borat und als Referenz ohne diesen Zusatzstoff methyliert. Borat wurde erfolgreich als stereo- und damit toposelektives Reagenz zur Kontrolle der Methylierung von KGM in Wasser oder Wasser/Aceton eingesetzt. Borat bildet reversible Komplexe mit Diolen in KGM, mit höherer Stabilität für *cis* 2,3-Diole (M) im Vergleich zu *trans* 2,3-Diolen (G). Mit steigendenn Äquivalenten von Borat wurde eine zunehmende Unterdrückung der 2- und 3-*O*-Methylierung von M beobachtet, während G hauptsächlich bei O-6 betroffen waren, jedoch in wesentlich geringerem Ausmaß. Erhöhung der Temperatur und Zugabe von aprotischem Aceton als Co-Lösungsmittel erhöhte die Reaktivität, aber auf Kosten der M/G-Regionalselektivität. M-KGMs mit einer DS-Differenz von bis zu 100 % zwischen M und G bei einem durchschnittlichen DS von 0,81 (DS_M 0,59, DS_G 1,18) wurden erhalten. Oligosaccharide, die durch partielle Hydrolyse nach vollständigem Schutz von M-KGM mit CH_3I-d_3 gewonnen worden waren, wurden mit *m*-ABA markiert und mit LC-ESI-MS gemessen. Die DS/DP-Profile stimmen mit der statistischen Verteilung der Methylgruppen überein. Außerdem wurde eine Übereinstimmung der experimentellen Daten mit der zufälligen M-G-Verteilung gefunden, wobei blockartige Strukturen ausgeschlossen werden konnten. Aus der LC-ESI-MS-Analyse von Oligosacchariden mit definierter Zusammensetzung (G_mM_n) wurde der Schluss gezogen, dass eine boratvermittelte Hemmung zu einem geringeren Methylierungsgrad in M-reichen Gebieten im Vergleich zu isoliertem M geführt haben könnte (kooperativer Effekt).

In einem zweiten Ansatz wurde die Differenz der Stereochemie an O-2 von M- und G-Resten verwendet, um verschiedene Grade und Muster der *O*-Methylierung in diesen beiden Glycosyleinheitendesselben Makromoleküls durch regioselektive Aktivierung mit Bu_2SnO zu erzeugen. Unter optimierten Bedingungen wurde M-KGM mit einem etwa doppelt so hohem DS für M wie für G erreicht, selbst bei einem sehr niedrigen Gesamt-DS (DS_{KGM} 0,11, DS_M 0,14, DS_G 0,07). Die Methylierung der sekundären OH wurde gegenüber der der primären OH-Gruppe bei M um den Faktor 6-10 und bei G um den Faktor 2-4 bevorzugt. Im *cis*-Diol (M) wurde die Position 3 leicht bevorzugt, während für das *trans*-Diol (G) die Position 2 in den meisten Fällen bevorzugt methyliert wurde. Referenzexperimente ohne Bu_2SnO unter sonst gleichen Bedingungen führten zu einem ähnlichen durchschnittlichen DS von M-KGM, jedoch mit völlig unterschiedlichem Methylmuster, was den Einfluss der Bildung von Stannylenacetalen als transiente Schutzgruppen für G und die selektive Aktivierung von Gruppen für den Menschen anzeigt. Die Eintopfreaktion unter lösungsmittelfreien Bedingungen führte zu M-KGM mit höheren DS-Werten, die Selektivität hinsichtlich G und M ging jedoch völlig verloren. Überraschenderweise wurde nun die primäre 6-OH-Gruppe stark bevorzugt, während 2-OH auch für M und G den geringsten Umsetzung zeigte. Der vielversprechendste Ansatz, den DS unter Beibehaltung der Selektivität zu steigern, war die wiederholte Stannylierung und Methylierung im optimierten System.

Zusammenfassend kann gesagt werden, dass das Glucomannanderivate interessante chemische und physikalische Eigenschaften aufweisen. So wird z.B. die thermische Stabilität durch Methylierung erhöht. Darüber hinaus zeigt die Analyse der Methylverteilung in oligomeren Sequenzen, dass eine blockartige Anordnung von Mannose und Glucose in KGM ausgeschlossen werden können und ein zufälliges G-M-Muster am wahrscheinlichsten ist. Darüber hinaus kann eine stereo- und damit auch toposelektive Methylierung in Gegenwart von Borat als temporäre Schutzgruppeoder oder über Stannylen-Acetale als dirigierende KGM-Zwischenprodukte durchgeführt werden, um die Eigenschaften der Polymere für spezifische Anwendungen zu modifizieren.

7 Material and Experimental

7.1 Chemicals and instrumentation

7.1.1 Reagents and materials

All reagents used were of high purity and were purchased from Roth, Sigma-Aldrich or TCI and used as obtained. Di-sodium tetraborate decahydrate ($Na_2B_4O_7 \cdot 10\ H_2O$) with 99.5% purity was purchased from Merck. Dibutyltin oxide (Bu_2SnO) with 95% purity was purchased from TCI. Dialysis tube Spectra/Por with MWCO of 3.5 and 14 kDa was purchased from Roth. Membrane filters, PTFE, 45 μm, were from Phenomenex. mol sieve (3 and 4 Å) was from Merck. 3 M MeOH/HCl is prepared by adding the calculated amount of acetyl chloride to dry methanol under ice-cooling.

KGM with M:G=1.6 (information given by the provider) was purchased from GfN, Herstellung von Naturextrakten GmbH, Germany. Mannan (Ivory nut, Megazyme Co. Wicklow, Ireland.), and methylcellulose (MC) (Sigma Aldrich, DS = 1.92) were used as standards for assigning the corresponding partially methylated derivatives of mannose and glucose in gas liquid chromatography (GLC) and of oligomers in LC-ESI-MS.

7.1.2 Instruments and methods

IR spectrometer

Instrument	Tensor 27, Bruker
Type	Diamond-ATR
Scan range	600 – 4000 cm^{-1} (32 scans)

Sonification

Ultrasonic homogenizer	Sonopuls, HD 3100 Generator
Generator	GM 3100
Ultrasonic transducer	UW 3100
Titanium plates	TT 13, 13 mm
HF-power	100 W
Working frequency	20 kHz
Sonotrode	KE 76, made of titanium, 137 mm × 6 mm
Amplitude	10 %
Immersion depth	5 cm
Break	5 s of operation with 2 s of break
Reaction temperature	15 ^{0}C

Heating and evaporation facilities

Heating blocks	Vapotherm Mobil S, Barkey GmbH & Co. KG Reacti-Therm with Reacti-Vap, Thermo Fisher Scientific
Evaporation	Reacti-Vap Evaporating Unit No. 18780, Pierce, Thermo Scientific
Vials	1 mL V-Vials, Supelco®, Sigma-Aldrich
	5 mL V-Vials, Supelco®, Sigma-Aldrich
Freeze drying	
Device	ALPHA2-4 Lock-1M, Heraeus Christ GmbH
Pump	Duo 5M, Pfeiffer Vacuum
Ethanol bath	Beta A, from Christ
Gas chromatography	
Instrument	GC-2010, Shimadzu
Column	ZB-5HT, phenomenex, 28.7 m × 0.25 mm ID × 0.25 µm FD
Injector mode	splitless, 250 °C
Carrier gas	hydrogen (64.7 kPa), linear velocity mode (45 cm^3/s)
Detector	FID, hydrogen (40 mL/min), synthetic air (400 mL/min) and nitrogen (make-up-Gas 30 mL/min)

Temperature programs

Rate (°C/min)	Temperature (°C)	Hold time (min)
(1) *O*-Ethyl-*O*-methyl-alditol acetates		
-	60	1
20	150	0
1	180	0
20	310	10
(2) 4-*O*-Acetyl- and 4-*O*-benzoyl-1,5-anhydro-D-glucitol/mannitols		
-	60	1
20	130	0
3	175	0
2	210	0
4	300	10
(3) Methyl *O*-methyl-*O*-trimethylsilyl-gluco-/manno-pyranoside		
-	60	1
20	130	0
2	210	0
4	300	10
(4) Methyl *O*-acetyl-*O*-Methyl-gluco-/manno-pyranoside		
-	60	1
20	130	0
1	180	0
30	310	5

Data analysis Shimadzu GC solution Chromatography Data SYSTEM Version 2.3

GLC-MS	
Device	Agilent 6890 gas chromatograph combined with a JMS-T100GC time of flight mass spectrometer
Mode	Electron ionization (EI), 70 eV
Column	ZB-5MS Phenomenex, 30 m × 0.25 mm ID × 0.25 μm FD
Injector	Split 1:10
Carrier gas	Helium
Software	Data Analysis (Bruker Dalonics, Bremen, Germany)
ESI-IT-MS	
Instrument	HCT Ultra ETDII (Bruker Daltonics, Bremen, Germany), equipped with an ion trap
Software	Data Analysis (Bruker Daltonics, Bremen, Germany)
Flow	200 μL/hour
Dry gas	N_2, 4L/min, 300 ^{0}C
Nebulizer gas	N_2, 10 psi
Mode	positive or negative ion mode, respectively
ICC target	100,000 (positive mode) and 70,000 (negative mode)
Average scans	100
Capillary voltage	3500-4000 V (negative mode)
End plate offset	-500 V (negative mode)
Capillary exit	-280 V (negative mode)
Skimmer	-40 V (negative mode)
Compound stability	1000%
Trap drive level	100%
Target Mass	1000
Solvent	Methanol
	mixture of acetonitrile and H_2O at various ratios (v/v 2:8, or 4:6 and 7:3)
LC-IT-MS	
Instrument	HCT Ultra ETDII (Bruker Daltonics, Bremen, Germany), equipped with an ion trap
Software	Data Analysis (Bruker Daltonics, Bremen, Germany)
Flow	0.2 mL/min
Column	RP-C_{18} (Phenomenex, Kinetex, 2.6 μm, 100 × 2.1 mm)
Mobile phase	A: H_2O/HOAc (99/1, v/v)

	B: acetonitrile/HOAc (99/1, v/v)
Pump	Binary pump, series 1100, G1312A, Agilent technologies
Autosampler	Series 1200, G1392B, Agilent technologies
DAD-Detector	200-600 nm, series 1100, G1315B, Agilent technologies
Gradient system	90% A (0 min) →20% A (60 min)
Dry gas	N_2, 9 L/min, 365 ^{0}C
Nebulizer gas	N_2, 40 psi
Voltages	3500-4000 V (negative mode)
Injection volume	15 μ L

Drying of organic solvents

For 250 mL of anhydrous solvent, 25 g of mol sieve (3 Å for MeOH, t-BuOH, ACN and 4 Å for dioxane, DMF, DMSO, pyridine, toluene) were activated at 115 °C for 12 hours and at 300 °C for 3 hours. Hereafter, the solvent and dried mol sieve were mixed in a bottle (bottle has been dried under heating and then cooled down) under a N_2 atmosphere. After 24 hours duration time, tried solvent could be used for reaction.

7.2 Reduction of molar mass by sonification

The KGM aqueous solution (2 mg/mL, 30 mL) was degraded by utilizing a SONOPULS Ultrasonic homogenizer in a 50 mL of centrifuge tube with KE 76 Sonotrode. The solution was stirred during the degradation and the centrifuge tube was placed in a 4 ℃ aquatic bath. After 3 hours, the clear solution was dialyzed (MWCO of 14 kDa) and lyophilized to retain dry KGM (→ sono-KGM, with 92% recovery yield).

7.3 Alkylation

7.3.1 Preparation of partially methylated KGM and mannan

In a round bottomed flask 1.6 g of KGM was stirred in 140 mL of distilled water overnight. Later 6 g of NaOH powder was added into the flask, automatic pH titrator was used for maintaining a constant pH of 13.6 of the aqueous system at room temperature. After adding NaOH KGM solution became clear. After cooling the solution to 15 °C, 10 mL of CH_3I was added to the reaction mixture which was let warming up to room temperature again. During the reaction the liquid was vigorously stirred to mix the two phases. During the reaction pulverized NaOH and CH_3I were repeatedly added to maintain pH and CH_3I-phase. By taking aliquots (30 mL) at various times (1, 5, 10, 22, 48 and 54 hours), a set of MKGMs was obtained, named M-KGM-1, M-KGM-2, M-KGM-3, M-KGM-4, M-KGM-5 and M-KGM-6,

indicating the hours of reaction. The yield was approximately 89% for all 6 samples on average. The withdrawn aliquots were purified by dialysis (MWCO 3500 Da) and subsequent lyophilization. Methylation of mannan was performed in the same system with defined amounts of NaOH and CH_3I to get partially methylated mannan with DS 1.06 (named MM). ATR-IR spectroscopy was used to check the progress of the methylation reaction.

7.3.2 Preparation of partially methylated KGM in the presence of borate

Approximate 50 mg of dialyzed and freeze-dried KGM was dissolved in 10 mL of distilled water (or solvent mixture) overnight. Different amounts of $Na_2B_4O_7 \cdot 10\ H_2O$ were added to KGM solution and gelation occurred instantly. 0.4 g of NaOH powder was added and the viscosity of KGM gel slowly decreased. After cooling to r.t., 2 mL of CH_3I was added and the two phase mixture was stirred for 48 hours at various temperatures. After 24 hours, the same amount of $Na_2B_4O_7 \cdot 10\ H_2O$ and NaOH powder and half the amount of CH_3I were added. The reaction conditions for the all samples are summarized in Table 4.1 in Chapter 4. As a reference, M-KGM was prepared in parallel under the same conditions, except the addition of borate.(Table 4.1 in Chapter 4). The yield of M-KGM was in the range of 93 – 101 %.

The products were purified by dialysis (MWCO of 3500 Da) and subsequently lyophilized. The entries M-KGM-8 to M-KGM-20 are listed in Table 4.1 in Chapter 4.

7.3.3 Preparation of fully ethylated M-KGM entry, MC and MM

For analysis of the methyl pattern, portions of ca. 10 mg of all M-KGM (M-KGM-1 to M-KGM-19) were perethylated in DMSO with NaOH/EtI at room temperature.[155] The *O*-ethyl-*O*-methyl-KGMs (EM-KGM) were isolated by dialysis and lyophilization (yield 82-94%). If necessary, ethylation was performed twice. Completeness of reaction was proved by the absence of significant OH vibration in ATR-IR. MM and MC were perethylated as well.

7.3.4 Preparation of fully deuteromethylated M-KGM entry

Perdeuteromethylation of M-KGM was performed according to the method of Ciucanu and Costello with NaOH/ CH_3I-d_3 in DMSO at room temperature.[156] The *O*-methyl/*O*-methyl-d_3-KGMs (DM-KGM) samples were purified as described above. Completeness of deuteromethylation was proved by ATR-IR spectroscopy.

7.3.5 Preparation of partially methylated KGM (M-KGM) via their tin-mediated complexes (in flask)

Sono-KGM (10-20 mg) was dissolved in a 250 mL round bottom flask with certain volume of dried solvent and the resulting suspension mixture was stirred for 24 hours. Depending on the sample preparation, 1.5-5 equiv. of Bu_2SnO (per glycosyl unit) were added either as a solid or

as a methanolic suspension (50 mg Bu_2SnO/ mL MeOH) and the reaction mixture was refluxed for 6 to 24 hours at a certain temperature. After removing the solvent by a rotary evaporator, the residue was dried under N_2 flow (→ stan-KGM). Small amounts of stan-KGM was submitted for ATR-IR analysis. The remaining stan-KGM was dissolved or suspended in the alkylating solvent and mixed with catalyst and a certain amount of methyl iodide. The reaction was carried out at different temperature for 24 to 66 hours. Hereafter, the products were purified by dialysis (MWCO of 3500 Da) and subsequently lyophilized (→ M-KGM). For the reduction of iodine, 5 mL of 5% sodium thiosulfate solution was added to the aqueous sample suspension during the dialysis. Relative molar composition of products (M-KGM-23 - 31, M-KGM-33 - 36) are listed at Table 9.8 in appendix and individual detailed reaction parameters are listed at Table 9.9 in appendix.

7.3.6 Preparation of partially methylated KGM (M-KGM) via their tin-mediated complexes (in vial)

8.5-15 mg of sono-KGM was dissolved in a 5 mL V-vial with 3-4 mL of dried pyridine (or mixture of dioxane and MeOH) and the resulting suspension mixture was stirred for 24 hours (8.5 mg starting material) or agitated in an ultrasonic bath (30 minutes, 15% amplitude, 15 mg starting material). 0.1 to 4 equiv. of Bu_2SnO (per glycosyl unit) were added as a methanolic suspension (50 mg Bu_2SnO/ mL MeOH) and the reaction mixture was heated to a certain temperature for 16 to 24 hours in a closed V-vial. The residue was dried by co-distillation with toluene under a stream of N_2 (→ stan-KGM). ATR-IR spectra were recorded from stan-KGM. The remaining stan-KGM was dissolved or suspended in the mixture of ACN and DMF (10:1, v/v) and mixed with catalyst (TBAB and K_2CO_3) and CH_3I. The reaction was carried out at different temperatures for 44-48 hours. After methylation, the solvent of the sample was removed under N_2 flow. The products were purified by dialysis (MWCO of 3500 Da) and subsequent lyophilized (→ M-KGM). Relative molar composition of all entries (M-KGM-21, 22, 32, 37, 40, 42 - 49) with their individual reaction parameters are found in Table 9.8 and Table 9.9 in appendix, respectively.

7.3.7 General procedure for dibutylstannylation of KGM (in vial)

15 mg of sono-KGM was dissolved in 3 mL of dry pyridine in a 5 mL V-vial and 2 equiv. of methanolic Bu_2SnO suspension was added. The stannylation was performed at 115 °C for 16 hours. After removal of the pyridine in a stream of N_2, stan-KGM was suspended in ACN:DMF (10:1), 1 equiv. of TBAB and 2 equiv. of K_2CO_3 were added, and the mixture was methylated at 70 °C for 48 hours with an excess of CH_3I. The product purification followed as previously described in section 7.3.8. Methyl α-D-mannoside and methyl α-D-glucoside were reacted according to the standard method to obtain regioselective methylated mannoside (MeMan-tin) and glucoside(MeGlc-tin). Relative molar composition of all entries (M-KGM-41, M-Man and M-Glc) with their individual reaction parameters are found in Table 9.8 and Table 9.9 in appendix, respectively.

7.3.8 Sample clean-up

10 mg of M-KGM-tin raw product still containing Bu_2SnO was suspended in 10 mL of MeOH in a 10 mL V-vial (stirred for 10 min) and then heated for 30 min in an oil bath (80 °C). M-KGM sedimented during cooling. After carefully removing the clear supernatant with a microliter syringe and drying the residue under a stream of N_2, purified M-KGM was obtained. M-KGM-37 - 44 were treated in this way.

7.3.9 Repeated stannylation/methylation according to 7.3.7

Sono-KGM (25 mg) was methylated to obtain M-KGM-21. Afterwards, M-KGM-21 was methylated one more time according to 7.3.7. However, considering the residual Bu_2SnO after the first methylation (no clean-up performed), we estimated that, 96 mg of M-KGM-21 raw product theoretically contains 27 % of M-KGM. Therefore, 15 mg of M-KGM-21 was submitted to stannylation in the presence of 1 equiv. of methanolic Bu_2SnO suspension, followed by methylation ($\rightarrow 2^{nd}$ run-1 eq., M-KGM-48). The other 15 mg of M-KGM-21 was stannylated in the presence of 2 equiv. of methanolic Bu_2SnO suspension, and subsequently submitted to methylation ($\rightarrow 2^{nd}$ run-2 eq., M-KGM-49).

7.3.10 Methylation of KGM in the presence of Bu_2SnO under solvent-free conditions

10-15 mg of KGM was homogenized in dry pyridine in a V-vial in an ultrasonic bath, and subsequently the solvent was removed. Methanolic Bu_2SnO suspension (1 equiv.), 0.5-1 equiv. of TBAB, 2 equiv. of K_2CO_3 or 4-6 equiv. of diisopropylethylamine (DIPEA) and an excess of CH_3I (ca. 70 equiv.) were added to the dry KGM. The mixture was heated for 12 or 24 hours to 90 or 100 °C. After evaporation of CH_3I the product was purified by dialysis

(MWCO 3.5 kDa) and subsequently lyophilized (→ M-KGM). Relative molar composition of all products (M-KGM-50 - 55) with their individual reaction parameters are found in Table 9.8 and Table 9.9 in appendix, respectively.

7.4 Analysis of the methyl pattern of M-KGM

7.4.1 Monomer analysis

Alditol acetate method (AAM)

Ca. 2 mg of EM-KGM was hydrolyzed in 2 M TFA at 120 °C for 2 hours, reduced to alditols with $NaBD_4$, and after removal of borate, acetylated with acetic anhydride in pyridine at 90 °C for 3 hours. Extracted alditol derivatives were analyzed by GLC-FID.[36] For peak assignment, *O*-ethyl-*O*-methyl cellulose and *O*-ethyl-*O*-methyl-mannan were converted to their alditol acetates, and analyzed by GLC-MS, respectively.

Reductive cleavage followed by acetylation or benzoylation (RCM-Ac/Bz)

Ca. 2 mg of EM-KGM was depolymerized by reductive cleavage method according to Gray et al.[37] Instead of acetylation with Ac_2O, benzoylation was performed with 50 mg of benzoic acid anhydride and 20 µL of 1-methylimidazole in pyridine, yielding 4-*O*-benzoyl-1,5-anhydroalditols for GLC-FID analysis.[38] For peaks assignment, *O*-ethyl-*O*-methyl cellulose and *O*-ethyl-*O*-methyl-mannan were submitted to the same procedure and analyzed by GLC-MS.

Methanolysis followed by acetylation or trimethylsilylation (MeOH-Ac/TMS)

Ca. 2 mg of M-KGM was depolymerized in freshly prepared 1.5 M methanolic HCl at 90 °C for 2 hours, followed by acetylation or trimethylsilylation after evaporation of MeOH/HCl.[39] The derivatives were analyzed by GLC-FID and GLC-MS to deduce position of methylation. Corresponding derivatives prepared from MM and MC were used as standards for peak evaluation.

7.4.2 Oligomer analysis of *O*-methyl/methyl-d_3-KGM

Partial hydrolysis of *O*-methyl/methyl-d_3-KGM

Ca. 2 mg of DM-KGM was dispersed in 750 µL of distilled water in a 1 mL-V-vial for 2 hours for better dissolution. Then 250 µL of 2 M HCl was added and the mixture was kept at 90 °C for 30 min. After cooling to room temperature, the sample was co-distilled with toluene to remove aqueous acid, and dried under a stream of N_2. The residue was dissolved in 500 µL of MeOH.

Labeling with *m*-amino benzoic acid

The partially hydrolyzed DM-KGM (ca. 2 mg) was dissoved in 0.5mL of MeOH and mixed with 0.3 mL of *m*ABA-solution (2 equiv./glycosyl unit) and 0.15 mL of glacial acetic acid. The reaction was holding at 40 °C for 30 min.[82] Reduction was performed by adding 50 μL of 2-picoline borane solution (2 equiv./glycosyl unit) and the mixture was holding at 40 °C for 45 min. The solvent was evaporated under a stream of N_2, 1 mL of MeOH was added and evaporated again. Using a mixture of ACN/H_2O/acetic acid (9.5/89.5/1, v/v/v) as solvent, the sample was dissolved to a concentration of 0.2 mg/mL.

ESI-MS analysis with syringe pump infusion

The analyte dissolved in various solvents (MeOH and mixtures of ACN and H_2O at various ratios (v/v 2:8, or 4:6 and 7:3)) were infused directly by means of a syringe pump at a flow rate of 200 µL/hour.

LC-ESI-MS analysis

For LC-ESI-MS the MS is coupled with an Agilent HPLC system consisting of a binary pump and a DAD. A RP_{18}-column (Phenomenex, Kinetex, 2.6 µm, 100 × 2.1 mm) was used with mobile phase H_2O/HOAc (99/1, v/v; A) and ACN/HOAc (99/1, v/v; B) in a linear gradient system (0 min, 90 vol% A and 60 min, 20 vol%A) and a flow rate of 0.2 mL/min. From the total mass spectrum of the DM-KGM oligomers, extracted ion chromatograms (EIC) were generated according to mass ranges of interest for the particular DPs.[64]

7.5 Thermo properties analysis

Differential scanning calorimetry (DSC)

DSC thermograms were recorded using a DSC 204 (NETZSCH) under N_2 atmosphere. M-KGMs were heated from -50 °C to 190 °C (first heating scan) at 30 °C/min, and then quenched to -50 °C. The second heating scan was run from -50 °C to 250 °C at a heating rate of 30 °C/min. To indicate the point of the heat capacity transition, an endothermic capacity change midpoint temperature (T) was recorded in the second heating scan. The processing of the data were performed with the Netzsch Proteus – Thermal Analysis software.

Thermogravimetric analysis (TGA)

TGA of M-KGMs were carried out using a TG 209 (NETZSCH) instrument under N_2 and synthetic air atmosphere. Thermograms were recorded from 25 °C to 550 °C at a heating rate of 10 °C/min and subsequently from 550 °C to 950 °C by 50 °C/min. The processing of the data were performed with the Netzsch Proteus – Thermal Analysis software.

8 References

1. W. L. A. Hetterscheid, *Blumea - Biodiversity, Evol. Biogeogr. Plants* **1994**, *39*, 237.
2. Y. Q. Zhang, B. J. Xie, X. Gan, *Carbohydr. Polym.* **2005**, *60*, 27.
3. S. S. Behera, R. C. Ray, *Food Rev. Int.* **2017**, *33*, 22.
4. B. Gómez, B. Míguez, R. Yáñez, J. L. Alonso, *J. Agric. Food Chem.* **2017**, *65*, 2019.
5. C. Tsuji, *J. Colloid Agric. Tokyo Imp. Univ.* **1895**, *2*, 103.
6. F. Smith, H. C. Srivastava, *J. Am. Chem. Soc.* **1959**, *81*, 1715.
7. K. Kato, K. Matsuda, *Agric. Biol. Chem.* **1969**, *33*, 1446.
8. N. Kishida, S. Okimasu, T. Kamata, *Agric. Biol. Chem.* **1978**, *42*, 1645.
9. M. Maeda, H. Shimahara, N. Sugiyama, *Agric. Biol. Chem.* **1980**, *44*, 245.
10. K. Katsuraya, K. Okuyama, K. Hatanaka, R. Oshima, T. Sato, K. Matsuzaki, *Carbohydr. Polym.* **2003**, *53*, 183.
11. S. Albrecht, G. C. J. Van Muiswinkel, J. Xu, H. A. Schols, A. G. J. Voragen, H. Gruppen, *J. Agric. Food Chem.* **2011**, *59*, 12658.
12. Q. Zhang, P. Mischnick, *Macromol. Chem. Phys.* **2017**, *218*, 1700119.
13. Z. Pan, J. Meng, Y. Wang, *Particuology* **2011**, *9*, 265.
14. K. Kato, T. Watanabe, K. Matsuda, *Agric. Biol. Chem.* **1970**, *34*, 532.
15. H. Shimahara, H. Suzuki, N. Sugiyama, K. Nisizawa, *Agric. Biol. Chem.* **1975**, *39*, 301.
16. P. Cescutti, C. Campa, F. Delben, R. Rizzo, *Carbohydr. Res.* **2002**, *337*, 2505.
17. J. Keithley, B. Swanson, *Altern. Ther. Health Med.* **2005**, *11*, 30.
18. X. Wen, T. Wang, Z. Wang, L. Li, C. Zhao, *Int. J. Biol. Macromol.* **2008**, *42*, 256.
19. J. Chatterji, J. K. Borchardt, *J. Pet. Technol.* **1981**, *33*, 2042.
20. M. Wang, W. He, S. Wang, X. Song, *Carbohydr. Polym.* **2015**, *125*, 334.
21. S. Singh, G. Singh, S. K. Arya, *Int. J. Biol. Macromol.* **2018**, *119*, 79.
22. S. Charoenrein, O. Tatirat, K. Rengsutthi, M. Thongngam, *Carbohydr. Polym.* **2011**, *83*, 291.
23. G. Xiong, W. Cheng, L. Ye, X. Du, M. Zhou, R. Lin, S. Geng, M. Chen, H. Corke, Y. Cai, *Food Chem.* **2009**, *116*, 413.
24. H. L. Chen, Y. C. Chen, Y. P. Liaw, W. H. H. Sheu, T. S. Tai, *J. Am. Coll. Nutr.* **2003**, *22*, 36.
25. F. Zhu, *Food Chem.* **2018**, *256*, 419.
26. J. Li, Y. Wang, W. Jin, B. Zhou, B. Li, *Food Hydrocoll.* **2014**, *35*, 375.
27. M. Triki, A. M. Herrero, F. Jiménez-Colmenero, C. Ruiz-Capillas, *Meat Sci.* **2013**, *93*, 351.

28. W. N. Haworth, *J. Chem. Soc.* **1915**, *107*, 8.
29. S. Hakomori, *J. Biochem.* **1964**, *55*, 205.
30. N. T. An, D. T. Thien, N. T. Dong, P. L. Dung, P. T. B. Hanh, T. T. Y. Nhi, D. A. Vu, *Carbohydr. Polym.* **2011**, *84*, 173.
31. C. Wang, Y. Zhu, M. Xu, Y. Qiao, W. Zhang, *Appl. Mech. Mater.* **2011**, *52–54*, 1340.
32. S. Bo, T. Muschin, T. Kanamoto, H. Nakashima, T. Yoshida, *Carbohydr. Polym.* **2013**, *94*, 899.
33. Y. Enomoto-Rogers, Y. Ohmomo, T. Iwata, *Carbohydr. Polym.* **2013**, *92*, 1827.
34. P. Mischnick, D. Momcilovic, *Adv. Carbohydr. Chem. Biochem.* **2010**, *64*, 117.
35. S. de Goeij, *Literature thesis*, Univ. van Amsterdam, **2013**.
36. K. Voiges, R. Adden, M. Rinken, P. Mischnick, *Cellulose* **2012**, *19*, 993.
37. A. J. D'Ambra, M. J. Rice, S. G. Zeller, P. R. Gruber, G. R. Gary, *Carbohydr. Res.* **1988**, *177*, 111.
38. L. E. Elvebak II, T. Schmitt, G. R. Gray, *Carbohydr. Res.* **1993**, *246*, 1.
39. A. Gonera, V. Goclik, M. Baum, P. Mischnick, *Carbohydr. Res.* **2002**, *337*, 2263.
40. S. Angyal, K. Dawes, *Aust. J. Chem.* **1968**, *21*, 2747.
41. C. K. Lee, E. J. Kim, *Carbohydr. Res.* **1999**, *320*, 223.
42. L. E. Elvebak II, H. J. Cha, P. McNally, G. R. Gray, *Carbohydr. Res.* **1995**, *274*, 71.
43. G. L. Sassaki, P. A. J. Gorin, L. M. Souza, P. A. Czelusniak, M. Iacomini, *Carbohydr. Res.* **2005**, *340*, 731.
44. R. K. Merkle, I. Poppe, *Methods Enzymol.* **1994**, *230*, 1.
45. D. P. Sweet, R. H. Shapiro, P. Albersheim, *Carbohydr. Res.* **1975**, *40*, 217.
46. M. Stefansson, *Carbohydr. Res.* **1998**, *312*, 45.
47. W. Tüting, G. Albrecht, B. Volkert, P. Mischnick, *Starch/Staerke* **2004**, *56*, 315.
48. M. Van Duin, J. A. Peters, A. P. G. Kieboom, H. Van Bekkum, *Tetrahedron* **1984**, *40*, 2901.
49. T. Wang, X. Yang, D. Wang, Y. Jiao, Y. Wang, Y. Zhao, *Carbohydr. Polym.* **2012**, *88*, 754.
50. K. Kobayashi, C. Huang, T. P. Lodge, *Macromolecules* **1999**, *32*, 7070.
51. K. Voiges, N. Lämmerhardt, P. Mischnick, *Cellulose* **2017**, *24*, 627.
52. K. Voiges, N. Lämmerhardt, C. Distelrath, P. Mischnick, *Cellulose* **2017**, *24*, 555.
53. R. Adden, W. Niedner, R. Müller, P. Mischnick, *Anal. Chem.* **2006**, *78*, 1146.
54. R. Adden, R. Müller, P. Mischnick, *Cellulose* **2006**, *13*, 459.
55. P. Mischnick, G. Kühn, *Carbohydr. Res.* **1996**, *290*, 199.

56. S. Gangula, M. Nimtz, P. Mischnick, *Int. J. Mass Spectrom.* **2016**, *402*, 57.
57. P. Mischnick, J. Heinrich, M. Gohdes, O. Wilke, N. Rogmann, *Macromol. Chem. Phys.* **2000**, *201*, 1985.
58. K. Wang, S. Gao, C. Shen, J. Liu, S. Li, J. Chen, X. Ren, Y. Yuan, *Carbohydr. Polym.* **2018**, *181*, 736.
59. K. Takechi, K. Furuhata, *Transaction* **1999**, *55*, 315.
60. N. Handa, R. Montgomery, *Carbohydr. Res.* **1969**, *11*, 467.
61. Y. Zhang, J. Li, M. E. Lindström, P. Mischnick, *Carbohydr. Res.* **2015**, *402*, 172.
62. C. L. Xu, C. Eckerman, A. Smeds, M. Reunanen, P. C. Eklund, R. Sjöholm, S. Willför, *Nord. Pulp Pap. Res. J.* **2011**, *26*, 167.
63. L. Maleki, U. Edlund, A. Albertsson, *Biomacromolecules* **2015**, *16*, 667.
64. P. Mischnick, R. Adden, *Macromol. Symp.* **2008**, *262*, 1.
65. S. N. Pawar, K. J. Edgar, *Biomaterials* **2012**, *33*, 3279.
66. R. J. Coleman, G. Lawrie, L. K. Lambert, M. Whittaker, K. S. Jack, L. Grøndahl, *Biomacromolecules* **2011**, *12*, 889.
67. E. C. Millard, L. R. Schroeder, N. S. Thompson, *Carbohydr. Res.* **1977**, *56*, 259.
68. A. H. Haines, *Adv. Carbohydr. Chem. Biochem.* **1976**, *33*, 11.
69. R. M. Izatt, L. D. Hansen, J. H. Rytting, J. J. Christensen, *J. Am. Chem. Soc.* **1965**, *87*, 2760.
70. P. Mares, J. Skorepa, M. Fridrich, *J. Chromatogr.* **1969**, *42*, 435.
71. K. Voiges, *Dissertation*, TU Braunschweig, **2015**.
72. J. Raßloff, *Diploma Thesis*, TU Braunschweig, **2017**.
73. H. M. Spurlin, *J. Am. Chem. Soc.* **1939**, *61*, 2222.
74. P. W. Arisz, H. J. J. Kauw, J. J. Boon, *Carbohydr. Res.* **1995**, *271*, 1.
75. S. Feng, C. Bagia, G. Mpourmpakis, *J. Phys. Chem. A* **2013**, *117*, 5211.
76. A. N. de Belder, B. Lindberg, O. Theander, *Acta Chem. Scand.* **1962**, *16*, 2005.
77. B. Norrman, *Acta Chem. Scand.* **1968**, *22*, 1623.
78. P. J. Garegg, *Acta Chem. Scand.* **1963**, *17*, 1343.
79. T. Kondo, A. Koschella, B. Heublein, D. Klemm, T. Heinze, *Carbohydr. Res.* **2008**, *343*, 2600.
80. J. Berglund, T. Angles d'Ortoli, F. Vilaplana, G. Widmalm, M. Bergenstråhle-Wohlert, M. Lawoko, G. Henrikasson, M. Lindström, J. Wohlert, *Plant J.* **2016**, *88*, 56.
81. R. Adden, M. Knarr, B. Huebner-Keese, R. Sammler (Dow Global Technologies Llc), *US20150045320*, **2015**.

82. J. Cuers, I. Unterieser, W. Burchard, R. Adden, M. Rinken, P. Mischnick, *Carbohydr. Res.* **2012**, *348*, 55.
83. H. H. Jensen, M. Bols, *Acc. Chem. Res.* **2006**, *39*, 259.
84. K. Kato, K. Matsuda, *Agric. Biol. Chem.* **1972**, *36*, 639.
85. T. Timell, *Can. J. Chem.* **1964**, *42*, 1456.
86. R. Moriana, Y. Zhang, P. Mischnick, J. Li, M. Ek, *Carbohydr. Polym.* **2014**, *106*, 60.
87. M. C. Ramos-Sanchez, F. J. Rey, M. L. Rodriguez, F. J. Martin-Gil, J. Martin-Gil, *Thermochim. Acta,* **1988**, *134*, 55.
88. S. C. Barros, A. A. da Silva, D. B. Costa, C. M. Costa, S. Lanceros- Méndez, M. N. T. Maciavello, J. L. G. Ribelles, F. Sentanin, A. Pawlicka, M. M. Silva, *Cellulose* **2015**, *22*, 1911.
89. N. K. Anuar, W. T. Wui, D. K. Ghodgaonkar, M. N. Taib, *J. Pharm. Biomed. Anal.* **2007**, *43*, 549.
90. M. J. Zohuriaan, F. Shokrolahi, *Polym. Test.* **2004**, *23*, 575.
91. M. G. Chudzinski, Y. Chi, M. S. Taylor, *Aust. J. Chem.* **2011**, *64*, 1466.
92. D. Wagner, J. P. H. Verheyden, J. G. Moffatt, *J. Org. Chem.* **1974**, *39*, 24.
93. M. E. Haque, T. Kikuchi, K. Yoshimoto, Y. Tsuda, *Chem. Pharm. Bull.* **1985**, *33*, 2243.
94. P. J. Kocieński, *Georg Thieme,* New York, **1994,** 21.
95. R. Eby, K. T. Webster, C. Schuerch, *Carbohydr. Res.* **1984**, *129*, 111.
96. Z. G. Chen, M. H. Zong, G. J. Li, *J. Appl. Polym. Sci.* **2006**, *102*, 1335.
97. A. B. Foster, *Adv. Carbohydr. Chem.* **1957**, *12*, 81.
98. S. Gao, J. Guo, K. Nishinari, *Carbohydr. Polym.* **2008**, *72*, 315.
99. J. Schott, J. Kretzschmar, M. Acker, S. Eidner, M. Z. Kumke, B. Drobot, A. Barkleit, S. Taut, V. Brendler, T. Stumpf, *Dalton Trans.* **2014**, *43*, 11516.
100. M. Makkee, A. P. G. Kieboom, H. Van Bekkum, *Recl. Trav. Chim. Pays-Bas* **1986**, *104*, 230.
101. M. P. Nicholls, P. K. C. Paul, *Org. Biomol. Chemitstry* **2004**, *2*, 1434.
102. R. Jasinski, D. Redwine, G. Rose, *J. Polym. Sci. Part B Polym. Phys.* **1996**, *34*, 1477.
103. S. W. Sinton, *Macromolecules* **1987**, *20*, 2430.
104. W. Jian, Y. Zeng, H. Xiong, J. Pang, *Carbohydr. Polym.* **2011**, *85*, 452.
105. E. W. Malcolm, J. W. Green, H. A. Swenson, *J. Chem. Soc.* **1964**, 4669.
106. R. G. P. Viera, G. R. Filho, R. M. N. de Assuncao, C. S. Meireles, J. G. Vieira, G. S. de Oliveira, *Carbohydr. Polym.* **2007**, *67*, 182.
107. J. Reuben, H. T. Conner, *Carbohydr. Res.* **1983**, *115*, 1.

108. B. T. Stokke, O. Smidsroed, F. Zanetti, W. Strand, G. Skjåk-Bræk, *Carbohydr. Polym.* **1993**, *21*, 39.
109. M. Bol, C. N. Sakellaris, C. R. Jacob, P. Mischnick, *Int. J. Mass Spectrom.* **2017**, *419*, 20.
110. M. Bishop, N. Shahid, J. Yang, A. R. Barron, *Dalt. Trans.* **2004**, *0*, 2621.
111. G. Dalessandro, G. Piro, D. H. Northcote, *Planta* **1986**, *169*, 564.
112. A. D. Elbein, *J. Biol. Chem.* **1968**, *244*, 1608.
113. G. Piro, A. Zuppa, G. Dalessandro, D. H. Northcote, *Planta* **1993**, *190*, 206.
114. A. D. Elbein, W. Z. Hassid, *Biochem. Biophys. Res. Commun.* **1966**, *23*, 311.
115. S. David, S. Hanessian, *Tetrahedron* **1985**, *41*, 643.
116. J. Lawandi, S. Rocheleau, N. Moitessier, *Tetrahedron* **2016**, *72*, 6283.
117. T. B. Grindley, *Adv. Carbohydr. Chem. Biochem.* **1998**, *53*, 17.
118. G. Yang, F. Kong, S. Zhou, *Carbohydr. Res.* **1991**, *211*, 179.
119. I. J. Boyer, *Toxicology* **1989**, *55*, 253.
120. L. Ballell, J. A. F. Joosten, F. A. el Maate, R. M. J. Liskamp, R. J. Pieters, *Tetrahedron Lett.* **2004**, *45*, 6685.
121. M. Giordano, A. Iadonisi, *J. Org. Chem.* **2014**, *79*, 213.
122. F. Peri, L. Cipolla, F. Nicotra, *Tetrahedron Lett.* **2000**, *41*, 8587.
123. H. Dong, Y. Zhou, X. Pan, F. Cui, W. Liu, J. Liu, O. Ramstroem, *J. Org. Chem.* **2012**, *77*, 1457.
124. T. B. Grindley, *Tin Chem. Fundam. Front. Appl.* **2008**, 497.
125. Y. Tsuda, M. E. Haque, K. Yoshimoto, *Chem. Pharm. Bull. (Tokyo).* **1983**, *31*, 1612.
126. S. David, A. Malleron, *Carbohydr. Res.* **2000**, *329*, 215.
127. G. Hodosi, P. Kováč, *Carbohydr. Res.* **1997**, *303*, 239.
128. H. Xu, Y. Lu, Y. Zhou, B. Ren, Y. Pei, H. Dong, Y. Pei, *Adv. Synth. Catal.* **2014**, *356*, 1735.
129. Z. Zhang, C. H. Wong, *Tetrahedron* **2002**, *58*, 6513.
130. P. H. Tam, T. L. Lowary, *Carbohydr. Res.* **2007**, *342*, 1741.
131. J. Alais, A. Maranduba, A. Veyrieres, *Tetrahedron Lett.* **1983**, *24*, 2383.
132. P. Fernández, J. Jiménez-Barbero, M. Martín-Lomas, *Carbohydr. Res.* **1994**, *254*, 61.
133. L. Xia, T. L. Lowary, *J. Org. Chem.* **2013**, *78*, 2863.
134. T. B. Grindley, R. Thangarasa, *Can. J. Chem.* **1990**, *68*, 1007.
135. X. Kong, B. T. Grindley, *Can. J. Chem.* **1994**, *72*, 2405.
136. S. David, A. Thieffry, A. Veyrières, *J. Chem. Soc. Perkin Trans.* **1981**, *1*, 1796.

137. M. Giordano, A. Iadonisi, *Tetrahedron Lett.* **2013**, *54*, 1550.
138. T. Ogawa, M. Matsui, *Carbohydr. Res.* **1978**, *62*, C1.
139. T. Ogawa, M. Matsui, *Carbohydr. Res.* **1977**, *56*, C1.
140. A. E. Manzi, A. S. Cerezo, *Carbohydr. Polym.* **1986**, *6*, 349.
141. S. Migdal, D. Gertner, A. Zilkha, *Isr. J. Chem.* **1967**, *5*, 163.
142. L. Ehrhardt, *Diploma Thesis*, Uni Hamburg, **1997**.
143. J. Raβloff, Q. Zhang, P. Mischnick, *Cellulose* **2019**, *25*, 4929.
144. A. Grönroos, P. Pirkonen, O. Ruppert, *Ultrason. Sonochem.* **2004**, *11*, 9.
145. Q. Zhang, P. Mischnick, *Macromol. Chem. Phys.* **2018**, *219*, 1700502.
146. V. Desai, M. A. Shenoy, P. R. Gogate, *Chem. Eng. Process. Process Intensif.* **2008**, *47*, 1451.
147. N. Schittenhelm, W. M. Kulicke, *Macromol. Chem. Phys.* **2000**, *201*, 1976.
148. L. H. Cheng, H. Nur Halawiah, B. N. Lai, H. M. Yong, S. L. Ang, *Int. Food Res. J.* **2010**, *17*, 1043.
149. A. G. Gonçalves, M. D. Noseda, M. E. R. Duarte, T. B. Grindley, *J. Org. Chem.* **2007**, *72*, 9896.
150. M. A. Nashed, L. Anderson, *Tetrahedron Lett.* **1976**, *17*, 3503.
151. R. Munavu, H. Szmant, *J. Org. Chem.* **1976**, *41*, 1832.
152. Y. Zhou, J. Li, Y. Zhan, Z. Pei, H. Dong, *Tetrahedron* **2013**, *69*, 2693.
153. T. A. Nguyen, T. T. Do, T. D. Nguyen, L. D. Pham, V. Du Nguyen, *Carbohydr. Polym.* **2011**, *84*, 64.
154. K. P. Sethi, K. P. R. Kartha, *Trends Carbohydr. Res.* **2016**, *8*, 29.
155. I. Ciucanu, F. Kerek, *Carbohydr. Res.* **1984**, *131*, 209.
156. I. Ciucanu, C. E. Costello, *J. Am. Chem. Soc.* **2003**, *125*, 16213.

9 Appendix

9.1 ATR-IR spectra of M-KGM-15/16

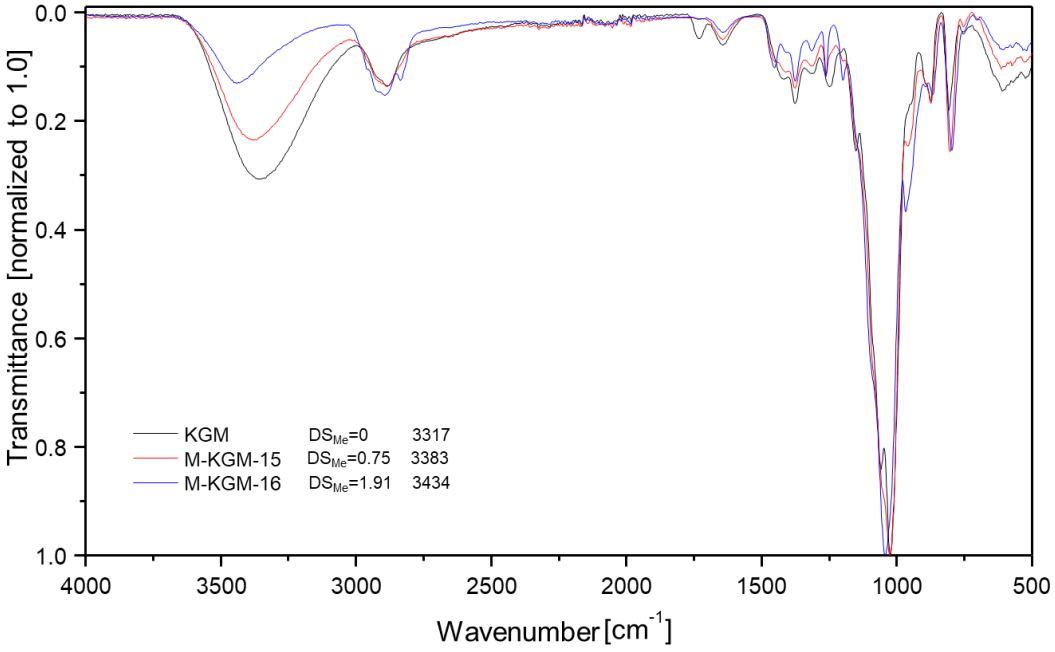

9.2 GLC-EI-MS spectra of M-KGM-derived mannose and glucose derivatives

Mass spectra of *O*-ethyl-*O*-methyl-glucitol acetate and mannitol acetate have been reported in the appendix of the thesis of Kristin Voiges.[71]

All mass spectra have been obtained by GLC-MS (temperature profile for setting described in section 7.1 according to various derivatization method).

9.2.1 4-*O*-Acetyl-*O*-ethyl-*O*-methyl-1,5-anhydroalditols

These mass spectra have been confirmed according to the publication of Gray et al.[42]

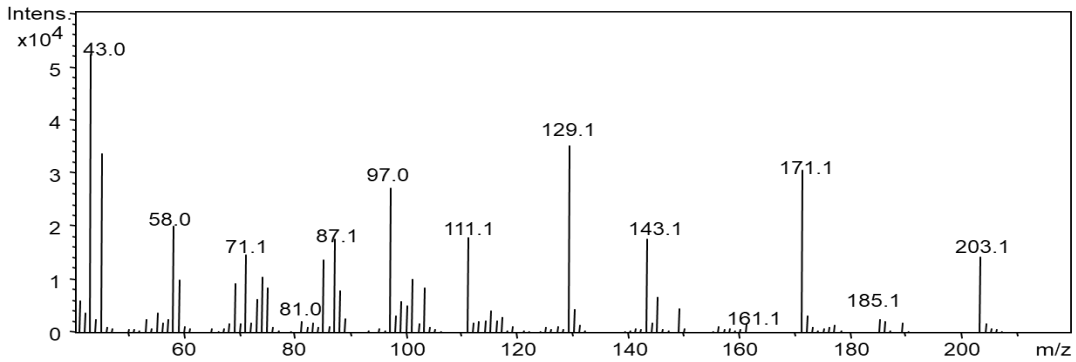

4-*O*-Acetyl-2,3,6-tri-*O*-methyl-1,5-anhydromannitol

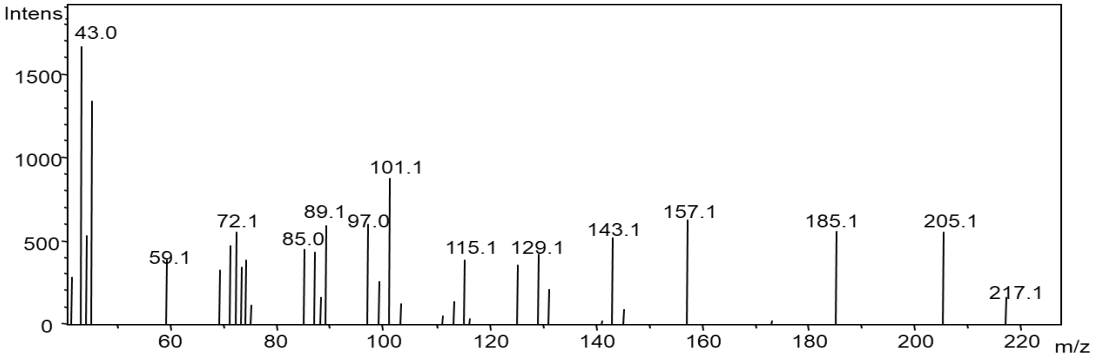

4-*O*-Acetyl-2-*O*-ethyl-3,6-di-*O*-methyl-1,5-anhydromannitol

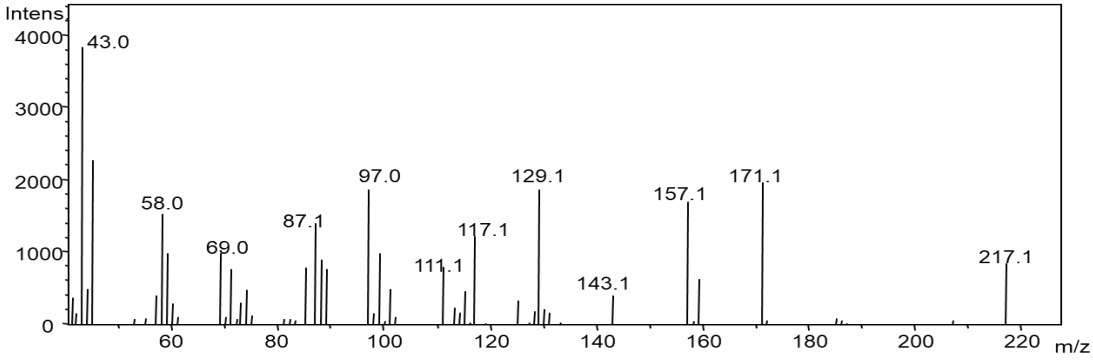

4-*O*-acetyl-3-*O*-ethyl-2,6-di-*O*-methyl-1,5-anhydromannitol

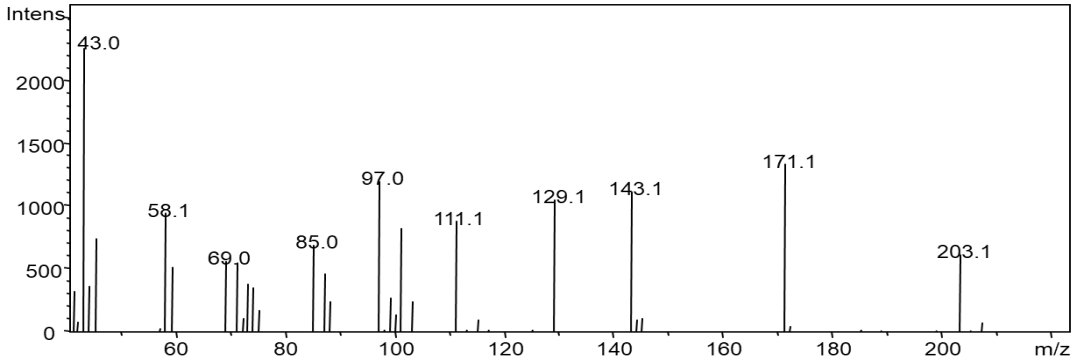

4-*O*-acetyl-6-*O*-ethyl-2,3-di-*O*-methyl-1,5-anhydromannitol

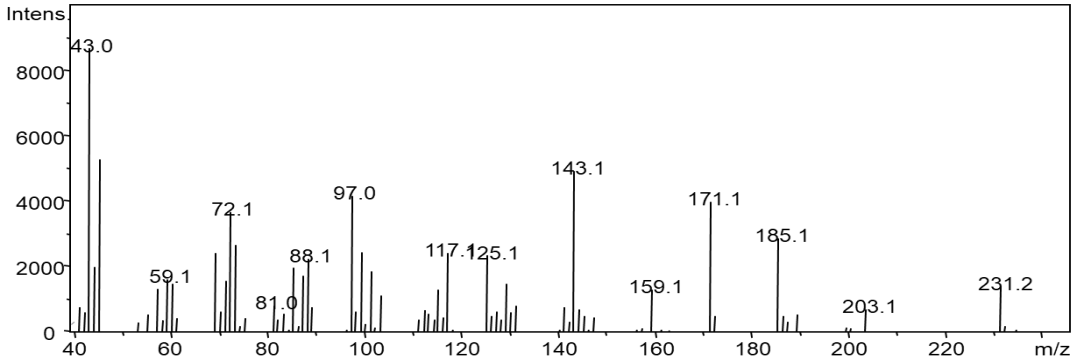

4-*O*-acetyl-2,3-di-*O*-ethyl-6-*O*-methyl-1,5-anhydromannitol

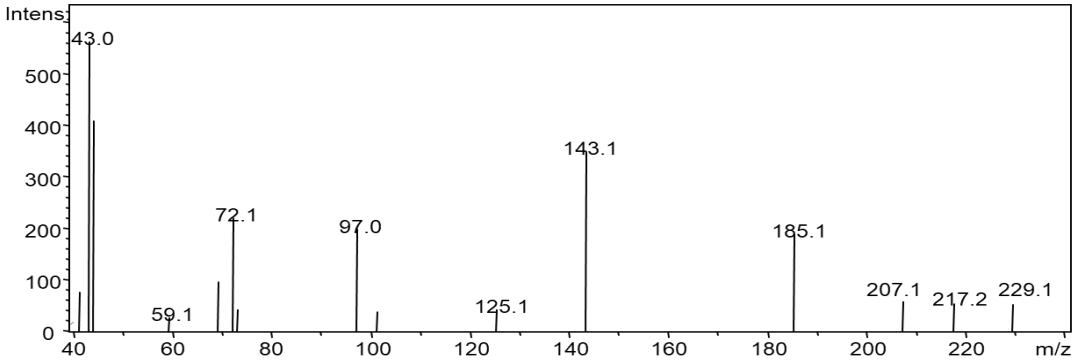

4-*O*-acetyl-2,6-di-*O*-ethyl-3-*O*-methyl-1,5-anhydromannitol

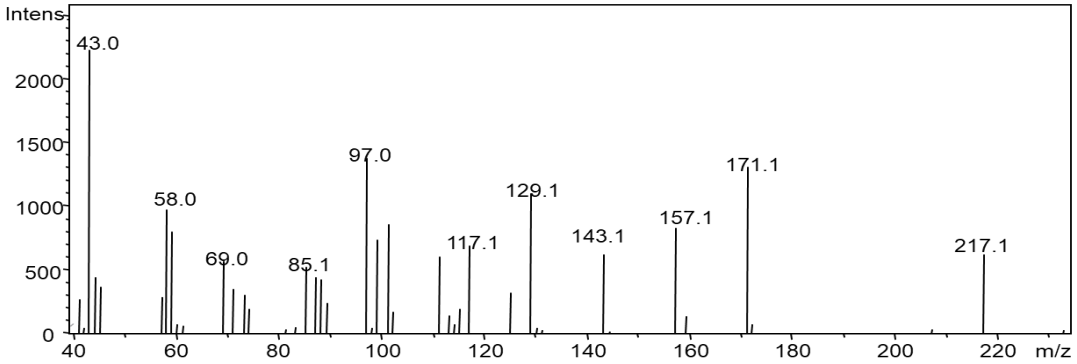

4-*O*-acetyl-3,6-di-*O*-ethyl-2-*O*-methyl-1,5-anhydromannitol

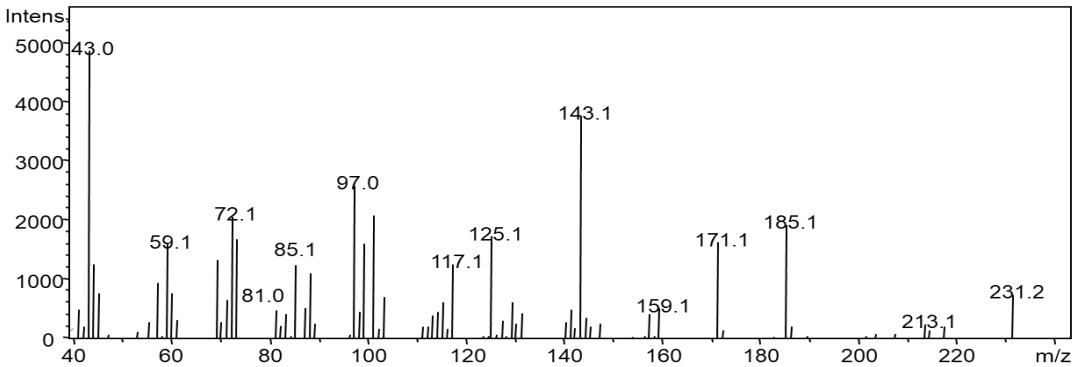

4-*O*-acetyl-2,3,6-tri-*O*-ethyl-1,5-anhydromannitol

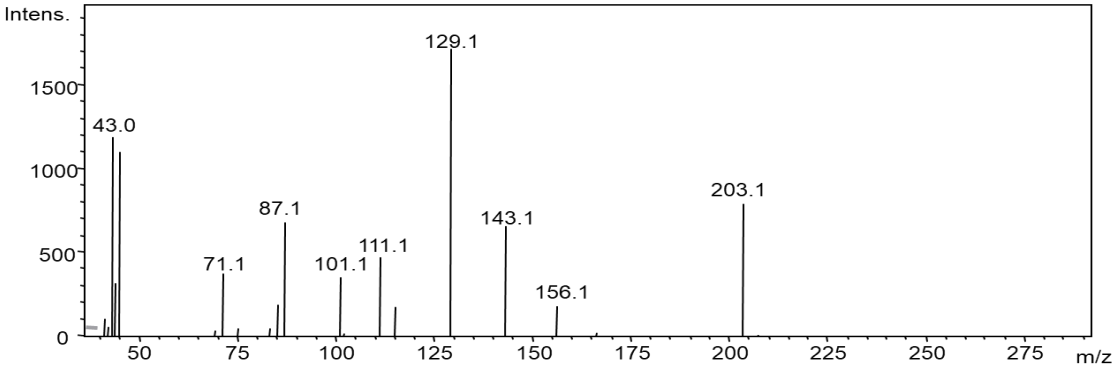

2,3,4,6-Tetra-*O*-methyl-1,5-anhydromannitol

9.2.2 4-*O*-Benzoyl-*O*-ethyl-*O*-methyl-1,5-anhydroalditols

These mass spectra have been confirmed according to the publication of Gray et al.[42]

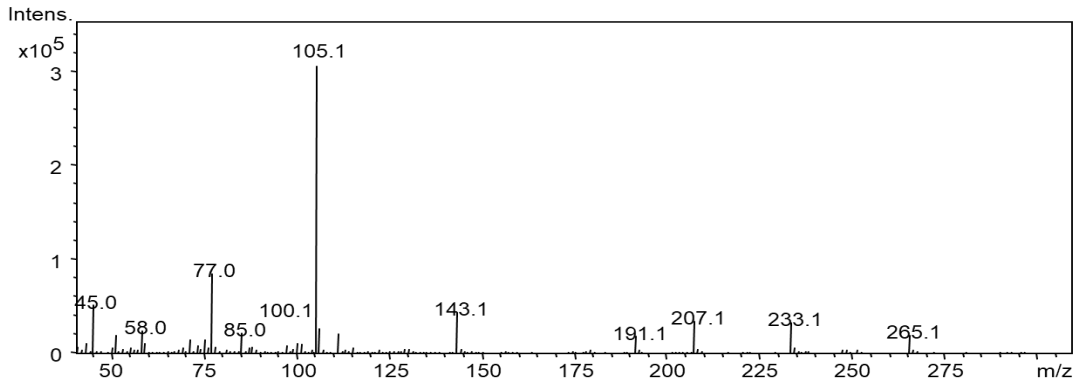

4-*O*-Benzoyl-2,3,6-tri-*O*-methyl-1,5-anhydromannitol

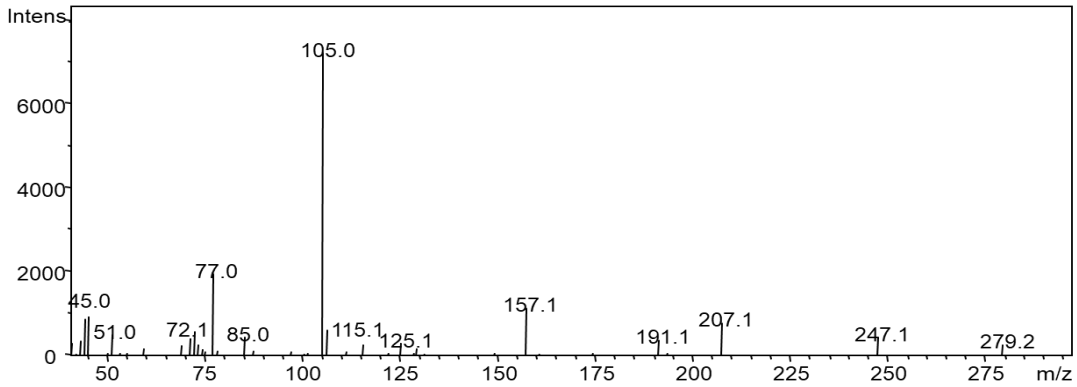

4-*O*-Benzoyl-2-*O*-ethyl-3,6-di-*O*-methyl-1,5-anhydromannitol

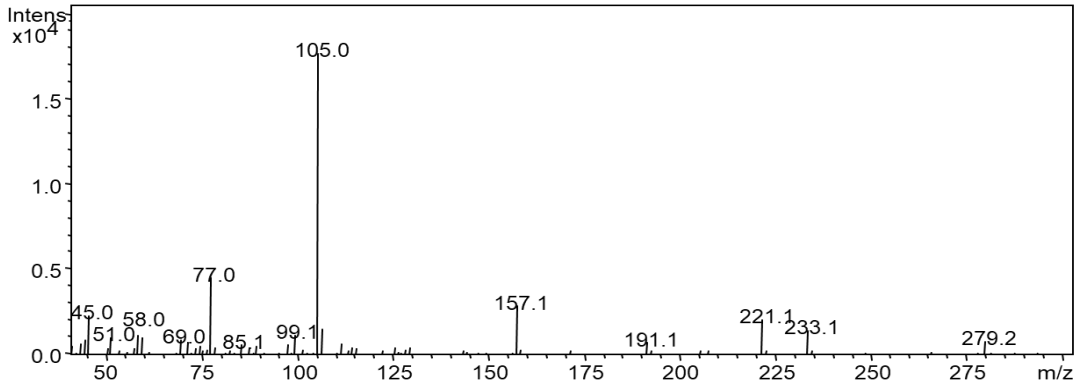

4-*O*-Benzoyl-3-*O*-ethyl-2,6-di-*O*-methyl-1,5-anhydromannitol

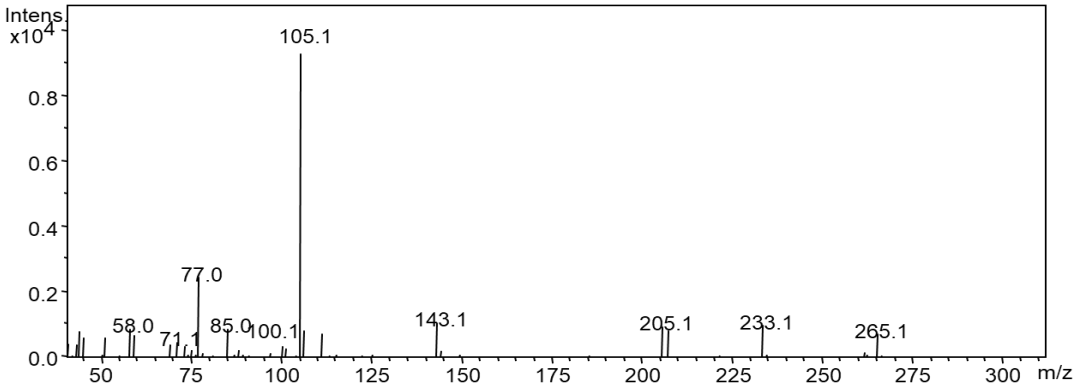

4-*O*-Benzoyl-6-*O*-ethyl-2,3-di-*O*-methyl-1,5-anhydromannitol

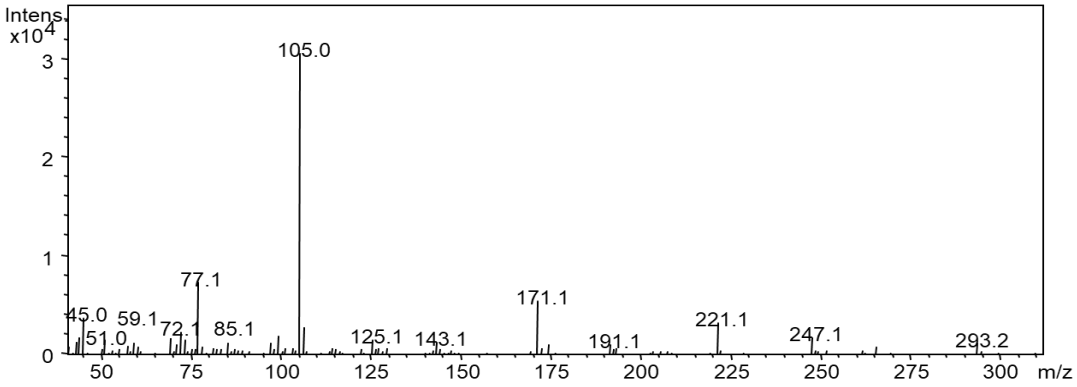

4-*O*-Benzoyl-2,3-di-*O*-ethyl-6-*O*-methyl-1,5-anhydromannitol

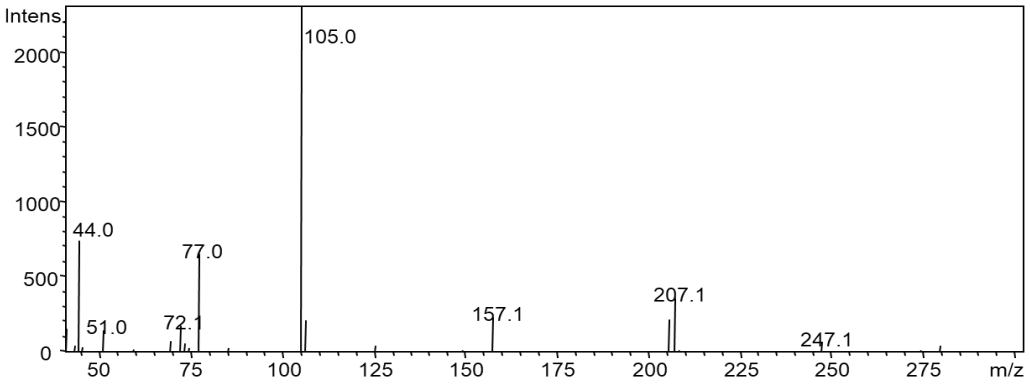

4-*O*-Benzoyl-2,6-di-*O*-ethyl-3-*O*-methyl-1,5-anhydromannitol

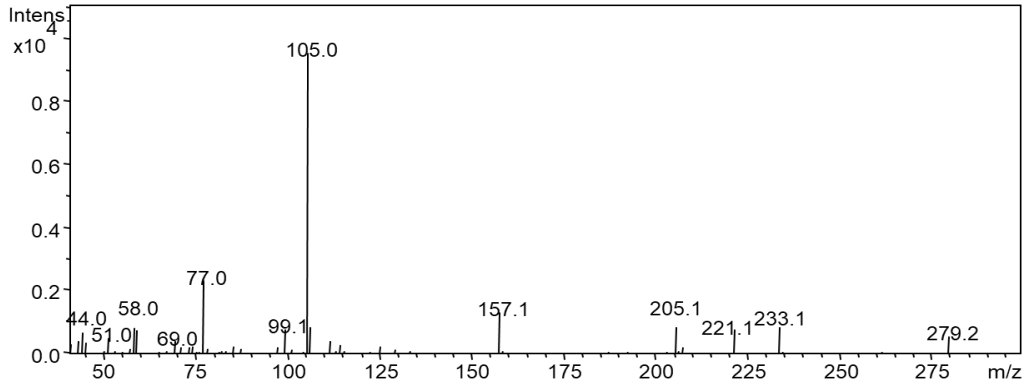

4-*O*-benzoyl-3,6-di-*O*-ethyl-2-*O*-methyl-1,5-anhydromannitol

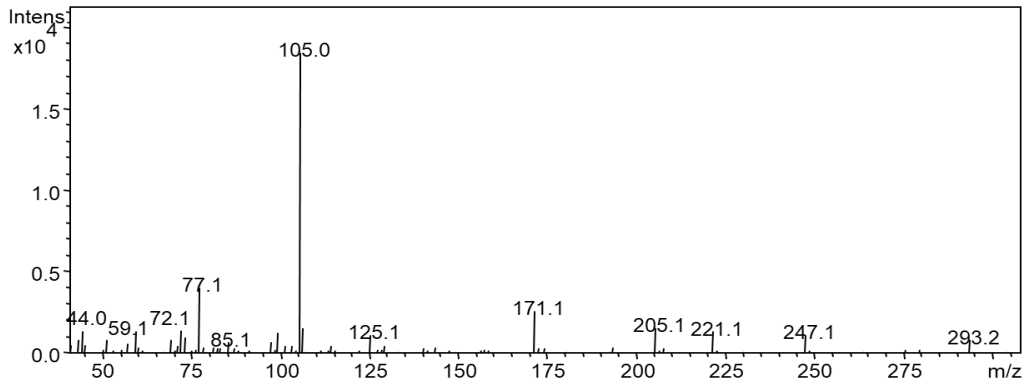

4-*O*-Benzoyl-2,3,6-tri-*O*-ethyl-1,5-anhydromannitol

9.2.3 Methyl *O*-acetyl-*O*-methyl-glucopyranoside

These mass spectra have been confirmed according to the publication of Merkle et al.[44]

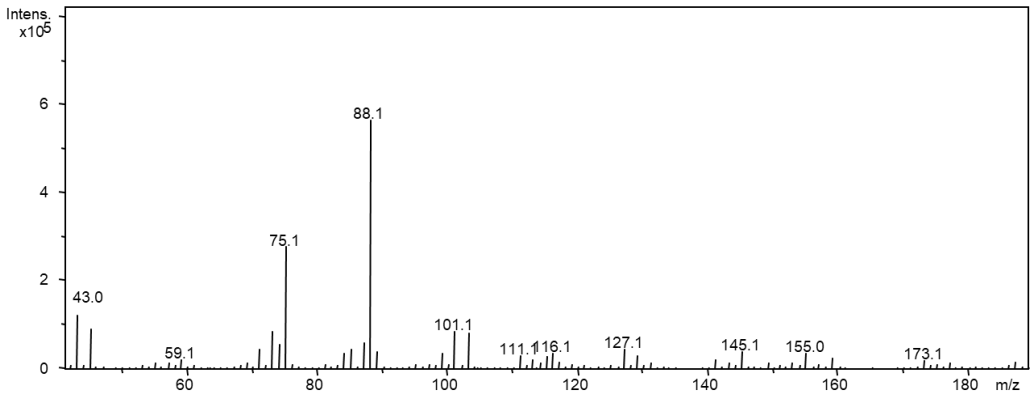

Methyl 4-*O*-acetyl-2,3,6-tri-*O*-methyl-mannopyranoside

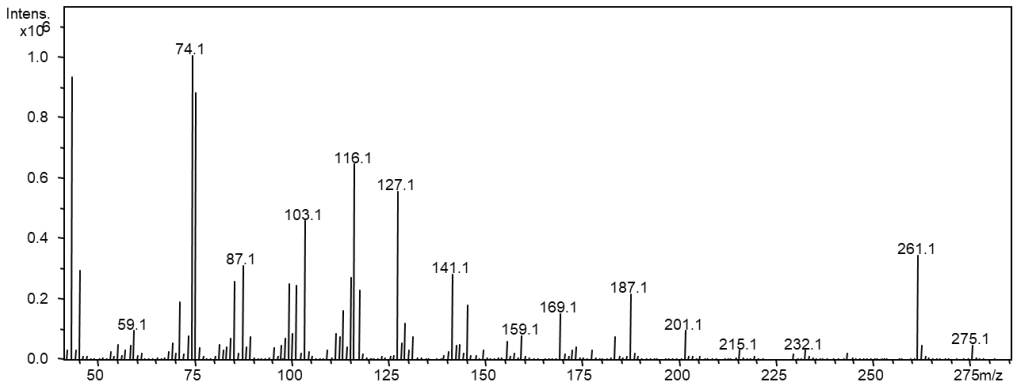

Methyl 2,4-di-*O*-acetyl-3,6-di-*O*-methyl-mannopyranoside

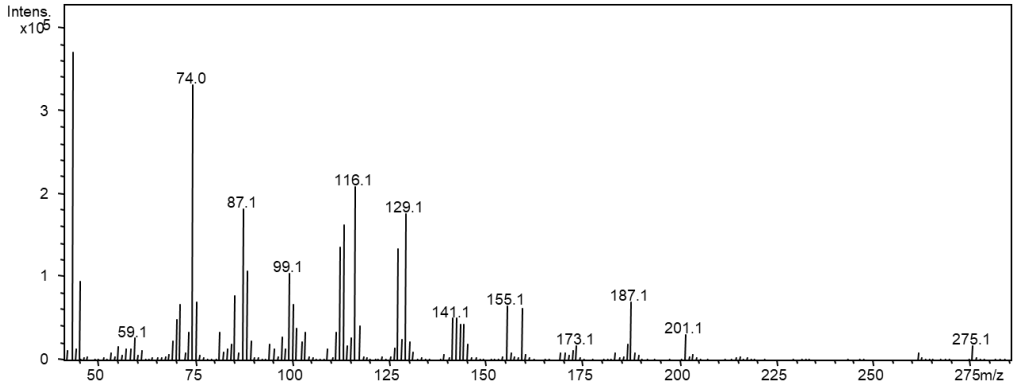

Methyl 3,4-di-*O*-acetyl-2,6-di-*O*-methyl-mannopyranoside

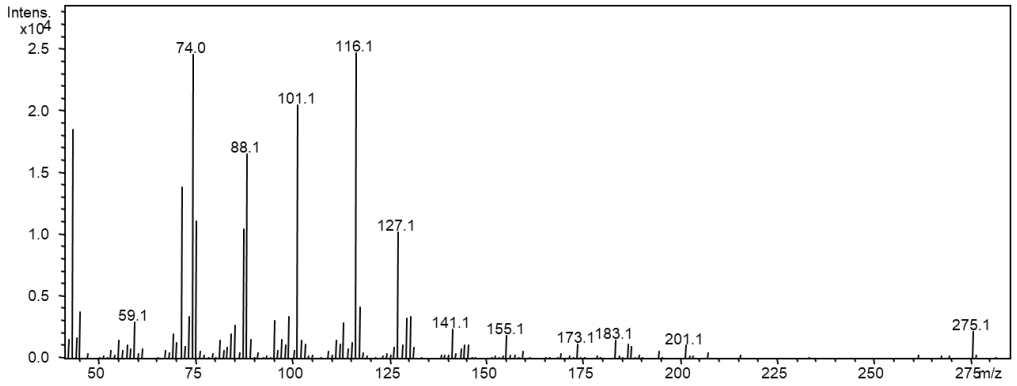

Methyl 4,6-di-*O*-acetyl-2,3-di-*O*-methyl-mannopyranoside

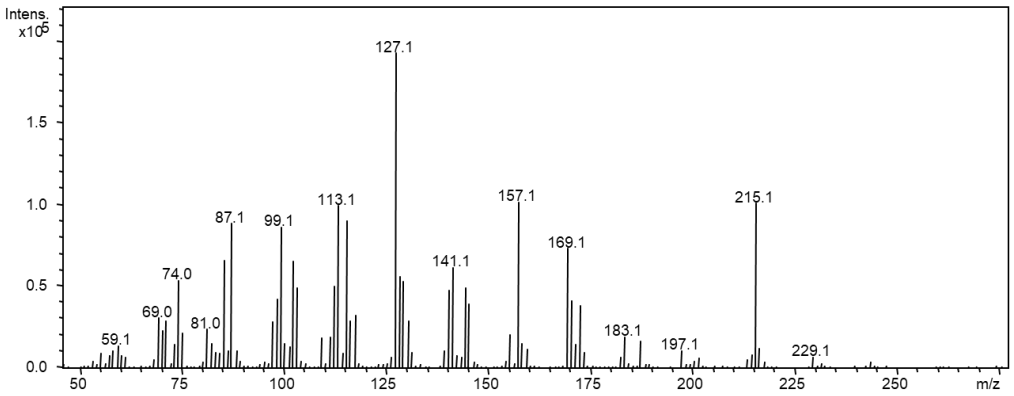

Methyl 2,3,4-tri-*O*-acetyl-6-*O*-methyl-mannopyranoside

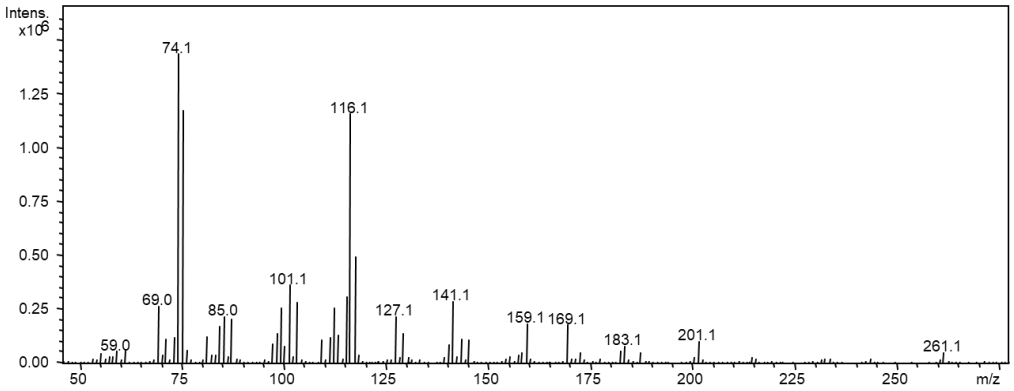

Methyl 2,4,6-tri-*O*-acetyl-3-*O*-methyl-mannopyranoside

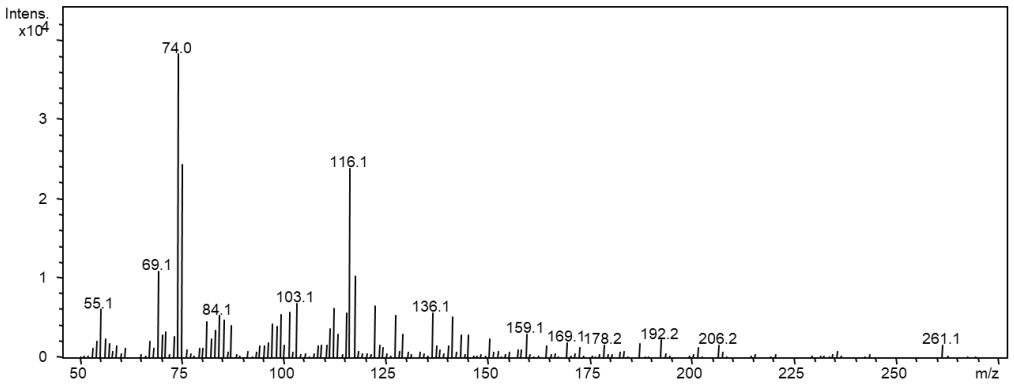

Methyl 3,4,6-tri-*O*-acetyl-2-*O*-methyl-mannopyranoside

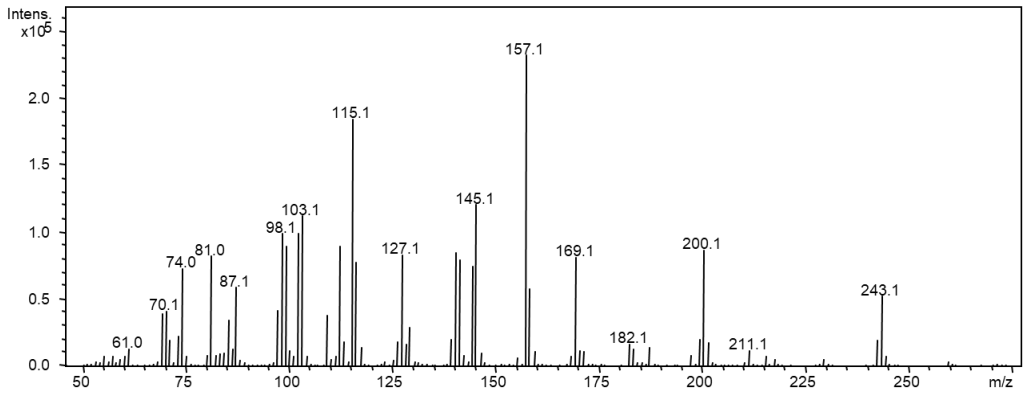

Methyl 2,3,4,6-tetra-*O*-acetyl-mannopyranoside

9.2.4 Methyl *O*-methyl-*O*-trimethylsily-glucopyranoside

These mass spectra have been confirmed according to the publication of Merkle et al.[44]

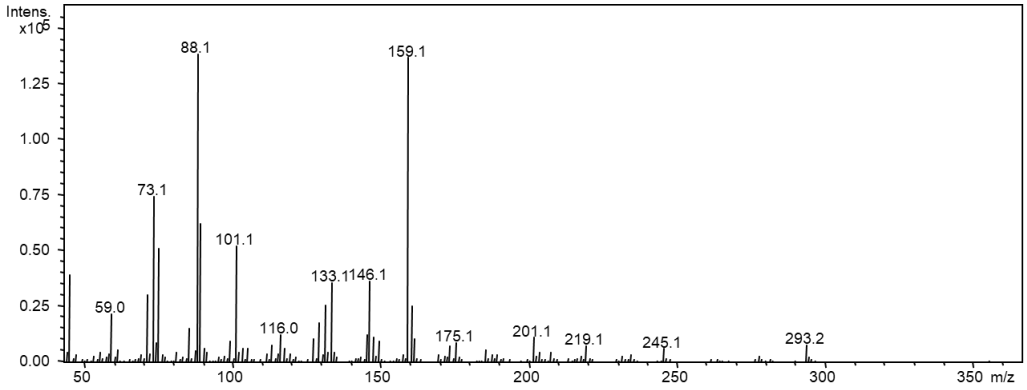

Methyl 2,3,6-tri-*O*-methyl-4-*O*-trimethylsilyl-mannopyranoside

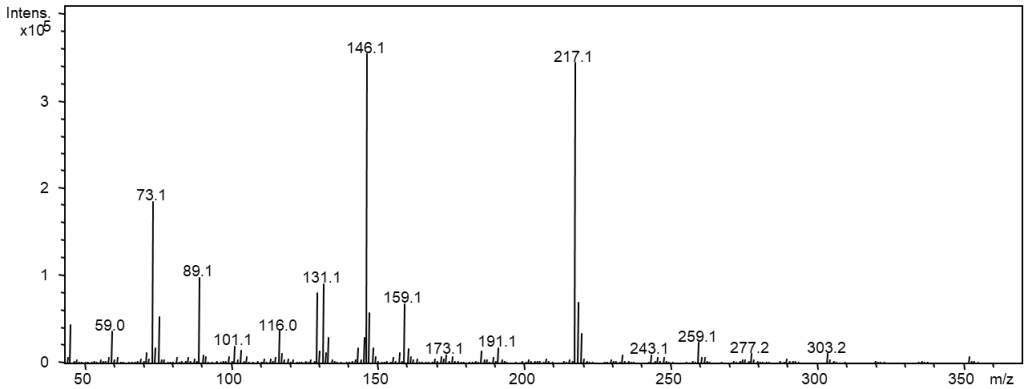

Methyl 3,6-di-*O*-methyl-2,4-di-*O*-trimethylsilyl-mannopyranoside

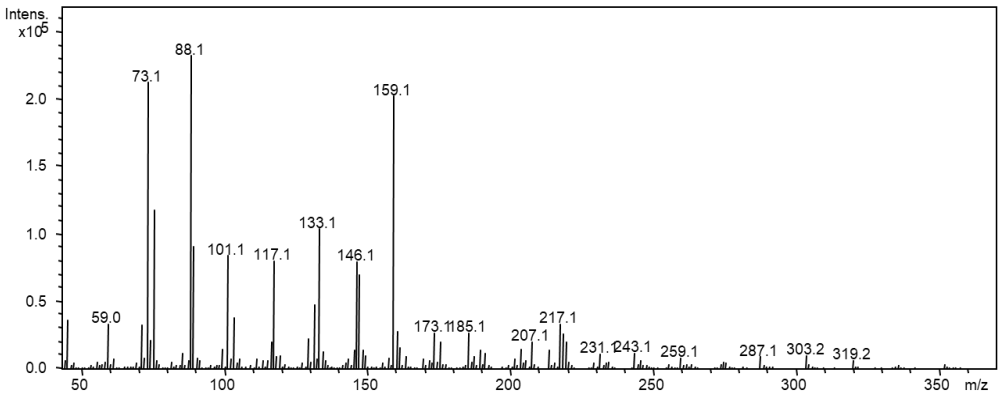

Methyl 2,3-di-*O*-methyl-4,6-di-*O*-trimethylsilyl-mannopyranoside

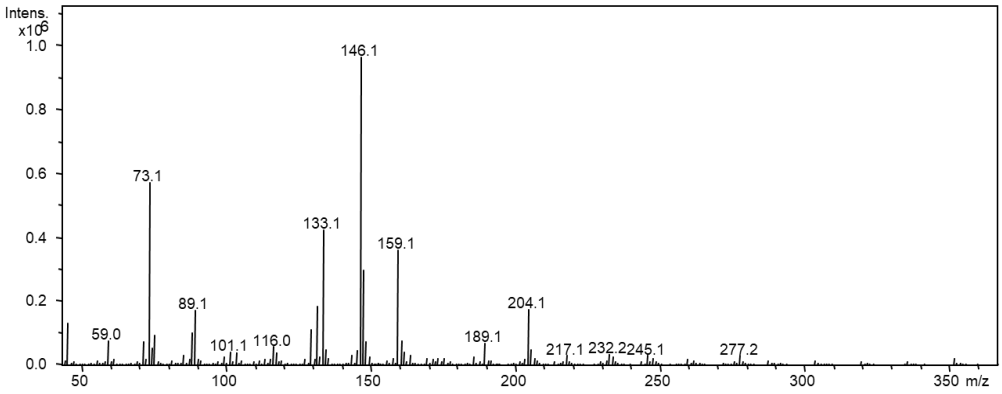

Methyl 2,6-di-*O*-methyl-3,4-di-*O*-trimethylsilyl-mannopyranoside

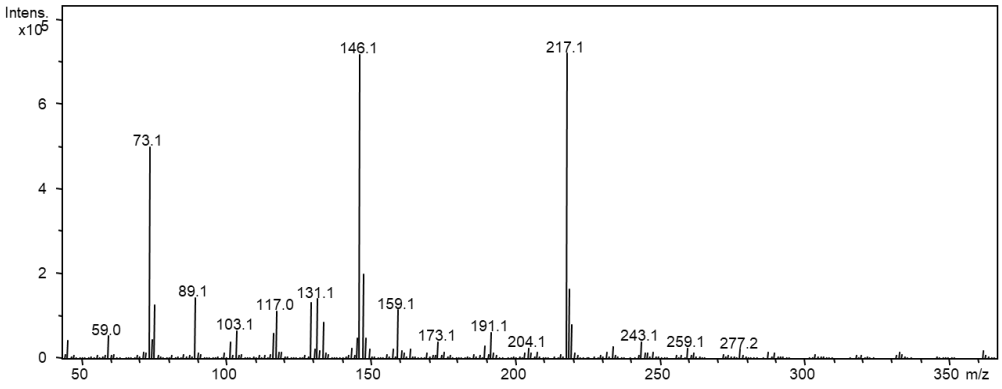

Methyl 3-*O*-methyl-2,4,6-tri-*O*-trimethylsilyl-mannopyranoside

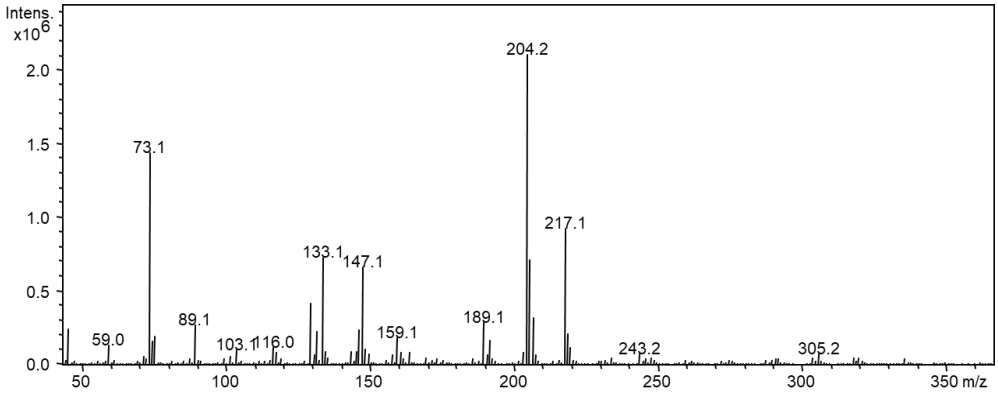

Methyl 6-*O*-methyl-2,3,4-tri-*O*-trimethylsilyl-mannopyranoside

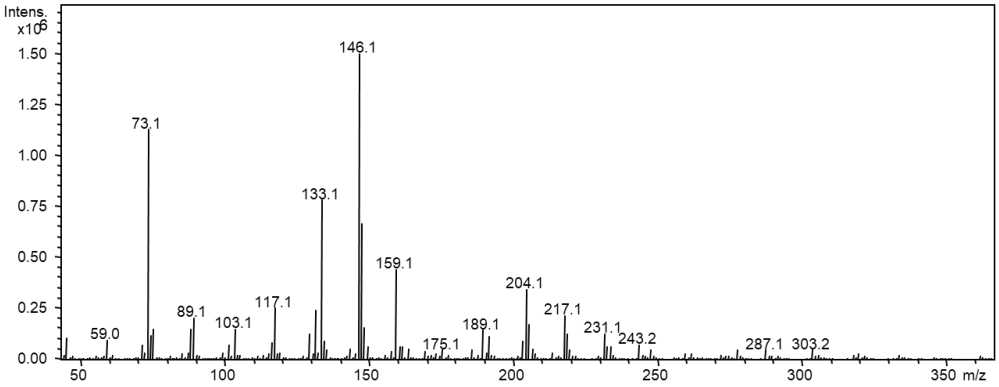

Methyl 2-*O*-methyl-3,4,6-tri-*O*-trimethylsilyl-mannopyranoside

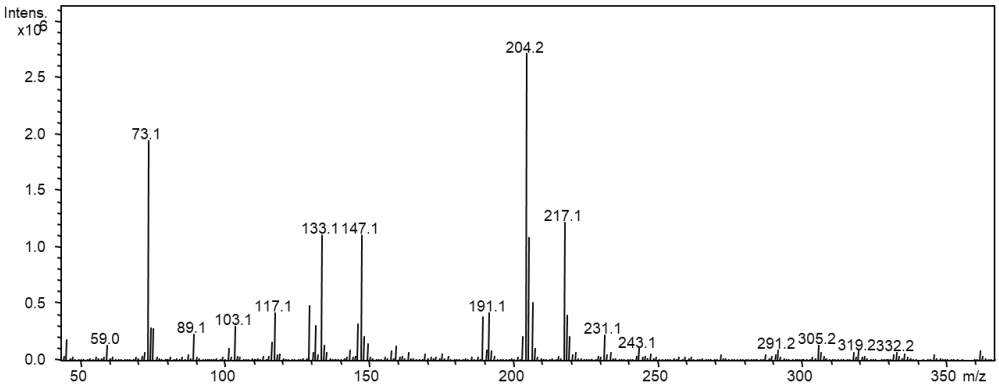

Methyl 2,3,4,6-tetra-*O*-trimethylsilyl-mannopyranoside

9.3 Constituents with respect to methyl pattern of M-KGM

Table 9.1. Relative molar composition (mol%) of M-KGM-1 regarding the glucose and mannose substituted at position *i* (s_i), molar fraction of *i*-fold substituted monomer units (c_i), partial DS-values x_i for individual hydroxyl groups in position i, and total DS, determined by various derivatization methods. Data are independently normalized for both glucose and mannose (n=2-3). Data are compared to calculated data on the models of Spurlin (S).[73] Sample preparation parameters are described at 7.3.1 and derivatization methods are described at 7.4.1.

Me in Position	**AAM**				**RCM-Ac**				**RCM-Bz**				**MeOH-Ac**				**MeOH-TMS**			
	Man	S	Glc	S	Man	S	Glc	S	Man	S	Glc	S	Man	S	Glc	S	Man	S	Glc	S
s_0	75.94	75.58	76.28	75.33	83.02	82.43	85.13	84.74	78.74	78.24	84.02	83.68	76.81	76.68	74.39	73.91	74.80	74.60	72.06	70.55
s_2	7.50	7.90	8.42	9.02	5.57	6.17	6.71	6.93	7.07	7.63	5.74	6.11	7.02	7.22	8.77	8.78	7.22	7.41	9.22	10.70
s_3	4.21	4.24	0.79	1.48	3.66	3.88	0.82	1.15	5.10	5.28	0.85	1.04	4.10	4.24	1.43	2.16	4.80	4.99	2.05	2.21
s_6	9.80	10.14	11.62	12.25	6.03	6.42	6.24	6.46	6.81	7.12	8.25	8.37	9.96	9.92	12.67	12.94	10.56	10.66	12.20	13.64
s_{23}	0.52	0.44	0.52	0.18	0.51	0.29	0.26	0.09	0.75	0.51	0.31	0.08	0.62	0.40	0.51	0.26	0.67	0.50	0.46	0.34
s_{26}	1.44	1.06	1.75	1.47	0.88	0.48	0.59	0.53	1.07	0.69	0.76	0.61	0.97	0.93	1.33	1.54	1.15	1.06	3.48	2.07
s_{36}	0.59	0.57	0.61	0.24	0.32	0.30	0.26	0.09	0.47	0.48	0.08	0.10	0.52	0.55	0.90	0.38	0.80	0.71	0.53	0.43
s_{236}	0.00	0.06	0.00	0.03	0.00	0.02	0.00	0.01	0.00	0.05	0.00	0.01	0.00	0.05	0.00	0.04	0.00	0.07	0.00	0.06
c_0	75.94	75.58	76.28	75.33	83.02	82.43	85.13	84.74	78.74	78.24	84.02	83.68	76.81	76.68	74.39	73.91	74.80	74.60	72.06	70.55
c_1	21.51	22.28	20.83	22.75	15.27	16.47	13.76	14.54	18.98	20.03	14.84	15.52	21.08	21.38	22.87	23.88	22.58	23.06	23.47	26.56
c_2	2.55	2.07	2.89	1.89	1.71	1.07	1.11	0.71	2.28	1.69	1.15	0.79	2.11	1.88	2.74	2.17	2.62	2.27	4.47	2.83
c_3	0.00	0.06	0.00	0.03	0.00	0.02	0.00	0.01	0.00	0.05	0.00	0.01	0.00	0.05	0.00	0.04	0.00	0.07	0.00	0.06
H_1	0.26		0.56		0.37		0.23		0.33		0.22		0.13		0.39		0.15		1.04	
x_2	0.09		0.11		0.07		0.08		0.09		0.07		0.09		0.11		0.09		0.13	
x_3	0.05		0.02		0.04		0.01		0.06		0.01		0.05		0.03		0.06		0.03	
x_6	0.12		0.14		0.07		0.07		0.08		0.09		0.11		0.15		0.13		0.16	
M/G ratio	1.63				2.24				2.07				1.74				1.60			
DS_M and DS_G	0.27		0.27		0.19		0.16		0.24		0.17		0.25		0.28		0.28		0.32	
DS_{KGM}	0.27				0.18				0.21				0.26				0.30			

Table 9.2. Relative molar composition (mol%) of M-KGM-2 regarding the glucose and mannose substituted at position *i* (s_i), molar fraction of *i*-fold substituted monomer units (c_i), partial DS-values x_i for individual hydroxyl groups in position *i*, and total DS, determined by various derivatization methods. Data are independently normalized for both glucose and mannose (n=2-3). Data are compared to calculated data on the models of Spurlin (S).[73] Sample preparation parameters are described at 7.3.1 and derivatization methods are described at 7.4.1.

Me in Position	**AAM**				**RCM-Ac**				**RCM-Bz**				**MeOH-Ac**				**MeOH-TMS**			
	Man	S	Glc	S	Man	S	Glc	S	Man	S	Glc	S	Man	S	Glc	S	Man	S	Glc	S
s_0	72.85	72.13	73.79	72.94	78.02	77.32	78.05	77.54	75.04	74.63	79.07	78.79	70.62	70.34	70.33	70.02	68.71	68.15	66.82	65.57
s_2	8.34	8.95	9.02	9.60	6.33	7.09	9.02	9.32	7.41	7.86	7.89	8.09	8.70	9.02	10.14	10.27	8.73	9.13	10.69	12.10
s_3	4.56	5.13	1.18	1.81	4.36	4.77	1.00	1.42	5.66	5.87	0.95	1.38	5.01	5.17	1.73	2.17	5.69	6.02	2.29	2.35
s_6	10.56	10.93	12.76	13.28	8.67	8.96	9.79	10.13	9.00	9.25	10.40	10.34	12.22	12.22	14.51	14.57	12.67	12.87	14.89	15.93
s_{23}	1.09	0.64	0.60	0.24	0.91	0.44	0.37	0.17	0.86	0.62	0.49	0.14	0.87	0.66	0.57	0.32	0.99	0.81	0.64	0.43
s_{26}	1.61	1.36	2.01	1.75	1.16	0.82	1.34	1.22	1.26	0.97	0.93	1.06	1.61	1.57	2.02	2.14	1.76	1.72	4.13	2.94
s_{36}	0.99	0.78	0.64	0.33	0.55	0.55	0.42	0.19	0.76	0.73	0.28	0.18	0.79	0.90	0.63	0.45	1.11	1.14	0.42	0.57
s_{236}	0.00	0.10	0.00	0.04	0.00	0.05	0.00	0.02	0.00	0.08	0.00	0.02	0.18	0.12	0.06	0.07	0.33	0.15	0.11	0.11
c_0	72.85	72.13	73.79	72.94	78.02	77.32	78.05	77.54	75.04	74.63	79.07	78.79	70.62	70.34	70.33	70.02	68.71	68.15	66.82	65.57
c_1	23.46	25.01	22.96	24.70	19.36	20.82	19.81	20.86	22.07	22.97	19.23	19.80	25.93	26.41	26.38	27.01	27.09	28.02	27.88	30.38
c_2	3.69	2.77	3.25	2.32	2.62	1.81	2.13	1.57	2.88	2.32	1.70	1.38	3.27	3.13	3.23	2.91	3.87	3.67	5.20	3.94
c_3	0.00	0.10	0.00	0.04	0.00	0.05	0.00	0.02	0.00	0.08	0.00	0.02	0.18	0.12	0.06	0.07	0.33	0.15	0.11	0.11
H_1	0.46		0.43		0.46		0.31		0.28		0.24		0.18		0.23		0.29		0.88	
x_2	0.11		0.12		0.08		0.11		0.10		0.09		0.11		0.13		0.12		0.16	
x_3	0.07		0.02		0.06		0.02		0.07		0.02		0.07		0.03		0.08		0.03	
x_6	0.13		0.15		0.10		0.12		0.11		0.12		0.15		0.17		0.16		0.20	
M/G ratio	1.69				1.86				1.70				1.67				1.60			
DS_M and DS_G	0.31		0.29		0.25		0.24		0.28		0.23		0.33		0.33		0.36		0.39	
DS_{KGM}	0.30				0.24				0.26				0.33				0.37			

Table 9.3. Relative molar composition (mol%) of M-KGM-3 regarding the glucose and mannose substituted at position *i* (s_i), molar fraction of *i*-fold substituted monomer units (c_i), partial DS-values x_i for individual hydroxyl groups in position *i*, and total DS, determined by various derivatization methods. Data are independently normalized for both glucose and mannose (n=2-3). Data are compared to calculated data on the models of Spurlin (S).[73] Sample preparation parameters are described at 7.3.1 and derivatization methods are described at 7.4.1.

Me in Position	**AAM**				**RCM-Ac**				**RCM-Bz**				**MeOH-Ac**				**MeOH-TMS**			
	Man	S	Glc	S	Man	S	Glc	S	Man	S	Glc	S	Man	S	Glc	S	Man	S	Glc	S
s_0	65.32	63.25	68.06	67.03	78.11	77.25	79.04	78.53	71.17	70.36	76.48	76.03	67.76	67.31	67.60	67.14	66.08	65.27	62.50	59.79
s_2	9.66	10.89	10.60	11.40	6.73	7.56	9.32	9.71	9.34	10.10	8.03	8.46	9.39	9.87	10.85	10.97	9.31	9.94	11.18	13.73
s_3	5.22	6.45	1.43	2.08	4.83	5.25	1.02	1.52	6.24	6.64	1.04	1.51	5.43	5.62	1.92	2.48	6.00	6.46	1.87	2.27
s_6	13.05	14.17	15.17	15.86	7.65	8.04	8.66	8.77	9.07	9.54	12.18	12.21	13.05	13.17	15.50	15.76	13.35	13.70	16.05	18.55
s_{23}	1.49	1.11	0.78	0.35	0.90	0.51	0.57	0.19	1.30	0.95	0.62	0.17	1.05	0.82	0.63	0.40	1.27	0.98	0.76	0.52
s_{26}	2.72	2.44	3.16	2.70	1.14	0.79	1.09	1.08	1.80	1.37	1.36	1.36	2.10	1.93	2.49	2.57	2.25	2.09	6.60	4.26
s_{36}	1.73	1.44	0.81	0.49	0.49	0.55	0.28	0.17	0.96	0.90	0.30	0.24	0.97	1.10	0.94	0.58	1.36	1.36	0.90	0.71
s_{236}	0.81	0.25	0.00	0.08	0.14	0.05	0.02	0.02	0.11	0.13	0.00	0.03	0.25	0.16	0.08	0.09	0.39	0.21	0.13	0.16
c_0	65.32	63.25	68.06	67.03	78.11	77.25	79.04	78.53	71.17	70.36	76.48	76.03	67.76	67.31	67.60	67.14	66.08	65.27	62.50	59.79
c_1	27.93	31.51	27.20	29.35	19.21	20.85	19.00	20.00	24.65	26.28	21.24	22.18	27.87	28.67	28.27	29.21	28.65	30.10	29.10	34.56
c_2	5.94	4.99	4.74	3.55	2.53	1.85	1.94	1.44	4.06	3.22	2.28	1.77	4.12	3.86	4.05	3.56	4.87	4.43	8.27	5.49
c_3	0.81	0.25	0.00	0.08	0.14	0.05	0.02	0.02	0.11	0.13	0.00	0.03	0.25	0.16	0.08	0.09	0.39	0.21	0.13	0.16
H_1	1.07		0.62		0.54		0.34		0.49		0.32		0.27		0.31		0.44		1.80	
x_2	0.15		0.15		0.09		0.11		0.13		0.10		0.13		0.14		0.13		0.19	
x_3	0.09		0.03		0.06		0.02		0.09		0.02		0.08		0.04		0.09		0.04	
x_6	0.18		0.19		0.09		0.10		0.12		0.14		0.16		0.19		0.17		0.24	
M/G ratio	1.61				1.99				1.71				1.68				1.56			
DS_M and DS_G	0.42		0.37		0.25		0.23		0.33		0.26		0.37		0.37		0.40		0.46	
DS_{KGM}	0.40				0.24				0.30				0.37				0.42			

Table 9.4. Relative molar composition (mol%) of M-KGM-4 regarding the glucose and mannose substituted at position *i* (s_i), molar fraction of *i*-fold substituted monomer units (c_i), partial DS-values x_i for individual hydroxyl groups in position *i*, and total DS, determined by various derivatization methods. Data are independently normalized for both glucose and mannose (n=2-3). Data are compared to calculated data on the models of Spurlin (S).[73] Sample preparation parameters are described at 7.3.1 and derivatization methods are described at 7.4.1.

Me in Position	**AAM**				**RCM-Ac**				**RCM-Bz**				**MeOH-Ac**				**MeOH-TMS**			
	Man	S	Glc	S	Man	S	Glc	S	Man	S	Glc	S	Man	S	Glc	S	Man	S	Glc	S
s_0	57.62	55.68	58.60	57.54	63.72	62.11	62.78	59.81	57.30	56.16	62.69	62.58	52.60	52.11	51.32	51.15	51.09	49.96	49.62	47.65
s_2	11.84	13.18	13.80	14.95	9.30	10.92	14.27	16.11	11.27	12.21	13.94	13.68	12.52	13.19	14.80	15.10	12.35	13.38	14.29	15.97
s_3	5.73	6.83	1.73	2.60	6.11	6.62	1.57	3.34	7.83	8.71	1.96	3.01	7.16	7.51	2.58	3.16	7.27	7.94	2.38	3.23
s_6	15.43	16.35	18.09	18.41	13.65	14.74	13.86	14.80	14.31	14.96	16.45	15.72	17.79	17.64	22.09	21.56	17.92	18.11	21.26	22.49
s_{23}	2.12	1.62	1.63	0.68	1.68	1.16	1.55	0.90	2.71	1.89	1.40	0.66	2.43	1.90	1.64	0.93	2.68	2.13	1.65	1.08
s_{26}	4.19	3.87	5.19	4.78	3.68	2.59	3.80	3.99	3.67	3.25	2.03	3.44	4.49	4.46	5.97	6.37	4.93	4.85	8.48	7.54
s_{36}	2.09	2.01	0.96	0.83	1.57	1.57	0.57	0.83	2.67	2.32	1.02	0.76	2.24	2.54	1.21	1.33	2.60	2.88	1.65	1.53
s_{236}	0.99	0.47	0.00	0.22	0.28	0.28	1.60	0.22	0.24	0.50	0.51	0.17	0.76	0.64	0.38	0.39	1.16	0.77	0.68	0.51
c_0	57.62	55.68	58.60	57.54	63.72	62.11	62.78	59.81	57.30	56.16	62.69	62.58	52.60	52.11	51.32	51.15	51.09	49.96	49.62	47.65
c_1	32.99	36.36	33.63	35.95	29.06	32.28	29.69	34.25	33.41	35.87	32.35	32.41	37.47	38.34	39.48	39.82	37.54	39.42	37.93	41.69
c_2	8.40	7.49	7.78	6.29	6.94	5.33	5.92	5.71	9.06	7.46	4.45	4.85	9.17	8.91	8.83	8.63	10.21	9.85	11.77	10.15
c_3	0.99	0.47	0.00	0.22	0.28	0.28	1.60	0.22	0.24	0.50	0.51	0.17	0.76	0.64	0.38	0.39	1.16	0.77	0.68	0.51
H_1	1.02		0.74		1.01		1.53		0.71		0.82		0.39		0.42		0.65		1.13	
x_2	0.19		0.21		0.15		0.21		0.18		0.18		0.20		0.23		0.21		0.25	
x_3	0.11		0.04		0.10		0.05		0.13		0.05		0.13		0.06		0.14		0.06	
x_6	0.23		0.24		0.19		0.20		0.21		0.20		0.25		0.30		0.27		0.32	
M/G ratio	1.60				1.74				1.72				1.72				1.60			
DS_M and DS_G	0.53		0.49		0.44		0.46		0.52		0.43		0.58		0.58		0.61		0.64	
DS_{KGM}	0.51				0.45				0.49				0.58				0.62			

Table 9.5. Relative molar composition (mol%) of M-KGM-5 regarding the glucose and mannose substituted at position *i* (s_i), molar fraction of *i*-fold substituted monomer units (c_i), partial DS-values x_i for individual hydroxyl groups in position *i*, and total DS, determined by various derivatization methods. Data are independently normalized for both glucose and mannose (n=2-3). Data are compared to calculated data on the models of Spurlin (S).[73] Sample preparation parameters are described at 7.3.1 and derivatization methods are described at 7.4.1.

Me in Position	**AAM**				**RCM-Ac**				**RCM-Bz**				**MeOH-Ac**				**MeOH-TMS**			
	Man	S	Glc	S	Man	S	Glc	S	Man	S	Glc	S	Man	S	Glc	S	Man	S	Glc	S
s_0	41.25	39.28	43.50	41.15	46.34	44.88	47.02	44.50	40.26	40.55	43.60	42.71	38.91	38.31	39.87	39.43	37.91	36.48	37.45	35.78
s_2	14.36	15.90	15.39	17.19	12.96	14.74	17.21	18.97	14.36	14.99	18.33	18.78	14.22	15.25	16.19	16.82	13.93	15.27	15.81	17.29
s_3	7.24	8.40	1.94	3.75	7.71	8.57	2.06	3.81	9.63	9.93	2.33	3.83	7.98	8.43	2.69	3.50	7.76	8.68	2.80	3.65
s_6	19.05	19.37	23.36	23.50	18.10	18.33	19.39	20.09	18.62	18.10	21.90	21.04	20.82	20.31	25.48	24.96	20.62	20.47	24.87	25.39
s_{23}	4.12	3.40	2.82	1.56	4.00	2.81	2.61	1.62	4.89	3.67	2.75	1.68	4.24	3.36	2.49	1.49	4.47	3.63	2.44	1.77
s_{26}	7.72	7.84	9.41	9.82	6.58	6.02	8.49	8.56	7.09	6.69	7.94	9.25	8.01	8.08	10.31	10.65	8.33	8.57	12.61	12.27
s_{36}	3.64	4.14	1.74	2.14	3.13	3.50	1.64	1.72	4.49	4.43	1.64	1.89	3.82	4.47	2.06	2.21	4.21	4.87	2.31	2.59
s_{236}	2.62	1.68	1.84	0.89	1.20	1.15	1.58	0.73	0.66	1.64	1.52	0.83	2.00	1.78	0.91	0.94	2.78	2.04	1.72	1.25
c_0	41.25	39.28	43.50	41.15	46.34	44.88	47.02	44.50	40.26	40.55	43.60	42.71	38.91	38.31	39.87	39.43	37.91	36.48	37.45	35.78
c_1	40.65	43.67	40.69	44.44	38.76	41.64	38.66	42.86	42.62	43.02	42.56	43.64	43.02	43.99	44.37	45.27	42.30	44.42	43.47	46.34
c_2	15.47	15.38	13.98	13.52	13.70	12.34	12.74	11.91	16.47	14.79	12.33	12.82	16.07	15.91	14.86	14.35	17.01	17.07	17.36	16.63
c_3	2.62	1.68	1.84	0.89	1.20	1.15	1.58	0.73	0.66	1.64	1.52	0.83	2.00	1.78	0.91	0.94	2.78	2.04	1.72	1.25
H_1	1.08		1.36		1.00		1.35		0.66		0.96		0.62		0.57		0.9		0.93	
x_2	0.29		0.29		0.25		0.30		0.27		0.31		0.28		0.30		0.30		0.33	
x_3	0.18		0.08		0.16		0.08		0.20		0.08		0.18		0.08		0.19		0.09	
x_6	0.33		0.36		0.29		0.31		0.31		0.33		0.35		0.39		0.36		0.42	
M/G ratio	1.68				1.82				1.89				1.65				1.58			
DS_M and DS_G	0.79		0.74		0.70		0.69		0.78		0.72		0.81		0.77		0.85		0.83	
DS_{KGM}	0.77				0.74				0.75				0.80				0.84			

Table 9.6. Relative molar composition (mol%) of M-KGM-6 regarding the glucose and mannose substituted at position *i* (s_i), molar fraction of *i*-fold substituted monomer units (c_i), partial DS-values x_i for individual hydroxyl groups in position *i*, and total DS, determined by various derivatization methods. Data are independently normalized for both glucose and mannose (n=2-3). Data are compared to calculated data on the models of Spurlin (S).[73] Sample preparation parameters are described at 7.3.1 and derivatization methods are described at 7.4.1.

Me in Position	**AAM**				**RCM-Ac**				**RCM-Bz**				**MeOH-Ac**				**MeOH-TMS**			
	Man	S	Glc	S	Man	S	Glc	S	Man	S	Glc	S	Man	S	Glc	S	Man	S	Glc	S
s_0	39.59	38.02	41.75	39.71	39.93	38.79	42.00	40.16	39.14	38.78	42.17	41.21	39.52	38.93	39.90	39.51	38.43	36.96	37.23	35.59
s_2	14.79	16.10	15.80	17.42	14.76	16.02	16.32	17.75	14.46	15.41	17.46	17.97	14.25	15.24	16.31	16.91	14.03	15.40	15.83	16.99
s_3	7.35	8.35	2.30	3.90	7.85	8.64	2.43	3.87	9.00	9.57	2.51	3.97	7.92	8.39	2.53	3.41	7.38	8.37	2.59	3.72
s_6	19.54	19.59	23.67	23.59	19.29	19.10	23.17	23.10	19.02	18.61	23.05	22.30	20.67	20.20	25.64	24.95	20.68	20.59	24.84	25.70
s_{23}	4.27	3.53	2.88	1.71	4.46	3.57	2.74	1.71	4.96	3.80	2.74	1.73	4.15	3.28	2.56	1.46	4.39	3.49	2.42	1.77
s_{26}	8.07	8.29	9.84	10.35	7.80	7.89	9.73	10.21	7.58	7.40	8.52	9.73	7.83	7.90	10.21	10.68	8.39	8.58	12.64	12.27
s_{36}	3.78	4.30	1.78	2.32	3.70	4.25	1.75	2.22	4.39	4.59	1.90	2.15	3.76	4.35	1.97	2.15	4.11	4.66	3.03	2.69
s_{236}	2.60	1.82	1.98	1.02	2.20	1.76	1.86	0.98	1.44	1.83	1.64	0.94	1.90	1.70	0.89	0.92	2.60	1.94	1.42	1.28
c_0	39.59	38.02	41.75	39.71	39.93	38.79	42.00	40.16	39.14	38.78	42.17	41.21	39.52	38.93	39.90	39.51	38.43	36.96	37.23	35.59
c_1	41.69	44.03	41.77	44.90	41.91	43.75	41.92	44.71	42.49	43.60	43.02	44.25	42.84	43.82	44.47	45.27	42.09	44.36	43.26	46.40
c_2	16.12	16.13	14.50	14.37	15.96	15.70	14.22	14.14	16.93	15.79	13.17	13.61	15.73	15.54	14.75	14.29	16.89	16.73	18.09	16.73
c_3	2.60	1.82	1.98	1.02	2.20	1.76	1.86	0.98	1.44	1.83	1.64	0.94	1.90	1.70	0.89	0.92	2.60	1.94	1.42	1.28
H_1	0.91		1.24		0.78		1.11		0.62		0.93		0.60		0.64		0.91		0.92	
x_2	0.30		0.30		0.29		0.31		0.28		0.30		0.28		0.32		0.29		0.32	
x_3	0.18		0.09		0.18		0.09		0.20		0.09		0.18		0.09		0.18		0.09	
x_6	0.34		0.37		0.33		0.37		0.32		0.35		0.34		0.42		0.36		0.42	
M/G ratio	1.68				1.76				1.89				1.67				1.56			
DS_M and DS_G	0.82		0.77		0.80		0.76		0.81		0.74		0.80		0.77		0.84		0.84	
DS_{KGM}	0.80				0.79				0.78				0.79				0.84			

Table 9.7. Relative molar composition (Mol %) of glucose and mannose of EM-KGM-8 to EM-KGM-20 substituted at position *i* (s_i), molar fraction in % of *i*-fold substituted monomer units (c_i), partial DS-values x_i for individual hydroxyl group in position *i*, and total DS. Data are independently normalized for both glucose and mannose. From each sample the value is an average of 3 individual analyses. Sample preparation parameters are described at 7.3.2 and derivatization methods are described at 7.4.1 (AAM).

Me in position	**M-KGM-8[1]**		**M-KGM-9[2]**		**M-KGM-10[2]**		**M-KGM-11[3]**		**M-KGM-12[4]**	
	Man	Glc	Man	Glc	Man	Glc	Man	Glc	Man	Glc
s_0	33.21±0.43	27.82±0.33	20.96±0.31	14.49±0.16	10.54±0.02	12.28±0.15	50.38±0.13	37.84±0.22	65.87±0.23	49.78±2.01
s_2	13.03±0.26	18.01±0.46	10.46±0.16	17.57±0.15	12.06±0.03	16.16±0.03	9.31±0.02	19.34±0.18	5.39±0.02	16.65±0.86
s_3	5.94±0.10	2.27±0.14	5.71±0.25	2.55±0.31	6.56±0.05	2.51±0.16	5.99±0.07	3.36±0.05	3.77±0.01	2.35±0.12
s_6	23.47±0.20	21.80±0.03	23.17±0.58	22.37±0.24	15.42±0.42	20.43±0.17	21.30±0.14	18.01±0.02	19.59±0.14	15.01±0.34
s_{23}	5.27±0.07	6.21±0.01	7.72±0.09	2.70±0.03	9.46±0.02	4.01±0.03	3.02±0.00	6.09±0.01	1.52±0.01	5.69±0.13
s_{26}	10.51±0.25	17.04±0.26	14.30±0.43	26.05±0.20	19.69±0.23	28.13±0.36	4.99±0.00	11.14±0.09	1.76±0.10	6.99±0.36
s_{36}	4.05±0.12	2.68±0.13	7.02±0.11	4.32±0.37	9.99±0.06	4.74±0.25	3.41±0.19	2.14±0.06	1.27±0.01	1.28±0.06
s_{236}	4.53±0.41	4.18±0.28	10.66±0.39	9.95±0.14	16.28±0.38	11.73±0.38	1.60±0.02	2.08±0.03	0.83±0.07	2.25±0.15
c_0	33.21±0.43	27.82±0.33	20.96±0.31	14.49±0.16	10.54±0.02	12.28±0.15	50.38±0.13	37.84±0.22	65.87±0.23	49.78±2.01
c_1	42.44±0.34	42.07±0.44	39.34±0.59	42.49±0.32	34.04±0.50	39.11±0.30	36.59±0.08	40.71±0.15	28.75±0.17	34.01±1.32
c_2	19.82±0.21	25.92±0.34	29.04±0.56	33.07±0.36	39.14±0.15	36.88±0.08	11.43±0.19	19.37±0.04	4.54±0.13	13.96±0.55
c_3	4.53±0.41	4.18±0.28	10.66±0.39	9.95±0.14	16.28±0.38	11.73±0.38	1.60±0.02	2.08±0.03	0.83±0.07	2.25±0.15
$H_{1(\text{Spurlin})}$	1.70	1.94	2.56	1.36	0.82	1.44	1.39	1.84	1.01	2.81
$H_{1(\text{Reuben})}$	0.46	0.76	0.72	1.26	0.38	0.92	0.67	0.68	0.27	0.93
x_2	0.33±0.7%	0.45±0.4%	0.43±0.7%	0.56±0.2%	0.57±0.6%	0.60±0.7%	0.19±0.0%	0.39±0.3%	0.09±0.1%	0.32±1.5%
x_3	0.20±0.4%	0.15±0.3%	0.31±0.6%	0.20±0.2%	0.42±0.2%	0.23±0.1%	0.14±0.3%	0.14±0.1%	0.07±0.0%	0.12±0.5%
x_6	0.43±0.4%	0.46±0.6%	0.55±0.4%	0.63±0.2%	0.61±0.1%	0.65±0.3%	0.31±0.1%	0.33±0.1%	0.23±0.2%	0.26±0.9%
M/G ratio	1.68		1.65		1.65		1.60		1.69	
DS_M and DS_G	0.96	1.06	1.29	1.38	1.61	1.48	0.64	0.86	0.40	0.69
DS_{KGM}	1.00		1.33		1.56		0.73		0.51	

[1]M-KGM-8 was prepared in H_2O/NaOH/CH_3I system at room temperature of 25 °C in the presence of 2 equiv. of borate.
[2]M-KGM-9 was prepared in H_2O/NaOH/CH_3I system at room temperature of 35 °C in the presence of 4 equiv. of borate. M-KGM-10 was reference experiment to M-KGM-9.
[3]M-KGM-11 was prepared in H_2O/NaOH/CH_3I system at room temperature of 20 °C in the presence of 8 equiv. of borate.
[4]M-KGM-12 was prepared in H_2O/NaOH/CH_3I system at room temperature of 20 °C in the presence of 20 equiv. of borate.

Table 9.7. (Continued)

Me in position	**M-KGM-13[1]**		**M-KGM-14[1]**		**M-KGM-15[2]**		**M-KGM-16[2]**	
	Man	Glc	Man	Glc	Man	Glc	Man	Glc
s_0	71.68±0.55	51.10±0.31	29.82±0.38	33.31±0.55	57.99±0.35	29.27±0.36	4.80±0.01	4.86±0.05
s_2	3.11±0.03	15.14±0.09	14.20±0.15	15.78±0.07	5.13±0.03	25.58±0.20	10.00±0.03	13.27±0.05
s_3	2.08±0.03	2.42±0.18	7.44±0.05	2.80±0.02	4.27±0.06	2.37±0.22	4.68±0.02	1.77±0.01
s_6	18.47±0.17	18.22±0.08	19.82±0.10	26.25±0.06	21.30±0.09	14.37±0.47	11.61±0.05	8.31±0.03
s_{23}	0.93±0.02	3.01±0.01	6.00±0.04	3.16±0.01	2.13±0.01	7.44±0.24	10.63±0.05	10.62±0.04
s_{26}	2.10±0.46	6.21±0.08	11.40±0.42	13.27±0.18	3.67±0.27	11.37±0.10	22.87±0.06	33.62±0.14
s_{36}	1.25±0.29	1.45±0.15	6.46±0.16	2.89±0.27	3.96±0.24	2.22±0.17	8.38±0.12	4.17±0.02
s_{236}	0.37±0.03	2.46±0.18	4.86±0.15	2.54±0.23	1.55±0.06	7.37±0.56	27.03±0.24	23.39±0.22
c_0	71.68±0.55	51.10±0.31	29.82±0.38	33.31±0.55	57.99±0.35	29.27±0.36	4.80±0.01	4.86±0.05
c_1	23.66±0.22	35.78±0.04	41.46±0.28	44.83±0.04	30.70±0.13	42.33±0.17	26.29±0.06	23.35±0.06
c_2	4.28±0.74	10.67±0.21	23.86±0.51	19.32±0.44	9.76±0.42	21.04±0.49	41.88±0.20	48.40±0.19
c_3	0.37±0.03	2.46±0.18	4.86±0.15	2.54±0.23	1.55±0.06	7.37±0.56	27.03±0.24	23.39±0.22
$H_{1(\text{Spurlin})}$	1.27	1.92	1.26	0.96	2.31	2.76	1.27	0.96
$H_{1(\text{Reuben})}$	0.94	0.87	0.76	0.33	1.70	1.49	0.52	0.68
x_2	0.07±0.4%	0.27±0.1%	0.36±0.4%	0.35±0.4%	0.12±0.3%	0.52±0.5%	0.71±0.1%	0.81±0.0%
x_3	0.05±0.3%	0.09±0.4%	0.25±0.3%	0.11±0.4%	0.12±0.3%	0.19±0.3%	0.51±0.1%	0.40±0.2%
x_6	0.22±0.6%	0.28±0.2%	0.43±0.6%	0.45±0.5%	0.30±0.4%	0.35±0.4%	0.70±0.1%	0.69±0.0%
M/G ratio	1.60		1.65		1.62		1.60	
DS_M and DS_G	0.33	0.64	1.04	0.91	0.55	1.07	1.91	1.90
DS_{KGM}	0.45		0.99		0.75		1.91	

[1]M-KGM-13 was prepared in H_2O/NaOH/CH_3I system at room temperature of 20 °C in the presence of 40 equiv. of borate. M-KGM-14 was reference experiment to M-KGM-13.
[2]M-KGM-15 was prepared in H_2O/NaOH/CH_3I system at 40 °C in the presence of 40 equiv. of borate. M-KGM-16 was reference experiment to M-KGM-15.

Table 9.7. (Continued)

Me in position	**M-KGM-17[1]**		**M-KGM-18[1]**		**M-KGM-19[2]**		**M-KGM-20[2]**	
	Man	Glc	Man	Glc	Man	Glc	Man	Glc
s_0	54.01±0.52	25.85±1.16	8.50±0.01	11.49±0.24	58.15±0.37	25.21±0.53	0.52±0.02	2.31±0.06
s_2	4.49±0.04	18.94±0.41	11.83±0.07	12.65±0.12	2.92±0.08	21.57±0.30	1.95±0.05	2.26±0.32
s_3	2.29±0.02	3.22±0.04	4.40±0.04	2.16±0.07	1.33±0.11	2.78±0.07	0.56±0.05	0.46±0.05
s_6	28.91±0.19	15.00±0.29	14.04±0.07	15.05±0.05	30.87±0.42	13.51±0.16	2.93±0.26	4.92±0.14
s_{23}	2.91±0.04	10.92±0.21	12.20±0.10	13.87±0.05	1.72±0.08	10.70±0.13	5.83±0.13	5.30±0.15
s_{26}	3.47±0.28	16.15±0.69	20.23±0.09	26.39±0.54	2.40±0.25	17.40±0.17	16.81±0.34	30.96±0.19
s_{36}	1.59±0.48	2.80±0.15	5.99±0.28	4.45±0.01	1.08±0.05	2.31±0.07	4.11±0.24	3.43±0.49
s_{236}	2.33±0.03	7.13±0.80	22.82±0.06	13.94±0.65	1.52±0.23	6.53±0.38	67.28±0.51	50.36±0.77
c_0	54.01±0.52	25.85±1.16	8.50±0.01	11.49±0.24	58.15±0.37	25.21±0.53	0.52±0.02	2.31±0.06
c_1	35.69±0.25	37.15±0.67	30.26±0.12	29.86±0.16	35.12±0.24	37.87±0.21	5.45±0.30	7.64±0.43
c_2	7.97±0.74	29.86±0.64	38.42±0.16	44.70±0.49	5.20±0.38	30.40±0.36	26.75±0.47	39.69±0.40
c_3	2.33±0.03	7.13±0.80	22.82±0.06	13.94±0.65	1.52±0.23	6.53±0.38	67.28±0.51	50.36±0.77
$H_{1(\text{Spurlin})}$	2.30	3.12	2.47	2.94	1.65	2.93	1.26	1.68
$H_{1(\text{Reuben})}$	0.70	1.26	0.47	2.09	0.62	1.36	0.38	1.00
x_2	0.13±0.3%	0.53±1.1%	0.67±0.2%	0.67±0.3%	0.09±0.6%	0.56±0.4%	0.92±0.4%	0.89±0.5%
x_3	0.09±0.5%	0.24±0.8%	0.45±0.2%	0.34±0.6%	0.06±0.5%	0.22±0.5%	0.78±0.5%	0.60±0.2%
x_6	0.36±0.6%	0.41±0.9%	0.63±0.2%	0.60±0.4%	0.36±0.1%	0.40±0.8%	0.91±0.2%	0.90±0.4%
M/G ratio	1.64		1.62		1.66		1.61	
DS_M and DS_G	0.59	1.18	1.76	1.61	0.50	1.18	2.61	2.38
DS_{KGM}	0.81		1.70		0.76		2.52	

[1]M-KGM-17 was prepared in H_2O/Acetone/NaOH/CH_3I system at room temperature of 20 °C in the presence of 40 equiv. of borate. M-KGM-18 was reference experiment to M-KGM-17.

[2]M-KGM-19 was prepared in H_2O/Acetone/NaOH/CH_3I system at 50 °C in the presence of 40 equiv. of borate. M-KGM-20 was reference experiment to M-KGM-19.

Table 9.8 Relative molar composition (Mol %) of M-KGM regarding mannose and glucose of M-KGM-21 - M-KGM-55, methylated at position *i* (s_i), relative distribution of methyl groups on the hydroxyl groups in position *i* in % (given instead of the very low partial DS values x_i), and DS of mannose, glucose and M-KGM. Data are normalized for both glucose and mannose. Relative molar composition of methyl α-D-mannoside and methyl α-D-glucoside are listed at the end. Sample preparation parameters are described at Table 9.9 and derivatization methods are described at 7.4.1 (MeOH-Ac).

Me in position	**M-KGM-21**		**M-KGM-22**		**M-KGM-23**		**M-KGM-24**		**M-KGM-25**		**M-KGM-26**		**M-KGM-27**		**M-KGM-28**	
	Man	Glc	Man	Glc	Man	Glc	Man	Glc	Man	Glc	Man	Glc	Man	Glc	Man	Glc
s_0	86.11	93.62	88.26	86.29	92.04	94.33	95.99	97.08	98.21	97.40	98.42	98.03	96.36	98.51	98.11	98.76
s_2	5.58	3.39	3.02	5.82	3.85	2.35	1.60	0.85	0.07	0.26	0.08	0.23	0.50	0.38	0.16	0.19
s_3	6.68	1.29	2.89	2.51	2.06	0.72	1.03	0.65	0.48	0.15	0.42	0.17	2.51	0.20	0.85	0.26
s_6	1.44	1.39	5.22	4.78	2.02	2.51	1.28	1.10	1.16	1.03	0.72	0.60	0.63	0.64	0.83	0.74
s_{23}	0.19	0.31	0.13	0.23	0.00	0.00	0.00	0.09	0.01	0.02	0.25	0.36	0.00	0.06	0.00	0.00
s_{26}	0.00	0.00	0.28	0.37	0.00	0.01	0.08	0.06	0.01	0.39	0.02	0.31	0.00	0.05	0.00	0.06
s_{36}	0.00	0.00	0.21	0.00	0.00	0.01	0.02	0.18	0.04	0.75	0.08	0.30	0.01	0.16	0.05	0.00
s_{236}	0.00	0.00	0.00	0.00	0.03	0.07	0.00	0.00	0.01	0.00	0.00	0.00	0.00	0.00	0.00	0.00
x_2 (%)	42.0	55.3	27.7	44.9	48.4	41.7	40.8	30.6	5.6	17.8	18.0	30.6	13.6	28.0	8.3	19.0
x_3 (%)	48.8	24.0	26.1	19.1	26.0	13.8	25.6	28.1	29.1	24.4	39.0	28.2	68.9	24.0	46.4	19.7
x_6 (%)	10.2	20.8	46.2	36.0	25.6	44.5	33.6	41.2	65.3	57.8	43.0	41.2	17.5	48.0	45.3	61.4
DS_M and DS_G	0.14	0.07	0.12	0.14	0.08	0.06	0.04	0.03	0.02	0.04	0.02	0.03	0.04	0.02	0.02	0.01
DS_{KGM}	0.11		0.13		0.07		0.04		0.03		0.02		0.03		0.02	

Table 9.8. (Continued)

Me in position	**M-KGM-29**		**M-KGM-30**		**M-KGM-31**		**M-KGM-32**		**M-KGM-33**		**M-KGM-34**		**M-KGM-35**		**M-KGM-36**	
	Man	Glc	Man	Glc	Man	Glc	Man	Glc	Man	Glc	Man	Glc	Man	Glc	Man	Glc
s_0	97.54	99.12	99.00	98.60	95.20	93.99	90.86	92.03	98.71	98.24	88.31	92.54	90.83	94.64	86.25	90.89
s_2	0.26	0.26	0.27	0.57	1.22	2.14	3.34	3.67	0.09	0.21	4.74	3.39	2.65	1.69	5.31	4.53
s_3	1.54	0.09	0.27	0.38	1.34	1.16	3.46	1.15	0.32	0.29	5.08	2.18	4.54	2.37	5.80	1.40
s_6	0.66	0.54	0.43	0.33	2.16	1.89	2.22	2.21	0.61	0.56	1.49	1.45	1.54	0.89	1.88	1.94
s_{23}	0.00	0.00	0.02	0.04	0.02	0.12	0.03	0.17	0.02	0.00	0.06	0.00	0.02	0.03	0.05	0.08
s_{26}	0.00	0.00	0.00	0.03	0.07	0.23	0.03	0.33	0.19	0.19	0.32	0.16	0.25	0.09	0.43	0.83
s_{36}	0.00	0.00	0.00	0.05	0.00	0.48	0.07	0.43	0.07	0.50	0.00	0.28	0.16	0.29	0.28	0.32
s_{236}	0.00	0.00	0.01	0.01	0.00	0.00	0.00	0.00	0.00	0.00	0.00	0.00	0.00	0.00	0.00	0.00
x_2 (%)	10.7	29.5	28.6	41.8	26.7	36.4	36.7	46.9	19.0	16.5	42.4	45.0	30.4	31.3	39.9	52.7
x_3 (%)	62.4	10.0	28.8	31.2	27.8	25.7	38.3	19.6	26.0	32.3	42.5	31.1	49.2	46.6	42.3	17.4
x_6 (%)	26.9	60.5	42.6	27.0	45.6	37.9	25.0	33.5	55.1	51.2	15.0	23.9	20.4	22.1	17.9	30.0
DS_M and DS_G	0.02	0.01	0.01	0.02	0.05	0.07	0.09	0.09	0.02	0.02	0.12	0.08	0.10	0.06	0.15	0.10
DS_{KGM}	0.02		0.01		0.06		0.09		0.02		0.11		0.08		0.13	

Table 9.8. (Continued)

Me in position	**M-KGM-37**		**M-KGM-38**		**M-KGM-39**		**M-KGM-40**		**M-KGM-41**		**M-KGM-42**		**M-KGM-43**		**M-KGM-44**	
	Man	Glc	Man	Glc	Man	Glc	Man	Glc	Man	Glc	Man	Glc	Man	Glc	Man	Glc
s_0	90.90	90.32	93.15	96.08	91.93	95.07	86.73	92.65	85.62	92.24	88.81	93.52	89.11	93.66	89.44	95.00
s_2	2.15	3.47	2.45	1.67	3.09	2.37	4.58	3.43	5.37	3.95	4.22	2.93	3.96	3.03	3.69	2.13
s_3	2.62	2.02	3.05	1.12	3.82	1.01	5.82	1.59	6.61	1.57	5.25	1.65	5.25	1.28	5.20	1.01
s_6	3.91	3.48	1.35	1.13	1.10	1.37	2.62	2.04	1.86	1.46	1.61	1.77	1.44	1.84	1.48	1.41
s_{23}	0.06	0.09	0.00	0.00	0.00	0.00	0.05	0.07	0.05	0.08	0.00	0.00	0.00	0.02	0.02	0.15
s_{26}	0.19	0.49	0.00	0.00	0.00	0.18	0.20	0.12	0.24	0.56	0.00	0.14	0.14	0.09	0.05	0.07
s_{36}	0.17	0.12	0.00	0.00	0.06	0.00	0.00	0.11	0.24	0.13	0.10	0.00	0.11	0.07	0.12	0.24
s_{236}	0.00	0.00	0.00	0.00	0.00	0.00	0.00	0.00	0.01	0.00	0.00	0.00	0.00	0.00	0.00	0.00
x_2 (%)	25.2	39.0	35.7	42.6	38.1	50.0	35.7	47.3	38.0	53.9	37.4	46.3	36.8	48.3	35.0	43.1
x_3 (%)	29.9	21.6	44.5	28.6	47.7	19.8	43.4	23.1	46.3	20.9	47.4	24.9	48.1	21.0	49.7	25.5
x_6 (%)	44.9	39.5	19.8	28.8	143	30.2	20.9	29.6	15.7	25.2	15.2	28.8	15.1	30.7	15.3	31.4
DS_M and DS_G	0.10	0.10	0.07	0.04	0.08	0.05	0.14	0.08	0.15	0.09	0.11	0.07	0.11	0.07	0.11	0.05
DS_{KGM}	0.10		0.06		0.07		0.11		0.12		0.10		0.10		0.09	

Table 9.8. (Continued)

Me in position	**M-KGM-45**		**M-KGM-46**		**M-KGM-47**		**M-KGM-48**		**M-KGM-49**		**M-KGM-50**		**M-KGM-51**		**M-KGM-52**	
	Man	Glc	Man	Glc	Man	Glc	Man	Glc	Man	Glc	Man	Glc	Man	Glc	Man	Glc
s_0	92.50	94.98	89.08	94.53	89.47	93.82	73.88	84.50	64.96	80.78	85.40	85.91	86.71	87.57	73.07	76.75
s_2	1.76	0.99	3.59	2.15	3.60	2.60	9.93	7.28	12.74	10.35	1.56	1.25	1.48	0.83	2.47	2.05
s_3	3.67	1.58	5.52	1.17	5.18	1.33	13.19	4.12	18.40	4.81	3.14	2.57	2.86	2.62	4.69	4.44
s_6	1.84	1.99	1.52	1.54	1.51	1.87	2.26	2.63	3.36	3.59	9.65	9.78	8.89	8.54	17.57	14.64
s_{23}	0.04	0.00	0.02	0.03	0.02	0.04	0.13	0.18	0.29	0.35	0.09	0.00	0.07	0.00	0.00	0.40
s_{26}	0.00	0.15	0.12	0.34	0.12	0.33	0.61	0.66	0.06	0.00	0.03	0.08	0.00	0.44	0.81	0.70
s_{36}	0.19	0.31	0.14	0.24	0.11	0.00	0.00	0.63	0.19	0.12	0.14	0.41	0.00	0.00	1.38	1.03
s_{236}	0.00	0.00	0.00	0.00	0.00	0.00	0.00	0.00	0.00	0.00	0.00	0.00	0.00	0.00	0.00	0.00
x_2 (%)	23.3	20.9	33.3	41.3	34.7	45.4	39.7	47.8	36.8	54.3	11.3	9.1	11.6	9.9	11.3	12.4
x_3 (%)	50.4	34.5	50.7	23.7	49.2	21.0	49.6	29.1	53.1	26.8	22.6	20.4	21.9	20.3	20.9	23.1
x_6 (%)	26.3	44.6	16.0	35.0	16.1	33.6	10.7	23.1	10.1	18.8	66.1	70.4	66.5	69.8	67.8	64.5
DS_M and DS_G	0.08	0.05	0.11	0.06	0.11	0.07	0.27	0.17	0.36	0.20	0.15	0.15	0.13	0.13	0.29	0.25
DS_{KGM}	0.07		0.09		0.09		0.23		0.28		0.15		0.13		0.28	

Table 9.8. (Continued)

Me in Position	**M-KGM-53**		**M-KGM-54**		**M-KGM-55**		**M-Man**	**M-Glc**	**M-KGM-7**	
	Man	Glc	Man	Glc	Man	Glc			Man	Glc
s_0	72.52	72.86	84.63	82.96	81.62	82.19	4.65	1.56	0.52	0.42
s_2	4.50	3.80	2.42	3.61	3.14	3.93	2.10	12.50	0.04	0.21
s_3	5.53	8.05	3.50	3.45	4.30	3.54	53.75	20.52	0.07	0.35
s_4							0.35	1.21		
s_6	14.55	13.15	7.98	8.17	9.29	9.23	2.61	0.86	0.44	0.59
s_{23}	0.49	0.52	0.31	0.51	0.00	0.00	10.69	26.28	0.84	0.96
s_{24}							0.44	0.18		
s_{34}							1.33	1.75		
s_{26}	1.25	0.99	0.36	1.02	0.71	0.58	3.50	8.92	0.39	0.42
s_{36}	1.16	0.63	0.79	0.28	0.94	0.53	17.74	14.64	0.35	0.26
s_{46}								0.25		
s_{236}							2.66	8.24	96.74	96.45
s_{234} or s_{246}	0.00	0.00	0.00	0.00	0.00	0.00	0.18	3.11		
s_{2346}									0.10	0.27
x_2 (%)	20.6	18.2	18.4	27.2	19.2	23.9	14.5	34.2	33.3	33.3
x_3 (%)	23.6	31.4	27.3	22.5	26.2	21.5	64.0	41.3	33.2	33.3
x_4 (%)							1.7	3.8		
x_6 (%)	55.8	50.4	54.3	50.3	54.6	54.6	19.8	20.8	33.1	33.2
DS_M and DS_G	0.30	0.29	0.17	0.19	0.20	0.19			2.96	2.95
DS_{KGM}	0.30		0.18		0.20		1.35	1.73	2.96	

9.4 Reaction conditions for the preparation of M-KGM-21 - 55

Table 9.9 Reaction parameters for synthesis of M-KGM-21 to 55, including the maximum of OH absorption of IR spectra after stannylation/methylation, respectively. The reaction parameters for the experiment of M-Man and M-Glc are listed at the end.

M-KGM	Weight (mg) / vessel	Solvent for Stan. (mL)	Bu_2SnO equiv./ glycosyl unit[1]	Stan. *t* (h)/T (°C)	Max. of OH absorption of stan-KGM (cm^{-1})	Solvent for Me. (mL)	CH_3I (eq)	Catalyst (eq)	Me. *t* (h)/T (°C)	Max. of OH absorption of M-KGM (cm^{-1})	DS
21	25.5 / in 3 Vials	Pyridine (4)	2 Sus.[2]	24/115	3363	ACN+DMF 10:1 (5)	61[3]	TBAB (1)+K_2CO_3 (2)	48/70	3442	0.11
22	8.5 / Vial	Pyridine (4)	2 Sus.[2]	24/115	3352	ACN+DMF 10:1 (5)	61[3]	TBAB (1)+K_2CO_3 (2)	48/75	3360	0.13
23	20 / Flask	MeOH (15)	2	6/75	----	ACN (7)	260	----	24/r.t.	3357	0.07
24	17 / Flask	MeOH (10)	1.5	6/78	----	DMF (10)	306	----	48/56	3365	0.04
25	10 / Flask	ACN (10)	2	24/80	3370	DMF (10)	521	----	72/40	3365	0.03
26	11 / Flask	DMSO+MeOH 2:1 (15)	2	24/72	3329	DMSO (10)	474	----	24/45	3385	0.02
27	10 / Flask	DMSO+MeOH 2:1 (15)	5	24/80	3319	DMSO (10)	521	10µL Me-imidazole	48/10	3386	0.03
28	10 / Flask	DMSO+MeOH 1:1(10)	2	24/80	3318	DMSO (5)	521	15µL Me-imidazole	30/r.t.	3372	0.02
29	11 / Flask	DMSO+ACN 1:1 (10)	5	20/110	3344	DMSO (5)	474	----	20/32	3414	0.02
30	11 / Flask	Dioxane (15)	5	6/110	3372	Dioxane (10)	474	---	24/36	3382	0.01
31	8 / Flask	t-BuOH+MeOH (8)	2	24/100	3371	ACN+DMF 10:1 (8)	16	TBAB (0.5)+K_2CO_3 (1.5)	48/60	3364	0.06
32	5 / Vial	Dioxane+ MeOH 1:1 (5)	2 Sus.[2]	24/80	3340	ACN+DMF 10:1 (5)	26	TBAB (0.5)+K_2CO_3 (1.5)	66/60	3347	0.09
33	10 / Flask	Toluene (20)	2 Sus.[2]	24/120	---	ACN+DMF 10:1 (10)	39[2]	TBAB (0.5)+K_2CO_3 (1.5)	39/70	3368	0.02
34	10 / Flask	Pyridine (10)	2 Sus.[2]	24/115	3363	ACN+DMF 10:1 (8)	65[3]	TBAB (1)+K_2CO_3 (2)	48/70	3366	0.11
35	10 / Flask	Pyridine (10)	2 Sus.[2]	24/115	3363	ACN+DMF 10:1 (8)	91[3]	TBAB (1.5)	48/70	3355	0.08
36	10 / Flask	Pyridine (10)	2 Sus.[2]	24/115	3363	ACN+DMF 10:1 (8)	78[3]	TBAB (1)+K_2CO_3 (2)	48/70	3357	0.13
37	15 / Vial	Pyridine (3)	0	16/115	3333	ACN+DMF 10:1 (5)	69[3]	TBAB (1)+K_2CO_3 (2)	48/70	3333	0.10
38	150 / Flask	Pyridine (35)	0.5 Sus.[2]	16/115	3341	ACN+DMF 10:1 (40)	69[3]	TBAB (1)+K_2CO_3 (2)	48/70	3362	0.06

Table 9.9 (Continued)

M-KGM	Weight (mg) / vessel	Solvent for Stan. (mL)	Bu_2SnO equiv./ glycosyl unit1	Stannylation t (h)/T (ºC)	Max. of OH absorption of stan-KGM (cm^{-1})	Solvent for Me. (mL)	CH_3I (eq)	Catalyst (eq)	Me. t (h)/T (ºC)	Max. of OH absorption of M-KGM (cm^{-1})	DS
39	150 / Flask	Pyridine (40)	1 Sus.[2]	16/115	3335	ACN+DMF 10:1 (40)	69[3]	TBAB (1)+K_2CO_3 (2)	48/70	3380	0.07
40	15 / Vial	Pyridine (3)	1.5 Sus.[2]	16/115	3333	ACN+DMF 10:1 (5)	69[3]	TBAB (1)+K_2CO_3 (2)	48/70	3359	0.10
41	15 / Vial	Pyridine (3)	2 Sus.[2]	16/115	3339	ACN+DMF 10:1 (5)	69[3]	TBAB (1)+K_2CO_3 (2)	48/70	3377	0.09
42	15 / Vial	Pyridine (3)	2.5 Sus.[2]	16/115	3333	ACN+DMF 10:1 (5)	69[3]	TBAB (1)+K_2CO_3 (2)	48/70	3333	0.10
43	15 / Vial	Pyridine (3)	3 Sus.[2]	16/115	3333	ACN+DMF 10:1 (5)	69[3]	TBAB (1)+K_2CO_3 (2)	48/70	3359	0.10
44	15 / Vial	Pyridine (3)	4 Sus.[2]	16/115	3339	ACN+DMF 10:1 (5)	69[3]	TBAB (1)+K_2CO_3 (2)	48/70	3377	0.09
45	15 / Vial	Pyridine (4)	2 Sus.[2]	16/115	3369	ACN+DMF 10:1 (5)	69[3]	TBAB(1)	44/70	3372	0.07
46	15 / Vial	Pyridine (4)	2 Sus.[2]	16/115	3340	ACN+DMF 10:1 (5)	69[3]	TBAB (1)+K_2CO_3 (0.5)	44/70	3359	0.09
47	15 / Vial	Pyridine (4)	2 Sus.[2]	16/115	3367	ACN+DMF 10:1 (5)	69[3]	TBAB (1)+K_2CO_3 (1)	44/70	3361	0.09
48	15/ Vial	Pyridine (4)	1 Sus.[2]	16/115	3350	ACN+DMF 10:1 (5)	69[3]	TBAB (1)+K_2CO_3 (1.5)	44/70	3350	0.23
49	30 / in 2 Vials	Pyridine (4)	2 Sus.[2]	16/115	3362	ACN+DMF 10:1 (5)	69[3]	TBAB (1)+K_2CO_3 (1.5)	44/70	3357	0.28
50	15 / Vial	Solv. free	1	---	---	Solv. free	69[3]	TBAB (1)+DIPEA (4)	12/90	3378	0.15
51	15 / Vial	Solv. free	1	---	---	Solv. free	69[3]	TBAB (1)+DIPEA (6)	12/90	3357	0.13
52	10 / Vial	Solv. free	1 Sus.[2]	---	---	Solv. free	69[3]	TBAB (0.5)+DIPEA (6)	24/100	3366	0.28
53	10 / Vial	Solv. free	1 Sus.[2]	---	---	Solv. free	67[3]	TBAB (0.5)+DIPEA (6)	24/90	3368	0.30
54	10 / Vial	Solv. free	1 Sus.[2]	---	---	Solv. free	67[3]	TBAB (0.5)+ K_2CO_3 (2)	24/90	3379	0.18
55	10 / Vial	Solv. free	1 Sus.[2]	---	---	Solv. free	67[3]	TBAB (0.5)+K_2CO_3 (2)	24/100	3383	0.20
M-Man	10 / Vial	Pyridine (4)	2 Sus.[2]	24/115	3335	ACN+DMF 10:1 (5)	61[3]	TBAB (1)+K_2CO_3 (2)	48/75	---	1.35
M-Glc	10 / Vial	Pyridine (4)	2 Sus.[2]	24/115	3286	ACN+DMF 10:1 (5)	61[3]	TBAB (1)+K_2CO_3 (2)	48/75	---	1.73

[1]Glycosyl unit = anhydro glucose unit / anhydro mannose unit in KGM.
[2]Sus. means Bu_2SnO boiled in MeOH at 50 mg/mL yielding a methanolic suspension of $Bu_2Sn(OMe)_2$ and Bu_2SnO.
[3]CH_3I was added in portions to the mixture during the reaction.